STATISTICAL MECHANICS OF THE AMORPHOUS SOLID STATE OF RANDOMLY CROSSLINKED MACROMOLECULES

Horacio Emilio Castillo, Ph.D.
Department of Physics
University of Illinois at Urbana-Champaign, 1999
Prof. Paul M. Goldbart, Advisor

In 1839 Charles Goodyear discovered the vulcanization of rubber: by heating natural rubber (which is a liquid), together with sulfur, he obtained an elastic solid material. This liquid-solid transformation was later found to entail the random crosslinking of the linear macromolecules forming natural rubber, until the crosslink density is high enough that an equilibrium phase transition—the vulcanization transition—from the liquid to the amorphous solid state occurs.

In this thesis a semi-microscopic theory of the vulcanization transition is developed, and the emergent amorphous solid state is studied in detail, close to the transition.

In the first part of this work a derivation is presented of the free energy functional for a system of randomly crosslinked linear macromolecules, starting from a semi-microscopic model. Stationary points of the free energy are obtained that represent, respectively, the liquid and the amorphous solid state. A continuous phase transition between the two states is found to occur. It is shown that in the liquid state all monomers are delocalized, but in the amorphous solid state, some fraction (called the "gel fraction") of the monomers become localized near random mean positions, and thermally fluctuate about these positions with random r.m.s. displacements (called "localization lengths"). The distribution of localization lengths is computed, and it is shown that both this distribution and the order parameter exhibit simple scaling properties near the transition. Both the gel fraction and the typical inverse localization length are found to vanish continuously at the transition.

In the second part of this work the stability of the amorphous solid state is analyzed for

a class of systems undergoing liquid–amorphous-solid phase transitions driven by the effect of random constraints. This class of systems includes vulcanized macromolecular systems, as well as others, including endlinked ones. This stability analysis is performed within two different formulations: one involving a Landau theory that is common to all systems in the class, and another involving the semi-microscopic theory for randomly crosslinked macromolecules (discussed in the first part of this work). The results are the same in the two formulations. The stability matrix is obtained for fluctuations around the stationary point corresponding to the amorphous solid state. All the eigenvalues of the stability matrix are shown to be non-negative near the transition. In fact, they are all positive, except for a zero mode associated with the spontaneously broken continuous translational symmetry of the system. Therefore the amorphous solid state is found to be stable.

Signatures of the transition to the amorphous solid state include not only the random localization of a fraction of the particles but also the emergence of a nonzero static shear modulus. In the third part of this work, a semi-microscopic statistical-mechanical theory of the latter signature is presented that accounts for both thermal fluctuations and quenched disorder. It is found that the shear modulus grows continuously from zero at the transition, and does so with the classical exponent, i.e., with the third power of the excess crosslink density. It is also found that, quite surprisingly, the external stresses do not spoil the spherical symmetry of the localization clouds of the particles near the transition.

To my parents,

to my wife Nancy

Acknowledgments

I would like to express my deepest gratitude to my thesis advisor, Prof. Paul Goldbart, for his guidance, and for his constant support and encouragement. His energy and enthusiasm have been a great inspiration to me. He somehow found the time to discuss physics, *and* to make sure that funding for this project was available. He is, above all, a great teacher.

I am also very grateful to Annette Zippelius, for her support and for a stimulating collaboration, and for her hospitality when she invited me to Goettingen.

I wish to thank Béla Joós, Michael Plischke, and Grzegorz Szamel for fruitful discussions and insightful criticism. I have benefited from discussions with Sandra Barsky, Nigel Goldenfeld, Ian Robinson, and Weiqun Peng. I am also grateful to Claudio Chamon, Eduardo Fradkin and Christopher Mudry, with whom I enjoyed collaborating in my "other life" as a quantum physicist.

I am grateful to my friends, here and all over the world, who helped me through these challenging and exciting times.

I want to thank my parents, always loving and generous. They are the ones who taught me to go always one step further. This thesis is dedicated to them, and to my wife, Nancy, for her love and for her constant support, and for all the times, happy and sad, that we have shared.

The work presented in this thesis was supported in part by the National Science Foundation through grants DMR94-24511, DMR91-57018, DMR91-22385, and DMR91-20000. Ad-

ditional support was provided by the University of Illinois at Urbana-Champaign through graduate fellowships, and by NATO through grant CRG 94090.

Table of Contents

List of Tables

List of Figures

Chapter 1

Introduction

1.1 Randomly crosslinked macromolecules

1.1.1 The vulcanization of rubber

Natural rubber, a substance obtained from the *Hevea brasiliensis* tree, had long been appreciated for being highly elastic and waterproof, but it was hampered for many uses because it yields (i.e., it "forgets" its original shape) under even the most feeble of stresses. For example, a sample of natural rubber will adopt the shape of the container holding it. In other words, it is a liquid.

In 1839, Goodyear discovered how to make a better material out of rubber, by the process of vulcanization. He found that when heating natural rubber with sulfur, the undesirable property of creep under small stress is eliminated. Vulcanized rubber is thus a solid, which makes it immensely more useful for practical applications than natural rubber.

Although since Goodyear's time much theoretical work has been done about this liquid-solid transition, and some aspects of the transition are well understood, there is still no detailed microscopic theory of it. This thesis attempts to provide some of the building blocks for such a theory.

1.1.2 Elastomers

Vulcanized rubber was the first historical example of an elastomer, a class of materials characterized by their unusual mechanical and structural properties [1]. An elastomer sample can be stretched by several hundred percent, and still will recover its original shape and size when the external stress is removed. By contrast, metals and glasses can rarely be deformed more than one per cent without introducing irreversibility.

This mechanical behavior hints at the structure of elastomers: their molecules must be able to adopt widely different spatial arrangements, stretching and bending significantly in response to stress. A long chain macromolecule at a temperature above its glass transition is a good candidate to exhibit such a behavior. It has very many accessible spatial configurations, which differ significantly in the spatial distances that separate the points of the chain. These linear macromolecules must be permanently attached (crosslinked) to each other in order for the system to be able to recover its original shape when the stress is removed. Otherwise, the macromolecules slide past one another, and the material yields permanently under stress, as happens for example with natural rubber.

The shear modulus of a typical elastomeric material increases approximately linearly with (absolute) temperature. This suggests that the elastic free energy of the system is dominated by the entropy rather than the internal energy. The thermal expansion coefficient is negative: the material releases heat and sometimes even undergoes partial crystallization upon stretching. This suggests that the entropy decreases when the system is stretched.

Before any detailed discussion of the thermodynamics of elastomers, let us review here some basic facts about linear chain polymers and crosslinks.

1.1.3 Polymers

Polymer chains are macromolecules, i.e., very large covalently bonded molecules, made up of many small, simple chemical units [4]. The individual units are called *repeat units* or

monomer residues, although we will mostly use the term *monomers*. The number of repeat units is called the "degree of polymerization" N_p. The degree of polymerization is usually more than 100 for a molecule to be called a polymer, but it is possible to have values of the order of 10^5 in synthetic polymers, and up to 10^9 in biological macromolecules. In Fig. (1.1) the chemical formulas are shown for some common polymer chains.

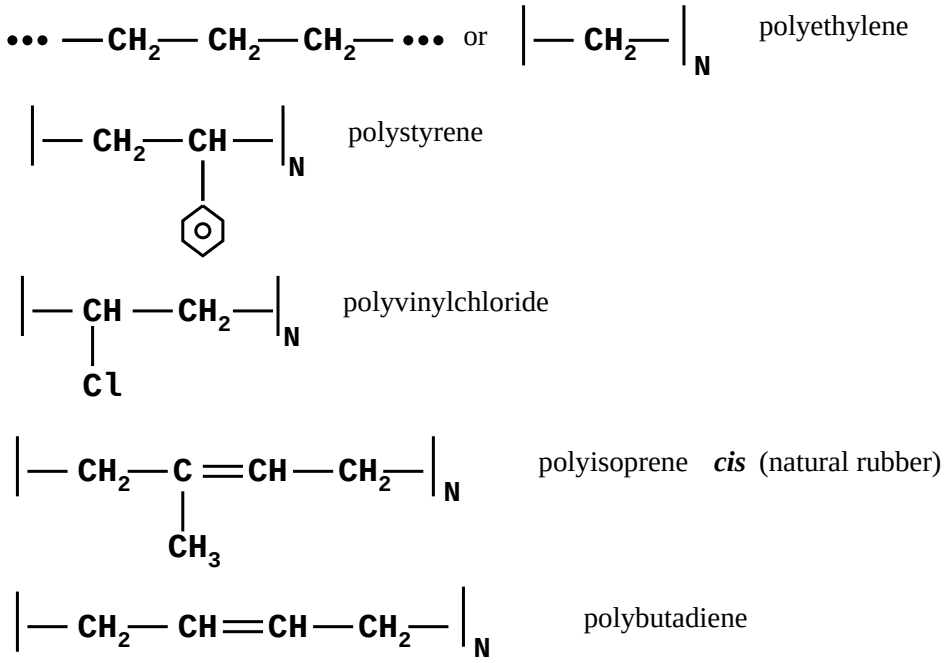

Figure 1.1: Some common linear polymers. The last two, polyisoprene*cis* and polybutadiene, give rise, when crosslinked, to elastomeric materials in common industrial use

Although many preparation procedures give wide distributions for the degree of polymerization, the distribution can be narrowed after the synthesis (for example by physical selection, using chromatography, precipitations, etc.), or a narrow range of degrees of polymerization can be obtained directly by using some special methods of synthesis, such as anionic polymerization.

In a carbon-carbon chain such as polyethylene, the length of each C–C bond and the valence angle θ between successive bonds are essentially fixed, but the angle between suc-

cessive units ϕ_n *around* the axis of the bond is not fixed. The conformation of the polymer is determined by the values of the $N_p - 1$ angles ϕ_n. The energy V of the bond between two monomer units is a function of ϕ_n that depends in its details on the specific chemical species involved but has some generic features common to typical polymers.

In the example of polyethylene, the potential energy $V(\phi)$ has three minima (at $\phi = \pi$, $\pi/3$, and $5\pi/3$), corresponding respectively to the *trans* and $\pm$*gauche* states (see Fig. 1.2). The deepest minimum is the one for the *trans* state, and the two *gauche* states are degenerate. This potential energy is characterized by two parameters: the energy difference $\Delta\epsilon$ between minima, and the energy barrier ΔE separating the minima. For polyethylene, $\Delta\epsilon \sim 400K$ and $\Delta E \sim 2000K$.

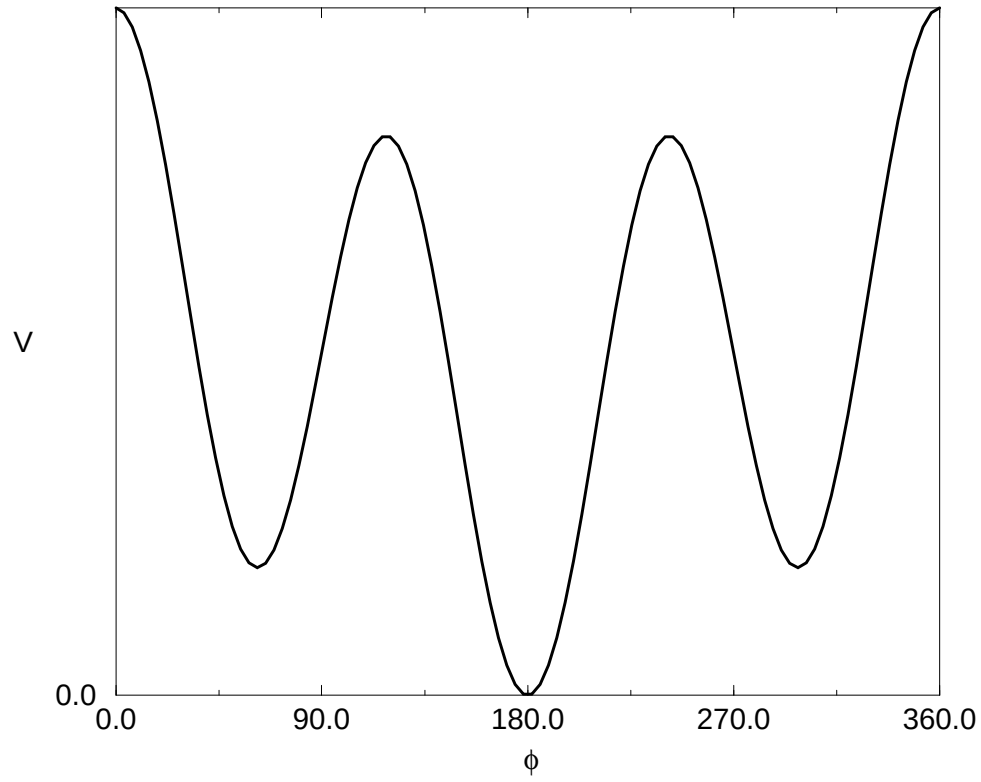

Figure 1.2: Bond energy V as a function of the angle ϕ around the bond (schematic).

The minimum energy configuration of the polymer is all *trans*, and is totally extended. However, for a typical degree of polymerization of 10000, there are of the order of 3^{10000} other configurations for the macromolecule. Most of them could be described as random coiled states, such as the one displayed in Fig. (1.3).

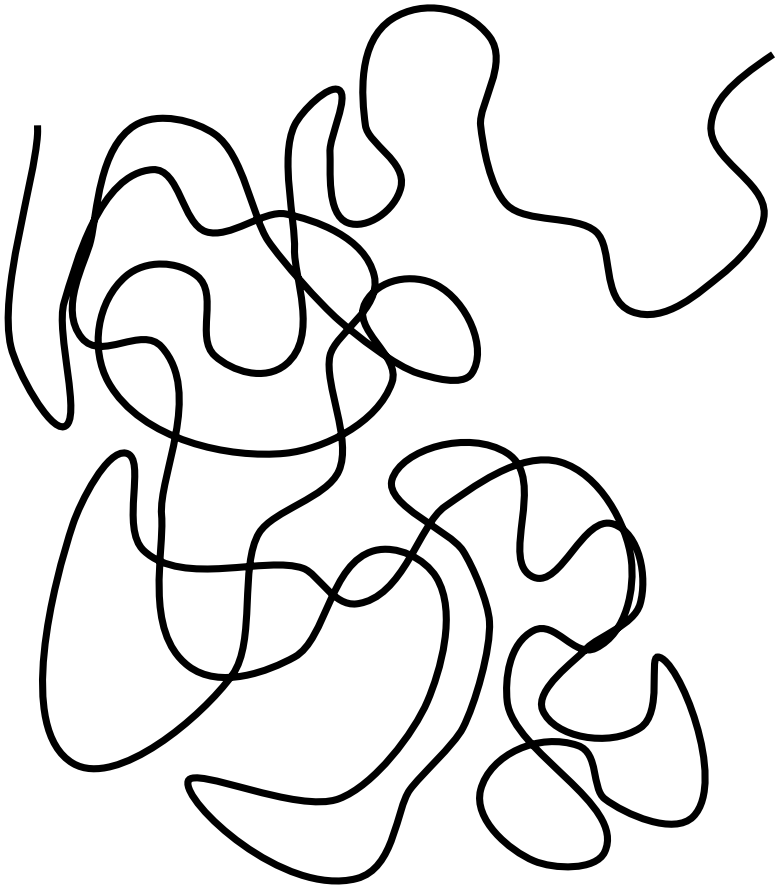

Figure 1.3: A randomly coiled polymer chain.

When $\Delta\epsilon$ is smaller than the thermal energy k_BT, the polymer is statically flexible. All three states for each bond have probabilities of the same order of magnitude, and therefore a huge number of configurations of the macromolecule have non-negligible thermodynamic weights. For slightly higher values of $\Delta\epsilon/k_BT$, there will be a definite preference for the *trans* state, and the polymer will be locally rigid. Still, on a large enough scale, it appears

as a flexible chain. This defines a parameter ℓ called the *persistence length*, such that for lengths larger than ℓ the chain appears continuous and flexible. The persistence length can be computed in terms of microscopic parameters:

$$\ell = \ell_0 \exp(\Delta\epsilon / k_B T), \tag{1.1}$$

where ℓ_0 is of the order of a few Angströms. If ℓ is much smaller than the total length L of the polymer, it is appropriate to consider the molecule as flexible for scales larger than ℓ. If ℓ is larger than L, the molecule has to be considered as a rigid rod at all scales.

Another important question related to polymer conformations is how fast the bonds can switch between *trans* and *gauche*. This depends on the height ΔE of the barrier between those states. The characteristic time associated with this process is called *persistence time* τ, and has the form

$$\tau = \tau_0 \exp(\Delta E / k_B T), \tag{1.2}$$

where τ_0 is of the order of 10^{-11}s. If the timescale of interest is longer than τ, the polymer can be considered to be dynamically flexible. For very high barriers ΔE, the polymer behaves like a random coil that is frozen in one conformation.

At low enough temperatures a system of polymers can partially crystallize, and at an even lower temperature it can undergo a glass transition, below which the individual molecules do not have enough thermal energy to change their conformations. In this work only the regime of temperatures above the glass transition and the crystallization transition will be considered. In this regime, the macromolecules can fluctuate freely and rapidly between different conformations.

A useful idealization that is very commonly employed in polymer physics is the concept of *ideal chain*. An ideal chain is a chain where the only interactions between monomers come from the rigidity of the backbone. It can be simply modeled as a random walk composed of L/ℓ uncorrelated steps represented by vectors $\{\mathbf{l}_m\}$, $m = 1, \ldots, L/\ell$, each one of length

ℓ. Its end to end distance $\mathbf{R} = \sum_m \mathbf{l}_m$ has the following statistical properties: due to the independence of the steps, the average square of $\mathbf{R}$ is linear in L/ℓ,

$$\langle \mathbf{R}^2 \rangle = \sum_{m=1}^{L/\ell} \langle {\mathbf{l}_m}^2 \rangle = (L/ell)\ell^2 = L\ell, \tag{1.3}$$

and in the case that $\ell \ll L$, the central limit theorem implies that the probability distribution of $\mathbf{R}$ is Gaussian, with the form

$$p(\mathbf{R}) = \Big(\frac{d}{2\pi\ell L}\Big)^{d/2} \exp\Big(-\frac{d}{2\ell L}\mathbf{R}^2\Big), \tag{1.4}$$

where d is the dimensionality of the space [7]. One can interpret $p(\mathbf{R})$ as the sum of the individual probabilities for all polymer conformations such that the total end to end distance of the polymer is $\mathbf{R}$. Therefore $p(\mathbf{R})$ is proportional to the constrained partition function of the polymer, and by taking its logarithm one immediately obtains the entropy for an individual polymer chain with its ends fixed at the origin and $\mathbf{R}$ (up to a constant):

$$S(\mathbf{R}) = S(\mathbf{0}) - \frac{d}{2\ell L}\mathbf{R}^2. \tag{1.5}$$

In addition to the interactions between monomers associated with the rigidity of the backbone chain, there are additional interactions that come about when monomers that are far apart along the backbone become spatially close to each other because the macromolecule is coiled. Because they act between monomers that are far apart along the backbone, these interactions are sometimes called "long range interactions" in the polymer literature, even when (as is usually the case, at least for electrically neutral systems) they are short-ranged in real space.

1.1.4 Gelation and vulcanization

Polymer gels are (random) networks of flexible polymer chains, and can be obtained by a variety of chemical or physical processes, generally involving the bonding, or *crosslinking*, of smaller units.

There are two kinds of gelation processes. If the crosslinks are, once made, completely stable (for the stresses and time scales involved in the relevant experiments), the process is called *strong gelation*. If the crosslinking reaction can proceed in both directions (i.e., bonding $\leftrightarrow$ non-bonding), the process is called *weak gelation*. Only strong gelation will be considered in this work.

For example, a common and conceptually simple method of gel preparation is based on the *condensation* of polyfunctional units. The number of bonding sites that a monomer has is referred to as the *functionality*. Bifunctional monomers can only combine to form linear macromolecules, but any monomer with functionality three or higher can form a branch point. For example, molecules with three bonding sites, such as trialcohool, can react with molecules that have two bonding sites, such as di-isocyanate, and after the reaction has proceeded long enough, a macroscopic branched object (the *gel*) is obtained. The part of the system that is not linked to the gel is made up of finite molecules, and it is called the *sol*.

The focus of this thesis is on the vulcanization transition, which is the special case of the sol-gel transition in which one starts from a dense system of long, linear chains and then crosslinks them (Fig. 1.4).

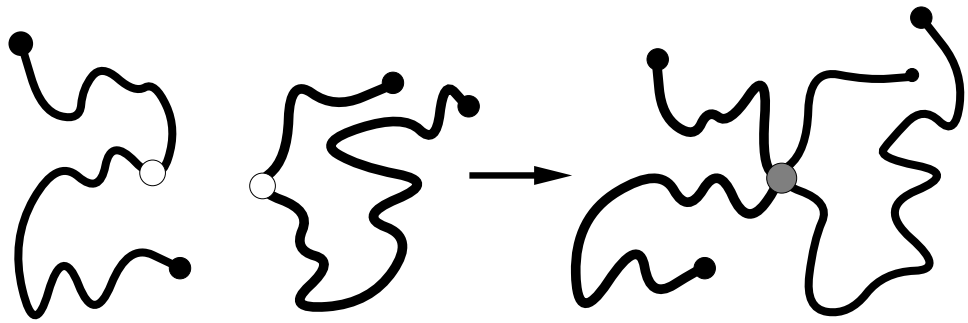

Figure 1.4: Crosslinking two polymer chains.

There are many ways to obtain the vulcanization transition in practice. In the process of

vulcanization discovered by Goodyear, sulfur reacts with double bonds along the polymers, resulting in a chain of between 2 and 4 sulfur atoms joining two chains of the original polymer (and forming a crosslink).

Another crosslinking reaction involves the use of peroxides. A peroxide radical removes hydrogen from the polymer chain and thus creates a radical site at the chain. This free radical migrates along the chain until it comes in close proximity with a similar radical from another chain. The two then combine to form a covalent bond that crosslinks the two chains. High-energy radiation, such as electrons, gamma photons, and ultraviolet light, can also be used to form free radicals, and hence generate crosslinks.

All of the above techniques produce crosslinking at random locations along the polymer chains. It is also possible to generate crosslinks at prescribed positions along the chains. The simplest example of this is to have polymer chains with reactive groups at both ends put in contact with small trivalent molecules, thus endlinking the polymers (i.e., linking them at their ends).

1.2 Theoretical approaches

In this section, some previous theoretical approaches to the vulcanization transition are discussed.

Before going into a discussion of specific theories, let us make here a general remark about the study of macromolecular systems. Generally speaking, there are two kinds of approaches. One centers on the detailed conformations and motions of individual monomers inside the polymer chain, and their dependence on the chemical species involved. This *local* point of view is extremely useful, e.g., when one wants to choose an optimal polymer for a given practical application. The other, *global*, point of view, centers on the dependence of physical properties on concentrations, crosslink densities, and a few basic interaction parameters. In

this point of view one tries to omit the details of chain structure as much as possible and to extract simple, universal, features which will remain true for a large class of macromolecular systems. This second, global, point of view is the one that will be adopted in this thesis.

1.2.1 Classical theory

The classical theory of gelation was pioneered by Flory and Stockmayer [6, 8, 9]. In the classical picture, the gelation process is modeled as a *branching process*. In more modern language, the classical picture can be thought of as percolation on a Cayley tree.

Let us discuss the ideas involved in the classical picture, in the simplest case of polymerization in a homogeneous system of f-functional monomers. In this case, one of the f-functional units as chosen as the root of the tree, and it is assumed that there is a probability α (the *reacted fraction*) that each one of the f reactive groups will react with another unit. All the monomers that react with it will form the first level of the tree. Each one has $f-1$ groups available to react. Some of those groups will react with free monomers (reactions within the tree are neglected in the classical theory), thus generating the second level of the tree, and so on. The expected number of members of the next level is $(f-1)\alpha$ times the number of members of a given level. This implies that there is a critical value of the reacted fraction $\alpha_c \equiv 1/(f-1)$ such that for $\alpha < \alpha_c$ the tree eventually dies down, whereas for $\alpha > \alpha_c$ the tree grows indefinitely. This is interpreted by saying that for $\alpha < \alpha_c$ the system is in the sol phase (all monomers belong to finite clusters), whereas for $\alpha > \alpha_c$ the system is in the gel phase (a nonzero fraction of the monomers belong to a macroscopic macromolecule).

The above picture can be extended immediately to the case of vulcanization. If all the monomers in the polymer can potentially participate in crosslinks, the number of monomers N_p of the chain plays the role of the functionality, and the rest of the argument follows through.

With a little more elaboration, the classical picture provides results for other physical quantities. The *gel fraction* q, (i.e., the fraction of the monomers that belong to the infinite cluster), can be shown, with no further physical assumptions, to grow linearly with $\alpha - \alpha_c$ [10]. With the additional assumption that all polymer segments are ideal chains, the *correlation length*, defined in this context as the r.m.s. average distance between monomers in the same finite cluster, can be shown to diverge as $(\alpha_c - \alpha)^{-1}$ as the system approaches the transition from the sol side [11].

A great deal of discussion has taken place within the framework of the classical theory with regards to the elastic properties of crosslinked polymer networks. We will briefly mention some of the results here. Consider a sample of dimensions L_x, L_y, L_z, and assume that a macroscopic distortion $L_j \to \lambda_j L_j$ $(j = x, y, z)$ is imposed on it. It is assumed in the classical theory that the change in free energy of the system is simply given by the absolute temperature times the sum of the changes in the entropies for those polymer segments that are considered "active". A polymer segment is defined to be a segment of linear polymer between two crosslinks. One way of defining an "active" segment is to say that it is a segment such that the distance between its ends changes when the system is deformed.

In the *affine network model* [14], it is assumed that for each elastically active segment a its end-to-end vector $\mathbf{R}_a$ changes in the form $R_{ja} \to \lambda_j R_{ja}$ $(j = x, y, z)$. Therefore, the free energy change for each elastically active segment a is

$$\Delta f_a(\lambda_x, \lambda_y, \lambda_z) = k_B T \frac{3}{2Ll}(\mathbf{R}_a^2(\{\lambda_j\}) - \mathbf{R}_a^2(\{1\})) \tag{1.6}$$

where k_B is Boltzmann's constant and T is the temperature, and the free energy change for the entire system is then

$$\Delta f(\lambda_x, \lambda_y, \lambda_z) = \sum_a k_B T \frac{3}{2Ll}(\mathbf{R}_a^2(\{\lambda_j\}) - \mathbf{R}_a^2(\{1\})) = \frac{N_{el} k_B T}{2}(\lambda_x^2 + \lambda_y^2 + \lambda_z^2 - 3), \tag{1.7}$$

where N_{el} is the number of elastically active segments. There is a competing model within the classical framework, called the *phantom network model*. In it, the end-to-end vector of each

segment is taken to be the sum of a mean value, which distorts affinely, and a fluctuation, which is uncorrelated with the mean value. In this model, it is assumed that chains can pass through one another (hence the name "phantom"), and the fluctuations of the end-to-end vector are found to be spherically symmetric even when the system is deformed [2]. The free energy change calculated in this model is qualitatively similar to, although not quite identical with, the result for the affine network model.

In most discussions of either the affine or the phantom network models, it is usually assumed that the system is in the well-crosslinked regime, and in fact the counting of elastically active segments is usually made by starting from a "perfect network", i.e., a network with no chain ends, and later making simple corrections to take into account some of the features of actual polymer networks. This procedure is not likely to produce accurate results close to the vulcanization transition, as in this regime the network barely exists at all and most chains are end chains.

However, it has been argued by Scanlan [16] and Case [17] that N_{el} scales as the third power of the excess crosslink density from the transition point. This immediately implies that the elastic free energy and, consequently, the shear modulus, also scale as the third power of the excess crosslink density from the transition point. The argument goes as follows [18]: an active junction point is defined as a point from which three "ties" (links leading to infinite sub-trees) radiate. Any point from which fewer "ties" radiate can always relax after deformation, and therefore does not contribute to the elastic free energy. An elastically active segment is a segment that has active junction points at its two ends. As the probability for a tree starting at a given point to be infinite defines the probability for a monomer to belong to the gel fraction, it follows that the probability for a junction point to be active goes like the third power of the gel fraction, and consequently as the third power of the excess crosslink density from the transition point.

The classical picture of gelation has had many successes, not the least of which was its

being the first picture to predict the existence of macroscopic molecules at all.

However, the classical approach does have some shortcomings. First, it is not a statistical mechanical theory. No prescriptions are given to compute the Boltzmann weights of configurations. There is also no attempt to analyze the interplay between the quenched disorder produced by random crosslinking and the thermal fluctuations of the system. In most cases, the architecture of the network is taken as an input. The classical picture does not provide more than a very rough picture of the structure of the system, essentially in terms of the behavior of the gel fraction. Finally, this is a mean field treatment, formulated in such a way that it is not obvious how to systematically improve upon it, in order to get a more accurate formulation. As it is well known, in most cases mean field theories break down close to continuous transitions (although, as we shall discuss later, vulcanization might be, an exception to this).

1.2.2 The Edwards formulation

Significant progress towards a statistical mechanical theory of polymer networks was made by Edwards and collaborators [19, 20, 21, 22]. Edwards proposed the effective hamiltonian of Eq. (2.6). Deam and Edwards wrote an explicit form for the partition function of a system of randomly crosslinked macromolecules, and were the first to apply the replica method to average thermodynamic quantities over the disorder in polymer physics. In their approach, both thermal fluctuations and quenched disorder were taken into account. They concentrated on the well-crosslinked regime, and resorted to a variational calculation to compute various physical quantities, including the elastic free energy and the r.m.s. size of the fluctuations in the positions of the crosslinks. In simple limits, they recovered the results of both the affine network and phantom network approaches.

This line of research has later been continued by Panyukov and collaborators [23, 24], who performed detailed computations of correlation functions accessible through scattering

experiments, and focused much of their attention on the effect of external strain on those correlation functions.

However, as already mentioned, the approaches of Edwards and collaborators and of Panyukov and collaborators only concentrate on the well crosslinked limit. In particular, they contain the assumption that all the polymers in the system can be combined together and represented in the model by a single extremely long macromolecule. Therefore this is a model for a network with no end chains. Close to the transition, most of the monomers in the gel belong to end chains. Therefore this model is completely inadequate to address the vulcanization transition.

The replica method

We will roughly sketch the replica method at this point, not only because it is a central part of the approach by Edwards and collaborators, but because it is also crucial to the approach followed in the present work.

In the study of systems with quenched disorder, it is generally desirable to compute averages over disorder of thermodynamic quantities, such as the Helmholtz free energy F or its derivatives. Let us consider, e.g., the free energy:

$$[F]/k_{\mathrm{B}}T = [-\ln Z], \tag{1.8}$$

where the symbols $[\cdots]$ stand for average over the disorder distribution. The expression on the r.h.s. of Eq. (1.8) is difficult to compute, due to the presence of the logarithm inside the average sign. This difficulty can be overcame by the use of the replica method, which is based on the use of the following expression:

$$[-\ln Z] = -\lim_{n\to 0} \frac{[Z^n]-1}{n}. \tag{1.9}$$

The validity of this expression follows from the form of the Taylor expansion of z^n in powers

of n:

$$z^n = 1 + n \ln z + \mathcal{O}(n^2). \tag{1.10}$$

Eq.1.9 is an exact statement, involving continuous values for the variable n. The next step in the replica approach is to compute $[Z^n]$ for *integer* values of n. In this case, Z^n can be interpreted as the partition function of a system containing n identical, noninteracting, copies (called "replicas", and labeled by the index $\alpha = 1, \ldots, n$) of the same realization of the original random system. From the technical point of view, the disorder average of a partition function is much easier to compute than the disorder average of its logarithm, because the partition function is a sum of Boltzmann weights, each one of which can usually be averaged over the disorder. Consequently it is possible in many cases to explicitly obtain $[Z^n]$. After disorder averaging, the randomness disappears from the problem, but there is a price to be paid: the replicas now interact with each other. Once a result has been obtained for $[Z^n]$ for integer values of n, the next stop in the approach is to take the explicit analytic expression for $[Z^n]$, and assume that n is really a continuous variable. At this point, the limit in Eq. 1.9 is taken, thus obtaining the free energy.

1.2.3 Percolation

A third theoretical approach to the gelation transition was put forward independently by De Gennes and by Stauffer. They proposed to identify [5, 25, 26, 27] gelation with percolation [28] on a lattice. One way to perform this identification [5] is to map sites in the lattice to monomer units, each one having a functionality equal to the number of nearest neighbors of each lattice site. Two neighboring monomers can react, and this corresponds (in the percolation analogy) to the presence of a formed bond between the corresponding sites. Thus the probability p of a bond being formed is identified with the reacted fraction α of the theory of gelation, and the gelation transition is identified with the percolation transition, in which an infinite cluster appears.

De Gennes further argued [25] that the elastic modulus E of a gel could be related to the macroscopic conductance Σ of a random resistor network with a fraction p of conducting links.

The proponents of the percolation point of view observed that the classical approach was equivalent to a model of percolation in a Cayley tree. They argued that the predictions about critical behavior (and, in particular, critical exponents) obtained in the classical approach should be modified to take into account the difference between percolation in dimension $d = 3$ and percolation in infinite dimensions (i.e., in the Cayley tree).

For the case of vulcanization in dimension $d = 3$ or larger, however, De Gennes pointed out [5, 29] that the mean field results should be correct, except for a region around the critical point of width going to zero in the long macromolecule limit (e.g., vanishing as $N_p^{-1/3}$ for $d = 3$).

The percolation approach suffers from many of the same drawbacks as the classical approach. It entails only a single statistical ensemble, and hence cannot treat the equilibration of thermal (i.e., annealed) freedoms in the presence of quenched freedoms (crosslinks, in the present case). Also, in the percolation approach there is no prescription for computing the Boltzmann weights of configurations. If the percolation ensemble is interpreted as describing the quenched freedoms then it can account for the appearance of an infinite network at a critical crosslink density, but it cannot account for the thermal fluctuations, which determine the physical properties of the liquid and amorphous solid states. If, on the other hand, the percolation ensemble is interpreted as describing the thermal fluctuations of the macromolecular freedoms then it may serve as a model for weak gelation, in which crosslinks continuously form and break up, but it cannot account for permanent, quenched crosslinks.

1.2.4 Microscopic theory of the vulcanization transition

Goldbart and Goldenfeld pointed out in a series of papers [30] that a true microscopic theory of the vulcanization transition was still lacking, as the theories that had been proposed this far either assumed the existence and architecture of the macromolecular network or neglected the interplay of thermal fluctuations, strong interactions and quenched disorder. They introduced and developed the point of view that the solid state of randomly crosslinked macromolecular networks represents an unusual, equilibrium state of matter, the equilibrium amorphous solid state.

In their work, they introduced a new order parameter, appropriate for detecting this amorphous solid state. This order parameter was inspired by the Edwards-Anderson order parameter of spin glasses [31, 32]. They also constructed a free energy functional starting from a minimal microscopic model, and they managed to show that the liquid state should be unstable for a sufficiently large density of crosslinks.

This whole approach drew much inspiration from both the Deam-Edwards theory of a single crosslinked macromolecule [20], as well as the Edwards-Anderson theory of spin glasses [31].

Further progress within this formulation was made by Zippelius, Goldbart and Goldenfeld [33]. They set up a self-consistent mean field theory in which the control parameter determined the density of crosslinks. They allowed for a fraction of the monomers (the gel fraction) to be localized, and the rest to be delocalized. They computed the gel fraction as a function of the control parameter, and found a liquid–amorphous-solid transition. They also studied nonlinear susceptibilities in the liquid phase, which turned out to diverge at the transition. However, the formalism they used only allowed for localization lengths of the order of the size of the system. This was believed by the authors to be due to the absence of correlations in their model for the crosslink distribution: as any monomer was equally likely to be crosslinked to any other monomer, the effective attractive potential produced by the

crosslinks was spread all over the system, instead of being concentrated at the sites of actual crosslinking.

This deficiency was resolved by Goldbart and Zippelius [34], who applied a prescription that had been proposed by Deam and Edwards to incorporate correlations into the crosslink distribution, and performed a variational calculation in which the localization length was the optimization parameter. In their work, they made two simplifying assumptions: that all monomers were either delocalized or localized simultaneously, and that the localization length was the same for all monomers. They obtained a localization length whose scale was set by the radius of gyration of the individual macromolecules (instead of being set by the size of the system), and which diverged at the transition (coming from the amorphous solid side) with the classical exponent $\nu = 1/2$. They also computed the rigidity exponent and found the value $t = 2$, (i.e., a value different from the classical one, but, as we shall see in Chap. 4, consistent with a subset of the experiments). However, their calculation predicted a liquid phase surviving well beyond its known region of stability, and therefore it was clear that the variational solution they obtained for the solid was a crude one, rather far (in order parameter space) from the true stationary point of the free energy functional. More significantly, the theory was formulated in a way that implied that the gel fraction had a discontinuity at the transition (all monomers were delocalized on one side, and localized on the other), whereas the gel fraction was known from experiments to be continuous at the transition.

The approach that we have been discussing in the present subsection is the one adopted in the present work in order to formulate a statistical mechanical theory of the vulcanization transition. Let us motivate this choice by reviewing some of the virtues of this approach.

First, both thermal freedoms (i.e.the macromolecular positions) and quenched freedoms (i.e.the crosslink locations) are incorporated, and handled appropriately, in contrast with percolative pictures. The replica technique provides the tool for accomplishing this. In fact,

it will be shown in Chap. 2 that the percolative picture emerges from the present approach in the form of statistical information concerning the presence of localized macromolecules. However, the present approach is considerably richer, additionally yielding statistical-mechanical information about the (thermally fluctuating) macromolecular system. In particular, it will allow a unified treatment of liquid and amorphous solid states. Second, the physical many-macromolecule character of the system is maintained, in contrast with approaches that consider instead the properties of a single linear macromolecule. Especially in the vicinity of the solidification transition, where the number of physical crosslinks is of order one per macromolecule, this is particularly significant, and allows for a theory of the solidification transition to be developed. Third, the present approach leads directly to an order parameter for the amorphous solid state, which is related to that of spin glass physics. The order parameter has a natural, physical interpretation, which facilitates the hypothesizing of an appropriate form for it (as it will be done in Chap. 2). Fourth, the physical freedoms, viz., the macromolecular configurations, appear directly throughout the development, not being exchanged for any problem-specific formal representation. (This is in contrast to other approaches, e.g., Ref. [24], in which the polymer degrees of freedom are formally represented using the $n \to 0$ limit of the n-vector model.) The macromolecular character of the system is therefore retained, especially when approximations are made. Indeed, the entire approach is very robust, so that, in addition to being of interest in the context of vulcanized macromolecular systems, it can readily be extended to address a wide range of other physical systems, such as crosslinked manifolds [35], endlinked systems of flexible, semi-flexible and rigid macromolecules [36], and continuous random network models of structural glasses [37, 38]. In addition, it should prove possible to extend the present approach to address issues of dynamics, and some progress in that direction has already been made [39]. Moreover, looking beyond the algebraic details, one sees a theoretical superstructure that is rather natural, direct and perhaps even conventional, at least from the point of view of statistical field theory.

Fifth, the use of the present approach has primarily been restricted to the mean-field level of approximation. However, as will be discussed in Chap. 2, it is possible in this approach to obtain an exact solution of the relevant stationary-point equations, as opposed to a variational approximation. This is a crucial point, as, e.g., the results for the elastic properties change significantly between the variational approximation and the calculation based on the exact stationary point. In addition, knowledge of the stationary point provides a promising starting point for future developments, such as going beyond mean field level.

Let us now point out the main limitations of this approach. First, for technical reasons, it is difficult to perform computations in the regime of high crosslinking (e.g., deep in the amorphous solid state). Other formulations, such as the original one by Edwards and collaborators, and also its continuation by Panyukov and collaborators, were designed with that regime in mind, and seem more appropriate to treat it. The present formulation, by contrast, is mainly intended to be used near the transition . Second, in its present form, this approach does not respect the interlocking of closed loops of macromolecules (as will be discussed further in Sec. 2.2.2) that crosslinking can induce. There is, in fact, no microscopic formulation that manages to take those interlockings into account, except for some rough approximate treatments [40]. Third, up to the present, the results from this formulation are obtained only to mean field level. No estimate has been obtained within the theory of the error that such approximation induces. However, considering De Gennes' argument that vulcanization should be well described by mean field theory, this is probably not a significant drawback.

1.3 Outline of this thesis

The work reviewed in the previous section had established that the microscopic formulation of Goldbart and collaborators does predict a liquid–amorphous-solid equilibrium phase tran-

sition. However, essentially all other questions about the nature of this transition were still not answered satisfactorily. For example, it was not yet clear whether a consistent theory could be developed that would start from a statistical mechanical formulation and address all of the following issues: (i) the existence of the transition, (ii) the continuous but singular change of the gel fraction at the transition, (iii) obtaining a physically sensible prediction for the localization lengths for the monomers in the amorphous solid, (iv) the form of the order parameter, and its role in determining the microscopic structure of the amorphous solid state, (v) the effect of external stresses on the structure of the state, and (vi) the existence and value of a a static shear modulus for the amorphous solid. In addition, in order to have a physically sensible theory, it is necessary to (vii) show that the states obtained are thermodynamically stable.

In this thesis an attempt is presented to address all of these issues within a consistent theoretical framework.

The organization of the thesis is as follows: Chap. 2 addresses issues (i) to (iv), Chap. 3 addresses issue (vii), and Chap. 4 addresses issues (v) and (vi).

The work presented in Chaps. 2 and 4 was done in collaboration with Paul Goldbart and Annette Zippelius. The work presented in Chap. 4 was done in collaboration with Paul Goldbart.

Chapter 2

The amorphous solid state of randomly crosslinked macromolecules

2.1 Introduction

In this chapter a general theoretical description is presented of the physical properties of systems of macromolecules that have been randomly and permanently crosslinked. The focus of this theoretical approach is on the equilibrium properties of such systems, especially in the regime of the vulcanization transition. As anticipated in Chap. 1, the term vulcanization transition refers to the sharp thermodynamic phase transition occurring when the mean density of crosslinks exceeds a certain critical value. At this critical crosslink-density, the equilibrium state of the system undergoes a continuous transition: for subcritical values the equilibrium state is a liquid state, in which all the macromolecules are delocalized; for supercritical values the equilibrium state is an amorphous solid state, in which a nonzero fraction of macromolecules form a macroscopic network, and spontaneously become localized about certain random locations. The focus of this chapter will be on the spontaneous emergence of the equilibrium amorphous solid state at the vulcanization transition, and the

structural properties of this unusual state of matter.

It should be pointed out that the theoretical description that is about to be presented recognizes strong influences from both the Deam-Edwards theory of a single crosslinked macromolecule [20], and the ideas and techniques developed in the field of spin glasses [32].

The basic ingredients of the present approach to the physical properties of randomly crosslinked macromolecular networks are as follows. A semi-microscopic description of the macromolecules is adopted, in which the detailed microscopic chemistry of the macromolecules and solvent (if any there be) feature only to the extent that they determine the following effective parameters: the total arclength of each macromolecule, the persistence length (i.e., the length of the statistically independent macromolecular segments, which are called monomers), and the excluded-volume strength (i.e., the parameter that describes the effective repulsion between monomers). Thus, the macromolecules are regarded as extended, featureless, flexible linear objects, each capable of exhibiting a large number of configurations, and classical equilibrium statistical mechanics is used to address the properties of systems composed of a thermodynamically large number of such macromolecules. The crosslinks are regarded as permanent elements that constrain certain randomly chosen monomers to remain adjacent to one another. Thus the crosslinked macromolecular system is a system with quenched disorder, in the sense that in addition to the macromolecular freedoms—the so-called annealed variables, which undergo equilibrium statistical-mechanical fluctuations—there are additional variables, those that specify the detailed realization of the crosslinking, that do not undergo equilibrium statistical-mechanical fluctuations. Instead, these variables—the so-called quenched random variables—vary only between realizations of the physical system. These quenched random variables are treated statistically, too, but their quenched nature is accounted for by invoking the replica technique.

What follows is an overview of the basic strategy used for determining the physical properties of randomly crosslinked macromolecular networks.

The plausible equilibrium states of the system—liquid, globule, crystalline solid, amorphous solid—are characterized in terms of an order parameter, designed to discriminate between these states. This order parameter is a more intricate object than the order parameters that arise, say, in the study of ferromagnetism or even spin glasses, and one must explore much larger spaces to find its equilibrium value. By investigating a simple caricature of the amorphous solid state, however, it is possible to identify a physically well-motivated scheme for parametrizing the amorphous solid state order parameter at a manageable level: via a single number—the fraction of spatially localized monomers—and a normalized probability distribution—the statistical distribution of localization lengths of the localized monomers.

The focus in this chapter is on the free energy and the order parameter for the system of interacting macromolecular freedoms subject to the crosslinking constraints. Application of the replica technique to these quantities allows for the elimination of the quenched random variables; the price for this elimination is the introduction of an effective coupling amongst the replicated macromolecular freedoms. The scheme used for parametrizing the order parameter leaves intact the permutation symmetry amongst the replicas. Next, a certain stochastic field is introduced, via which the replicated macromolecular description is transformed into a field-theoretic one. In this representation, the individual macromolecules are coupled to one another only indirectly, via their coupling to the fluctuations of the stochastic field, although the replicas of any given macromolecule remain directly coupled to each other.

In order to elucidate the physical properties of the system a mean-field approach is adopted, which amounts to approximating, via the stationary-point method, the averages over the stochastic field in the field-theoretic expressions for the free energy and order parameter. The state of the physical system then follows from the form of the appropriate stationary value of the stochastic field or, equivalently, from the form of the self-consistent value of the order parameter. For mean crosslink densities smaller than a certain critical

value, of order one crosslink per macromolecule, there is only one stationary value, which is elementary, and the corresponding state is the liquid state. For supercritical crosslink densities the appropriate stationary value corresponds to the amorphous solid state. At the critical crosslink density the system undergoes a continuous vulcanization transition from the liquid state to the amorphous solid state.

To determine the properties of the amorphous solid state itself, we hypothesize that the self-consistent value of the order parameter lies within the family of order-parameter values reachable via our (severely restrictive but nevertheless physically plausible) parametrization. Quite remarkably, this is indeed the case: our parametrization does not merely yield a variational approximation to the amorphous solid state. Instead, although one has no *a priori* reason to suppose that it should, it permits an *exact* mean-field description of randomly crosslinked macromolecular networks to be constructed. What emerges is an amorphous solid state characterized by a nonzero fraction of localized monomers. The precise value of this fraction depends on the crosslink density, and vanishes continuously at the transition and in the liquid state. This fraction depends on the crosslink density in a manner identical to that found in random graph theory and percolation. The state is further characterized by a crosslink-density–dependent distribution of localization lengths, which quantifies the manner in which the localized monomers have become localized around their random mean positions. The typical localization length diverges continuously at the transition and in the liquid state. In the vicinity of the transition, the distribution of localization lengths has a scaling form governed by a universal function, which we compute. To date, we have been unable to obtain conclusive results for the distribution of localization lengths far from the amorphous solidification transition. The reason for this is purely technical: at a certain stage in the development we employ a perturbative calculation, in which the small parameter is the fraction of localized particles (or, equivalently, the characteristic inverse localization length, measured in units of the radius of gyration of a single, noninteracting macromolecule), this

parameter being zero in the liquid state, and small in the amorphous solid state only in the vicinity of the transition.

The present chapter is organized as follows. In the present, introductory, section we provide an overview of the chapter. In Sec. 2.2 we discuss the basic elements of the model of macromolecular systems on which the present approach is based, including the level of description of macromolecular configurations, the Edwards measure for their statistical weights, and the notion of crosslinks as quenched random variables. We also discuss the partition function, free energy and issues of indistinguishability, along with the statistical characterization of the crosslinks, and the notion of disorder averages of certain physically relevant quantities. In Sec. 2.3 we develop the general subject of order parameters appropriate for the amorphous solid and other states, discussing the properties that such order parameters should possess. We explore a simple scenario for the amorphous solid state, which provides physical motivation for a certain specific hypothesis that we make for the form taken by the amorphous solid order parameter in the amorphous solid state. At this stage we introduce the concept of gel and sol fractions and the statistical distribution of localization lengths associated with localized monomers. We also analyze the symmetry properties of the ordered state, and discuss some ways of experimentally probing the order parameter. In Sec. 2.4 we address the statistical mechanics of randomly crosslinked macromolecular networks, invoking the replica technique in order to eliminate the (quenched random) crosslink variables. In Sec. 2.5 we reformulate the statistical mechanics of randomly crosslinked macromolecular networks in field-theoretic terms by introducing a certain stochastic field, which is closely related to the amorphous solid state order parameter. In Sec. 2.6 we explore the properties of the resulting field theory within the context of a natural mean-field approximation. We exhibit the instability of the liquid state, and we compute the free energy and self-consistent order parameter in the vicinity of the transition. We also describe the characteristics of the amorphous solid state that emerge from this approach. In Sec. 2.7 we present a compari-

son of our results with the results later obtained by Barsky and Plischke in their molecular dynamics simulations of randomly crosslinked polymers systems. These simulations give strong support to the physical picture presented in this Chapter. In Sec. 2.8 we briefly review some published works that extend this approach to related systems and develop a Landau theory that captures the essential elements of the liquid–amorphous-solid transition without resorting to a microscopic model. In Sec. 2.9 we make some concluding remarks. We have organized this chapter so that the main text is, to a large degree, free of lengthy mathematical details. Wherever possible such details have been relegated to appendices.

The research discussed in the present chapter has been reported on in Refs. REF:epl and [42].

2.2 Model of the macromolecular system

2.2.1 Macromolecular system prior to crosslinking

We consider a system consisting of a large number N of long, flexible macromolecules, initially identical, and contained in a large d-dimensional hypercube of volume V. The macromolecules are characterized by their common arclength L and (weakly temperature-dependent) persistence length $\ell(\ll L)$, so that the number of effectively statistically independent segments comprising each macromolecule is of order $L/\ell \gg 1$. Semi-microscopic spatial configurations of the system are characterized by the collection of spatial configurations of the macromolecules $\{\mathbf{R}_i(\sigma)\}_{i=1}^N$, in which $\mathbf{R}_i(\sigma)$ is the d-dimensional position vector of the monomer an arclength distance σ from a specific end of macromolecule i, the (discrete) macromolecule index i ranging from 1 to N and the (continuous) arclength variable σ ranging from 0 to L.

It is convenient to exchange the dimensionful position vector $\mathbf{R}$ and arclength σ for

dimensionless versions $\mathbf{c}$ and s via the transformation

$$\mathbf{R}_i(\sigma) \equiv \sqrt{\ell L/d}\ \mathbf{c}_i(s), \tag{2.1}$$

$$\sigma \equiv L\, s. \tag{2.2}$$

Thus, we shall be measuring spatial distances in units of $(\ell L/d)^{1/2}$ (i.e., the root mean squared end-to-end distance of a free macromolecule divided by $\sqrt{d}$), and arclength distances in units of the total arclength L. We shall measure energies in units such that $k_{\rm B}T$ is unity.

At the level of the present semi-microscopic description, and prior to the incorporation of the effects of either monomer-monomer interactions or crosslinks, we account for the connectivity of the constituent macromolecules by adopting the Wiener measure [19, 22, 46], in terms of which the statistical weight [47] of the configuration of the system $\{\mathbf{c}_i(s)\}_{i=1}^N$ is proportional to $\exp(-W_1)$, where

$$W_1 \equiv \frac{1}{2}\sum_{i=1}^{N}\int_0^1 ds \left|\frac{d}{ds}\mathbf{c}_i(s)\right|^2. \tag{2.3}$$

The subscript 1 on W_1 anticipates the introduction of replicas of the system, which we shall need to make below. We shall often need to consider normalized expectation values taken with respect to the Wiener measure, which we shall denote by the angle-bracket pair $\langle\cdots\rangle_1^{\rm W}$, defined by

$$\left\langle \cdots \right\rangle_1^{\rm W} \equiv \frac{\int \mathcal{D}\mathbf{c}\, \exp\left(-W_1\right)\cdots}{\int \mathcal{D}\mathbf{c}\, \exp\left(-W_1\right)}, \tag{2.4}$$

where the dots represent an arbitrary function of the configuration of the system, and the measure

$$\mathcal{D}\mathbf{c} \equiv \prod_{i=1}^{N}\prod_{0\le s\le 1} d\mathbf{c}_i(s) \tag{2.5}$$

indicates functional integration over all spatial configurations of the system, i.e., over all configurations of the N macromolecules. The subscript 1 on $\langle\cdots\rangle_1^{\rm W}$ also indicates that the average is taken only over the configurations of a single copy of the system, also anticipating the introduction of replicas.

We account for monomer-monomer interactions in a phenomenological manner, by augmenting the Wiener measure with an additional factor that has the effect of suppressing the statistical weight of configurations in which pairs of monomers occupy common regions of space [19, 22, 46]. To this end, we replace the Wiener measure, Eq. (2.3), by the Edwards measure, in terms of which the statistical weight of the configuration $\{\mathbf{c}_i(s)\}_{i=1}^N$ is proportional to $\exp(-H_1)$, where

$$H_1 = \frac{1}{2}\sum_{i=1}^{N}\int_0^1 ds \Big|\frac{d}{ds}\mathbf{c}_i(s)\Big|^2 + \frac{\lambda^2}{2}\sum_{i,i'=1}^{N}\int_0^1 ds\int_0^1 ds'\,\delta^{(d)}(\mathbf{c}_i(s)-\mathbf{c}_{i'}(s')). \tag{2.6}$$

Here, $\delta^{(d)}(\mathbf{c})$ is the d-dimensional Dirac δ-function, and the dimensionless (real, positive) parameter λ^2 characterizes the strength of the suppression of statistical weight due to the (repulsive) excluded-volume interaction between monomers [19, 22, 46]. The excluded-volume interaction is suitably modified so as to exclude interactions between adjacent monomers on a common macromolecule (i.e., monomers for which $|s-s'| < \ell/L$). The system can be regarded as a melt of macromolecules, in which case the interaction parameter λ^2 is intended to account for the monomer-monomer interaction. Alternatively, it can be regarded as a solution of macromolecules dissolved in a good solvent, in which case λ^2 is intended to represent the effective monomer-monomer interaction (i.e., the bare interaction renormalized by the monomer-solvent and solvent-solvent interactions, the solvent degrees of freedom having been integrated out). In both cases, λ^2 is weakly temperature-dependent. Even at the level of mean-field theory, the excluded-volume interaction plays a crucial role: it partially compensates the effective monomer-monomer attraction due to the crosslinks in just such a fashion as to maintain the macroscopic homogeneity of the system while allowing for the possibility of transition from the liquid to the amorphous solid state.

We shall need to consider normalized expectation values taken with respect to the Edwards measure, which we shall denote by the angle-bracket pair $\langle\cdots\rangle_1^{\mathrm{E}}$, defined by

$$\Big\langle\cdots\Big\rangle_1^{\mathrm{E}} \equiv \frac{\int \mathcal{D}\mathbf{c}\,\mathrm{e}^{-H_1}\cdots}{\int \mathcal{D}\mathbf{c}\,\mathrm{e}^{-H_1}}, \tag{2.7}$$

where the dots represent an arbitrary function of the configuration of the system, and once again $\mathcal{D}\mathbf{c}$ indicates functional integration over all configurations of the system. Again, the subscripts 1 on H_1 and $\langle\cdots\rangle_1^{\mathrm{E}}$ anticipate the introduction of replicas.

It should be noted that neither the Wiener measure nor the Edwards measure explicitly breaks translational or rotational symmetry: the statistical weight of a configuration remains unchanged if all the monomers are simultaneously translated through a common amount or rotated through a common angle about a common axis.

2.2.2 Crosslinks as quenched random variables

Our aim is to address the statistical mechanics of thermodynamically large systems of macromolecules into which a large number of crosslinks have been permanently introduced at random. Each crosslink has the effect of constraining two randomly selected monomers, the locations of which were kinematically independent prior to the introduction of the crosslink, to occupy a common spatial location. Thus the effect of the crosslinks is to eliminate from the ensemble of configurations of the system all configurations that do not obey the entire set of random constraints enforced by the crosslinks. Our task is therefore to address the statistical mechanics of macromolecular systems in the presence of a large number of random constraints.

A specific realization of the crosslinking is fully described by specifying which randomly selected pairs of monomers are connected by each crosslink, i.e., that the crosslink labeled by the index e serves to connect the monomer at arclength s_e on macromolecule i_e to the monomer at arclength s'_e on macromolecule i'_e, for $e = 1, \ldots, M$, with M being the total number of crosslinks. Thus, only those configurations that satisfy the constraints

$$\mathbf{c}_{i_e}(s_e) = \mathbf{c}_{i'_e}(s'_e), \qquad (\text{with } e = 1, \ldots, M) \tag{2.8}$$

are retained in the ensemble. It should be noted that these constraints do not explicitly

break translational symmetry.

In principle, of course, neither the crosslinks nor the integrity of the macromolecules are truly permanent. However, in many physical realizations of crosslinked macromolecular systems there is a very wide separation between the time-scale required for the crosslink-constrained macromolecular system to relax to a state of thermodynamic equilibrium and the much longer time-scale required for either the crosslinks or the macromolecules to break. For such systems, and it is such systems that we have in mind, the crosslinks and the macromolecules should be regarded as permanent, so that the number and identity of the monomers participating in crosslinks, $\chi \equiv \{i_e, s_e; i'_e, s'_e\}_{e=1}^{M}$, should be treated as nonequilibrating (i.e., quenched) random variables. The unconstrained macromolecular freedoms are regarded as reaching equilibrium in the presence of fixed values of the quenched variables. Thus, it is a meaningful task to address the equilibrium statistical mechanics of permanently crosslinked macromolecular systems.

It should be remarked that the relative statistical weights of the configurations that do satisfy the crosslinking constraints are hypothesized, at least *a priori*, to be unaffected by the introduction of crosslinks. That is, the statistical weights are proportional to $\exp(-H_1)$ for configurations satisfying the crosslinks and zero otherwise. However, as we shall see in detail below, for a sufficiently large density of crosslinks the translational and rotational symmetry of the equilibrium state of the system is spontaneously broken. That is, in a given (pure) state the statistical weights of configurations that are translations and rotations of one another are no longer identical, and thus localization can arise. Indeed, only one member of a family of translated and rotated configurations has a nonzero weight in a given (pure) state. The associated transition to an amorphous solid state is precisely the transition on which we are focusing. We remark that in the present context of amorphous solidification, translational and rotational symmetry are spontaneously broken in an unusual sense, in that they remain fully intact at the macroscopic level.

A second mechanism that leads to the violation of the hypothesis mentioned in the previous paragraph arises because sufficient crosslinking is liable to give a topological character to the system of macromolecules, at least in three spatial dimensions, in the sense that for a given set of crosslinks there will be families of configurations allowed by the crosslinks that are mutually inaccessible. We mean by this that, because of the possibility of interlocking closed loops formed by macromolecules, there will be families of configurations between which the system cannot continuously evolve without the necessity either of the breaking of at least one crosslink or the passage of one monomer through another. We distinguish between constraints arising indirectly from crosslinking via the interlocking of closed loops and constraints arising directly from the crosslinks themselves by referring to the former as *anholonomic* constraints and the latter as *holonomic* constraints. In principle, a statistical-mechanical approach should incorporate, at most, those configurations that are mutually accessible, i.e., should respect both holonomic and anholonomic constraints. The theory presented here treats the holonomic constraints as quenched but the anholonomic constraints as annealed, therefore not incorporating the latter. We know of no explicit semi-microscopic strategy that is capable of handling the anholonomic constraints.

2.2.3 Partition function

We define the "naïve" statistical-mechanical partition function $\tilde{Z}(\{i_e, s_e; i'_e, s'_e\}_{e=1}^M)$ that characterizes one particular realization $\chi = \{i_e, s_e; i'_e, s'_e\}_{e=1}^M$ of the crosslinked system via

$$\bar{Z}(\{i_e, s_e; i'_e, s'_e\}_{e=1}^M) \equiv \int \mathcal{D}\mathbf{c}\ \mathrm{e}^{-H_1} \prod_{e=1}^{M} \delta\Big(\mathbf{c}_{i_e}(s_e) - \mathbf{c}_{i'_e}(s'_e)\Big)\,. \tag{2.9}$$

The product of Dirac δ-functions serves to remove from the sum over configurations implicit in the angle brackets (2.7) any configuration that fails to satisfy the constraints (2.8) [49], the remaining configurations contributing with weights given by the Edwards measure (2.6).

We also define a correlator $\tilde{Z}(\{i_e, s_e; i'_e, s'_e\}_{e=1}^M)$

$$\tilde{Z}(\{i_e, s_e; i'_e, s'_e\}_{e=1}^M) \equiv \left\langle \prod_{e=1}^M \delta(\mathbf{c}_{i_e}(s_e) - \mathbf{c}_{i'_e}(s'_e)) \right\rangle_1^{\mathrm{E}}, \tag{2.10}$$

that probes the contact points between macromolecules. This correlator is exactly identical to the ratio between the naïve partition function for the given crosslink realization, and the naïve partition function for the system with no crosslinks. This means that it can be interpreted as a "normalized partition function" which only probes the changes in the system due to the crosslinking.

At first sight, the quantity $\bar{Z}(\{i_e, s_e; i'_e, s'_e\}_{e=1}^M)$ in Eq. (2.9), which we are calling the naïve partition function, appears to be precisely the physical partition function of the crosslinked system. However, for a straightforward reason associated with the notion of indistinguishability, a reason that we discuss in Secs. 2.2.4 and 2.2.6, $\bar{Z}(\{i_e, s_e; i'_e, s'_e\}_{e=1}^M)$ as defined in Eq. (2.9) is not quite the correct definition of the physical partition function. However, as we shall see, the naïve partition function $\bar{Z}(\{i_e, s_e; i'_e, s'_e\}_{e=1}^M)$ will turn out to be adequate for our purposes, and we will simply call it "partition function" except when we want to specifically distinguish it from the true partition function.

2.2.4 Indistinguishability

As first pointed out by Gibbs [50], the (configurational aspect of the) physical partition function for systems involving one or more species of identical constituents is to be found by summing over all configurations of the system while ignoring the issue of the distinguishability of the constituents, and subsequently dividing by an appropriate combinatorial factor to account for the indistinguishability of the constituents. This strategy compensates for the over-counting of configurations that has arisen from the neglect of indistinguishability.

What are the implications of indistinguishability in the present context? For the case of the system of N identical uncrosslinked macromolecules, the appropriate factor is $N!$, and

thus the physical partition function is given by

$$\frac{1}{N!}\int \mathcal{D}\mathbf{c}\, \exp\left(-H_1\right). \tag{2.11}$$

If, for the case of the crosslinked system, the appropriate factor were also $N!$ (which it is not) then its physical partition function would be given by

$$\frac{1}{N!}\int \mathcal{D}\mathbf{c}\, \exp\left(-H_1\right) \prod_{e=1}^{M} \delta^{(d)}(\mathbf{c}_{i_e}(s_e) - \mathbf{c}_{i'_e}(s'_e)). \tag{2.12}$$

However, the process of crosslinking alters the system from one that comprises N copies of a single species of identical elements. Instead, the crosslinked system will contain a variety of species, such as macromolecules that do not participate in any crosslinks, as well as clusters of macromolecules of many types. By clusters we mean assemblages of macromolecules that are (directly or indirectly) connected by crosslinks or interlockings, and therefore cannot be separated by arbitrary distances. Examples of clusters include pairs of macromolecules that participate in a single crosslink, that crosslink being located between some specific pair of arclength locations [say $(s, s') = (0.12, 0.57)$], single macromolecules crosslinked to themselves at some specific pair of arclength locations, triplets of macromolecules connected by two specifically located crosslinks, as well as more complicated species such as pairs of self-crosslinked macromolecules interlocking one another.

Let us label the various possible cluster species by the index $a = 1, 2, 3, \ldots$, and let $a = 0$ label the uncrosslinked macromolecule species. Then, for a specific realization of the disorder (i.e., the crosslinks and the interlockings) let the number of uncrosslinked macromolecules be ν_0, and the number of clusters of species a be ν_a [51]. Then the incorrect combinatorial factor of $N!$ should be replaced by the correct factor $\sigma(\chi) = \prod_a \nu_a!$, this factor varying across disorder realizations. The physical partition function for a given realization of the system is then given by

$$Z(\{i_e, s_e; i'_e, s'_e\}_{e=1}^{M}) \equiv \frac{1}{\prod_a \nu_a!}\int \mathcal{D}\mathbf{c}\, \exp\left(-H_1\right) \prod_{e=1}^{M} \delta^{(d)}(\mathbf{c}_{i_e}(s_e) - \mathbf{c}_{i'_e}(s'_e)). \tag{2.13}$$

This correction of the combinatorial factor is mirrored by the absence, due to the constraints, in the summation over system configurations of those configuration in which macromolecules participating in a cluster are widely separated, which results in the loss of volume factors. Together, the corrected combinatorial factor and the loss of volume factors conspire to yield a thermodynamic free energy that is properly extensive.

In common with much work on the physics of disordered systems, we shall not focus on the statistical mechanics of a system having a particular realization of the disorder. Instead we shall take a probabilistic approach, focusing on the typical properties of randomly crosslinked macromolecular systems. To do this, we shall need to consider the statistical distribution of crosslink locations. In fact, we shall also allow the number of crosslinks to fluctuate across realizations.

2.2.5 Deam-Edwards crosslink distribution

To compute physical quantities characterizing the system of randomly crosslinked macromolecules for a specific realization of the large set of quenched random variables $\{i_e, s_e; i'_e, s'_e\}_{e=1}^{M}$ is, of course, neither possible nor particularly useful. Instead we shall focus on *typical* values of physical quantities, constructed by suitably averaging them over the quenched random variables. To perform this averaging we shall need to choose a probability distribution that assigns a sensible statistical weight $\mathcal{P}_M(\{i_e, s_e; i'_e, s'_e\}_{e=1}^{M})$ to each possible realization of the number M and location $\{i_e, s_e; i'_e, s'_e\}_{e=1}^{M}$ of the crosslinks. Following an elegant strategy due to Deam and Edwards [20], we assume that the normalized crosslink distribution is given by

$$\mathcal{P}_M(\{i_e, s_e; i'_e, s'_e\}_{e=1}^{M}) = \frac{(\mu^2 V/2N)^M \, \tilde{Z}(\{i_e, s_e; i'_e, s'_e\}_{e=1}^{M})}{M! \left\langle \exp\left(\frac{\mu^2 V}{2N} \sum_{i,i'=1}^{N} \int_0^1 ds \int_0^1 ds' \, \delta^{(d)}(\mathbf{c}_i(s) - \mathbf{c}_{i'}(s'))\right)\right\rangle_1^{\mathrm{E}}}, \qquad (2.14)$$

where $\tilde{Z}(\{i_e, s_e; i'_e, s'_e\}_{e=1}^{M})$ is given by Eq. (2.10), and can be regarded as probing the equilibrium correlations of the underlying uncrosslinked liquid [52]. Such correlations were omitted from the crosslink distribution in certain previous works [30, 33], which led to difficulties in

obtaining a quantitative description of the amorphous solid state. It is not, at present, clear whether this omission is significant for the liquid state.

The Deam-Edwards distribution can be envisaged as arising from a realistic vulcanization process, in which crosslinks are introduced simultaneously and instantaneously into the liquid state in equilibrium [53]. Specifically, it incorporates the notion that all pairs of monomers that happen (at some particular instant) to be nearby are, with a certain probability controlled by the crosslink density parameter μ^2, crosslinked. Thus, the correlations of the crosslink distribution reflect the correlations of the uncrosslinked liquid, and it follows that realizations of crosslinks only acquire an appreciable statistical weight if they are compatible with some reasonably probable configuration of the uncrosslinked liquid. This good feature of the Deam-Edwards distribution is compatible with the random, space-filling, *frozen liquid*, nature of the equilibrium amorphous state that is achieved upon sufficient crosslinking.

We allow the number of crosslinks to fluctuate in a quasi-Poisson manner, controlled by the parameter μ^2. All that we shall need to know about μ^2 is that the mean number of crosslinks per macromolecule, which we denote by $[M]/N$, is a smooth, monotonically-increasing function of μ^2 that can, in principle, be determined using the distribution $\mathcal{P}$ [54]. We remark that the control parameter μ^2 appears in Eq. (2.14) divided by N/V. This factor is simply the (dimensionless) density of macromolecules, which is an intensive quantity. As we shall see, this choice leads to an equation of state that does not depend on the density of macromolecules, at least at the level of mean-field theory. We also remark that no delicate scaling of the control parameter is needed to achieve a good thermodynamic limit, in contrast with the case of the Sherrington-Kirkpatrick spin-glass model [55].

As discussed in Sec. 2.2.2, at least in three dimensions crosslinking confers anholonomic topological constraints on the network as well as holonomic ones. Thus, the statistical-mechanical tool for constructing the crosslink distribution is not entirely correct. In principle,

crosslink-realizations should be labeled not only by $\{i_e, s_e; i'_e, s'_e\}_{e=1}^{M}$, i.e., by the number and arclength locations of the crosslinks, but also by the precise topology of the realization, i.e., by the manner in which the macromolecules thread through the closed loops made by one another. Then the statistical weight attributed to a crosslink-and-topology realization would be better modeled as arising from those configurations of the underlying equilibrium liquid that not only satisfy the holonomic constraints but also the anholonomic ones. As remarked in Sec. 2.2.2, no mathematical tool yet exists for accomplishing this refinement analytically. In other words, we are treating the random topology of the system as annealed rather than quenched.

One should pause to notice the striking feature that at the heart of the Deam-Edwards crosslink distribution is the normalized partition function $\tilde{Z}(\{i_e, s_e; i'_e, s'_e\}_{e=1}^{M})$ of the crosslinked system, i.e., the crosslink distribution is itself proportional to the partition function, the logarithm of which it is to be used to average. This fact gives the development a structure that is rather appealing, at least from the point of view of form. This will become especially apparent in Sec. 2.4 in the context of the replica technique, in which this distribution is generated via an additional (i.e., zeroth) replica, the permutation aspect of the symmetry of the theory thereby being enlarged from the permutation group $\mathcal{S}_n$ to $\mathcal{S}_{n+1}$, where n is the number of replicas [56, 57]. There is, however, no physical basis for restricting attention *solely* to crosslink distributions generated by the partition function identical to that of the crosslinked system. For example, one might imagine crosslinking at a different temperature or solvent quality, (or, as in Chap. 4, crosslinking and later deforming the system), which would break the symmetry between the crosslink distribution and the partition function of the crosslinked system; then, in the context of the replica technique, the permutation aspect of the symmetry of the theory would remain $\mathcal{S}_n$.

2.2.6 Disorder averages and symmetry factors

How are we to use the Deam-Edwards crosslink distribution? As is well known, it is generally inappropriate in disordered systems to average the partition function itself over the quenched random variables, as this would amount to treating the quenched random variables as annealed variables (i.e., equilibrated variables having the same status as the variables describing the configurations of the system that can be accessed during equilibrium fluctuations). Rather, it is thermodynamically extensive or intensive quantities, such as the free energy or the order parameter, that should be averaged over the quenched random variables [32]. To illustrate this point, consider the free energy $-\ln \hat{Z}$. (Recall that we are measuring energies in units such that $k_{\rm B}T = 1$.) Then the disordered-average of the free energy per macromolecule per space dimension, which we denote by f, is given by

$$-dNf = \left[\ln Z(\{i_e, s_e; i'_e, s'_e\}_{e=1}^{M})\right], \tag{2.15}$$

where the square brackets indicate a disorder-average, viz.,

$$\left[\mathcal{O}_M(\{i_e, s_e; i'_e, s'_e\}_{e=1}^{M})\right] \equiv \mathcal{P}_0\mathcal{O}_0 + \sum_{M=1}^{\infty} \int_0^1 ds_1 \cdots ds_M \int_0^1 ds'_1 \cdots ds'_M$$
$$\sum_{i_1=1}^{N} \cdots \sum_{i_M=1}^{N} \sum_{i'_1=1}^{N} \cdots \sum_{i'_M=1}^{N} \mathcal{P}_M(\{i_e, s_e; i'_e, s'_e\}_{e=1}^{M})\, \mathcal{O}_M(\{i_e, s_e; i'_e, s'_e\}_{e=1}^{M}), \tag{2.16}$$

where $\mathcal{O}_M(\{i_e, s_e; i'_e, s'_e\}_{e=1}^{M})$ is an arbitrary function of the realization of crosslinks. The average over the locations of the crosslinks excludes realizations of the disorder in which two positions on the same macromolecule located closer than a persistence length participate in crosslinks. This can be accomplished by suitably cutting off the arclength integrations.

In practice, it is easier to compute disorder averages for the logarithm of the naïve partition function $\bar{Z}$ than for the logarithm of the physical partition function Z itself. The relation between the two is given by

$$f = -\frac{1}{dN}\left[\ln \frac{Z(\chi)}{\sigma(\chi)}\right] = \bar{f} + \frac{1}{dN}[\ln \sigma(\chi)] \tag{2.17}$$

where the naïve free energy per macromolecule per space dimension is

$$\bar{f} \equiv \frac{1}{N}[\log \bar{Z}]. \tag{2.18}$$

The difference between the two free energies,

$$\Delta f \equiv f - \bar{f} = \frac{1}{dN}\left[\ln\left(\prod_a \nu_a!\right)\right], \tag{2.19}$$

is in general proportional to $\ln N$ (for large N). The constant of proportionality is, in general, difficult to compute. It will be, however, close to d^{-1} for the case of lightly crosslinked systems, in which σ is close to $N!$, and it will approach zero for the high-crosslinking limit, in which all macromolecules are connected to a single cluster. (For the uncrosslinked system $\Delta f = \ln N/d$.) Thus, $\bar{f}$ $(= f - \Delta f)$ contains a term proportional to the logarithm of the size of the system, i.e., is not intensive. Despite this unphysical feature of $\bar{f}$, it is $\bar{f}$ that we shall be computing, rather than f, because our inability to compute $[\ln \prod_a \nu_a!]$ precludes us from computing f. However, the physical properties of the system, such as the order parameter, e.g., are determined by certain disorder-averaged quantities that we shall show to be insensitive to the indistinguishability factor $\prod_a \nu_a!$, and which can thus be computed in the present approach.

2.3 Order parameter for the amorphous solid state

2.3.1 General properties of the order parameter

We now discuss a certain order parameter constructed with the intention of distinguishing between equilibrium states that are liquid (in which the monomers are all delocalized), crystalline solid (in which a nonzero fraction are localized in a spatially periodic fashion), globular (in which the monomers have condensed within a spatial subvolume of the system), and amorphous solid (in which a nonzero fraction are localized in a spatially random fashion) [30].

Consider the real space density for one particular monomer to be at position $\mathbf{r}$ in the sample,

$$\rho_{i,s,\chi}(\mathbf{r}) = \langle \delta(\mathbf{r} - \mathbf{c}_i(s)) \rangle_\chi \tag{2.20}$$

and its Fourier transform

$$\langle \exp(i\mathbf{k} \cdot \mathbf{c}_i(s)) \rangle_\chi = \int_V d\mathbf{r}\, \rho_{i,s,\chi}(\mathbf{r}) \exp(i\mathbf{k} \cdot \mathbf{r}), \tag{2.21}$$

where $\mathbf{k}$ is any wave vector. The angle brackets $\langle \cdots \rangle_\chi$ indicate an average over the equilibrium state in question for a particular realization of the disorder, indicated by the subscript χ. Such equilibrium states may correspond to situations in which the translational symmetry of the system is spontaneously broken, in which case they are not ergodic. However, we shall not dwell here on the possibility of further ergodicity-breaking (e.g., of the type commonly associated with the concept of replica-symmetry breaking; see Ref. [32]). This restriction is consistent with the results presented below. For a discussion of the issue of ergodicity-breaking in systems of crosslinked macromolecular networks, see Refs. [30, 56].

First, consider the case of a delocalized monomer, i.e., a monomer (i, s) that can be found, with equal probability, in the vicinity of any location in the container. Consequently, the equilibrium expectation value of its real space density is the constant V^{-1}, and the Fourier transform vanishes (except for the trivial case of $\mathbf{k} = \mathbf{0}$).

Next, consider the case of a monomer (i, s) that is localized in the vicinity of specific point $\mathbf{b}_i(s)$ in space, albeit exhibiting thermal fluctuations about this point. In this case, the real space density $\rho_{i,s,\chi}(\mathbf{r})$ will be more or less sharply peaked around $\mathbf{b}_i(s)$ and, correspondingly, $\langle \exp(i\mathbf{k} \cdot \mathbf{c}_i(s)) \rangle_\chi$ will not vanish identically, instead varying with $\mathbf{k}$ so as to reflect the spatial localization of the monomer (i, s). For this case

$$\langle \exp(i\mathbf{k} \cdot \mathbf{c}_i(s)) \rangle_\chi = \exp(i\mathbf{k} \cdot \mathbf{b}_i(s))\, \wp_{(i,s)}(\mathbf{k}) \tag{2.22}$$

where $\wp_{(i,s)}(\mathbf{k})$ is a (nonzero) form factor that describes the thermal fluctuations of the monomer around its mean position.

One could be tempted simply to propose the disorder average of the total density in Fourier space (i.e., the sum of all individual monomer densities) as the order parameter. In fact, this kind of order parameter allows one to distinguish between a liquid phase, in which all elements of the system are delocalized, and a crystalline phase, in which the system forms some kind of regular lattice in real space, or a globule phase, in which the density is concentrated in one particular region in real space (see Table 2.1). However, an amorphous solid phase, in which some of the monomers are localized, but in a random and homogeneous manner, would give the same value of the order parameter as a liquid (except for corrections of subleading order in the thermodynamic limit). Thus, we need an order parameter that probes the structure of the system in a subtler way.

A similar problem appears in the the context of a class of amorphous magnetic systems known as spin glasses, in which a system of N spins $\{\mathbf{S}_i\}_{i=1}^N$ are subject to random frustrated interactions. The total magnetization $\mathbf{M} = (1/N)\sum_i \langle \mathbf{S}_i \rangle$ (i.e., the sum of the thermal averages of all the spins in the system), is zero both in the paramagnetic phase, where each term in the sum is zero, and in the spin glass phase, in which individual spins are frozen with nonzero but random values, so that terms in the sum end up canceling each other because of their random orientation. The solution to this difficulty in the spin glass case was found by Edwards and Anderson [31, 32]: one simply needs to take a sum of *scalar products* of the local mean values: $(1/N)\sum_i \langle \mathbf{S}_i \rangle \cdot \langle \mathbf{S}_i \rangle$, and the cancelation of terms no longer occurs. A related approach also works in the context of vulcanization, where the order parameter is an extension, *mutatis mutandis*, of the order parameter introduced by Edwards and Anderson for spin glasses.

For a specific realization of the crosslinks (i.e., prior to disorder averaging), the appropriate order parameter is given by [30]

$$\frac{1}{N}\sum_{i=1}^{N}\int_0^1 ds\, \langle \exp\left(i\mathbf{k}^1 \cdot \mathbf{c}_i(s)\right)\rangle_\chi \langle \exp\left(i\mathbf{k}^2 \cdot \mathbf{c}_i(s)\right)\rangle_\chi \cdots \langle \exp\left(i\mathbf{k}^g \cdot \mathbf{c}_i(s)\right)\rangle_\chi, \tag{2.23}$$

for $g = 1, 2, 3, \ldots$, none of the d-dimensional wave vectors $\{\mathbf{k}^1, \ldots, \mathbf{k}^g\}$ being zero.

The disorder-averaged order parameter is denoted by

$$\Omega_{\mathbf{k}^1,\mathbf{k}^2,\ldots,\mathbf{k}^g} \equiv \left[\frac{1}{N}\sum_{i=1}^{N}\int_0^1 ds\,\langle\exp\left(i\mathbf{k}^1\cdot\mathbf{c}_i(s)\right)\rangle_\chi\langle\exp\left(i\mathbf{k}^2\cdot\mathbf{c}_i(s)\right)\rangle_\chi\cdots\langle\exp\left(i\mathbf{k}^g\cdot\mathbf{c}_i(s)\right)\rangle_\chi\right]. \tag{2.24}$$

For any particular positive integer g, this order parameter may be regarded as the g^{th} moment of the distribution of random static density fluctuations $\mathcal{N}(\{\rho_{\mathbf{k}}\})$ (see Ref. [33]), which is defined by

$$\mathcal{N}(\{\rho_{\mathbf{k}}\}) \equiv \left[\frac{1}{N}\sum_{i=1}^{N}\int_0^1 ds\prod_{\mathbf{k}}{}^{\dagger}\delta_{\mathrm{c}}\Big(\rho_{\mathbf{k}}-\langle\exp\left(i\mathbf{k}\cdot\mathbf{c}_i(s)\right)\rangle_\chi\Big)\right], \tag{2.25}$$

where $\prod_{\mathbf{k}}^{\dagger}$ denotes the product over all d-vectors $\mathbf{k}$ in the half-space given by the condition $\mathbf{k}\cdot\mathbf{n}>0$ for a suitable unit d-vector $\mathbf{n}$, and the Dirac δ-function of complex argument $\delta_{\mathrm{c}}(z)$ is defined by $\delta_{\mathrm{c}}(z)\equiv\delta(\mathrm{Re}\,z)\,\delta(\mathrm{Im}\,z)$, where $\mathrm{Re}\,z$ and $\mathrm{Im}\,z$ respectively denote the real and imaginary parts of the complex number z. Thus,

$$\begin{aligned}\int\prod_{\mathbf{k}}{}^{\dagger}d\,\mathrm{Re}\,\rho_{\mathbf{k}}\,d\,\mathrm{Im}\,\rho_{\mathbf{k}}\;\mathcal{N}(\{\rho_{\mathbf{k}}\})\;\rho_{\mathbf{k}^1}\rho_{\mathbf{k}^2}\cdots\rho_{\mathbf{k}^g}&\\ =\left[\frac{1}{N}\sum_{i=1}^{N}\int_0^1 ds\,\langle\exp\left(i\mathbf{k}^1\cdot\mathbf{c}_i(s)\right)\rangle_\chi\langle\exp\left(i\mathbf{k}^2\cdot\mathbf{c}_i(s)\right)\rangle_\chi\cdots\langle\exp\left(i\mathbf{k}^g\cdot\mathbf{c}_i(s)\right)\rangle_\chi\right].&\end{aligned} \tag{2.26}$$

To see why formula (2.23) is indeed an order parameter appropriate for distinguishing between liquid, crystalline, globular and amorphous solid states, let us examine its qualitative properties.

First, suppose that the state is liquid. Then each monomer is delocalized, and consequently the Fourier transformed density vanishes for all nonzero $\mathbf{k}$. Thus, for a liquid state the order parameter (2.23) vanishes, all terms in the summation over monomers vanishing identically. This corresponds to a state having full translational and rotational symmetry.

Next, consider the case when a nonzero fraction of monomers are localized in the vicinity of specific points in space, albeit exhibiting thermal fluctuations about these points. In this case, for many monomers (i,s) the Fourier transformed density will be nonvanishing and

given by Eq. (2.22). In such a state, translational invariance is broken at the microscopic level. However, the symmetry of the state of the system at the macroscopic level is not settled without further information.

What possibilities present themselves in the situation in which a nonzero fraction of the monomers are localized? If the mean locations $\{\mathbf{b}_i(s)\}$ of the localized monomers are distributed randomly and homogeneously over the volume of the system then the state is said to be macroscopically translationally invariant (MTI), the inclusion of rotational invariance being understood. We mean by this that there is no periodicity, or any other macroscopic feature capable of distinguishing one equilibrium state from any global translation or rotation of it. We refer to such states as (equilibrium) amorphous solid states. On the other hand, if the mean locations $\{\mathbf{b}_i(s)\}$ of the localized monomers are distributed inhomogeneously over the volume of the system then the state is said to break translational invariance macroscopically. Examples of such states are the globular state [58], in which the monomers have condensed (in space) within a subvolume of the system, and the crystalline state, in which the mean locations of the monomers are arranged in a periodic lattice (and the monomers may be regarded as having condensed in wave vector space).

How are the various possible states diagnosed by the order parameter? As we showed above, the order parameter is zero for all $\{\mathbf{k}^1,\ldots,\mathbf{k}^g\}$ in a state that is translationally invariant at the microscopic level (i.e., a liquid). On the other hand, it will take at least some nonzero values for any state in which translational invariance is broken at the microscopic level. By using Eq. (2.22) we see that in such a state the order parameter (2.23) becomes

$$\frac{1}{N}\sum_{i=1}^{N}\int_0^1 ds\,\wp_{(i,s)}(\mathbf{k}^1)\wp_{(i,s)}(\mathbf{k}^2)\cdots\wp_{(i,s)}(\mathbf{k}^g)\,\exp\Big(i(\mathbf{k}^1+\mathbf{k}^2+\cdots+\mathbf{k}^g)\cdot\mathbf{b}_i(s)\Big). \qquad (2.27)$$

This order parameter also provides a way to distinguish between nonliquid states that are MTI and those that are not. In the case of an MTI state the summation of complex phase factors will totally destructively interfere unless the wave vectors happen to sum to zero, the random locations of the mean monomer-positions otherwise leading to random phase

cancelations. Hence, the order parameter will only fail to vanish for values of the wave vectors $\{\mathbf{k}^1, \mathbf{k}^2, \ldots, \mathbf{k}^g\}$ that sum to zero. This property of being MTI is a fundamental characteristic of the amorphous solid state. In the non-MTI case total destructive interference is avoided not only if the wave vectors sum to zero but also under other circumstances. Hence, in this case the order parameter will also fail to vanish for certain values of the wave vectors $\{\mathbf{k}^1, \mathbf{k}^2, \ldots, \mathbf{k}^g\}$ that do not sum to zero. To establish this, consider how formula (2.27) transforms under a global translation by an arbitrary vector $\mathbf{a}$:

$$\begin{aligned}
&\frac{1}{N}\sum_{i=1}^{N}\int_0^1 ds\, \wp_{(i,s)}(\mathbf{k}^1)\wp_{(i,s)}(\mathbf{k}^2)\cdots\wp_{(i,s)}(\mathbf{k}^g)\, \exp\Big(i(\mathbf{k}^1+\mathbf{k}^2+\cdots+\mathbf{k}^g)\cdot\mathbf{b}_i(s)\Big) \\
&\quad\to \exp\Big(i(\mathbf{k}^1+\mathbf{k}^2+\cdots+\mathbf{k}^g)\cdot\mathbf{a}\Big) \\
&\quad\times\frac{1}{N}\sum_{i=1}^{N}\int_0^1 ds\, \wp_{(i,s)}(\mathbf{k}^1)\wp_{(i,s)}(\mathbf{k}^2)\cdots\wp_{(i,s)}(\mathbf{k}^g)\, \exp\Big(i(\mathbf{k}^1+\mathbf{k}^2+\cdots+\mathbf{k}^g)\cdot\mathbf{b}_i(s)\Big).
\end{aligned} \tag{2.28}$$

In situations of MTI, this transformation must leave the order parameter unchanged for all vectors $\mathbf{a}$. This enforces the condition that for MTI situations the order parameter must vanish unless $\mathbf{k}^1+\mathbf{k}^2+\cdots+\mathbf{k}^g=\mathbf{0}$, and thus the order parameter becomes

$$\delta_{\mathbf{0},\mathbf{k}^1+\cdots+\mathbf{k}^g}\,\frac{1}{N}\sum_{i=1}^{N}\int_0^1 ds\, \wp_{(i,s)}(\mathbf{k}^1)\cdots\wp_{(i,s)}(\mathbf{k}^g), \tag{2.29}$$

where $\delta_{\mathbf{p}^1,\mathbf{p}^2}$ is a d-dimensional Kronecker δ-factor, which is nonzero only if the d-vectors $\mathbf{p}^1$ and $\mathbf{p}^2$ have all components equal, in which case it has the value unity. In this state, in contrast with the crystalline state, there is no periodicity associated with the spatial pattern of localized monomers, and thus there will not be a collection of reciprocal lattice vectors for which the order parameter fails to vanish. In particular, the order parameter vanishes for $g=1$. (One may equivalently regard the amorphous solid state as the special case of the crystalline state in which the unit cell of the crystal is the entire sample, i.e., a realization of Schrödinger's "aperiodic solid." [59]) The equilibrium amorphous solid state is characterized

by the presence of random (i.e., nonperiodic) static density fluctuations, which spontaneously break translational symmetry at the microscopic (but not the macroscopic) level.

In the non-MTI case, either the transformation (2.28) must leave the order parameter unchanged for a discrete lattice of vectors $\mathbf{a}$, or it need not leave the order parameter unchanged for any value of $\mathbf{a}$. When there is invariance for a discrete lattice of vectors (i.e., in the crystalline state), the order parameter must vanish unless $\mathbf{k}^1 + \mathbf{k}^2 + \cdots + \mathbf{k}^g = \mathbf{G}$, where $\mathbf{G}$ is any reciprocal lattice vector of the crystal (including the zero reciprocal lattice vector). When there is no vector for which the invariance holds (i.e., in the globular state) the order parameter need not vanish on symmetry grounds for any values of the wave vectors $\{\mathbf{k}^1, \ldots, \mathbf{k}^g\}$.

To summarize, the values of the order parameter for the various values of g and the wave vectors $\{\mathbf{k}^1, \mathbf{k}^2, \ldots, \mathbf{k}^g\}$ serve to distinguish between liquid, crystalline, globular and amorphous solid states: for liquid states the order parameter vanishes for $g = 1, 2, 3, \ldots$; for amorphous solid states it vanishes for all wave vectors that do not sum to zero (and thus vanishes for $g = 1$); for crystalline states it only vanishes for wave vectors that fail to sum to a reciprocal lattice vector (and therefore is nonzero for some $\{\mathbf{k}^1, \mathbf{k}^2, \ldots, \mathbf{k}^g\}$, even when $g = 1$); and for globular states it need not vanish in symmetry grounds for any values of $\{\mathbf{k}^1, \mathbf{k}^2, \ldots, \mathbf{k}^g\}$. Table 2.1 summarizes this discussion.

There is a simple generalization of the order parameter, which emerges naturally from the replica theory to be presented in Sec. 2.4. This generalized order parameter probes correlations between the actual state of the system and the state of the system before crosslinking. It differs from Eq. (2.24 by the inclusion of an additional Fourier density factor $\langle \exp(i\mathbf{k}^0 \cdot \mathbf{c}_i(s)) \rangle_{\bar{\chi}}$, defined as the thermal average over the configurations of the system before crosslinking that satisfy the set χ of constraints:

$$\Omega_{\mathbf{k}^0, \mathbf{k}^1, \ldots, \mathbf{k}^g} \equiv \left[\frac{1}{N} \sum_{i=1}^{N} \int_0^1 ds \, \langle \exp\left(i\mathbf{k}^0 \cdot \mathbf{c}_i(s)\right) \rangle_{\bar{\chi}} \langle \exp\left(i\mathbf{k}^1 \cdot \mathbf{c}_i(s)\right) \rangle_{\chi} \cdots \langle \exp\left(i\mathbf{k}^g \cdot \mathbf{c}_i(s)\right) \rangle_{\chi} \right]. \tag{2.30}$$

Table 2.1: Order parameter and states of the system.

State	Density for one monomer	Order parameter $\Omega_{\mathbf{k}^1,\ldots,\mathbf{k}^g}$	Translational symmetries
LIQUID	$\langle e^{i\mathbf{k}\cdot\mathbf{r}_j}\rangle = \delta_{\mathbf{k},\mathbf{0}}$ (all)	$= \delta_{\mathbf{k}^1,\mathbf{0}} \times \cdots \times \delta_{\mathbf{k}^g,\mathbf{0}}$	Macroscopic and Microscopic
AMORPHOUS SOLID	$\langle e^{i\mathbf{k}\cdot\mathbf{r}_j}\rangle \sim e^{i\mathbf{k}\mathbf{c}_j}$ (some) $\langle e^{i\mathbf{k}\cdot\mathbf{r}_j}\rangle = \delta_{\mathbf{k},\mathbf{0}}$ (others)	$\sim \delta_{\mathbf{k}^1+\cdots+\mathbf{k}^g,\mathbf{0}}$	Macroscopic
CRYSTAL	$\langle e^{i\mathbf{k}\cdot\mathbf{r}_j}\rangle \sim e^{i\mathbf{k}\mathbf{c}_j}$	$\sim \delta_{\mathbf{k}^1+\cdots+\mathbf{k}^g,\mathbf{G}}$ $\mathbf{G} \in$ reciprocal lattice	Macroscopic only by lattice vectors
GLOBULE (with density $\rho(\mathbf{r})$)	$\langle e^{i\mathbf{k}\cdot\mathbf{r}_j}\rangle \sim e^{i\mathbf{k}\mathbf{c}_j}$ (some) $\langle e^{i\mathbf{k}\cdot\mathbf{r}_j}\rangle = \delta_{\mathbf{k},\mathbf{0}}$ (others)	$= S(\mathbf{k}^1 + \cdots + \mathbf{k}^g)$ $(S(\mathbf{k}) \equiv \int \mathbf{dk}\, \mathbf{e}^{\mathbf{ik}\cdot\mathbf{r}}\rho(\mathbf{r}))$	None

This expression clearly reduces to the order parameter of Eq. (2.24) in the particular case $\mathbf{k}^0 = \mathbf{0}$. The distinction between the definitions of $\langle\cdots\rangle_{\bar{\chi}}$ and $\langle\cdots\rangle_{\chi}$ is only relevant for situations in which alterations other than crosslinking are made to the system after crosslinking.

2.3.2 A simple idealization: generalized Einstein model

To illustrate the general properties of the order parameter, and to motivate the specific hypothesis for the form of the order parameter described in Sec. 2.3.3 and applied in Sec. 2.6, we examine a simple caricature of the amorphous solid state. We refer to this caricature as a generalized Einstein model, by analogy with the Einstein model of a crystalline solid adopted for the computation of the specific heat, in which it is assumed that every atom is independently localized by an identical harmonic potential [60]. In the context of amorphous solidification, the caricature is obtained by asserting that a fraction $(1-q)$ of the monomers

(the so-called sol fraction) are delocalized, with each monomer (i,s) of the remaining fraction q (the so-called gel fraction) being localized near a random mean position $\mathbf{b}_i(s)$, its location exhibiting thermal fluctuations about that mean position. We emphasize that our usage of the terms gel and sol in this chapter refers solely to the issue of whether or not a monomer is localized. Ultimately, however, we shall see that the gel fraction defined in this way coincides with the more common architectural definition, in the sense that localization will be seen to occur only for crosslink densities for which the network spans the entire system. It is further asserted that the probability distribution for the fluctuations in location of each localized monomer (i,s) about its mean position is gaussian and isotropic, and characterized by an inverse square localization length $\tau_i(s) = 1/\xi_i(s)^2$. This assumption is physically reasonable, for example, if one considers the thermal fluctuations of a monomer in the near parabolic region around the bottom of a local minimum of the potential that the rest of the system exerts on the particular monomer. Then, for the localized monomer (i,s), the Fourier-transformed density would be given by

$$\langle \exp\left(i\mathbf{k}\cdot\mathbf{c}_i(s)\right)\rangle_\chi = \exp\left(i\mathbf{k}\cdot\mathbf{b}_i(s)\right)\exp\left(-k^2/2\tau_i(s)\right), \tag{2.31}$$

so that the order parameter (prior to disorder-averaging) becomes

$$(1-q)\prod_{a=1}^{g}\delta^{(d)}_{\mathbf{0},\mathbf{k}^a} + \frac{1}{N}\sum_{i=1}^{N}\int_0^1 ds\,\exp\Big(i\mathbf{b}_i(s)\cdot\sum_{a=1}^{g}\mathbf{k}^a\Big)\,\exp\Big(-\sum_{a=1}^{g}|\mathbf{k}^a|^2/2\tau_i(s)\Big), \tag{2.32}$$

where it is understood that the summation in the second term only includes localized monomers.

To obtain the disorder-average of the order parameter we make the natural assumption that in the disorder ensemble the random variables $\mathbf{b}_i(s)$ and $\tau_i(s)$ are uncorrelated. Furthermore, we assume that $\mathbf{b}_i(s)$ is uniformly distributed over the volume V, and denote by $p(\tau)$ the probability distribution for the inverse square localization length. In this case the order parameter becomes

$$(1-q)\prod_{a=1}^{g}\delta^{(d)}_{\mathbf{0},\mathbf{k}^a} + q\,\delta^{(d)}_{\mathbf{0},\sum_{a=1}^{g}\mathbf{k}^a}\int_0^\infty d\tau\,p(\tau)\exp\Big(-\sum_{a=1}^{g}|\mathbf{k}^a|^2/2\tau\Big). \tag{2.33}$$

The first term accounts for the delocalized monomers, and the second term accounts for the localized monomers. If $q = 0$ then the state described by this order parameter is the liquid state. If $q \neq 0$ then it describes an amorphous solid state. The Kronecker δ factor in front of the second term is a reflection of the MTI that characterizes the amorphous solid state. This hypothesis is a refinement of the gaussian hypothesis used in a number of contexts [61]. It is useful to observe that the gel fraction q can be extracted from the order parameter Eq. (2.23) by taking the limit of the order parameter as $\{\mathbf{k}^1, \ldots, \mathbf{k}^g\} \to \{\mathbf{0}, \ldots, \mathbf{0}\}$ through a sequence for which $\sum_{a=1}^{g} \mathbf{k}^a = \mathbf{0}$. Let us observe here that even if we did not *assume* $p(\tau)$ to be a probability distribution (and therefore a non-negative normalized function), the normalization condition for $p(\tau)$ would emerge simply from the condition that the order parameter is unity at the origin.

2.3.3 Replica order-parameter hypothesis: gel fraction and distribution of localization lengths

Having discussed the physical order parameter capable of diagnosing equilibrium amorphous solidification, we now anticipate the development of the replica approach by describing the particular form that we shall hypothesize for the replica order parameter, i.e., the order parameter that emerges from the application of the replica technique and represents, in the replica approach, the physical order parameter discussed in the previous two subsections of the present section. This form is motivated by the general characterization of amorphous solidification in terms of the gel fraction q and the distribution of inverse square localization lengths $p(\tau)$ given in Sec. 2.3.2. Below, in Sec. 2.6, we shall show that within the context of a certain model of randomly crosslinked macromolecular networks the form that we now hypothesize for the replica order parameter is sufficiently broad to allow us to provide an exact and physically appealing mean-field–level description of the transition to and properties of the equilibrium amorphous solid state of randomly crosslinked macromolecular networks.

As we shall see in detail in Sec. 2.4, the replica representation of the physical order parameter is given by

$$\Big\langle \frac{1}{N} \sum_{i=1}^{N} \int_0^1 ds \, \exp\big(i \sum_{\alpha=0}^{n} \mathbf{k}^\alpha \cdot \mathbf{c}_i^\alpha(s)\big) \Big\rangle_{n+1}^{\mathrm{P}}, \tag{2.34}$$

in the replica limit, $n \to 0$. As we shall also see there, $\langle \cdots \rangle_{n+1}^{\mathrm{P}}$ denotes an expectation value for a pure (i.e., quenched-disorder–free) system of $n+1$ coupled replicas of the original macromolecular system. Note the inclusion of degrees of freedom associated with a replica labeled by $\alpha = 0$. Strictly speaking, only the special case of $\mathbf{k}^0 = \mathbf{0}$ in Eq. (2.34) is necessary to obtain the order parameter of Eq. (2.24). However, the keeping of nonzero values of $\mathbf{k}^0$ has two advantages: (i) it allows to probe correlations between the state of the system before crosslinking and the present state of the system via the generalized order parameter of Eq. (2.30), and (ii) the general form of Eq. (2.34) with $\mathbf{k}^0$ not necessarily zero emerges naturally from the replica theory.

For the sake of notational convenience we introduce hatted vectors (e.g., $\hat{k}$ or $\hat{c}$), which are $(n+1)d$-component vectors comprising $(n+1)$-fold replicated sets of d-component vectors (e.g., the wave vectors $\{\mathbf{k}^0, \mathbf{k}^1, \ldots, \mathbf{k}^n\}$ or the position vectors $\{\mathbf{c}^0, \mathbf{c}^1, \ldots, \mathbf{c}^n\}$). We define the extended scalar product $\hat{k} \cdot \hat{c}$ by $\hat{k} \cdot \hat{c} \equiv \sum_{\alpha=0}^{n} \mathbf{k}^\alpha \cdot \mathbf{c}^\alpha$, having the special cases $\hat{k}^2 \equiv \hat{k} \cdot \hat{k}$ and $\hat{c}^2 \equiv \hat{c} \cdot \hat{c}$. In terms of this notation, the order parameter becomes

$$\Big\langle \frac{1}{N} \sum_{i=1}^{N} \int_0^1 ds \, \exp\big(i\hat{k} \cdot \hat{c}_i(s)\big) \Big\rangle_{n+1}^{\mathrm{P}}. \tag{2.35}$$

By translating formula (2.33) into the replica language, through the use of Eq. (2.59), we are led to the assumption that the replica order parameter takes on values expressible in the following form:

$$(1-q)\, \delta_{\tilde{k},\hat{0}}^{(nd+d)} + q\, \delta_{\tilde{\mathbf{k}},\mathbf{0}}^{(d)} \int_0^\infty d\tau \, p(\tau) \, \exp(-\hat{k}^2/2\tau), \tag{2.36}$$

where $\tilde{\mathbf{k}} \equiv \sum_{\alpha=0}^{n} \mathbf{k}^\alpha$ is a permutation-invariant d-vector built by summing the elements of the replicated vector $\hat{k}$, and $\delta_{\hat{p},\hat{q}}^{(nd+d)} \equiv \prod_{\alpha=0}^{n} \delta_{\mathbf{p}^\alpha,\mathbf{q}^\alpha}^{(d)}$. Thus, we parametrize the order parameter in

terms of the gel fraction q and the distribution of (inverse square) localization lengths $p(\tau)$ [62]. This parametrization is severely restrictive mathematically but physically plausible. In order for $p(\tau)$ to be interpreted as a probability distribution it must be non-negative. This condition is not imposed *a priori*, but emerges from the stationarity condition. The ranging of τ only over positive values reflects the fact that inverse square localization lengths are positive. Moreover, delocalized monomers are accounted for by the term proportional to $(1-q)$, so that $p(\tau)$ must not contain a Dirac δ-function–like piece at $\tau = 0$. The factor $\delta^{(d)}_{\tilde{\mathbf{k}},\mathbf{0}}$ incorporates the MTI property into the hypothesized form. It should be emphasized that the hypothesized form is invariant under the permutation of the replicated vectors $\{\mathbf{k}^0, \mathbf{k}^1, \ldots, \mathbf{k}^n\}$, which is a manifestation of its replica-symmetric character.

2.3.4 Symmetry properties of the order parameter hypothesis

We now state explicitly the symmetry properties of the order parameter hypothesis (2.36) that we shall use throughout the remainder of this chapter. As we shall see in Sec. 2.5, the free energy functional of the replica theory turns out to have the following symmetries: (i) *independent* translations or rotation of the replicas, and (ii) permutations of the replicas. In the liquid state the order parameter retains all these symmetries. In the amorphous solid state the symmetry of the order parameter is reduced. By invoking our hypothesis for the order parameter we are assuming that in the amorphous solid state the residual symmetries become: (i′) *common* translations and rotations of the replicas, and (ii) permutations of the replicas. In other words, in the transition to the amorphous solid state the symmetry of independent translations and rotations of the replicas is spontaneously broken. As a consequence of the spontaneous breaking of certain symmetries there is a manifold of symmetry-related values of the order parameter that describe the solid state.

In this chapter we have restricted our attention to order-parameter hypotheses that are invariant under the permutations of all $(n+1)$ replicas (i.e., that are replica-symmetric).

This mathematical restriction is equivalent to the physical condition that, upon amorphous solidification, the (overwhelming fraction of the) system must exhibit one member of a unique family of equilibrium states (i.e., statistical arrangements of the macromolecules), this unique family of states being related by global translations and rotations. While the occurrence of a unique family would not be an unreasonable consequence of crosslinking, especially in view of our exclusion of the anholonomic constraints that crosslinking introduces into the physical system, one might anticipate that crosslinking would cause the full physical system to exhibit many families of states (i.e., there would be states that are not related by global translations and rotations). Such an occurrence would be signaled by an order parameter that is no longer invariant under permutations of the replicas (i.e., for which replica symmetry is spontaneously broken). For discussions of these matters, see Ref. [56] as well as Refs. [30].

It must, however, be emphasized that, regardless of the issue of the intactness of permutation symmetry, the primary physical phenomenon at hand in the formation of the equilibrium amorphous solid state is the spontaneous breaking of translation symmetry (viz., the spontaneous random localization of macromolecules). The issue of replica-symmetry–breaking is not an alternative to translational-symmetry–breaking: it simply addresses whether or not a system with given realization of crosslinking possesses one or many un–symmetry-related ways for the macromolecules to be randomly localized. To allow for the possibility that replica-symmetry–breaking accompanies translational-symmetry–breaking is to explore a more general class of behaviors of the system.

2.3.5 Connection with scattering experiments

The order parameter that we have been addressing in the present section is, in principle, accessible via neutron scattering experiments [64, 65], at least for the case $g = 2$. In fact,

the elastic part of the differential scattering cross-section (per atom) can be written as

$$\frac{1}{N}\frac{d^2\sigma}{d\Omega} = S^{\rm el}(\mathbf{q}) = \lim_{t\to\infty}\Big(\frac{|b_{\rm coh}|^2}{N}\Big\langle\sum_{i,i'=1}^{N}\int_0^1 ds\,ds'\exp\big(-i\mathbf{q}\cdot\mathbf{c}_i(s;0)\big)\exp\big(i\mathbf{q}\cdot\mathbf{c}_{i'}(s';t)\big)\Big\rangle + \frac{|b_{\rm incoh}|^2}{N}\Big\langle\sum_{i=1}^{N}\int_0^1 ds\exp\big(-i\mathbf{q}\cdot\mathbf{c}_i(s;0)\big)\exp\big(i\mathbf{q}\cdot\mathbf{c}_i(s;t)\big)\Big\rangle\Big), \quad (2.37)$$

where $b_{\rm coh}$ is the average scattering length, $b_{\rm incoh}$ is the variance of the scattering length, $\mathbf{c}_i(s;t)$ is the position of monomer s on macromolecule i at time t, and $\langle\cdots\rangle$ indicates a time-dependent equilibrium expectation value. The second part on the right hand side is the *incoherent* contribution, and can be extracted in some cases. By using the fact that the connected correlators vanish for $t\to\infty$, we see that this second part reduces to

$$\frac{|b_{\rm incoh}|^2}{N}\sum_{i=1}^{N}\int_0^1 ds\Big\langle\exp\big(-i\mathbf{q}\cdot\mathbf{c}_i(s)\big)\Big\rangle\Big\langle\exp\big(i\mathbf{q}\cdot\mathbf{c}_i(s)\big)\Big\rangle, \quad (2.38)$$

i.e., formula (2.23) evaluated for the special case of $\{\mathbf{k}^1,\mathbf{k}^2,\ldots,\mathbf{k}^g\} = \{-\mathbf{q},\mathbf{q},\mathbf{0},\ldots,\mathbf{0}\}$. Thus, the order parameter for $g=2$ is proportional to the incoherent part of the elastic neutron scattering cross-section.

Oeser *et al.* [66] have measured the time persistent part of the incoherent scattering function in neutron-spin-echo experiments. They fit their data, which are taken in the high crosslinking limit, to a gaussian in wave vector space characterized by a typical length scale l, which turns out to be comparable to the radius of gyration. A potential critique of neutron scattering experiments results from the available time scales, of order 10 ns, which make it difficult to extrapolate to infinite time in order to extract the time-persistent part of the autocorrelation. This may not be a severe problem in the high crosslinking limit, in which one expects rather small time scales associated with small distances between crosslinks. However, it may become prohibitive for weakly crosslinked systems, which barely sustain an infinite cluster.

Pulsed field gradient NMR (see, e.g., Ref. [67]) is another experimental technique for measuring the intermediate-time incoherent scattering function with a spatial and temporal

resolution that is complementary to neutron scattering experiments. Typical time scales in NMR experiments are of order milliseconds, and length scales are restricted to be greater than 10 nm. An example of such measurements are the detection of spatial fluctuations in swollen networks in Ref. [68].

Another technique that may be useful to probe the order parameter is dynamic light scattering (DLS). In this technique, light is scattered from the sample, and the scattered intensities at different times and for a fixed scattering wave-vector $\mathbf{q}$ are correlated [69]. From those correlations it is possible to obtain the normalized intermediate scattering function $f(\mathbf{q}, t)$, where t is the time delay. [$f(\mathbf{q}, t)$ is proportional to the second term in the right hand side of Eq. (2.37).] In one experiment with brownian particles trapped in a polyacrylamide gel [70], intensity correlations for time intervals of microseconds to tens of seconds were measured, for scattering wave-vectors between 0.01 and 0.03 nm^{-1}. In this case, by analyzing the long time limit of $f(\mathbf{q}, t)$, localized particles were detected and r.m.s. localization lengths of between 6 and 35 nm were measured for them. The authors claim that the results of the experiment are not compatible with the existence of a unique localization length, and that a distribution of localization lengths is necessary to fit the data, although they are not able to determine it.

2.4 Replica approach for disorder-averaged quantities

Having prepared the way by discussing the model and the construction of a suitable probability distribution for the disorder, and defining an order parameter capable of diagnosing the possible states of the system, we now turn to the computation of disorder-averages of important physical quantities, such as the free energy, order parameter and certain correlators. A direct assault on this task, as it stands, seems prohibitively difficult, but it can be rendered tractable by the use of the replica technique [32], pioneered in the context of

macromolecular networks by Deam and Edwards [20]. In this approach, we do not consider just the original degrees of freedom but, instead, a system comprising $n+1$ interacting copies (i.e., replicas) of it that will be labeled by the superscript $\alpha = 0, 1, \ldots, n$. In this new system, the quenched randomness disappears from the formulation, at the price of introducing an inter-replica interaction.

Let us first consider, for example, the naive free energy $\bar{f}$. Within the framework of the replica technique, its disorder average is obtained from

$$\bar{f} = \frac{-1}{ndN}[\log \bar{Z}] = \lim_{n\to 0} \frac{-1}{ndN} \log [\bar{Z}^n], \tag{2.39}$$

where $\bar{Z}^n$ is interpreted as the partition function for a system comprised of n identical copies (or *replicas*) of the original system [32].

For the Deam-Edwards distribution, the disorder average of Eq. (2.39) takes the form

$$[\bar{Z}^n] = \mathcal{C} \sum_{\chi} \frac{1}{M_\chi!} \left(\frac{\mu^2 V}{2N}\right)^{M_\chi} \tilde{Z}(\chi) \bar{Z}^n(\chi), \tag{2.40}$$

where M_χ is the number of crosslinks for the disorder realization χ, and $\mathcal{C}$ is a normalization constant:

$$\mathcal{C}^{-1} = \left\langle \exp\{\frac{\mu^2 V}{2N} \sum_{i,j=1}^{N} \int_0^1 ds \int_0^1 dt\, \delta\left(\mathbf{c}_i(s) - \mathbf{c}_j(t)\right)\} \right\rangle_1^{\mathrm{E}}. \tag{2.41}$$

As anticipated before, the presence of the $\tilde{Z}$ factor makes it necessary to introduce an additional replica, besides the n replicas associated with the n factors of $\bar{Z}$. The additional replica, labeled by $\alpha = 0$, represents the degrees of freedom of the original system before crosslinking, or, equivalently, describes the crosslink distribution. Consequently, any changes in the system *after* the permanent constraints have been created will affect replicas $\alpha = 1, \ldots, n$, but not replica $\alpha = 0$ [20].

2.4.1 Computing $[\bar{Z}^n]$ explicitly: particle density variables

A more explicit expression for $[\bar{Z}^n]$ can be obtained by combining Eqs. (2.9), (2.10) , (2.41) and (2.40):

$$\begin{aligned}[\bar{Z}^n] &= \frac{\int \mathcal{D}\mathbf{c}^0 \cdots \mathcal{D}\mathbf{c}^n \;\; \mathrm{e}^{-\sum_{\alpha=0}^n H^\alpha} \sum_\chi \frac{1}{M_\chi!} \left(\frac{\mu^2 V}{2N}\right)^{M_\chi} \prod_{\alpha=0}^n \prod_{e=1}^{M_\chi} \delta\left(\mathbf{c}_{i_e}^\alpha(s_e) - \mathbf{c}_{i'_e}^\alpha(s'_e)\right)}{\int \mathcal{D}\mathbf{c} \;\; \exp\{ -H + \frac{\mu^2 V}{2N} \sum_{i,j=1}^N \int_0^1 ds \int_0^1 dt \, \delta\left(\mathbf{c}_i(s) - \mathbf{c}_j(t)\right) \}} \\ &= \frac{\int \mathcal{D}\hat{c} \;\; \exp\left\{ -\sum_{\alpha=0}^n H^\alpha + \frac{\mu^2 V}{2N} \sum_{i,j=1}^N \int_0^1 ds \int_0^1 dt \, \delta\left(\hat{c}_i(s) - \hat{c}_j(t)\right) \right\}}{\int \mathcal{D}\mathbf{c} \;\; \exp\{ -H + \frac{\mu^2 V}{2N} \sum_{i,j=1}^N \int_0^1 ds \int_0^1 dt \, \delta\left(\mathbf{c}_i(s) - \mathbf{c}_j(t)\right) \}} \end{aligned} \tag{2.42}$$

Here quantities with superscripts 0, α, and n are respectively associated with replicas 0, α, and n; and $\int \mathcal{D}\hat{c}$ is equivalent to $\int \mathcal{D}\mathbf{c}^0 \cdots \mathcal{D}\mathbf{c}^n$. At this point it is convenient to exploit the translation invariance of the above expression by switching from coordinates representing the polymer configurations $\mathbf{c}_i(s)$ and $\hat{c}_i(s)$ to variables representing Fourier transformed monomer densities, defined by

$$Q_{\mathbf{p}}^\alpha = \frac{1}{N} \sum_{i=1}^N \int_0^1 ds \; \mathrm{e}^{i\mathbf{p}\cdot\mathbf{c}_i^\alpha(s)}, \tag{2.43}$$

$$Q_{\hat{q}} = \frac{1}{N} \sum_{i=1}^N \int_0^1 ds \; \mathrm{e}^{i\hat{q}\cdot\hat{c}_i(s)}. \tag{2.44}$$

We start by using the decompositions of the Dirac delta function in terms of plane waves, given by

$$\delta(\mathbf{c}) = \frac{1}{V} \sum_{\mathbf{p}} \exp\left(i\mathbf{p}\cdot\mathbf{c}\right) \tag{2.45}$$

in d-dimensional space and by

$$\delta(\hat{c}) = \frac{1}{V^{1+n}} \sum_{\hat{q}} \exp\left(i\hat{q}\cdot\hat{c}\right) \tag{2.46}$$

in replicated space, which allow us to write

$$\frac{1}{2N} \sum_{i,j=1}^N \int_0^1 ds \int_0^1 dt \, \delta\left(\mathbf{c}_i^\alpha(s) - \mathbf{c}_j^\alpha(t)\right) = \frac{N}{2} \sum_{\mathbf{p}} |Q_{\mathbf{p}}^\alpha|^2 \tag{2.47}$$

$$\frac{1}{2N} \sum_{i,j=1}^N \int_0^1 ds \int_0^1 dt \, \delta\left(\hat{c}_i(s) - \hat{c}_j(t)\right) = \frac{N}{2} \sum_{\hat{q}} |Q_{\hat{q}}|^2. \tag{2.48}$$

Throughout this calculation we employ periodic boundary conditions in real space, and this determines the set $r^{\rm u}$ of allowed d-dimensional wave vectors $\mathbf{p}$ that enter the sums in the right hand sides of Eqs. (2.45) and (2.47). The set $R^{\rm u}$ of allowed replicated wave vectors $\hat{q}$ in the right hand sides of Eqs. (2.46) and (2.48) is obtained by simply taking all combinations of $(n+1)$ allowed d-dimensional wave vectors. Here the superscript u stands for "unstrained system". In Chap. 4, when we discuss deformations of the system, these deformations will directly change the boundary conditions in real space, and consequently the set of allowed wave vectors.

We now introduce a particularly convenient decomposition of the terms in a summation over a replicated wave vector $\hat{q}$, such as that appearing in Eq. (2.48). Consider a generic replicated vector $\hat{q} \equiv \{\mathbf{q}^0, \mathbf{q}^1, \ldots, \mathbf{q}^n\}$. Of the $n+1$ component d-vectors, establish the number h that are nonzero d-vectors. Then we say that the replicated vector $\hat{q}$ resides in the h-replica sector. For example, if $\hat{q} \equiv \{\mathbf{0}, \mathbf{0}, \mathbf{q}^2, \mathbf{0}, \mathbf{q}^4, \mathbf{0}, \mathbf{0}, \ldots, \mathbf{0}\}$ with $\mathbf{q}^2$ and $\mathbf{q}^4$ both nonzero d-vectors then $h = 2$, and we say that $\hat{q}$ resides in the 2-replica sector. The decomposition that we are introducing amounts to separating from the summation over $\hat{q}$ the term in the 0-replica sector (i.e., the term corresponding to $\hat{q} = \hat{0} \equiv \{\mathbf{0}, \mathbf{0}, \ldots, \mathbf{0}\}$), and also separating the terms in the 1-replica sector (i.e., terms corresponding to those values of $\hat{q}$ in which exactly one d-vector is nonzero). Thus we shall decompose summations over $\hat{q}$ into contributions from: (i) the 0-replica sector; (ii) the 1-replica sector; and (iii) the remainder, which we refer to as the higher-replica sector, and which contains the h-replica sectors for $2 \leq h \leq n+1$. Schematically, the decomposition can be expressed in the following way for a generic quantity $\mathcal{Q}_{\hat{q}}$:

$$\sum_{\hat{q}} \mathcal{Q}_{\hat{q}} \equiv \mathcal{Q}_{\hat{0}} + \sum_{\alpha=0}^{n} \sum_{\mathbf{p}}{}' \mathcal{Q}_{\mathbf{p}}^{\alpha} + \overline{\sum_{\hat{k}}} \mathcal{Q}_{\hat{k}} \tag{2.49}$$

where $\sum_{\mathbf{p}}'$ denotes a summation over all values of the d-vector $\mathbf{p}$ except that the $\mathbf{p} = \mathbf{0}$ term is omitted (i.e., it comprises terms in the 1-replica sector), $\mathcal{Q}_{\mathbf{p}}^{\alpha}$ denotes the value of $\mathcal{Q}_{\hat{p}}$ when $\hat{p}$ is in the 1-replica sector (i.e., the $\alpha^{\rm th}$ d-vector entry in $\hat{p}$ is $\mathbf{p} \neq \mathbf{0}$, all other entries being

zero), and $\overline{\sum}_{\hat{k}}$ denotes a summation over replicated vectors $\hat{k}$ residing in the higher replica sector. An alternative form for the decomposition reads

$$\sum_{\hat{q}} \mathcal{Q}_{\hat{q}} \equiv \mathcal{Q}_{\hat{0}} + \tilde{\sum}_{\hat{p}} \mathcal{Q}_{\hat{p}} + \overline{\sum}_{\hat{k}} \mathcal{Q}_{\hat{k}}, \tag{2.50}$$

where the symbol $\tilde{\sum}_{\hat{p}}$ denotes a sum over replicated wave vectors in the one replica sector. With a view to subsequent decoupling transformations, it is useful to use the Fourier representations of the Dirac δ-functions and the replica-sector decomposition in order to re-express the Dirac δ-function interactions, i.e., the non-Wiener measure terms that couple the replicated degrees of freedom. Thus, the delta-function interaction terms that were expressed as a function of densities in Eqs. (2.47) and (2.48) can be written as follows

$$\begin{aligned} \frac{N}{2} \sum_{\hat{q}} |Q_{\hat{q}}|^2 &= \frac{N}{2} + \frac{N}{2} \sum_{\alpha=0}^{n} \sum_{\mathbf{p}}{}' |Q^{\alpha}_{\mathbf{p}}|^2 + \frac{N}{2} \overline{\sum}_{\hat{k}} |Q_{\hat{q}}|^2 \\ &= \frac{N}{2} + \frac{N}{2} \sum_{\alpha=0}^{n} \sum_{\mathbf{p}}{}^{\dagger} |Q^{\alpha}_{\mathbf{p}}|^2 + N \overline{\sum}_{\hat{k}}{}^{\dagger} |Q_{\hat{q}}|^2, \end{aligned} \tag{2.51}$$

$$\begin{aligned} \frac{N}{2} \sum_{\alpha=0}^{n} \sum_{\mathbf{p}} |Q^{\alpha}_{\mathbf{p}}|^2 &= (n+1)\frac{N}{2} + \frac{N}{2} \sum_{\alpha=0}^{n} \sum_{\mathbf{p}}{}' |Q^{\alpha}_{\mathbf{p}}|^2 \\ &= (n+1)\frac{N}{2} + N \sum_{\alpha=0}^{n} \sum_{\mathbf{p}}{}^{\dagger} |Q^{\alpha}_{\mathbf{p}}|^2. \end{aligned} \tag{2.52}$$

For each of the left hand sides we have performed two steps. In the first step we performed the replica-sector decomposition, according to Eq. (2.49). In the second step, we have recognized that the summands in the summations over wave vectors of the second step are even functions of the relevant wave vector. Furthermore, none of the summations includes a zero wave vector. Thus, in each case the summation can be restricted to half of the relevant wave vector space, provided a factor of two is included to compensate. To represent this, we have introduce the notation $\sum^{\dagger}_{\mathbf{k}}$ to denote $\sum'_{\mathbf{k}}$ but with $\mathbf{k}$ restricted to the half space via the additional condition $\mathbf{k} \cdot \mathbf{n} > 0$ for a suitable unit d-vector $\mathbf{n}$, and $\overline{\sum}^{\dagger}_{\hat{k}}$ to denote $\overline{\sum}_{\hat{k}}$ but with $\hat{k}$ restricted to the half space via the additional condition $\hat{k} \cdot \hat{n} > 0$ for a suitable unit $(n+1)d$-vector $\hat{n}$. The virtue of this procedure is that in our subsequent development it will enable us to avoid the introduction of kinematically non-independent fields.

Using the decompositions just introduced to rewrite in terms of Fourier transformed monomer densities the delta-functions appearing in the expression of Eq. (2.42) for $[\bar{Z}^n]$ we obtain,

$$[\bar{Z}^n] = \frac{\mathrm{e}^{-Nn\phi} \int \mathcal{D}\hat{c} \;\; \exp\left\{ -\frac{1}{2}\sum_{i=1}^{N} \int_0^1 ds \left|\frac{d\hat{c}_i(s)}{ds}\right|^2 - N\tilde{\lambda}_n^2 \frac{N}{V} \tilde{\sum}_{\hat{p}}^{\dagger} |Q_{\hat{p}}|^2 + N\frac{\mu^2}{V^n} \overline{\sum}_{\hat{k}}^{\dagger} |Q_{\hat{k}}|^2 \right\}}{\int \mathcal{D}\mathbf{c} \;\; \exp\left\{ -\frac{1}{2}\sum_{i=1}^{N} \int_0^1 ds \left|\frac{d\mathbf{c}_i(s)}{ds}\right|^2 - N\tilde{\lambda}_0^2 \frac{N}{V} \sum_{\mathbf{p}}^{\dagger} |Q_{\mathbf{p}}|^2 \right\}}. \quad (2.53)$$

Here we have introduced the effective excluded-volume parameter

$$\tilde{\lambda}_n^2 \equiv \lambda^2 - \frac{\mu^2 V}{N V^n}, \quad (2.54)$$

i.e., the bare excluded-volume parameter λ^2 renormalized to a smaller value by a correction term proportional to the crosslink density parameter μ^2. The theory to be presented here is only valid in the regime in which this parameter is positive,

$$\tilde{\lambda}_0^2 > 0 \quad (2.55)$$

or, equivalently, in the regime

$$0 \leq \mu^2 < \lambda^2 \frac{N}{V}. \quad (2.56)$$

A negative value of $\tilde{\lambda}_n^2$ seems to be associated with an instability towards a collapse of the system into a high density condensate in real space, although the simple model we are studying is probably too crude to handle that regime. On the other hand, a positive value of $\tilde{\lambda}_n^2$ disfavors any configuration with nonzero values of $Q_{\mathbf{p}}^{\alpha}$, and therefore favors MTI.

The constant $\phi \equiv \frac{N}{2V}\lambda^2 + \frac{\mu^2}{2}\log V + \mathcal{O}(n)$ arises from terms in the 0-replica sector, and plays no further role in the theory.

2.4.2 Computing the order parameter explicitly

Having obtained a more explicit expression for $[\bar{Z}^n]$, it is instructive to do the same with the order parameter. The order parameter is a sum of terms of the form $[\langle \mathcal{O}_0 \rangle_\chi \cdots \langle \mathcal{O}_g \rangle_\chi]$, i.e., disorder averages of products of thermal averages of observables $\mathcal{O}_i$, $i = 0, \ldots, g$. We

assume here that the system has not been modified after crosslinking, and therefore drop the distinction between $\langle\cdots\rangle_{\bar{\chi}}$ and $\langle\cdots\rangle_{\chi}$; the extension to the general case is straightforward. Since $\langle 1\rangle_{\chi} = 1$ for any disorder realization χ, it is clear that

$$\begin{aligned}
[\langle\mathcal{O}_0\rangle_{\chi}\cdots\langle\mathcal{O}_g\rangle_{\chi}] &= \lim_{n\to 0}\left[\langle\mathcal{O}_0\rangle_{\chi}\cdots\langle\mathcal{O}_g\rangle_{\chi}\langle 1_{g+1}\rangle_{\chi}\cdots\langle 1_n\rangle_{\chi}\right], \\
&= \lim_{n\to 0}\left[\frac{\int\mathcal{D}\mathbf{c}_0 \mathrm{e}^{-H^0}\Delta_0(\chi)\mathcal{O}_0}{\int\mathcal{D}\mathbf{c}_0 \mathrm{e}^{-H^0}\Delta_0(\chi)}\cdots\frac{\int\mathcal{D}\mathbf{c}_g \mathrm{e}^{-H^g}\Delta_g(\chi)\mathcal{O}_g}{\int\mathcal{D}\mathbf{c}_g \mathrm{e}^{-H^g}\Delta_g(\chi)}\right. \\
&\qquad \left.\times\frac{\int\mathcal{D}\mathbf{c}_{g+1} \mathrm{e}^{-H^{g+1}}\Delta_{g+1}(\chi)}{\int\mathcal{D}\mathbf{c}_{g+1} \mathrm{e}^{-H^{g+1}}\Delta_{g+1}(\chi)}\cdots\frac{\int\mathcal{D}\mathbf{c}_n \mathrm{e}^{-H^n}\Delta_n(\chi)}{\int\mathcal{D}\mathbf{c}_n \mathrm{e}^{-H^n}\Delta_n(\chi)}\right] \\
&= \lim_{n\to 0}\left[\int\mathcal{D}\mathbf{c}_0 \mathrm{e}^{-H^0}\Delta_0(\chi)\mathcal{O}_0\cdots\int\mathcal{D}\mathbf{c}_g \mathrm{e}^{-H^g}\Delta_g(\chi)\mathcal{O}_g\right. \\
&\qquad \left.\times\int\mathcal{D}\mathbf{c}_{g+1} \mathrm{e}^{-H^{g+1}}\Delta_{g+1}(\chi)\cdots\int\mathcal{D}\mathbf{c}_n \mathrm{e}^{-H^n}\Delta_n(\chi)\right].
\end{aligned} \tag{2.57}$$

Here we have denoted by $\Delta(\chi)$ a quantity that implements the constraints, i.e., that is nonzero only for those configurations that satisfy the constraints given by χ.

We can perform the disorder average explicitly, thus obtaining an expression analogous to Eq. (2.42) (when computing $\Omega_{\mathbf{k}^0,\cdots,\mathbf{k}^g}$ in the replica approach, both here and later, we choose $\hat{l}$ so that $\mathbf{l}^{\alpha} = \mathbf{k}^{\alpha}$ for $\alpha = 0,\cdots,g$ and $\mathbf{l}^{\alpha} = \mathbf{0}$ for $\alpha = g+1,\cdots,n$ [71]),

$$\begin{aligned}
\Omega_{\mathbf{k}^0,\cdots,\mathbf{k}^g} &= \lim_{n\to 0}\frac{1}{N}\sum_{j=1}^{N}\int_0^1 ds\,\left[\langle e^{i\mathbf{k}^0\cdot\mathbf{c}_j(s)}\rangle_{\chi}\cdots\langle e^{i\mathbf{k}^g\cdot\mathbf{c}_j(s)}\rangle_{\chi}\langle 1_{g+1}\rangle_{\chi}\cdots\langle 1_n\rangle_{\chi}\right] \\
&= \lim_{n\to 0}\frac{1}{N}\sum_{j=1}^{N}\int_0^1 ds\,\left[\prod_{\alpha=0}^{n}\langle e^{i\mathbf{l}^{\alpha}\cdot\mathbf{c}_j(s)}\rangle_{\chi}\right] \\
&= \lim_{n\to 0}\frac{\int\mathcal{D}\mathbf{c}^0\cdots\mathcal{D}\mathbf{c}^n\,\left\{\frac{1}{N}\sum_{j=1}^{N}\int_0^1 ds\;\mathrm{e}^{i\sum_{\alpha=0}^{n}\mathbf{l}^{\alpha}\cdot\mathbf{c}_i^{\alpha}(s)}\right\}\mathrm{e}^{-\sum_{\alpha=0}^{n}H^{\alpha}}}{\int\mathcal{D}\mathbf{c}\;\;\exp\{-H+\frac{\mu^2V}{2N}\sum_{i,j=1}^{N}\int_0^1 ds\int_0^1 dt\,\delta\left(\mathbf{c}_i(s)-\mathbf{c}_j(t)\right)\}} \\
&\qquad\times\sum_{\chi}\frac{1}{M_{\chi}!}\left(\frac{\mu^2V}{2N}\right)^{M_{\chi}}\prod_{\alpha=0}^{n}\prod_{e=1}^{M_{\chi}}\delta\left(\mathbf{c}_{i_e}^{\alpha}(s_e)-\mathbf{c}_{i'_e}^{\alpha}(s'_e)\right) \\
&= \lim_{n\to 0}\frac{\int\mathcal{D}\hat{c}\;Q_{\hat{l}}\;\exp\left\{-\sum_{\alpha=0}^{n}H^{\alpha}+\frac{\mu^2V}{2N}\sum_{i,j=1}^{N}\int_0^1 ds\int_0^1 dt\,\delta\left(\hat{c}_i(s)-\hat{c}_j(t)\right)\right\}}{\int\mathcal{D}\mathbf{c}\;\;\exp\{-H+\frac{\mu^2V}{2N}\sum_{i,j=1}^{N}\int_0^1 ds\int_0^1 dt\,\delta\left(\mathbf{c}_i(s)-\mathbf{c}_j(t)\right)\}}
\end{aligned} \tag{2.58}$$

Clearly, the value of the above expression is unchanged by dividing by $1 = [\langle 1_1\rangle_{\chi}\cdots\langle 1_g\rangle_{\chi}]$.

This leads to

$$\begin{aligned}\Omega_{\mathbf{k}^1,\cdots,\mathbf{k}^g} &= \lim_{n\to 0} \frac{\int \mathcal{D}\hat{c}\; Q_{\hat{l}}\; \exp\Big\{ -\sum_{\alpha=0}^{n} H^{\alpha} + \frac{\mu^2 V}{2N} \sum_{i,j=1}^{N} \int_0^1 ds \int_0^1 dt\, \delta\left(\hat{c}_i(s) - \hat{c}_j(t)\right) \Big\}}{\int \mathcal{D}\hat{c}\;\; \exp\Big\{ -\sum_{\alpha=0}^{n} H^{\alpha} + \frac{\mu^2 V}{2N} \sum_{i,j=1}^{N} \int_0^1 ds \int_0^1 dt\, \delta\left(\hat{c}_i(s) - \hat{c}_j(t)\right) \Big\}}, \\ &= \lim_{n\to 0} \langle Q_{\hat{l}} \rangle_{n+1}^{\mathrm{P}}\,, \end{aligned} \tag{2.59}$$

where $\langle \cdots \rangle_{n+1}^{\mathrm{P}}$ denotes an average for an effective pure (i.e. disorder-free) system of $n+1$ coupled replicas of the original system, defined for a generic observable O by

$$\langle O \rangle_{n+1}^{\mathrm{P}} = \frac{\int \mathcal{D}\hat{c}\;\; O \;\; \exp\Big\{ -\frac{1}{2}\sum_{i=1}^{N} \int_0^1 ds \left| \frac{d\hat{c}_i(s)}{ds} \right|^2 - N\tilde{\lambda}_n^2 \frac{N}{V} \tilde{\sum}_{\hat{p}}^{\dagger} |Q_{\hat{p}}|^2 + N \frac{\mu^2}{V^n} \overline{\sum}_{\hat{k}}^{\dagger} |Q_{\hat{p}}|^2 \Big\}}{\int \mathcal{D}\hat{c}\;\; \exp\Big\{ -\frac{1}{2}\sum_{i=1}^{N} \int_0^1 ds \left| \frac{d\hat{c}_i(s)}{ds} \right|^2 - N\tilde{\lambda}_n^2 \frac{N}{V} \tilde{\sum}_{\hat{p}}^{\dagger} |Q_{\hat{p}}|^2 + N \frac{\mu^2}{V^n} \overline{\sum}_{\hat{k}}^{\dagger} |Q_{\hat{p}}|^2 \Big\}}. \tag{2.60}$$

2.5 Field theory

All the above expressions contain interactions between macromolecules that complicate any analytic treatment. We now decouple those interactions by performing a Hubbard-Stratonovich transformation that eliminates the Fourier transformed density variables $Q_{\hat{k}}$ in favor of stochastic fields $\Omega_{\hat{k}}$ [72]. This strategy has the following virtues. First, the task of summing over the configurations of the system of N replicated macromolecules is reduced to the task of summing over the configurations of a *single* replicated macromolecule. The monomers that constitute this replicated macromolecule remain coupled to each other via the Wiener measure, Eq. (2.3), and by the stochastic field to which they are coupled. Second, the stochastic field itself has a natural physical interpretation: it is related in a direct manner to the order parameter. Third, the expressions in terms of sums over the values of the stochastic field are more readily computable than the formal expressions in terms of sums over polymer configurations that we have been dealing with up to now.

We make use of the formulas:

$$\exp\left(-a\,|w|^2\right) = (a/\pi) \int d(\mathrm{Re}\, z)\; d(\mathrm{Im}\, z)\;\; \exp\left(-a\,|z|^2\right) \exp\left(2ia\,\mathrm{Re}\, z w^*\right), \tag{2.61}$$

$$\exp\left(+a\,|w|^2\right) = (a/\pi) \int d(\mathrm{Re}\, z)\; d(\mathrm{Im}\, z)\;\; \exp\left(-a\,|z|^2\right) \exp\left(2a\,\mathrm{Re}\, z w^*\right), \tag{2.62}$$

where w is an arbitrary complex number, a is a real and positive (but otherwise arbitrary) number, and the integrals are taken over the entire complex z plane. The upper formula can be applied to the terms that come from excluded volume repulsions, which provide contributions with negative prefactors in the exponents in Eq. (2.53); whereas the lower formula can be applied to the term originated in the disorder distribution, which comes with a positive prefactor proportional to μ^2.

By combining Eq. (2.53) with Eqs. (2.61) and (2.62) in the way just outlined, we obtain:

$$[\bar{Z}^n] = \mathcal{N} \int \mathcal{D}\Omega \ \exp\{-ndN\mathcal{F}_n(\{\Omega_{\hat{k}}\})\}, \tag{2.63}$$

where $\mathcal{F}_n(\{\Omega_{\hat{k}}\})$ is a replicated free energy functional and $\mathcal{N}$ is a normalization constant. The symbol $\int\mathcal{D}\Omega$ denotes integration over all possible configurations for the fields $\{\Omega_{\hat{k}}\}$, where the independent set of variables is the set of all the complex-valued $\Omega_{\hat{k}}$ for $\hat{k}$ in the half-space determined by the condition that $\hat{k}\cdot\hat{n}$ be positive for a fixed unit vector $\hat{n}$, and it is always assumed that $\Omega_{-\hat{k}} = \Omega^*_{\hat{k}}$. The free energy functional $\mathcal{F}_n(\{\Omega_{\hat{k}}\})$ has the expression

$$\begin{aligned} nd\mathcal{F}_n(\{\Omega_{\hat{k}}\}) = {} & \tilde{\lambda}_n^2 \frac{N}{V} \tilde{\sum_{\hat{p}}}^{\dagger} |\Omega_{\hat{p}}|^2 + \frac{\mu^2}{V^n} \overline{\sum_{\hat{k}}}^{\dagger} |\Omega_{\hat{k}}|^2 \\ & - \ln \left\langle \exp\left(i\tilde{\lambda}_n^2 \frac{2N}{V} \tilde{\sum_{\hat{p}}}^{\dagger} \mathrm{Re}\, \Omega_{\hat{p}} \rho^*_{\hat{p}} + \frac{2\mu^2}{V^n} \overline{\sum_{\hat{k}}}^{\dagger} \mathrm{Re}\, \Omega_{\hat{k}} \rho^*_{\hat{k}} \right) \right\rangle^W_{n+1}, \end{aligned} \tag{2.64}$$

where the one-macromolecule Fourier transformed density $\rho_{\hat{k}}$ is

$$\rho_{\hat{k}} \equiv \int_0^1 ds \ \mathrm{e}^{i\hat{k}\cdot\hat{c}(s)} \tag{2.65}$$

for a macromolecular configuration $\hat{c}(s)$, and the Wiener replicated average is defined by

$$\langle O \rangle^W_{n+1} \equiv \frac{\int \mathcal{D}\hat{c} \ O \ \exp\left\{ -\frac{1}{2}\int_0^1 ds \left| \frac{d\hat{c}(s)}{ds} \right|^2 \right\}}{\int \mathcal{D}\hat{c} \ \exp\left\{ -\frac{1}{2}\int_0^1 ds \left| \frac{d\hat{c}(s)}{ds} \right|^2 \right\}}. \tag{2.66}$$

We see that indeed the set of Hubbard-Stratonovich transformations has led to the decoupling of the N (replicated) macromolecules from each other, and that in the end we have obtained an expression involving only one macromolecule interacting with the stochastical field $\Omega_{\hat{q}}$.

We can compute the free energy functional $\mathcal{F}_n(\{\Omega_{\hat{k}}\})$ perturbatively, order by order, in powers of $\{\Omega_{\hat{k}}\}$. This perturbative construction of the Landau-Ginzburg-Wilson free energy functional is equivalent to that arising in many other contexts in statistical physics.

The normalization constant $\mathcal{N}$ in Eq. (2.63) is given by the expression

$$\begin{aligned} \mathcal{N} &= \frac{\mathrm{e}^{-Nn\phi}}{\int \mathcal{D}\mathbf{c}\ \exp\{-\frac{1}{2}\sum_{i=1}^{N}\int_0^1 ds \left|\frac{d\mathbf{c}_i(s)}{ds}\right|^2 - N\tilde{\lambda}_0^2\frac{N}{V}\sum_{\mathbf{p}}^{\dagger}|Q_{\mathbf{p}}|^2\}} \\ &= \mathrm{e}^{-Nn\phi}\,\mathcal{C}\int\mathcal{D}\mathbf{c}\ \exp\{-H_1\}. \end{aligned} \tag{2.67}$$

Let us now discuss the symmetry properties of the free energy functional. Under independent translations of all the replicas, i.e., $\mathbf{c}_i^{\alpha} \to \mathbf{c}_i^{\alpha} + \mathbf{a}^{\alpha}$, the replica order parameter, Eq. (2.34), transforms as

$$\Omega_{\hat{k}} \to \Omega'_{\hat{k}} = \mathrm{e}^{i\sum_{\alpha=0}^{n}\mathbf{k}^{\alpha}\cdot\mathbf{a}^{\alpha}}\Omega_{\hat{k}}. \tag{2.68}$$

For later reference, let us calculate the change in the order parameter for the case of small displacements:

$$\delta\Omega_{\hat{k}} \equiv \Omega'_{\hat{k}} - \Omega_{\hat{k}} = i\,\hat{k}\cdot\hat{a}\,\Omega_{\hat{k}} + \mathcal{O}(a^2). \tag{2.69}$$

Under independent rotations of the replicas, defined by $\hat{R}\hat{v} \equiv \{R^0\mathbf{v}^0, \cdots, R^n\mathbf{v}^n\}$ and $\mathbf{c}_i^{\alpha} \to R^{\alpha}\mathbf{c}_i^{\alpha}$, the order parameter transforms as

$$\Omega_{\hat{k}} \to \Omega'_{\hat{k}} = \Omega_{\hat{R}^{-1}\hat{k}}. \tag{2.70}$$

By inserting the transformed order parameter for either of the above operations into the free energy functional Eq. (2.123), we see that in both cases:

$$nd\mathcal{F}_n(\{\Omega'_{\hat{k}}\}) = nd\mathcal{F}_n(\{\Omega_{\hat{k}}\}), \tag{2.71}$$

i.e., that the free energy functional is invariant under *independent* translations and rotations of the replicas. Besides, since both the replicated Wiener average and the sums over replicated wave vectors in Eq. (2.64) are intrinsically replica symmetric, the free energy functional is invariant under permutations of the $n+1$ replicas.

We can now compute the order parameter in terms of sums over the stochastic field, and show the direct relation between the two that was mentioned before. For the computation of the order parameter, besides Eqs. (2.61) and (2.62), we make use of the formulas:

$$iw \exp\left(-a\,|w|^2\right) = (a/\pi) \int d(\mathrm{Re}\, z)\; d(\mathrm{Im}\, z)\; z\; \exp\left(-a\,|z|^2\right) \exp\left(2ia\,\mathrm{Re}\, zw^*\right), \quad (2.72)$$

$$w \exp\left(+a\,|w|^2\right) = (a/\pi) \int d(\mathrm{Re}\, z)\; d(\mathrm{Im}\, z)\; z\; \exp\left(-a\,|z|^2\right) \exp\left(2a\,\mathrm{Re}\, zw^*\right), \quad (2.73)$$

where the symbols have the same meaning as before. A calculation similar to the one for the partition function gives rise to the expressions [72]

$$\langle Q^{\alpha}_{\mathbf{k}} \rangle^{\mathrm{P}}_{n+1} = -i \langle \Omega^{\alpha}_{\mathbf{k}} \rangle^{\mathcal{F}}_{n+1}, \quad (2.74)$$

$$\langle Q_{\hat{k}} \rangle^{\mathrm{P}}_{n+1} = \langle \Omega_{\hat{k}} \rangle^{\mathcal{F}}_{n+1}. \quad (2.75)$$

Here, the expectation value $\langle \cdots \rangle^{\mathcal{F}}_{n+1}$ is defined via

$$\left\langle \cdots \right\rangle^{\mathcal{F}}_{n+1} \equiv \frac{\int \mathcal{D}\Omega \;\cdots \exp\{-ndN\mathcal{F}_n(\{\Omega_{\hat{k}}\})\},}{\int \mathcal{D}\Omega \;\exp\{-ndN\mathcal{F}_n(\{\Omega_{\hat{k}}\})\},}. \quad (2.76)$$

Thus, by using Eq. (2.59) we see that we can relate the order parameter to the expectation value of the stochastic field $\Omega_{\hat{k}}$:

$$\left[\frac{1}{N}\sum_{i=1}^{N}\int_0^1 ds\, \langle \exp\left(i\mathbf{k}^0 \cdot \mathbf{c}_i(s)\right)\rangle_{\chi} \langle \exp\left(i\mathbf{k}^1 \cdot \mathbf{c}_i(s)\right)\rangle_{\chi} \cdots \langle \exp\left(i\mathbf{k}^g \cdot \mathbf{c}_i(s)\right)\rangle_{\chi}\right] = \lim_{n\to 0} \langle \Omega_{\hat{l}} \rangle^{\mathcal{F}}_{n+1}, \quad (2.77)$$

where $\hat{l} = \{\mathbf{k}^0, \mathbf{k}^1, \ldots, \mathbf{k}^g, \mathbf{0}, \ldots, \mathbf{0}\}$. In the following section we make explicit use of this development in order to compute the order parameter.

Let us notice here that the normalization constant $\mathcal{N}$ drops out of the computation of any pure averages because of a cancelation between numerator and denominator. This immediately implies that it plays no role in determining the order parameter. Even when in Chap. 4 we look at the change in free energy due to a deformation of the system, $\mathcal{N}$ will be unaffected, because it only depends on the state of the system before crosslinking. Therefore, we will ignore $\mathcal{N}$ from now on.

2.6 Stationary-point approximation

In the preceding sections we have developed an exact, formal, field-theoretic representation of the statistical mechanics of randomly crosslinked macromolecular networks. In the present section we shall explore the properties of such systems, focusing our attention on the regime of crosslink densities near to the equilibrium phase transition from the liquid state to the amorphous solid state that sufficient crosslinking causes. We shall do this by analyzing the field-theoretic representation at the level of mean-field theory, considering in detail expressions for the free energy and the order parameter.

The mean-field level of approximation follows from computing the functional integral in Eq. (2.63) by using the stationary-point method. This amounts to replacing the functional integral by the value of its integrand that is stationary with respect to variations of $\{\Omega_{\hat{q}}\}$, so that, omitting unimportant constants, we obtain the following approximations for $\bar{f}$, $\langle\Omega^{\alpha}_{\mathbf{k}}\rangle^{\mathcal{F}}_{n+1}$, and $\langle\Omega_{\hat{k}}\rangle^{\mathcal{F}}_{n+1}$.

$$\bar{f} = \lim_{n\to 0}\mathcal{F}_n(\{\bar{\Omega}_{\hat{q}}\}) \tag{2.78}$$

$$i\langle\Omega_{\hat{p}}\rangle^{\mathrm{P}}_{n+1} = \langle\Omega_{\hat{p}}\rangle^{\mathcal{F}}_{n+1} = \bar{\Omega}_{\hat{p}}, \tag{2.79}$$

$$\langle Q_{\hat{k}}\rangle^{\mathrm{P}}_{n+1} = \langle\Omega_{\hat{k}}\rangle^{\mathcal{F}}_{n+1} = \bar{\Omega}_{\hat{k}}, \tag{2.80}$$

where $\hat{p}$ is any replicated wave-vector in the one replica sector and $\hat{k}$ is any replicated wave-vector in the higher replica sector. The particular values $\{\bar{\Omega}_{\hat{q}}\}$ for the stochastic field are those that satisfy the stationarity conditions

$$\left.\frac{\delta\mathcal{F}_n}{\delta\Omega^{*}_{\hat{q}}}\right|_{\{\bar{\Omega}_{\hat{q}}\}} = 0. \tag{2.81}$$

By inserting the explicit expression of Eq. (2.64) for the free energy functional, the stationarity conditions are shown to be

$$\bar{\Omega}_{\hat{p}} = i\langle\rho_{\hat{p}}\rangle^{W,\bar{\Omega}}_{n+1} \qquad \bar{\Omega}_{\hat{k}} = \langle\rho_{\hat{k}}\rangle^{W,\bar{\Omega}}_{n+1} \tag{2.82}$$

for $\hat{p}$ in the one replica sector and $\hat{k}$ in the higher replica sector. Here we have defined the average

$$\langle O \rangle_{n+1}^{W,\bar{\Omega}} = \frac{\left\langle O \exp\left(i\tilde{\lambda}_n^2 \frac{N}{V} \tilde{\sum}_{\hat{p}} \bar{\Omega}_{\hat{p}} \rho_{\hat{p}}^* + \frac{\mu^2}{V^n} \overline{\sum}_{\hat{k}} \bar{\Omega}_{\hat{k}} \rho_{\hat{k}}^* \right) \right\rangle_{n+1}^{W}}{\left\langle \exp\left(i\tilde{\lambda}_n^2 \frac{N}{V} \tilde{\sum}_{\hat{p}} \bar{\Omega}_{\hat{p}} \rho_{\hat{p}}^* + \frac{\mu^2}{V^n} \overline{\sum}_{\hat{k}} \bar{\Omega}_{\hat{k}} \rho_{\hat{k}}^* \right) \right\rangle_{n+1}^{W}}. \tag{2.83}$$

The stationary-point condition of Eq. (2.82) can thus be interpreted as a self-consistent equation for the stochastic fields $\{\Omega_{\hat{q}}\}$. In the Weiss molecular field theory of magnetism one postulates that the thermal average of the spin under the effect of an effective field produced by the mean field magnetization has to be equal to the mean field magnetization. In the present theory, the appropriate thermal averages of the Fourier transformed densities for a macromolecule under the influence of an effective field produced by the stochastic variables $\{\Omega_{\hat{q}}\}$, have to reproduce the same values of those stochastic variables $\{\Omega_{\hat{q}}\}$.

Although the general physical interpretation of the set of stationarity conditions in Eq. (2.82) seems clear, it is not at all obvious how to solve those equations. The available space that the fields $\{\Omega_{\hat{q}}\}$ span is enormous. For example, in the replica theory of spin glasses, even though the unknown $Q_{\alpha\beta}$ (an $n \times n$ matrix associated with the correlations of spins in replicas α and β) is a much simpler object than the set of $\{\Omega_{\hat{q}}\}$ that one needs to determine in the present theory, much effort was necessary before a satisfactory solution to the stationary-point equations was discovered by Parisi.

In our problem, it seems out of the question to search exhaustively for solutions. Instead, we proceed by steps. First, in Sec. 2.6.1 we analyze the stationary point corresponding to the liquid state, and find its region of thermodynamic stability. Later on, in Sec. 2.6.2, we take a variational approach to the problem of the amorphous solid state, by restricting the order parameter to the family described by the parametrization presented in Sec. 2.3.3. Finally, in Sec. 2.6.3 we show that the optimal solution found within a restricted hypothesis is a true stationary point.

2.6.1 Instability of the liquid state

In the context of the mean-field approximation, the liquid state corresponds to $\bar{\Omega}_{\hat{q}} = 0$, which can readily be checked to solve Eq. (2.82). To address the stability of this state we expand perturbatively Eq. (2.64) for $\mathcal{F}_n(\{\Omega_{\hat{q}}\})$ about $\bar{\Omega}_{\hat{q}} = 0$ to second order in $\Omega_{\hat{q}}$. This gives

$$\begin{aligned} nd\mathcal{F}_n(\{\Omega_{\hat{q}}\}) &= \tilde{\lambda}_n^2 NV^{-1} \sum_{\alpha=0}^{n} \sum_{\mathbf{k}}^{\dagger} \left(1 + \tilde{\lambda}_n^2 NV^{-1} g_0(|\mathbf{k}|^2)\right) |\Omega_{\mathbf{k}}^{\alpha}|^2 \\ &\quad + \mu^2 V^{-n} \overline{\sum}_{\hat{k}}^{\dagger} \left(1 - \mu^2 V^{-n} g_0(|\hat{k}|^2)\right) |\Omega_{\hat{k}}|^2 + \cdots . \end{aligned} \tag{2.84}$$

The correlators necessary to calculate the terms in this expansion are computed in App. A, and the function $g_0(|\mathbf{k}|^2)$ resulting from the subsequent arclength integrations is defined in App. B and has the value

$$g_0(|\mathbf{k}|^2) = \frac{\mathrm{e}^{-k^2/2} - \left(1 - \frac{1}{2}k^2\right)}{\frac{1}{2}\left(\frac{1}{2}k^2\right)^2} \sim \begin{cases} 1 - k^2/6, & \text{if } k^2 \ll 1; \\ 4/k^2 & \text{if } k^2 \gg 1. \end{cases} \tag{2.85}$$

As we anticipated at the end of Sec. 2.4.1, the stability of the 1-replica sector is controlled by the coefficient of the $|\Omega_{\mathbf{k}}^{\alpha}|^2$ term in this expansion. This coefficient, together with the positive-definiteness of $g_0(|\mathbf{k}|^2)$, show that provided the crosslink-renormalized excluded-volume parameter $\tilde{\lambda}_n^2$, Eq. (2.54), is positive, the 1-replica sector is locally stable. Thus, the stationary-point value $\bar{\Omega}_{\mathbf{k}}^{\alpha}$ is zero. The positive-definiteness of $\tilde{\lambda}_n^2$ requires that

$$\lambda^2 > \frac{\mu^2 V}{NV^n}, \tag{2.86}$$

i.e., that the repulsive character of the physical excluded-volume parameter λ^2 is sufficiently strong to enable the system to withstand the effective tendency towards collapse afforded by the crosslinking. Thus, we see that even at the level of mean-field theory it is only as a consequence of the presence of the excluded-volume interaction that the system can, at the same time, be stable with respect to collapse to the (inhomogeneous) globular state and yet unstable with respect to the formation of the (macroscopically homogeneous) amorphous solid state.

The stability of the higher-replica sector is controlled by the coefficient of the $|\Omega_{\hat{k}}|^2$ term in the expansion, Eq. (2.84), i.e., by

$$1 - \mu^2 V^{-n} g_0(|\hat{k}|^2) \tag{2.87}$$

(considering, as we do, $\mu^2 \geq 0$). The two contributions to this coefficient enter with competing signs, owing to the attractive nature of the effective term arising from crosslinking, and thus provide the opportunity for the loss of positivity of this coefficient. Indeed, the coefficient indicates that the liquid state will be stable for $\mu^2 < 1$ and unstable for $\mu^2 > 1$, i.e., stable only for sufficiently small crosslink density, the factor of V^{-n} in Eq. (2.87) being eliminated by first taking the limit $n \to 0$, and subsequently taking the thermodynamic limit ($V \to \infty$, $N \to \infty$, N/V fixed, μ^2 fixed) [73]. The least stable modes correspond to long wavelengths, $\hat{k}^2 \to 0$, for which $g_0(|\hat{k}|^2) \to 1$ from below [74].

The linear stability analysis of the present subsection indicates that the liquid state, as characterized by the order parameter discussed in Sec. 2.3, is stable when the mean number of crosslinks per macromolecule $[M]/N$ is smaller than a certain critical value M_c/N, i.e., those mean crosslink densities corresponding to $\mu^2 < 1$. However, for larger crosslink densities, $([M]/N) > (M_c/N)$, i.e., $\mu^2 > 1$, the liquid state is unstable [75], being replaced by an alternative state which, as we shall see in the following two subsections, is an amorphous solid state, characterized by $\Omega_{\hat{k}} \neq 0$ for $\hat{k}$ in the higher replica sector but $\Omega^{\alpha}_{\mathbf{p}} = 0$. In fact, the state that replaces the liquid state will turn out to have the property of macroscopic translational invariance (see Sec. 2.3.1), so that even though it has $\Omega_{\hat{k}} \neq 0$ this is compatible with and does not disturb the fact that the 1-replica sector remains stable and that $\Omega^{\alpha}_{\mathbf{p}}$ remains zero.

2.6.2 Variational approach

We now set about exploring the nature of the amorphous solid state with respect to which the liquid state is unstable for $\mu^2 > 1$. Initially, we do this by following the strategy outlined before of making $\mathcal{F}_n$ stationary with respect to the fields $\Omega^\alpha_{\mathbf{p}}$ and $\Omega_{\hat{k}}$. However, we are unable to parametrize the entire space of possible fields. Instead, we consider the class of fields for which physical motivation was presented in Sec. 2.3.2 [see Eq. (2.36)],

$$\Omega^\alpha_{\mathbf{k}} = \quad 0, \qquad \text{(1-replica sector)}, \tag{2.88}$$

$$\Omega_{\hat{k}} = \quad q\,\delta^{(d)}_{\tilde{\mathbf{k}},\mathbf{0}} \int_0^\infty d\tau\, p(\tau) \exp\left(-\hat{k}^2/2\tau\right), \qquad \text{(higher-replica sector)}, \tag{2.89}$$

evaluate $\mathcal{F}_n$ for such fields, and make the resulting quantity stationary with respect to the variational quantities, the gel fraction q (a number) and the distribution of (inverse square) localization lengths $p(\tau)$ (a normalized function). This amounts to making a variational mean-field approximation. However, as we shall see in the following subsection, the hypothesis we make for the stationary point will actually turn out to contain an exact stationary point of $\mathcal{F}_n$.

By inspecting Eq. (2.64) and employing Eq. (2.88) we see that there are two contributions to the free energy: a term quadratic in $\Omega_{\hat{k}}$, and a term that can be identified as the logarithm of the partition function of a single replicated macromolecule coupled to $\Omega_{\hat{k}}$. The explicit details of the evaluation of these terms when $\Omega_{\hat{k}}$ is given by Eq. (2.89) are presented in App. C. Then the variational mean-field approximation to the free energy is given by

$$\bar{f} \approx \lim_{n\to 0} \min_{\Omega_{\hat{q}}} \mathcal{F}_n(\{\Omega_{\hat{q}}\}) \approx \min_{q,\,p(\tau)} \bar{f}^{\rm var}\{q,p\}, \tag{2.90}$$

where we have omitted constants independent of the variational parameters q and $p(\tau)$, and the variational free energy $\bar{f}^{\rm var}\{q,p\}$ is given by

$$\begin{aligned}\bar{f}^{\rm var}\{q,p\} \;=\; & -\frac{1}{2}\Big(\exp(-\mu^2 q) - (1-\mu^2 q) - \frac{1}{2}\mu^2 q^2\Big)\ln\left(V^{2/d}/2\pi\mathrm{e}\right) \\ & + \frac{1}{4}\mu^2 q^2 \int_0^\infty d\tau_1\, p(\tau_1) \int_0^\infty d\tau_2\, p(\tau_2) \ln\left((\tau_1^{-1}+\tau_2^{-1})^{-1}\right)\end{aligned}$$

$$+\frac{1}{2}\mathrm{e}^{-\mu^2 q}\sum_{r=1}^{\infty}\frac{\mu^{2r}q^r}{r!}\int_0^1 ds_1\cdots ds_r$$
$$\times\int_0^\infty d\tau_1 p(\tau_1)\cdots d\tau_r p(\tau_r)\ln\left(\mathcal{W}^{(r)}\det{}^{(r)}\mathcal{R}^{(r)}_{\rho\rho'}\right). \qquad (2.91)$$

Here, $\det^{(r)}$ denotes the determinant of an $r\times r$ matrix, $\mathcal{R}^{(r)}_{\rho\rho'}$ is an $(r\times r)$-matrix–valued function of the r arclength coordinates $\{s_\nu\}_{\nu=1}^r$ and the r inverse square localization lengths $\{\tau_\nu\}_{\nu=1}^r$, and $\mathcal{W}^{(r)}$ is a single such function, $\mathcal{R}^{(r)}_{\rho\rho'}$ and $\mathcal{W}^{(r)}$ being respectively defined in Eqs. (E.1) and (E.3) of App. E.

As anticipated in Sec. 2.2.6, in addition to intensive terms we find a nonintensive term, proportional to $\ln V$, owing to the omission of the disorder-average of the Gibbs symmetry factor. The presence of the $\ln V$ factor signals the fact that the configuration integral produces additional powers of V. These powers of V can only be due to degrees of freedom that are allowed to vary over the entire sample, i.e., to the fraction of macromolecules that are delocalized. Thus this term depends on the gel fraction q, but it cannot (and does not) depend on $p(\tau)$, which only describes the localized degrees of freedom. In the following subsection we shall analyze the self-consistency condition for the order parameter directly and, although no quantity proportional to $\ln V$ will appear, we will re-obtain the exact same results as in the present subsection. This approach will be seen to have the additional substantial virtue of demonstrating that the hypothesized form of the order parameter, Eq. (2.36), used in the present section as a variational hypothesis, in fact provides an *exact stationary point* of the free energy, not merely a variational approximation.

As a first step towards minimizing $\bar{f}^{\mathrm{var}}$ we regard the term proportional to $\ln V$ as dominant, and make it stationary with respect to the gel fraction q. This leads to the condition [33, 76]

$$\exp(-\mu^2 q) = 1 - q, \qquad (2.92)$$

For all values of μ^2 this equation has the root $q = 0$, corresponding to the liquid state. However, for $\mu^2 > 1$ an additional root appears, emerging continuously from $q = 0$ at $\mu^2 = 1$,

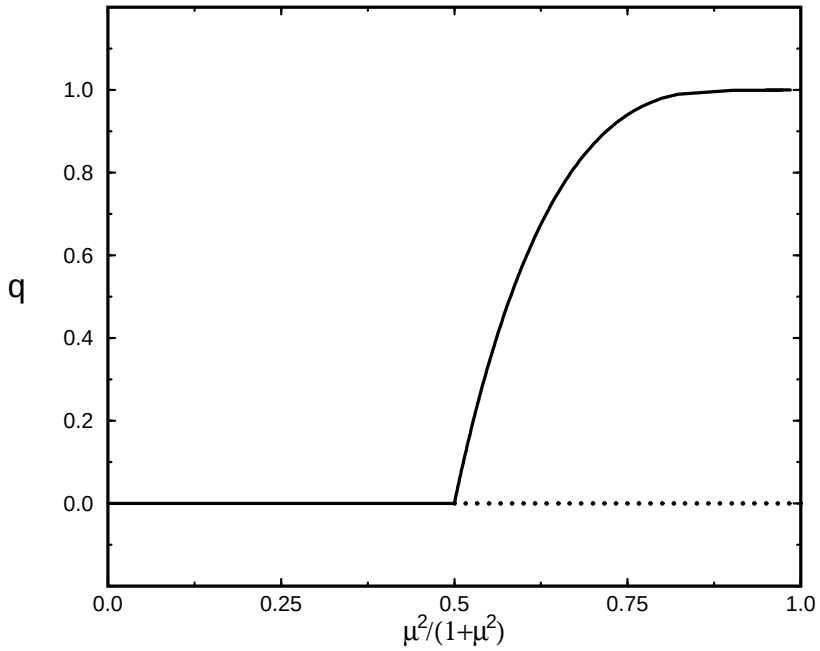

Figure 2.1: Dependence of the gel fraction q on the crosslink density control parameter μ^2.

and describing the equilibrium amorphous solid state. In Fig. (2.1) we show the dependence of the gel fraction on μ^2. For $\mu^2 \gg 1$, i.e., the highly crosslinked regime, q approaches unity asymptotically as $q \sim 1 - \exp(-\mu^2)$. In the critical regime, $0 \leq \mu^2 - 1 \ll 1$, it is convenient to exchange μ^2 for the new control parameter ϵ, defined via

$$\mu^2 \equiv 1 + \epsilon/3, \tag{2.93}$$

with $0 \leq \epsilon \ll 1$. We may then solve perturbatively for q, obtaining

$$q = 2\epsilon/3 + \mathcal{O}(\epsilon^2). \tag{2.94}$$

Having determined the condition satisfied by q we now turn our attention to the dependence of $\bar{f}^{\rm var}$ on the distribution $p(\tau)$ of inverse square localization lengths. As we are primarily interested in crosslink densities in the vicinity of the vulcanization transition (i.e., $0 \leq \epsilon \ll 1$), we use the result that, to order ϵ, we have $q = 2\epsilon/3$. This allows us to retain in the summation over r in Eq. (2.91) only the terms $r = 2, 3$ (the $r = 1$ term vanishing identically by the construction of $\mathcal{W}^{(r)}$). Next, we assume that the inverse square localization lengths having appreciable statistical weight in $p(\tau)$ are also of order ϵ, i.e., small compared to unity, in units such that $\sqrt{\ell L/d} = 1$, so that localization is on length scales much larger than the size of a free macromolecule. (We shall confirm the consistency of this assumption *a posteriori*.) Thus, we may use the result from App. E to expand $\ln\left(\mathcal{W}^{(r)} \det{}^{(r)} \mathcal{R}^{(r)}_{\rho\rho'}\right)$ in Eq. (2.91) for small $\{\tau_\rho\}_{\rho=1}^{r}$, retaining terms to order τ_ρ. Then we integrate over the arclength variables $\{s_1, \ldots, s_r\}$ by using the results of App. E. Omitting terms that are independent of $p(\tau)$ we find that, to $\mathcal{O}(\epsilon^3)$,

$$\bar{f}^{\rm var} = -\frac{1}{8}\left(\frac{2\epsilon}{3}\right)^3 \left\{\ln\left(\frac{\tau_1+\tau_2}{\tau_1\tau_2}\right)\right\}_\tau + \frac{1}{12}\left(\frac{2\epsilon}{3}\right)^3 \left\{\ln\left(\frac{\tau_1+\tau_2+\tau_3}{\tau_1\tau_2\tau_3}\right)\right\}_\tau + \frac{1}{12}\left(\frac{2\epsilon}{3}\right)^2 \left\{\frac{\tau_1\tau_2}{\tau_1+\tau_2}\right\}_\tau, \tag{2.95}$$

where the curly brace carrying the subscript τ indicates averaging over the localization lengths, i.e., $\{\Psi(\tau_1, \tau_2, \ldots)\}_\tau \equiv \int_0^\infty d\tau_1 p(\tau_1) d\tau_2 p(\tau_2) \cdots \Psi(\tau_1, \tau_2, \ldots)$, as many lengths $\tau_1, \tau_2, \ldots$ as feature as arguments of the arbitrary function Ψ.

For future reference we note that if we suppose that the distribution of localization lengths is sharp, i.e., has no fluctuations, so that $p(\tau) = \delta(\tau - \xi^{-2})$, where ξ is the sharp value of the localization lengths, then the expression for $\bar{f}^{\rm var}$ simplifies, becoming

$$\bar{f}^{\rm var} = \frac{1}{24}\left(\frac{2\epsilon}{3}\right)^3 \ln\left(\xi^2\right) + \frac{1}{24}\left(\frac{2\epsilon}{3}\right)^2 \frac{1}{\xi^2}, \tag{2.96}$$

correct to $\mathcal{O}(\epsilon^3)$. In this case, demanding that $\bar{f}^{\rm var}$ be stationary with respect to ξ^2 yields, to $\mathcal{O}(\epsilon)$,

$$\frac{1}{\xi^2} = \begin{cases} 0, & \text{if } \mu^2 \leq 1; \\ 2\epsilon/3, & \text{if } \mu^2 \geq 1. \end{cases} \tag{2.97}$$

We now return to the general situation, in which the distribution of localization lengths is not constrained to be sharp. Rather than demand that $\bar{f}^{\rm var}$ be explicitly stationary with respect to $p(\tau)$ itself, it is convenient to exchange its dependence on $p(\tau)$ for dependence on the Laplace transform $\hat{p}(\hat{\tau})$ given by

$$\hat{p}(\hat{\tau}) \equiv \int_0^\infty d\tau p(\tau) \exp(-\hat{\tau}\tau). \tag{2.98}$$

The details of this exchange are deferred to App. G; what results is the following expression for $\bar{f}^{\rm var}$, correct to $\mathcal{O}(\epsilon^3)$:

$$\begin{aligned} \bar{f}^{\rm var} &= -\frac{1}{8}\left(\frac{2\epsilon}{3}\right)^3 \int_0^\infty \frac{d\hat{\tau}}{\hat{\tau}} \left(-\hat{p}(\hat{\tau})^2 + 2\hat{p}(\hat{\tau}) - \mathrm{e}^{-\hat{\tau}}\right) \\ &\quad + \frac{1}{12}\left(\frac{2\epsilon}{3}\right)^3 \int_0^\infty \frac{d\hat{\tau}}{\hat{\tau}} \left(-\hat{p}(\hat{\tau})^3 + 3\hat{p}(\hat{\tau}) - 2\mathrm{e}^{-\hat{\tau}}\right) \\ &\quad + \frac{1}{12}\left(\frac{2\epsilon}{3}\right)^2 \int_0^\infty d\hat{\tau} (d\hat{p}/d\hat{\tau})^2. \end{aligned} \tag{2.99}$$

This expression has the virtue of being a local functional of $\hat{p}(\hat{\tau})$, so that the consequent stationarity condition will be a differential equation for $\hat{p}(\hat{\tau})$. Moreover, the (global) constraint that $p(\tau)$ be normalized to unity, $\int_0^\infty d\tau p(\tau) = 1$, is exchanged for the (local) boundary condition $\hat{p}(0) = 1$.

We now demand that $\bar{f}^{\rm var}$ be stationary with respect to $\hat{p}(\hat{\tau})$, i.e., that $\delta \bar{f}^{\rm var}/\delta \hat{p}(\hat{\tau}) = 0$. The details of computing the functional derivative of $\bar{f}^{\rm var}$ with respect to $\hat{p}(\hat{\tau})$ are deferred to App. G; what results is the following stationarity condition, correct to $\mathcal{O}(\epsilon^4)$:

$$0 = \frac{\delta \bar{f}^{\rm var}}{\delta \hat{p}(\hat{\tau})} = -\left(\frac{2\epsilon}{3}\right)^3 \frac{1}{4\hat{\tau}}\Big(1 - \hat{p}(\hat{\tau})\Big) + \left(\frac{2\epsilon}{3}\right)^3 \frac{1}{4\hat{\tau}}\left(1 - \hat{p}(\hat{\tau})^2\right) - \left(\frac{2\epsilon}{3}\right)^2 \frac{1}{6}\frac{d^2\hat{p}}{d\hat{\tau}^2}, \tag{2.100}$$

or, equivalently,

$$\hat{\tau}\frac{d^2\hat{p}}{d\hat{\tau}^2} = \epsilon\, \hat{p}(\hat{\tau})\left(1 - \hat{p}(\hat{\tau})\right), \tag{2.101}$$

correct to $\mathcal{O}(\epsilon)$. Normalization of $p(\tau)$ leads to the boundary condition $\hat{p}(0) = 1$. As $p(\tau)$ does not contain a δ-function contribution at $\tau = 0$ (see [78]), $\hat{p}$ obeys the additional boundary condition $\hat{p}(\infty) = 0$.

Before solving the stationarity condition we note that $p(\tau)$ depends parametrically on the crosslink density, so it would be more accurate to denote it by $p(\tau;\epsilon)$. We now introduce the scaling function $\pi(\theta)$ in terms of which $p(\tau;\epsilon)$ is given by $p(\tau;\epsilon) = (2/\epsilon)\pi(2\tau/\epsilon)$. In other words we transform the dependent and independent variables as follows:

$$\epsilon p(\tau;\epsilon)/2 = \pi(\theta), \tag{2.102}$$

$$\tau = \epsilon\theta/2.. \tag{2.103}$$

In this way, up to an elementary factor, the dependence of $p(\tau;\epsilon)$ on τ and ϵ is combined into a dependence on a single scaling variable θ; see [79]. Then the Laplace transform of the scaling function $\hat{\pi}(\hat{\theta})$ is defined via

$$\hat{\pi}(\hat{\theta}) \equiv \int_0^\infty d\theta \pi(\theta) \exp(-\hat{\theta}\theta), \tag{2.104}$$

so that

$$\hat{p}(\hat{\tau}) = \hat{\pi}(\hat{\theta}) \tag{2.105}$$

$$\epsilon\hat{\tau}/2 = \hat{\theta}. \tag{2.106}$$

In terms of $\hat{\pi}(\hat{\theta})$, and neglecting $\mathcal{O}(\epsilon)$ contributions, the stationarity condition then becomes

$$\hat{\theta}\frac{d^2\hat{\pi}}{d\hat{\theta}^2} = 2\hat{\pi}(\hat{\theta})\left(1 - \hat{\pi}(\hat{\theta})\right), \tag{2.107}$$

subject to the boundary conditions $\hat{\pi}(0) = 1$ and $\hat{\pi}(\infty) = 0$.

We have been unable to solve this nonlinear ordinary differential equation for $\hat{\pi}(\hat{\theta})$ analytically. One might consider solving this differential equation numerically, and then inverting the solution numerically to obtain $\pi(\theta)$ and hence $p(\tau)$. While this is possible in principle, the numerical inversion of Laplace transforms is notoriously unstable. Instead, we have found it preferable to take the inverse-transform of the differential equation analytically, and thus we obtain the following nonlinear integro-differential equation and constraint for $\pi(\theta)$:

$$\frac{\theta^2}{2}\frac{d\pi}{d\theta} = (1-\theta)\,\pi(\theta) - \int_0^\theta d\theta' \pi(\theta')\pi(\theta-\theta'), \tag{2.108}$$

$$\int_0^\infty d\theta\, \pi(\theta) = 1, \tag{2.109}$$

the constraint resulting from normalization.

We shall obtain $\pi(\theta)$ [and hence $p(\tau)$] in Sec. 2.6.4, and discuss the consequences of the physical values of q and $p(\tau)$. Before doing so, we shall adopt a different point of view, in which we focus not on the variational extremization of the free energy but instead on the self-consistent equation for the order parameter.

2.6.3 Self-consistency condition for the order parameter

In Sec. 2.6.2 we enforced the stationarity of the free energy functional only with respect to the parameters q and $p(\tau)$ of our order parameter hypothesis, and not with respect to arbitrary variations. As a consequence, we are not yet in a position to address whether or not the resulting order parameter is a true stationary point of the free energy functional. In the present subsection we establish that the solution that we have found is indeed a true stationary point of the free energy functional by directly analyzing the stationarity conditions (2.82) themselves. We emphasize that this approach allows us to circumvent the difficulties discussed in Sec. 2.2.6 that arise in the computation of the contribution to the free energy associated with changes in the indistinguishability factors introduced by the crosslinks.

We insert the hypothesis given in Eqs. (2.88) and (2.89) into the stationarity conditions (2.82) to obtain

$$\begin{aligned}
&(1-q)\delta_{\hat{q},\hat{0}} + q\,\delta_{\tilde{\mathbf{q}},\mathbf{0}} \int_0^\infty d\tau\, p(\tau)\, \exp\left(-\hat{q}^2/2\tau\right) \\
&\qquad \Big\langle \int_0^1 dt\, \exp\left(i\hat{q}\cdot\hat{c}(t)\right) \\
&\qquad\qquad \times \exp\left(\mu^2 V^{-n} q \textstyle\sum_{\hat{k}} \delta_{\tilde{\mathbf{k}},\mathbf{0}} \displaystyle\int_0^\infty d\tau\, p(\tau) \exp\left(-\hat{k}^2/2\tau\right) \int_0^1 ds\, \mathrm{e}^{i\hat{k}\cdot\hat{c}(s)}\right) \Big\rangle_{n+1}^{\mathrm{W}} \\
&= \frac{\qquad\qquad\qquad\qquad\qquad\qquad\qquad\qquad\qquad\qquad\qquad\qquad}{\Big\langle \exp\left(\mu^2 V^{-n} q \textstyle\sum_{\hat{k}} \delta_{\tilde{\mathbf{k}},\mathbf{0}} \displaystyle\int_0^\infty d\tau\, p(\tau) \exp\left(-\hat{k}^2/2\tau\right) \int_0^1 ds\, \mathrm{e}^{i\hat{k}\cdot\hat{c}(s)}\right) \Big\rangle_{n+1}^{\mathrm{W}}}.
\end{aligned} \tag{2.110}$$

Here, in both the numerator and the denominator we have relaxed the constraints on the summations having coefficient μ^2 by: (i) doubling the range of the summations to include

the entire higher-replica sector by making use of the property of the hypothesis $\Omega_{\hat{k}} = \Omega^*_{-\hat{k}}$; (ii) including the 1-replica sector terms (which vanish by the MTI of the order parameter hypothesis); and (iii) inserting identical factors associated with the 0-replica sector. It should be noted that Eq. (2.110) also follows from the direct application of the Weiss molecular-field method.

As shown at the end of App. H, evaluation of the numerator and denominator of the right-hand side yields

$$\begin{aligned}(1-q)\,\delta_{\hat{q},\hat{0}} \;+\; & q\,\delta_{\tilde{\mathbf{q}},\mathbf{0}} \int_0^\infty d\tau\, p(\tau)\, \mathrm{e}^{-\hat{q}^2/2\tau} \\ = \;& \mathrm{e}^{-\mu^2 q}\,\delta_{\hat{q},\hat{0}} + \mathrm{e}^{-\mu^2 q}\,\delta_{\tilde{\mathbf{q}},\mathbf{0}} \int_0^\infty d\tau\, \mathrm{e}^{-\hat{q}^2/2\tau} \sum_{r=1}^\infty \frac{\mu^{2r} q^r}{r!} \int_0^1 ds_1 \cdots ds_{r+1} \\ & \times \int_0^\infty d\tau_1 \cdots d\tau_r\, p(\tau_1) \cdots p(\tau_r)\, \delta(\tau - \Upsilon^{(r)}), \qquad (2.111)\end{aligned}$$

$$\frac{1}{\Upsilon^{(r)}} \;\equiv\; \frac{1}{\mathcal{W}^{(r)}} + \mathcal{S}_{r+1,r+1} - \frac{2}{\mathcal{W}^{(r)}} \sum_{\rho=1}^r \mathcal{U}_\rho^{(r)}\, \mathcal{S}_{\rho,r+1} - \sum_{\rho,\rho'=1}^r \mathcal{S}_{r+1,\rho}\, \mathcal{C}_{\rho\rho'}^{(r)}\, \mathcal{S}_{\rho',r+1}, \qquad (2.112)$$

where the limit $n \to 0$ has been taken everywhere except in the dimension of $\hat{q}$, and where $\mathcal{S}_{\rho\rho'}$, $\mathcal{U}^{(r)}$, $\mathcal{W}^{(r)}$ and $\mathcal{C}^{(r)}$ are, respectively, defined in Eqs. (A.3), (E.2), (E.3) and (E.4), and depend on $\{s_1, \ldots, s_{r+1}\}$ and $\{\tau_1, \ldots, \tau_{r+1}\}$. It should be emphasized that Eq. (2.111) is not solved by any sharp distribution of localization lengths $p(\tau) = \delta(\tau - \xi^{-2})$. Thus, a variational hypothesis involving a sharp distribution gives at best a variational approximation, whereas a variational hypothesis involving a non-sharp distribution has the potential to yield an exact stationary point, and we shall find such an exact stationary point below, at least in the vicinity of the vulcanization transition.

We now extract information about q and $p(\tau)$ from Eq. (2.111). First, we take the limit $\hat{q}^2 \to 0$, via a sequence for which $\tilde{\mathbf{q}} = \mathbf{0}$. In this limit, the left hand side becomes q, and on the right side each integral gives a factor of unity, yielding the self-consistency condition for the gel fraction q:

$$q = 1 - \mathrm{e}^{-\mu^2 q}, \qquad (2.113)$$

i.e., precisely the self-consistency condition for q found from the free energy approach is Sec. 2.6.2 and discussed there.

Having decoupled the issue of the gel fraction q from the issue of the distribution $p(\tau)$ we now return to $p(\tau)$ itself. By considering Eq. (2.112) for a fixed nonzero value of $\hat{q}^2$, and using Lerch's uniqueness theorem for Laplace transforms [80] we find that indeed the hypothesis solves the self-consistency condition for $\{\Omega^{\alpha}_{\mathbf{k}}, \Omega_{\hat{k}}\}$ provided that the distribution $p(\tau)$ satisfies the condition

$$q\, p(\tau) = \mathrm{e}^{-\mu^2 q} \sum_{r=1}^{\infty} \frac{\mu^{2r} q^r}{r!} \int_0^1 ds_1 \cdots ds_{r+1} \int_0^{\infty} d\tau_1 \cdots d\tau_r\, p(\tau_1) \cdots p(\tau_r)\, \delta(\tau - \Upsilon_r). \qquad (2.114)$$

This equation for $p(\tau)$ is, for all values of μ^2, identically satisfied if $q = 0$.

We have not, thus far, made any approximations beyond that of mean field theory. In order to render Eq. (2.114) tractable, we now restrict our attention to the vicinity of the transition regime in the solid state, i.e., to values of ϵ, as defined in Eq. (2.93), satisfying $0 \leq \epsilon \ll 1$. This restriction allows us to assume that q is small, and that only localization lengths much larger than the free-macromolecule radius of gyration have an appreciable probability, i.e., $p(\tau)$ only gives appreciable weight for $0 < \tau \ll 1$. Thus, we need retain in Eq. (2.114) only terms for which r is 1 or 2, and may expand $\Upsilon^{(1)}$ to $\mathcal{O}(\tau^2)$ and $\Upsilon^{(2)}$ to $\mathcal{O}(\tau^1)$. As discussed in App. I, in terms of the scaling function $\pi(\theta)$ introduced in Eq. (2.102), we recover Eq. (2.108) subject to the normalization condition Eq. (2.109), i.e., precisely the stationarity condition for $p(\tau)$ found from the free energy approach.

Thus, the condition that the order parameter be self-consistent turns out to be identical to the condition that the free energy functional be stationary with respect to variations within the subspace spanned by the hypothesized form of the order parameter. The form for the order parameter hypothesized in Eq. (2.36) is not merely a variational form but in fact gives an exact stationary point of the free energy functional, Eq. (2.64).

We have obtained the equation for the gel fraction q, Eq. (2.92), and the equations for the scaled distribution $\pi(\theta)$, Eqs. (2.108) and (2.109), from two different points of view. In the

previous subsection we have discussed the consequences of Eq. (2.92) for q. In the following subsection we shall discuss the solution of Eqs. (2.108) and (2.109) for $\pi(\theta)$, and elaborate on the physical consequences of our results for q and $p(\tau)$.

2.6.4 Characteristics of the amorphous solid state

For the sake of completeness we first restate the results concerning the gel fraction q that were found in Sec. 2.6.2 from the self-consistency condition on q, Eq. (2.92). For all values of μ^2 we find the solution $q = 0$, corresponding to the liquid state. For $\mu^2 > 1$ an additional solution appears, emerging continuously from $q = 0$ at $\mu^2 = 1$, and describing the equilibrium amorphous solid state, as shown in Fig. (2.1). For $\mu^2 \gg 1$, i.e., the highly crosslinked regime, q approaches unity asymptotically as $q \sim 1 - \exp(-\mu^2)$. In terms of the deviation of the crosslink density from criticality, i.e., ϵ defined in Eq. (2.93), the critical regime is $0 \leq \epsilon \ll 1$. In this regime we may solve perturbatively for q, obtaining $q = 2\epsilon/3 + \mathcal{O}(\epsilon^2)$, Eq. (2.94).

It should be noted that the stationarity condition on q, Eq. (2.92), is precisely the condition obtained by Erdős and Rényi in the context of random graph theory [76], which can also be interpreted as a mean-field treatment of percolation. In particular, Erdős and Rényi showed that that for a random graph of N points and $\mu^2 N/2$ edges the probability for the fraction of points in the largest component to differ from the solution q of Eq. (2.92) vanishes in the $N \to \infty$ limit. A related approach to the theory of macromolecular networks [33] has also led to Eq. (2.92). This is physically quite reasonable: one would anticipate that the transition from liquid to solid would occur when the density of crosslinks is sufficient to create a macroscopically extended network of crosslinked macromolecules.

We now address the distribution of localization lengths via the scaling form $\pi(\theta)$. We have solved both the integro-differential equation (2.108) and the differential equation (2.107) numerically [81, 82], and the solution of Eq. (2.108) is shown in Fig. (2.2). As we see in this figure, the scaling function $\pi(\theta)$ has a single maximum near $\theta = 1$, away from which

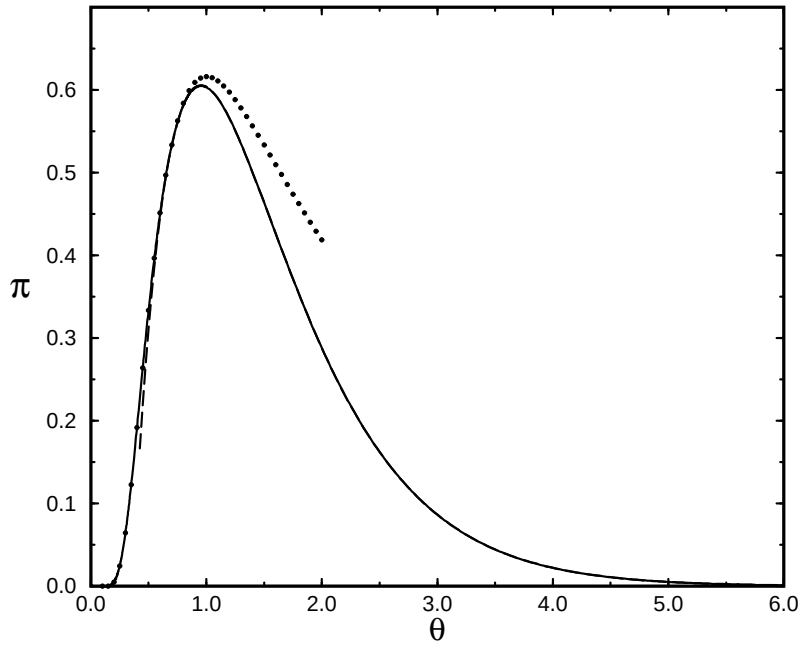

Figure 2.2: Scaling function $\pi(\theta)$ for the probability distribution of localization lengths. Exact scaling function (full line); asymptotic form for $\theta \to 0$ (dotted line); asymptotic form for $\theta \to \infty$ (broken line).

it decays rapidly. In fact, states for which $\pi(\theta)$ takes negative values are not ruled out by the hypothesis Eq. (2.36), but are not found as solutions of the stationarity condition Eqs. (2.108) and (2.109).

We are able to obtain asymptotic properties of $\pi(\theta)$ analytically. The asymptotic form $\pi(\theta) \sim a\theta^{-2} \exp(-2/\theta)$ (for $\theta \ll 1$) is obtained from Eq. (2.108) by neglecting the second term on the right hand side. Notice the essential singularity at the origin: $\pi(\theta)$ vanishes very rapidly indeed as $\theta \to 0$. The coefficient $a \approx 4.554$ cannot be obtained from local asymptotic analysis. Instead we have obtained it separately by the numerical solution of Eq. (2.107), as

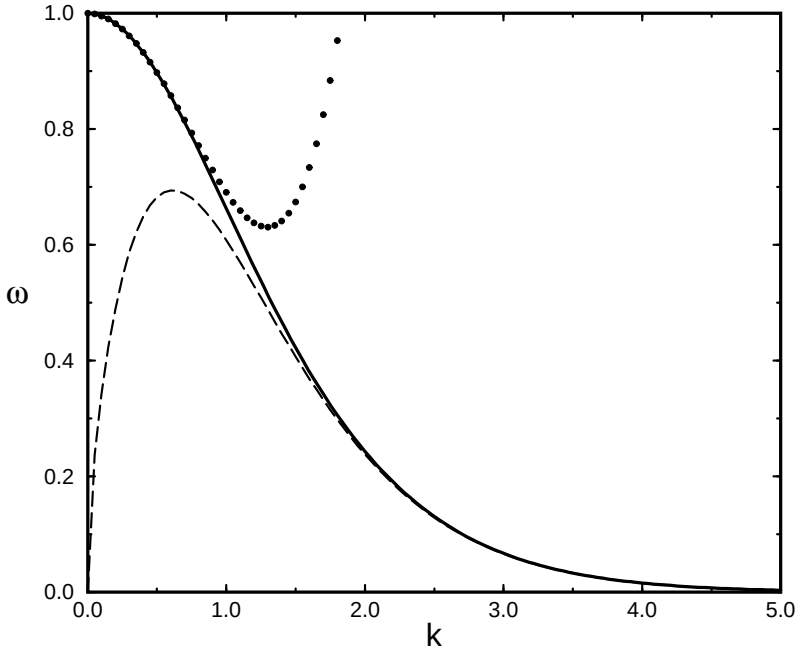

Figure 2.3: Scaling function $\omega(k)$ for the order parameter. Exact scaling function (full line); asymptotic form for $k \to 0$ (dotted line); asymptotic form for $k \to \infty$ (broken line).

discussed in footnote [82]. The asymptotic form $\pi(\theta) \sim 3(b\theta - 3/5)\exp(-b\theta)$ (for $\theta \gg 1$) is obtained by computing the inverse Laplace transform of the approximate analytical solution of Eq. (2.107) near the point $\hat{\theta} = -b$, at which $\hat{\pi}(\hat{\theta})$ diverges. The coefficient $b \approx 1.678$ was obtained separately by determining the (negative) value of $\hat{\theta}$ at which the numerical solution of Eq. (2.107) diverges. Notice the exponential decay of $\pi(\theta)$ for large θ: $\pi(\theta)$ goes to zero quickly as $\theta \to \infty$. For the sake of comparison with the numerical results, the small- and large-θ asymptotic forms for $\pi(\theta)$ are also shown in Fig. (2.2). A distribution of localization lengths also features in Panyukov's approach to the well-crosslinked regime; see [84].

In addition to providing the distribution of localization lengths, knowledge of $\pi(\theta)$ allows us to construct the order parameter, $\Omega_{\hat{k}}$. By using Eqs. (2.102) and (2.103) in Eq. (2.36) we obtain

$$\Omega_{\hat{k}} = (1-2\epsilon/3)\,\delta_{\hat{k},\hat{0}} + (2\epsilon/3)\,\delta_{\tilde{\mathbf{k}},\mathbf{0}}\,\omega\Big(\sqrt{2\hat{k}^2/\epsilon}\Big), \tag{2.115}$$

$$\omega(k) \equiv \int_0^\infty d\theta\,\pi(\theta)\,\mathrm{e}^{-k^2/2\theta}. \tag{2.116}$$

Although we do not have an exact analytical expression for $\pi(\theta)$, we can compute $\omega(k)$ numerically. We do this by inserting the the numerical values of $\pi(\theta)$ into Eq. (2.116), and show the result for $\omega(k)$ in Fig. (2.3). We are able to obtain analytical asymptotic expressions for $\omega(k)$. For $k \ll 1$ the result simply follows from expanding the exponential function in Eq. (2.116) in powers of k, thus obtaining

$$\omega(k) \sim 1 - \frac{k^2}{2}\int_0^\infty d\theta\,\theta^{-1}\pi(\theta) + \frac{k^4}{8}\int_0^\infty d\theta\,\theta^{-2}\pi(\theta) + \cdots \tag{2.117}$$

$$= 1 - 0.4409\,k^2 + 0.1316\,k^4 + \cdots, \qquad \text{for} \quad k \ll 1. \tag{2.118}$$

We see that $\omega(k)$ departs quadratically from its absolute maximum of unity at the origin. For $k \gg 1$ one can replace $\pi(\theta)$ by its large-θ asymptotic form in Eq. (2.116) to obtain

$$\omega(k) \sim \left(\frac{9\pi k^3}{\sqrt{8b}}\right)^{1/2} \mathrm{e}^{-\sqrt{2bk^2}}\left(1 + \frac{27}{40\sqrt{2bk^2}} + \cdots\right), \qquad \text{for} \quad k \gg 1. \tag{2.119}$$

We see that $\omega(k)$ decays exponentially to zero for large k. For the sake of comparison with the numerical results, the small- and large-k asymptotic forms for $\omega(k)$ are also shown in Fig. (2.3).

To summarize, as shown in Sec. 2.6.1 the liquid state of a system of randomly crosslinked macromolecules becomes unstable when the mean number of crosslinks per macromolecule $[M]/N$ is increased beyond a certain critical value M_c/N, corresponding to $\mu^2 = 1$. At this critical point the system exhibits a continuous phase transition from the liquid state to the amorphous solid state. As shown in Secs. 2.6.2 and 2.6.3, this solid state is characterized by a gel fraction q, which grows from a value of zero at the critical point with the classical

exponent $\beta = 1$ (see Ref. [85]): $q \sim \epsilon \sim \mu^2 - 1 \sim ([M] - M_c)/N$. The amorphous solid state is further characterized by the statistical distribution of localization lengths $2\xi^{-3}p(\xi^{-2})$. In the vicinity of the transition the dependence of this distribution on the control parameter ϵ and the (inverse square) localization length τ is determined by a universal scaling function (of a single variable) $\pi(\theta)$, i.e., $p(\tau) = (2/\epsilon)\pi(2\tau/\epsilon)$. This universality guarantees that $\pi(\theta)$ need only be computed once for all near-critical crosslink densities. As already mentioned in the present subsection, $\pi(\theta)$ has a single maximum, away from which it decays rapidly. Hence, the fraction of localized monomers that are localized on length scales much larger than $\epsilon^{-1/2}$ is exceedingly small. Our result for $p(\tau)$ also predicts that the fraction of localized monomers with localization lengths much smaller than $\epsilon^{-1/2}$ is also exceedingly small. This provides an *a posteriori* confirmation of the internal consistency of the perturbation expansion in powers of ξ^{-2} upon which our results rely. However, the detailed form of the distribution for localization lengths much smaller than $\epsilon^{-1/2}$ (e.g., for localization lengths of the order of the radius of gyration of a free macromolecule) is unreliable because such localization lengths are not within the range of validity of the perturbation expansion. The rapid decay of $p(\tau)$ away from its maximum guarantees that its moments are finite. This character, together with the scaling form of $p(\tau)$ ensures that the moments scale in the following manner: $[\xi^{-2m}] \sim (([M] - M_c)/N)^{m+1}$. Furthermore, as the distribution has single maximum it is sensible to define a typical localization length ξ_{typ} associated with the most probable localization length. This length ξ_{typ} obeys the scaling relation $\xi_{\text{typ}} \sim (\mu^2 - 1)^{-1/2}$. Thus, a simple, reasonable approximation to the true distribution $p(\tau)$ would be a sharp distribution, e.g., $\delta(\tau - \epsilon/2)$.

We have seen in Sec. 2.6.3 that the order parameter hypothesized in Sec. 2.3.3 and determined in Secs. 2.6.2 and 2.6.3 is a solution of the stationarity condition for the free energy Eq. (2.82). This is in contrast with the hypothesis analyzed in Ref. [34], in which it was assumed that $q = 1$ and $p(\xi^{-2}) = \delta(\xi^{-2} - \bar{\xi}^{-2})$ (i.e., that all monomers share a common

localization length). The hypothesis of Ref. [34] does not satisfy the stationarity condition, and therefore only provides a variational bound on the free energy. That our result for the order parameter is a stationary point of the free energy, rather than merely a variational bound, is a feature of considerable significance. The consequent exact vanishing of the linear term in the expansion of the free energy functional Eq. (2.64) in powers of the departure from the known stationary value streamlines further analysis of, e.g., linear stability, fluctuations, correlations, and response to perturbations.

2.7 Comparison with numerical simulations

The purpose of the present section is to compare the results just presented with the results of extensive molecular dynamics simulations, performed by Barsky and Plischke [86, 87]. These simulations address the amorphous solidification transition in the context of randomly crosslinked macromolecular systems, by using an off-lattice model of macromolecules interacting via a Lennard-Jones potential. It should be emphasized that there are substantial differences between ingredients and calculational schemes used in the analytical and simulational approaches. In particular, the analytical approach: (i) invokes the replica technique; (ii) retains inter-particle interactions only to the extent that macroscopically inhomogeneous states are disfavored (i.e., the one-replica sector remains stable at the transition); (iii) neglects order-parameter fluctuations, its conclusions therefore being independent of the space-dimension; and (iv) is solved via an Ansatz, which is not guaranteed to capture the optimal solution. Nevertheless, and rather strikingly, the simulations yield an essentially identical picture for the transition to and properties of the amorphous solid state, inasmuch as they indicate that (i) there exists a (crosslink–density controlled) continuous phase transition from a liquid state to an amorphous solid state; (ii) the critical crosslink density is very close to one crosslink per macromolecule; (iii) q varies linearly with the density of crosslinks, at least

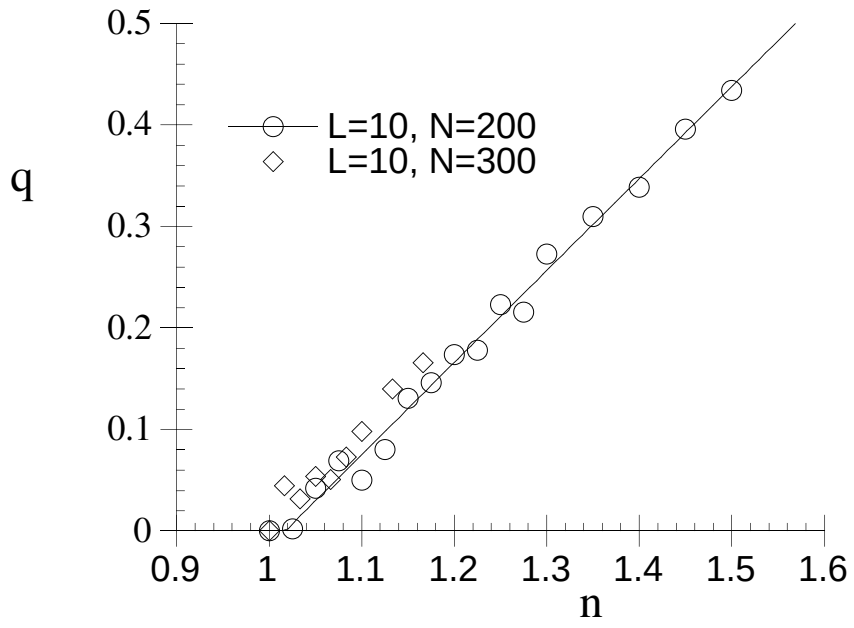

Figure 2.4: Molecular dynamics results for the gel fraction as a function of the crosslink density. Localized fraction q as a function of the number of crosslinks per macromolecule n, as computed in molecular dynamics simulations by Barsky and Plischke (1997, unpublished). L is the number of monomers in each macromolecule; N is the number of macromolecules in the system. The straight line is a linear fit to the $N = 200$ data. Note the apparent existence of a continuous phase transition near $n = 1$, as well as the apparent linear variation of q with n, both features being consistent with the mean-field description.

in the vicinity of this transition (see Fig. 2.4); (iv) when scaled appropriately (i.e., by the mean localization length), the simulation data for the distribution of localization lengths exhibit very good collapse on to a universal scaling curve for the several (near-critical) crosslink densities and macromolecule lengths considered (see Figs. 2.5 and 2.6); and (v) the form of this universal scaling curve appears to be in remarkably good agreement with the precise form of the analytical prediction for this distribution.

Let us now look more critically at the comparison between the results of the simulation and the mean-field theory. With respect to the localized fraction, the theory, as it stands at present, is only capable of showing the linearity of the dependence, near the transition, on

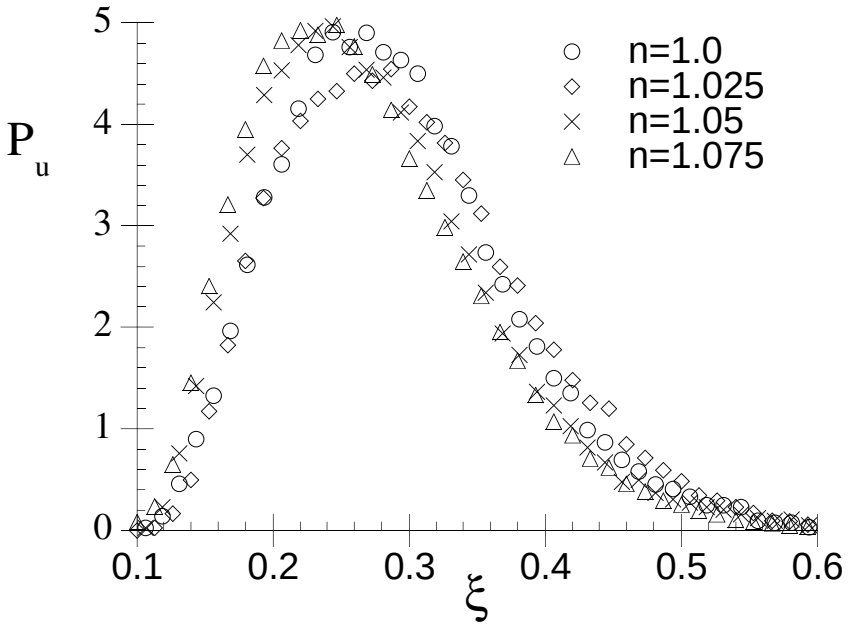

Figure 2.5: Molecular dynamics results for the probability distribution of localization lengths. Unscaled probability distribution P_{u} of localization lengths ξ (in units of the linear system size), as computed in molecular dynamics simulations by Barsky and Plischke (1997, unpublished). In the simulations the number of segments per macromolecule is 10; and the number of macromolecules is 200.

the excess crosslink density, leaving undetermined the proportionality factor. The simulation results are consistent with this linear dependence, giving, in addition, the amplitude. There are two facets to the universality of the distribution of localization lengths. First, that the distributions can, for different systems and different crosslink densities, be collapsed on to a universal scaling curve, is verified by the simulations, as pointed out above. Second, the question of how the scaling parameter depends on the excess crosslink density is difficult to address in current simulations, because the dynamic range for the mean localization length accessible in them is limited, so that its predicted divergence at the transition is difficult to verify.

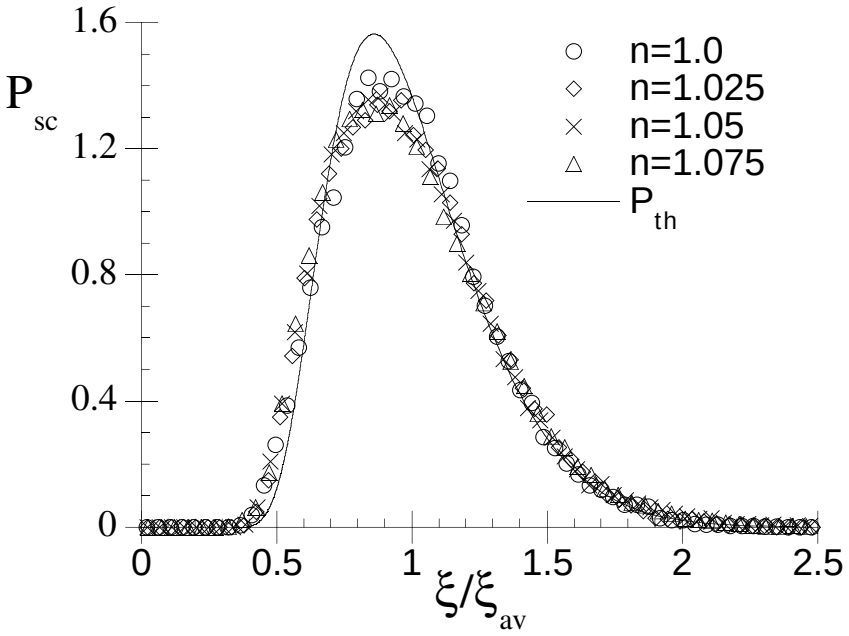

Figure 2.6: Molecular dynamics results for the scaled probability distribution of localization lengths. Probability distribution $P_{\rm s}$ of localization lengths ξ, scaled with the sample-average of the localization lengths $\xi_{\rm av}$, as computed in molecular dynamics simulations by Barsky and Plischke (1997, unpublished). Note the apparent collapse of the data on to a single universal scaling distribution, as well as the good quantitative agreement with the mean-field prediction for this distribution (solid line). In the simulation the number of segments per macromolecule is 10; and the number of macromolecules is 200. The mean-field prediction for $P_{\rm sc}(\xi/\xi_{\rm av})$ is obtained from the universal scaling function $\pi(\theta)$ by $P_{\rm sc}(y) = (2s/y^3)\,\pi(s/y^2)$, where the constant $s \simeq 1.224$ is fixed by demanding that $\int_0^\infty dy\, y\, P_{\rm sc}(y) = 1$.

2.8 Universality and Landau theory

In this section a brief review is presented of some theoretical developments that have emerged essentially as extensions of the theory presented in this chapter. This includes both semi-microscopic models of other systems and also a Landau theory approach. This Landau theory applies both to randomly crosslinked macromolecules and to other systems that undergo similar amorphous solidification transitions. As the Landau theory is technically simpler than any of the semi-microscopic theories for specific systems, it will be used in the next

section to help construct a proof of the thermodynamic stability of the amorphous solid state.

The theory of the vulcanization transition for randomly crosslinked macromolecular systems has been extended to study randomly *end-linked* macromolecular systems [36], and also randomly crosslinked *manifolds* (i.e., higher dimensional objects) [35]. In the original case of randomly crosslinked macromolecular systems, the macromolecules were modeled as flexible, with a short-ranged excluded-volume interaction, and the crosslinks were imposed at random arc-length locations. By contrast, in the case of *end-linked* systems, although the excluded-volume interaction remained the same, the macromolecules were now modeled as either flexible or stiff, and the random linking was restricted to the ends of the macromolecules. Despite the differences between the unlinked systems and the styles of linking, in all cases identical critical behavior has been obtained in mean-field theory, right down to the precise form of the statistical distribution of scaled localization lengths.

Perhaps even more strikingly, in the numerical simulations of randomly crosslinked macromolecular systems discussed in the previous section, Barsky and Plischke [86, 87] have employed an off-lattice model of macromolecules interacting via a Lennard-Jones potential. Yet again, an essentially identical picture has emerged for the transition to and properties of the amorphous solid state, despite the substantial differences between physical ingredients incorporated in the simulation and in the analytical theory.

In the light of these observations, it was proposed by Peng, Castillo, Goldbart and Zippelius [88] that a common theoretical formulation of the amorphous solidification transition (of which the vulcanization transition is a prime example) should exist that exhibits the emergent collective properties of all these systems that are model-independent, and therefore provide useful predictions for a broad class of experimentally realizable systems. In Ref. [88], they presented two different (but related) formulations: one of them is a Landau theory written in terms of a replica order parameter and derived from symmetry considera-

tions and physical assumptions, but without resorting to microscopic models; the other one is also a Landau theory, but it is written in terms of the distribution of random static density fluctuations of Eq. (2.26, and is derived from the previous one. These two formulations give rise to identical physical results, but only the first one will be discussed here.

2.8.1 Replica Landau theory: Order parameter, symmetries, and free energy

Here we briefly review the physical arguments that were used in the construction of the replica Landau theory for a system that undergoes a liquid–amorphous-solid transition that is controlled by the density of random constraints imposed on it.

In a system characterized by static random density fluctuations, the appropriate order parameter is a generalization of the one used for randomly crosslinked macromolecules:

$$\Omega_{\mathbf{k}^1,\mathbf{k}^2,\cdots,\mathbf{k}^g} \equiv \left[\frac{1}{N}\sum_{i=1}^{N}\langle e^{i\mathbf{k}^1\cdot\mathbf{c}_i}\rangle_\chi\langle e^{i\mathbf{k}^2\cdot\mathbf{c}_i}\rangle_\chi\cdots\langle e^{i\mathbf{k}^g\cdot\mathbf{c}_i}\rangle_\chi\right], \tag{2.120}$$

where now N is the total number of particles, $\mathbf{c}_i$ (with $i = 1,\ldots,N$) is the position of particle i, the wave-vectors $\mathbf{k}^1,\mathbf{k}^2,\cdots,\mathbf{k}^g$ are arbitrary, $\langle\cdots\rangle_\chi$ denotes a thermal average for a particular realization χ of the disorder, and $[\cdots]$ represents averaging over the disorder. The particles considered correspond to the thermodynamically independent units of the system. For example, they can be all the monomers, or at least all portions of length ℓ of polymer chain (in the case of flexible macromolecules); or only the ends of the polymers (in the case of rigid macromolecules that can be only end-linked).

Under the Deam-Edwards assumption [20] that the statistics of the disorder is determined by the instantaneous correlations of the unconstrained system, obtaining disorder averages with the replica technique involves working with the $n \to 0$ limit of systems of $n+1$, as opposed to n, replicas. The additional replica, labeled by $\alpha = 0$, represents the degrees of freedom of the original system before adding the constraints, or, equivalently, describes the

constraint distribution.

In the replica formalism, the order parameter is represented by the analog of Eq. (2.34):

$$\Omega_{\hat{k}} \equiv \Big\langle \frac{1}{N} \sum_{i=1}^{N} \exp\left(i\hat{k} \cdot \hat{c}_i\right) \Big\rangle_{n+1}^{\mathrm{P}}. \tag{2.121}$$

In the Landau theory, the order parameter in the one-replica sector represents spatial variations in the disorder-averaged mean particle-density, and is always taken to be strictly zero.

In the stationary-point approximation, the disorder-averaged free energy f (per particle and space dimension) is given by [32, 89, 72]:

$$f = \lim_{n \to 0} \min_{\{\Omega_{\hat{k}}\}} \mathcal{F}_n(\{\Omega_{\hat{k}}\}), \tag{2.122}$$

The Landau free energy functional is constructed from the following assumptions, which generalize properties of the vulcanization transition: (i) there is no external potential, and therefore no term linear in the order parameter in the Landau free energy, (ii) the amorphous solidification transition is continuous, and therefore it is sufficient to keep only terms quadratic and cubic in the order parameter to construct the Landau free energy, (iii) any localization near the transition should occur only on long length scales, and therefore it is permissible to Taylor expand the coefficients in the free energy functional to low orders in the wavevectors, (iv) by analyticity and rotational invariance, only functions of $\{|\mathbf{k}^0|^2, \ldots, |\mathbf{k}^n|^2\}$ can appear in the coefficients, and (v) by the permutation symmetry among the replicas, the wavevectors can only enter the expressions for the coefficients in the form $\hat{k}^2$.

These considerations lead to the following form for the Landau free energy functional:

$$nd\mathcal{F}_n(\{\Omega_{\hat{k}}\}) = \overline{\sum}_{\hat{k}} \Big(-\epsilon + \frac{|\hat{k}|^2}{2} \Big) |\Omega_{\hat{k}}|^2 - \overline{\sum}_{\hat{k}_1 \hat{k}_2 \hat{k}_3} \Omega_{\hat{k}_1} \Omega_{\hat{k}_2} \Omega_{\hat{k}_3} \delta_{\hat{k}_1 + \hat{k}_2 + \hat{k}_3, \hat{0}}\,. \tag{2.123}$$

Here ϵ is the control parameter, which is proportional to the amount by which the constraint density exceeds its value at the transition. As before, the symbol $\overline{\sum}$ denotes a sum over replicated wave vectors $\hat{k}$ in the higher-replica sector.

2.8.2 Stationary-point approximation

Demanding that variations of $\mathcal{F}_n(\{\Omega_{\hat{k}}\})$ with respect to the order parameter should be zero results in the stationary point equations equations:

$$0 = 2(-\epsilon + \frac{1}{2}|\hat{k}|^2)\Omega_{\hat{k}} - 3\overline{\sum_{\hat{k}_1\hat{k}_2\in R^{\mathrm{u}}}}\Omega_{\hat{k}_1}\,\Omega_{\hat{k}_2}\,\delta_{\hat{k}_1+\hat{k}_2,\hat{k}}\,. \tag{2.124}$$

The stationary-point equations Eq. (2.124) are satisfied (in the limit $n \to 0$) by the hypothesis Eqs. (2.36), provided that

$$\begin{aligned} 0 = \delta_{\tilde{\mathbf{k}},\mathbf{0}}\Big\{ & 2\left(3q^2 - \epsilon q + q\hat{k}^2/2\right)\int_0^\infty d\tau\, p(\tau)\, \mathrm{e}^{-\hat{k}^2/2\tau} \\ & - 3q^2\int_0^\infty d\tau_1\, p(\tau_1)\int_0^\infty d\tau_2\, p(\tau_2)\,\mathrm{e}^{-\hat{k}^2/2(\tau_1+\tau_2)}\Big\}\,. \end{aligned} \tag{2.125}$$

By taking the limit $\hat{k}^2 \to 0$, the above equation reduces to a condition for the gel fraction:

$$0 = -2q\epsilon + 3q^2. \tag{2.126}$$

For negative or zero ϵ, corresponding to crosslink densities less than or equal to the critical value, the only physical solution is $q = 0$, corresponding to the liquid state. For positive ϵ, corresponding to crosslink densities in excess of the critical value, there are two solutions. One, unstable, is the continuation of the liquid state $q = 0$; the other, stable, corresponds to a nonzero gel fraction, i.e., to the amorphous solid state,

$$q = \frac{2}{3}\epsilon. \tag{2.127}$$

As mentioned above, the gel fraction, and consequently the order parameter, change continuously at the transition, which means that at $\epsilon = 0$ there is a continuous phase transition between the liquid and the amorphous solid state (thus justifying *a posteriori* the hypothesis that was made when the Landau theory was proposed).

In the the amorphous solid state, by assuming that Eq. (2.126) is satisfied, Eq. (2.125) reduces to an equation involving only the distribution of (inverse square) localization lengths

$p(\tau)$:

$$\frac{\tau^2}{2}\frac{dp}{d\tau} = \Big(\frac{\epsilon}{2} - \tau\Big)p(\tau) - \frac{\epsilon}{2}\int_0^\tau d\tau_1\, p(\tau_1)\, p(\tau - \tau_1). \tag{2.128}$$

The form of this equation immediately suggests that, to this level of approximation, all ϵ dependence can be eliminated by the scaling [90]:

$$p(\tau) = (2/\epsilon)\,\pi(\theta); \qquad \tau = (\epsilon/2)\,\theta. \tag{2.129}$$

Thus, the universal scaling function $\pi(\theta)$ satisfies

$$\frac{\theta^2}{2}\frac{d\pi}{d\theta} = (1-\theta)\,\pi(\theta) - \int_0^\theta d\theta'\pi(\theta')\pi(\theta-\theta'), \tag{2.130}$$

together with the normalization condition

$$1 = \int_0^\infty d\theta\,\pi(\theta). \tag{2.131}$$

This normalization condition directly follows from the fact that the order parameter of Eq. (2.24) has to be unity at the origin.

Eqs. (2.130) and (2.131) are respectively identical to Eqs. (2.108) and (2.109). This implies that the order parameter obtained in the Landau theory for the amorphous solid state is the same as the one obtained in the semi-microscopic theory for randomly crosslinked macromolecules, i.e., the one described by Eqs. (2.115) and (2.116).

2.9 Concluding remarks

In the present chapter we have presented a theoretical description of the physical properties of systems of macromolecules that have been randomly crosslinked. Our focus has been on the equilibrium properties of such systems, especially in the regime of the vulcanization transition. Up to now, the results we have obtained refer mainly to the structure of the amorphous solid state.

To construct our picture of their physical properties, we have developed a field-theoretic representation of the statistical mechanics of randomly crosslinked macromolecular systems. The order parameter capable of distinguishing between the various candidate states (liquid, amorphous, crystalline solid and globular) easily fits into this representation. The presence of quenched as well as annealed variables has been addressed by invoking the replica technique. We have derived the stationary-point equation from the free energy functional of this field-theoretic representation, this equation being equivalent to the self-consistent mean-field equation satisfied by the order parameter. While it is not apparent how one might obtain the most general solution for the order parameter, we have proposed a physically motivated form for it, which allows for the possibilities of a liquid state and an amorphous solid state. This form is parametrized by the fraction of localized monomers, together with the statistical distribution of localization lengths. In fact, this form turns out to yield an exact solution of the stationary-point equation. It should be noted that we are only able to proceed with the calculation in the vicinity of the amorphous solidification transition, where the typical localization length is substantially larger than the radius of gyration of an isolated non–self-interacting macromolecule.

The quantitative picture of randomly crosslinked macromolecular systems that emerges from our field-theoretic representation has the following primary elements. At the mean-field level of approximation there is, for any crosslink density, a stationary point of the free energy functional that corresponds to the liquid state. However, for crosslink densities greater than a certain critical value, this liquid state is unstable. At this critical crosslink density a new stationary point of the free energy functional bifurcates continuously from the liquid-state stationary point. This new stationary point, which is characterized by a nonzero gel-fraction and a specific distribution of localization lengths, corresponds to the amorphous solid state. The transition between the liquid and amorphous solid states is therefore continuous: in particular, the gel fraction and the inverse-square of the typical localization length both

increase from zero linearly with the excess of the crosslink density from its critical value. Moreover, the entire distribution of (inverse-square) localization lengths has a scaling form determined by a universal function of a single variable (which only need be computed once for all near-critical crosslink densities). Detailed results for the gel fraction and the distribution of localization lengths have been given.

There are several other contexts in which one can make use of the circle of ideas that we have been using to explore the physical properties of randomly crosslinked macromolecular systems.

First, as we mentioned in Sec. 2.8, one can apply them to a wide class of random-network–forming systems. Indeed, a straightforward extension [35] of the present work yields a theory of randomly crosslinked manifolds (i.e., higher-dimensional analogs of linear macromolecules [91, 92]). Similarly, one can address macromolecular networks formed via a random *endlinking* (rather than crosslinking) process, in which one end from each of several randomly selected macromolecules is linked to one other [36]. One can also consider networks formed via the (freely-jointed) endlinking of rigid or semi-flexible rods [36], subjects that are of particular relevance to certain biological structures. All these examples, together with the case of randomly crosslinked flexible macromolecules, are described by a Landau theory [88] reviewed in Sec. 2.8.

This circle of ideas has also been used to develop a statistical-mechanical theory of continuous random (atomic or molecular) networks, and thus to develop a view of the structural glass transition [37]. In this case, what emerges is a picture of glass-formation in which atomic or molecular units are (permanently chemically) bonded together at random, so as to develop an infinite network. Not only do the translational freedoms of the units become localized but also do the orientational freedoms.

Chapter 3

Stability of the amorphous solid state near the amorphous solidification transition

3.1 Introduction

In Chap. 2 a physically plausible candidate for the amorphous solid state was obtained, and its structural properties were discussed in detail. This amorphous solid state was first proposed as a variational hypothesis and later shown to be an exact solution to the stationary-point equations for the free energy functional. However, such stationary points may be unstable, in which case they do not provide an acceptable description of an equilibrium thermodynamic state. The aim of the present Chapter is to show that the proposed amorphous solid state stationary point indeed is locally *stable*, at least near the amorphous solidification transition.

The amorphous solid state is highly symmetric: although it breaks translational invariance and rotational invariance at the microscopic level (as a fraction of the molecules

are localized), the disorder averaged density remains spatially uniform, and the state remains macroscopically translationally (and rotationally) invariant (MTI), and also replica-symmetric.

This situation bears some resemblance to what happens in another system under the effects of quenched randomness, namely the Sherrington-Kirkpatrick (SK) model for spin glasses [55]. In the SK model with no external magnetic field and symmetric spin-spin couplings, the spin glass state found by Sherrington and Kirkpatrick is characterized by the presence of nonzero frozen-in magnetization at the level of individual spins, but the disorder averaged total magnetization remains zero in the spin glass phase, and the solution is replica symmetric.

It was shown by de Almeida and Thouless [93] that this highly symmetric SK stationary point is locally unstable for all temperatures below the spin glass transition. In fact, the SK stationary point is certain to be incorrect at very low temperatures, as it gives rise to a negative entropy in the limit of zero temperature. This difficulty was resolved by Parisi [94], who found a replica-symmetry-breaking solution to the stationary-point equations. This solution has a positive entropy at all positive temperatures and is locally marginally stable [95].

By analogy to the spin glass case, it would not be entirely surprising if in systems undergoing a liquid–amorphous-solid transition because of the effect of random constraints, the stationary point of the free energy proposed above, corresponding to the amorphous solid state turned out to be locally unstable, and in need of being superseded by a less symmetric solution of the stationary point equations. However, it is shown in this Chapter that the amorphous solid state proposed above is locally stable near the liquid-amorphous solid transition. More specifically, the Hessian matrix that describes changes of the free energy functional for fluctuations around the stationary point corresponding to the amorphous solid state is computed, and it is shown that, to linear order in the excess constraint density, all eigenvalues of the Hessian matrix are positive, except for a unique (and expected) zero (or

Goldstone) mode associated with the spontaneously broken continuous translational symmetry of the system. In order to show this, a description is constructed for the space of fluctuations around the stationary point that allows the eigenvalue problem in replicated space to be reduced, in essence, to an integral eigenvalue equation in one dimension.

Only the region near the transition is addressed here. In this region, the free energy functionals for the Landau theory and for the semi-microscopic theory of randomly crosslinked macromolecules differ only in terms that do not play any role in the mean field theory. In the study of fluctuations, these additional terms do make the algebra slightly simpler for the Landau theory, without altering the physical picture. For this reason, the Landau theory is addressed first, and the semi-microscopic theory subsequently. The slight difference between the Landau theory and the semi-microscopically derived theory is due to the fact that, while in the former only states with a spatially homogeneous disorder averaged particle density are admitted in the theory, in the latter states having spatial variations are (in principle) allowed but ultimately are suppressed by the repulsive inter-particle interactions.

The rest of this chapter is organized as follows. In Sec. 3.2 the Hessian matrix for the amorphous solid state is computed in the context of the Landau theory described in Sec. 2.8, and the continuous symmetry of the problem is exploited to choose a basis set that significantly simplifies the eigenvalue equation for the Hessian matrix. In Sec. 3.3 positive lower bounds are found for all the eigenvalues of the Hessian matrix, except for one zero eigenvalue that is present due to the spontaneously broken continuous symmetry. In Sec. 3.4 these results are extended to the case of the semi-microscopically derived free energy functional for randomly crosslinked macromolecules, and in Sec. 3.5 some concluding remarks are presented.

An article on the research discussed in the present chapter is in preparation [43].

3.2 Landau theory: Hessian matrix

In this section the stability matrix for the Landau theory is computed, and the symmetries of the system are exploited to simplify its diagonalization. In essence, the simplification goes along the same lines as the separation of radial and angular variables in the Schroedinger equation for a particle in central potential in quantum mechanics. There are technical differences, of course, since the space in the present case has a dimensionality that depends on the number of replicas.

3.2.1 Hessian matrix elements

Consider any variation of the $\{\Omega_{\hat{k}}\}$ around a stationary point. To first order, the variation of the free energy functional has to be zero. We see from Eq. (2.123) that the lowest order variation $\delta[\mathcal{F}_n(\{\Omega_{\hat{k}}\})]$ is given by

$$\delta[nd\mathcal{F}_n(\{\Omega_{\hat{k}}\})] = \overline{\sum}_{\hat{k}} \left(-\epsilon + \frac{|\hat{k}|^2}{2}\right) |\delta\Omega_{\hat{k}}|^2 - 3\overline{\sum}_{\hat{k}_1\hat{k}_2\hat{k}_3} \delta_{\hat{k}_1+\hat{k}_2+\hat{k}_3,\hat{0}}\, \Omega_{\hat{k}_1}\, \delta\Omega_{\hat{k}_2}\, \delta\Omega_{\hat{k}_3} + \mathcal{O}((\delta\Omega)^3). \tag{3.1}$$

Now consider expanding around the liquid state for any value of ϵ. In this case, the variation reduces, to quadratic order, to

$$\delta^{(2)}[nd\mathcal{F}_n(\{\Omega_{\hat{k}}\})] = \overline{\sum}_{\hat{k}} \left(-\epsilon + \frac{|\hat{k}|^2}{2}\right) |\delta\Omega_{\hat{k}}|^2, \tag{3.2}$$

which evidently indicates that the liquid state is stable for $\epsilon < 0$ and unstable for $\epsilon > 0$. For $\epsilon > 0$ the only candidate for a stable thermodynamic state is the amorphous solid discussed in Chap. 2. From now on we focus only on this state.

By inserting the value of the order parameter, Eqs. (2.115) and (2.116), into the three-wavevector sum in Eq. (3.1), we obtain:

$$\begin{aligned}
&\overline{\sum}_{\hat{k}_1\hat{k}_2\hat{k}_3} \delta_{\hat{k}_1+\hat{k}_2+\hat{k}_3,\hat{0}}\; \delta_{\tilde{\mathbf{k}}_1,\mathbf{0}}\, \frac{2\epsilon}{3}\, \omega\left(\sqrt{2\hat{k}_1^2/\epsilon}\right) \delta\Omega_{\hat{k}_2}\, \delta\Omega_{\hat{k}_3} \\
&\quad = \overline{\sum}_{\hat{k}_2\hat{k}_3} \delta_{\tilde{\mathbf{k}}_2+\tilde{\mathbf{k}}_3,\mathbf{0}}\, \frac{2\epsilon}{3}\, \omega\left(\sqrt{\frac{2}{\epsilon}\left(\hat{k}_2+\hat{k}_3\right)^2}\right) \delta\Omega_{\hat{k}_2}\, \delta\Omega_{\hat{k}_3} - \frac{2\epsilon}{3}\overline{\sum}_{\hat{k}} |\delta\Omega_{\hat{k}}|^2 + \mathcal{O}((\delta\Omega)^3)
\end{aligned} \tag{3.3}$$

Thus we can rewrite the quadratic part of the variation in terms of the Hessian matrix $H_{\hat{q},\hat{q}'}$:

$$\delta^{(2)}\left[nd\mathcal{F}_n(\{\Omega_{\hat{q}}\})\right] = \sum_{\hat{q},\hat{q}'} H_{\hat{q},\hat{q}'}\,\delta\Omega_{\hat{q}}\,\delta\Omega_{-\hat{q}'} \tag{3.4}$$

where H is defined by

$$H_{\hat{k},\hat{l}} \equiv \frac{1}{2!}\frac{\delta^2\left[nd\mathcal{F}_n\right]}{\delta\Omega_{\hat{k}}\,\delta\Omega_{-\hat{l}}}. \tag{3.5}$$

(For later convenience, we have chosen a definition that differs from the standard one by a factor of 1/2.) More explicitly, we have

$$H_{\hat{k},\hat{l}} \;=\; \delta_{\hat{k},\hat{l}}\left(\epsilon + \frac{\hat{k}^2}{2}\right) - \delta_{\tilde{\mathbf{k}},\tilde{\mathbf{l}}}2\epsilon\int_0^\infty d\theta\,\pi(\theta)\mathrm{e}^{-(\hat{k}-\hat{l})^2/\epsilon\theta} + \mathcal{O}(\epsilon^2). \tag{3.6}$$

As we are interested only in the matrix elements to leading (i.e., first) order in ϵ, we neglect higher orders from now on.

3.2.2 Exploiting the symmetries: change of basis

We now exploit the symmetries of the problem in order to simplify the diagonalization the Hessian matrix. As a direct consequence of the invariance of the free energy functional under translations, as well as the MTI property of the amorphous solid state, the matrix element $H_{\hat{k},\hat{l}}$ only connects wavevectors such that $\tilde{\mathbf{k}} = \tilde{\mathbf{l}}$. This already reduces the complexity of the problem by making the Hessian block diagonal.

As $H_{\hat{k},\hat{l}}$ depends on $\hat{k}^2$, $\hat{l}^2$, and $\hat{k}\cdot\hat{l}$, one could expect to find a symmetry under rotations in $(n+1)d$ dimensions that would simplify the diagonalization of H still further. However, the factor $\delta_{\tilde{\mathbf{k}},\tilde{\mathbf{l}}}$ is not invariant under those rotations. Instead, H only displays a rotational symmetry in nd dimensions, but this will enable us to simplify the problem in much the same way as is commonly done for central potentials in quantum mechanics.

In order to make this symmetry explicit, we choose a *fixed* matrix $T \in SO((1+n)d)$ such that, for any vector $\hat{v}$ in replicated space, we explicitly isolate $\tilde{\mathbf{v}}$ from the other nd

independent coordinates, which we call $\breve{v}$:

$$T\hat{v} = \begin{pmatrix} \frac{\tilde{\mathbf{v}}}{\sqrt{1+n}} \\ \breve{v} \end{pmatrix}. \tag{3.7}$$

Due to T being orthogonal, scalar products are simple to write in the new coordinates

$$\hat{v} \cdot \hat{w} = \frac{\tilde{\mathbf{v}} \cdot \tilde{\mathbf{w}}}{1+n} + \breve{v} \cdot \breve{w} \tag{3.8}$$

In the new coordinates, we have

$$H_{\tilde{\mathbf{k}}\breve{k},\tilde{\mathbf{l}}\breve{l}} = \delta_{\tilde{\mathbf{k}},\tilde{\mathbf{l}}}\{\delta_{\breve{k},\breve{l}}[\epsilon + \frac{1}{2}(\breve{k}^2 + \frac{\tilde{\mathbf{k}}^2}{1+n})] - 2\epsilon \int_0^\infty d\theta\, \pi(\theta) \mathrm{e}^{-(\breve{k}-\breve{l})^2/\epsilon\theta}\}. \tag{3.9}$$

The above expression, taken naively, would immediately tell us that the Hessian is invariant under rotations in nd dimensions:

$$\forall R \in SO(nd): \qquad H_{\tilde{\mathbf{k}}R\breve{k},\tilde{\mathbf{l}}R\breve{l}} = H_{\tilde{\mathbf{k}}\breve{k},\tilde{\mathbf{l}}\breve{l}}. \tag{3.10}$$

However, there is an important caveat. Our Hessian is only defined for wavevectors in the higher replica sector, but the proposed rotations can take a vector in the higher replica sector and transform it into a vector in the one replica sector. For the moment we are going to ignore this difficulty, and simply diagonalize the matrix obtained by using Eq. (3.6) as its definition, with $\hat{k}$ and $\hat{l}$ taking *any* nonzero values, both in the higher and in the lower replica sector. After doing that, we will return to the issue of the one replica sector. Let us just anticipate part of the results by mentioning that in the replica limit $n \to 0$, the only effect of this extension of the Hessian on its spectrum of eigenvalues is the addition of one spurious eigenvalue corresponding to a fluctuation in the one replica sector. We will use the self explanatory names "original Hessian" and "extended Hessian" whenever it is necessary to make such distinctions.

For this modified problem, the $SO(nd)$ symmetry holds, and Eq. (3.10) is correct without caveats.

In what follows, we will use the same strategies as in the diagonalization of the quantum mechanical hamiltonian for a particle in a central potential. The role of the hamiltonian will be played by $H_{\hat{k},\hat{l}}$. We will also exploit the symmetries of the problem: the rotational symmetry in nd dimensional space will allow us to write each eigenfunction as a product of a radial part, that will be obtained by solving a one dimensional eigenvalue equation, and an angular part that will be simply a surface harmonic in nd dimensions. The quantity $\tilde{\mathbf{k}}$, which is exactly conserved by $H_{\hat{k},\hat{l}}$, will play the role of an additional conserved quantum number. We will obtain different eigenfunctions for each fixed value of $\tilde{\mathbf{k}}$.

We are going to work in the Hilbert space of complex functions of the variable $\hat{k}$. The scalar product in this space is defined as follows:

$$\langle f|g\rangle \equiv \frac{1}{V^n}\sum_{\hat{k}\neq\hat{0}} f^*(\hat{k})g(\hat{k}), \tag{3.11}$$

and simplifies in the thermodynamic limit to:

$$\begin{aligned}\langle f|g\rangle &\simeq V\int \frac{d\hat{k}}{(2\pi)^{(1+n)d}} f^*(\hat{k})g(\hat{k}) \\ &= V\int \frac{d\tilde{\mathbf{k}}d\breve{k}}{(1+n)^{d/2}(2\pi)^{(1+n)d}} f^*(\tilde{\mathbf{k}},\breve{k})g(\tilde{\mathbf{k}},\breve{k}).\end{aligned} \tag{3.12}$$

We define a basis set for this Hilbert space by

$$\varphi_{p\tilde{\mathbf{p}}\sigma}(\tilde{\mathbf{k}},\breve{k}) \equiv (1+n)^{d/4}(2\pi)^{nd/2}\delta_{\tilde{\mathbf{p}}\tilde{\mathbf{k}}}\delta(|\breve{k}|-p)p^{\frac{1-nd}{2}}S_\sigma(\phi_{\breve{k}}), \tag{3.13}$$

Here $S_\sigma(\phi)$ is a normalized surface harmonic defined on the unit sphere in nd-dimensional space [96] (surface harmonics are generalizations of spherical harmonics to space dimensions other than $d=3$). The notation $\phi_{\breve{k}} \equiv \breve{k}/|\breve{k}|$ denotes the unit nd-dimensional vector along the direction of $\breve{k}$. The elements of the basis set $\{\varphi_{p\tilde{\mathbf{p}}\sigma}\}$ are orthogonal and normalized under the scalar product of Eq. (3.11):

$$\langle\varphi_{p'\tilde{\mathbf{p}}'\sigma'}|\varphi_{p\tilde{\mathbf{p}}\sigma}\rangle = \delta(p'-p)\delta_{\tilde{\mathbf{p}}'\tilde{\mathbf{p}}}\delta_{\sigma',\sigma}. \tag{3.14}$$

As suggested above, we propose to write each eigenfunction for the problem in the form:

$$\begin{aligned}\psi_{r,\tilde{\mathbf{p}},\sigma}(\tilde{\mathbf{k}},\breve{k}) &= (1+n)^{d/4}(2\pi)^{nd/2}\delta_{\tilde{\mathbf{p}},\tilde{\mathbf{k}}}|\breve{k}|^{\frac{1-nd}{2}}R_r(|\breve{k}|)S_\sigma(\phi_{\breve{k}}),\\ &= \int_0^\infty dp\, R_r(p)\,\varphi_{p,\tilde{\mathbf{p}},\sigma}(\tilde{\mathbf{k}},\breve{k}),\end{aligned} \tag{3.15}$$

where the discrete δ function ensures that the eigenfunction is concentrated on points with a fixed value of $\tilde{\mathbf{k}}$, the surface harmonic S_σ gives the angular dependence on $\breve{k}$ and the radial function R_r gives the radial dependence on $\breve{k}$. Using the normalization condition for the basis set, we obtain the normalization condition for the radial part:

$$\int_0^\infty dk\,|R_r(k)|^2 = 1 \tag{3.16}$$

We now compute the matrix elements of the Hessian between the elements of the basis set $\{\varphi_{p,\tilde{\mathbf{p}},\sigma}\}$.

Consider first the part H^D of the Hessian that is diagonal in $\breve{k}$, i.e., the first term in the rhs of Eq. (3.9). This part is also diagonal in the basis $\{\varphi_{p,\tilde{\mathbf{p}},\sigma}\}$, with the matrix elements:

$$\langle\varphi_{p'\tilde{\mathbf{p}}'\sigma'}|H^D|\varphi_{p\tilde{\mathbf{p}}\sigma}\rangle = \delta(p'-p)\delta_{\tilde{\mathbf{p}}'\tilde{\mathbf{p}}}\delta_{\sigma',\sigma}[\epsilon+\frac{1}{2}(p^2+\frac{\tilde{\mathbf{p}}^2}{1+n})]. \tag{3.17}$$

The non-diagonal part H^O of the Hessian, given by the second term in the rhs of Eq. (3.9), has in the new basis matrix elements that only connect different values of the radial coordinate p, but are still diagonal in $\tilde{\mathbf{p}}$ and σ. It is shown in App. J that the matrix elements of H^O have the form

$$\langle\varphi_{p'\tilde{\mathbf{p}}'\sigma'}|H^O|\varphi_{p\tilde{\mathbf{p}}\sigma}\rangle = \delta_{\tilde{\mathbf{p}}',\tilde{\mathbf{p}}}\delta_{\sigma',\sigma}(-2\epsilon)\epsilon^{-1/2}C_n\,\eta^{(n)}_{|\sigma|}(p'/\sqrt{\epsilon},p/\sqrt{\epsilon}), \tag{3.18}$$

with

$$C_n \equiv (\epsilon/4\pi)^{nd/2}(1+n)^{-d/2} \tag{3.19}$$

and

$$\eta^{(n)}_l(x',x) \equiv 2\sqrt{x'x}\int_0^\infty \frac{d\theta\,\pi(\theta)}{\theta^{1-nd/2}}\,\mathrm{e}^{-(x'^2+x^2)/\theta}\,I_{l-1+nd/2}(\frac{2x'x}{\theta}), \tag{3.20}$$

where $I_\nu(x)$ is the modified Bessel function of order ν. The label $l(\equiv|\sigma|)$ is the degree of the surface harmonic S_σ (each surface harmonic is a homogeneous trigonometric polynomial). The constant C_n satisfies the condition

$$\lim_{n\to 0} C_n = 1, \tag{3.21}$$

which makes it disappear from the eigenvalue equation in the replica limit. The kernel function $\eta_l^{(n)}(x',x)$ is real and symmetric, and controls the non-diagonal nature of the matrix elements. Due to the positivity of $I_\nu(y)$ for $\nu \geq -1$ and $y > 0$, $\eta_l^{(n)}(x',x)$ is positive for $xx' > 0$. For $xx' = 0$, $\eta_l^{(n)}(x',x)$ vanishes, except if $l = 0$ and $nd > 0$, in which case it is divergent.

Since both H^D and H^O are diagonal on the $\tilde{\mathbf{p}}$ and σ labels, the eigenvalue equation for the Hessian:

$$H|\psi\rangle = \kappa|\psi\rangle \tag{3.22}$$

can now be simplified to a radial equation:

$$\begin{aligned} \kappa R(p) &= \int_0^\infty dp' \,\langle\varphi_{p\tilde{\mathbf{p}}\sigma}|H|\varphi_{p'\tilde{\mathbf{p}}\sigma}\rangle R(p'), \\ &= [\epsilon + \frac{1}{2}(p^2 + \frac{\tilde{\mathbf{p}}^2}{1+n})]R(p) - 2\epsilon C_n \int_0^\infty \frac{dp'}{\sqrt{\epsilon}}\,\eta_{|\sigma|}^{(n)}(p/\sqrt{\epsilon}, p'/\sqrt{\epsilon})\; R(p'). \end{aligned} \tag{3.23}$$

This radial equation can be simplified further by the rescaling:

$$\begin{aligned} \zeta &= \frac{1}{\epsilon}[\kappa - (\epsilon + \frac{\tilde{\mathbf{p}}^2}{2(1+n)})], \\ x &= p/\sqrt{\epsilon}, \qquad u(x) = \epsilon^{1/4} R(\sqrt{\epsilon}x), \end{aligned} \tag{3.24}$$

which removes the ϵ dependence from the eigenvalue equation, thus making both the eigenvalue ζ and the eigenfunction $u(x)$ ϵ-independent:

$$\zeta u(x) = \frac{x^2}{2}u(x) - 2\,C_n \int_0^\infty dx'\,\eta_{|\sigma|}^{(n)}(x,x')\; u(x'). \tag{3.25}$$

In the replica limit $n \to 0$ the radial equation reduces to:

$$\zeta u(x) = \frac{x^2}{2}u(x) - 2\int_0^\infty dx'\,\eta_{|\sigma|}^{(0)}(x,x')\; u(x'). \tag{3.26}$$

In most cases, this limit is straightforward, because $\eta^{(n)}_{|\sigma|}(x,x')$ smoothly converges to $\eta^{(0)}_{|\sigma|}(x,x')$. The only exception is the case of $|\sigma| = 0$ near the origin, in which the limit $n \to 0$ for $\eta^{(n)}_{|\sigma|}(x,x')$ is singular. In Sec. 3.3.3 we show, however, that the only difference between the limit for $n \to 0$ of the eigenvalue spectrum of Eq. (3.25) and the eigenvalue spectrum of Eq. (3.26) is that in the later the spurious eigenvalue corresponding to the 1rs is removed. For the moment, then, we only consider Eq. (3.26).

Both of the above equations are eigenvalue equations for Hermitian operators. This guarantees the existence of a basis of eigenfunctions, all of them with real eigenvalues. Notice also the nontrivial fact that the radial equation is well defined in the replica limit $n \to 0$.

The form of the radial eigenvalue equations tell us that the eigenfunctions and eigenvalues have to depend on the degree $l = |\sigma|$ of the respective surface harmonics (which plays a role analogous to the quantum number l in the central potential problem for a quantum mechanical particle), and on an additional label r, playing a role analogous to the radial quantum number in quantum mechanics. Therefore, the eigenvalues of the extended Hessian are given by the relation:

$$\kappa_{lr}(\tilde{\mathbf{k}}) = (1 + \zeta_{lr})\epsilon + \frac{\tilde{\mathbf{k}}^2}{2}. \tag{3.27}$$

Let us observe here that, since $I_{-1}(z) = I_1(z)$ for all values of the variable z, we have the equality

$$\eta^{(0)}_0(x,x') = \eta^{(0)}_2(x,x'), \tag{3.28}$$

which means that the radial equations for $|\sigma| = 0$ and $|\sigma| = 2$ are identical.

3.3 Landau theory: eigenvalues of the Hessian matrix

In this section we find positive lower bounds for all the eigenvalues of the Hessian in the Landau theory, except for the zero mode associated with translational symmetry. Since it is easier to work with scaled variables, let us first translate the condition $\kappa \geq 0$ in terms of ζ.

The relation between the two can be written in the form:

$$\frac{\kappa}{\epsilon} = \zeta + 1 + \frac{\tilde{\mathbf{k}}^2}{2\epsilon}. \tag{3.29}$$

Taking the worst possible case, corresponding to $\tilde{\mathbf{k}} = \mathbf{0}$, we get:

$$\kappa > 0 \iff \zeta + 1 > 0. \tag{3.30}$$

The right hand side of the equivalence sign is the condition that we are going to establish in what follows.

3.3.1 Obtaining the zero mode

We will first consider the eigenfluctuation associated with the translational symmetry, and show that it is a zero mode. From Eq. (2.69), the fluctuation can be written as

$$\begin{aligned} \delta\Omega_{\hat{k}} &= i\hat{k}\cdot\hat{a}\,(2\epsilon/3)\,\delta_{\tilde{\mathbf{k}},\mathbf{0}} \int_0^\infty d\theta\,\pi(\theta)\,\mathrm{e}^{-\hat{k}^2/\epsilon\theta}\,, \\ &= i\breve{k}\cdot\breve{a}\,(2\epsilon/3)\,\delta_{\tilde{\mathbf{k}},\mathbf{0}} \int_0^\infty d\theta\,\pi(\theta)\,\mathrm{e}^{-\breve{k}^2/\epsilon\theta}\,. \end{aligned} \tag{3.31}$$

The only angular dependence of $\delta\Omega_{\hat{k}}$ is given by the prefactor $\breve{k}\cdot\breve{a}$, which is a first degree polynomial in $\breve{k}$. This means that $|\sigma| = 1$. By taking the scalar product with the appropriate element [98] in the $\{\varphi_{p,\tilde{\mathbf{p}},\sigma}\}$ basis we obtain the radial function associated with $\delta\Omega_{\hat{k}}$:

$$\begin{aligned} R(k) &= \langle\varphi_{p,\tilde{\mathbf{p}}=\mathbf{0},\sigma=(1,0)}|\delta\Omega\rangle, \\ &= iA_n\epsilon k^{(1+nd)/2} \int_0^\infty d\theta\,\pi(\theta)\,\mathrm{e}^{-k^2/\epsilon\theta}\,, \end{aligned} \tag{3.32}$$

where A_n is a numerical prefactor, which we can ignore in what follows. Taking now the replica limit, and translating into scaled variables, we obtain:

$$u(x) = \sqrt{x} \int_0^\infty d\theta\,\pi(\theta)\,\mathrm{e}^{-x^2/\theta}\,. \tag{3.33}$$

We now show that this scaled radial function is a solution of the scaled radial eigenfunction equation Eq. (3.26) with $\zeta = -1$.

Let us first consider the diagonal term. By inserting the explicit form for $u(x)$ and later performing an integration by parts we obtain

$$\begin{aligned}\frac{x^2}{2}u(x) &= \frac{\sqrt{x}}{2}\int_0^\infty d\theta\,\pi(\theta)\theta^2\frac{d}{d\theta}(\mathrm{e}^{-x^2/\theta}),\\ &= -\frac{\sqrt{x}}{2}\int_0^\infty d\theta\,\mathrm{e}^{-x^2/\theta}\frac{d}{d\theta}[\theta^2\pi(\theta)],\\ &= -\sqrt{x}\int_0^\infty d\theta\,\mathrm{e}^{-x^2/\theta}[\frac{\theta^2}{2}\frac{d}{d\theta}\pi(\theta)+\theta\pi(\theta)]. \end{aligned} \tag{3.34}$$

Now the nondiagonal term gives us

$$\begin{aligned}&-2\int_0^\infty dx'\eta_1^{(0)}(x,x')\;u(x')\\ &= -2\int_0^\infty dx'd\theta d\theta' 2\sqrt{xx'}\frac{\pi(\theta)}{\theta}\mathrm{e}^{-(x^2+x'^2)/\theta}I_0(\frac{2xx'}{\theta})\sqrt{x'}\pi(\theta')\mathrm{e}^{-x'^2/\theta'}. \end{aligned} \tag{3.35}$$

By making use of the identity [99]

$$2\int_0^\infty dx x\mathrm{e}^{-ax^2}I_0(bx)=\frac{\mathrm{e}^{b^2/4a}}{a}, \tag{3.36}$$

we perform the integration over x' in Eq. (3.35), thus obtaining

$$\begin{aligned}-2\int_0^\infty dx'\eta_1^{(0)}(x,x')\;u(x') &= -2\sqrt{x}\int_0^\infty d\theta d\theta'\frac{\theta'\pi(\theta)\pi(\theta')}{\theta+\theta'}\mathrm{e}^{-x^2/(\theta+\theta')},\\ &= -\sqrt{x}\int_0^\infty d\theta\,\mathrm{e}^{-x^2/\theta}\int_0^\theta d\theta'\pi(\theta)\pi(\theta'). \end{aligned} \tag{3.37}$$

Finally, we combine Eqs. (3.34) and (3.37) to obtain

$$\begin{aligned}&u(x)+\frac{x^2}{2}u(x)-2\int_0^\infty dx'\eta_{|\sigma|}^{(0)}(x,x')\;u(x')\\ &= \sqrt{x}\int_0^\infty d\theta\,\mathrm{e}^{-x^2/\theta}[-\frac{\theta^2}{2}\frac{d}{d\theta}\pi(\theta)+(1-\theta)\pi(\theta)-\int_0^\theta d\theta'\pi(\theta)\pi(\theta')],\\ &= 0. \end{aligned} \tag{3.38}$$

The justification of the last equality comes from the factor in square brackets being zero by the stationary point condition, Eq. (2.108).

We have thus shown that Eq. (3.26) is satisfied by $u(x)$ with the eigenvalue $\zeta=-1$. By Eq. (3.29), this proves that the corresponding $\delta\Omega_{\hat{k}}$ given by Eq. (3.31) is an eigenvector of the Hessian with zero eigenvalue.

3.3.2 Positive lower bounds for the eigenvalues

Having obtained the zero mode for a specific kind of fluctuation, we now discuss general fluctuations in the order parameter field, and show that for all $|\sigma| \neq 1$, the eigenvalues are positive definite.

Consider one particular scaled radial eigenfunction $u(x)$. To simplify the argument we will temporarily switch to the normalization

$$\int_0^\infty dx\, |u(x)| = 1, \tag{3.39}$$

and we define the quantity

$$s(x) = \mathrm{sgn}(u(x)). \tag{3.40}$$

By combining Eqs. (3.26), (3.39), and (3.40), we write the eigenvalue in a slightly complicated but very useful form

$$\begin{aligned} \zeta &= \zeta \int_0^\infty dx\, |u(x)| = \int_0^\infty dx\, s(x)\, \zeta\, u(x) \\ &= \int_0^\infty dx\, s(x) \Big[\frac{x^2}{2} u(x) - 2 \int_0^\infty dx'\, \eta^{(0)}_{|\sigma|}(x,x')\, u(x') \Big] \\ &= \int_0^\infty dx\, \frac{x^2}{2}\, |u(x)| - 2 \int_0^\infty dx dx'\, \eta^{(0)}_{|\sigma|}(x',x)\, |u(x)|\, s(x)\, s(x'). \end{aligned} \tag{3.41}$$

(In the last line we interchanged the dummy variables x and x'.) From the above, it follows immediately that:

$$\zeta \geq \int_0^\infty dx\, \gamma_{|\sigma|}(x)\, |u(x)| \geq \bar{\gamma}_{|\sigma|}, \tag{3.42}$$

with the definitions:

$$\gamma_l(x) \equiv \frac{x^2}{2} - 2 \int_0^\infty dx'\, \eta^{(0)}_l(x',x), \tag{3.43}$$

$$\bar{\gamma}_l \equiv \inf_x \gamma_l(x). \tag{3.44}$$

Here the symbol inf indicates the greatest lower bound [100] for a set of real numbers.

It is convenient to write $\gamma_l(x)$ in terms of another function $\beta_l(v)$ as follows

$$\gamma_l(x) = \int_0^\infty d\theta\, \pi(\theta)\, \beta_l(x/\sqrt{\theta}) \tag{3.45}$$

$$\beta_l(v) \equiv \frac{v^2}{2\langle\theta^{-1}\rangle_\pi} - 4\int_0^\infty du\, \sqrt{uv}\mathrm{e}^{-(u^2+v^2)} I_{l-1}(2uv). \tag{3.46}$$

Here we have used the definition of average with respect to the scaled distribution $\pi(theta)$ that characterizes the order parameter

$$\langle f(\theta)\rangle_\pi \equiv \int_0^\infty d\theta\, \pi(\theta)\, f(\theta), \tag{3.47}$$

and we need in particular the numerical value

$$\langle\theta^{-1}\rangle_\pi = 0.881768 \tag{3.48}$$

Since $\pi(\theta)$ is normalized to unity, Eq. (3.45) implies that

$$\zeta \geq \bar{\gamma}_{|\sigma|} \geq \bar{\beta}_{|\sigma|}, \tag{3.49}$$

where

$$\bar{\beta}_l \equiv \inf_v \beta_l(v). \tag{3.50}$$

The bounds for different indices l are not independent. In fact, because $I_l(x) < I_{l-1}(x)$ for $x > 0$ and $l \geq 1$, we have the inequality $\eta_{l+1}^{(0)}(x,x') < \eta_l^{(0)}(x,x')$ for $xx' > 0$ and $l \geq 1$, and from this inequality it follows that all the bounds defined up to now: $\gamma_l(x)$, $\bar{\gamma}_l$, $\beta_l(v)$, and $\bar{\beta}_l$, are *increasing* functions of l for $l \geq 1$. Thus, if we obtain a positive lower bound for one value of $l \geq 1$, the same bound applies for all larger values of l.

In order to obtain more concrete results, we need an explicit expression for $\beta_l(v)$. In App. (K) we obtain the exact expression

$$\beta_l(v) = \frac{v^2}{2\langle\theta^{-1}\rangle_\pi} - 2\frac{\Gamma(\frac{l}{2}+\frac{1}{4})}{\Gamma(l)} v^{l-1/2} M(\frac{l}{2}-\frac{1}{4}, l, -v^2), \tag{3.51}$$

along with the asymptotic forms $\beta^{(>)}(v)$ and $\beta^{(<)}(v)$, given by

$$\beta_l(v) \sim \beta^{(>)}(v) \equiv \frac{v^2}{2\langle\theta^{-1}\rangle_\pi} - 2 \qquad \text{for } v \gg 1, \tag{3.52}$$

$$\beta_l(v) \sim \beta^{(<)}(v) \equiv \frac{v^2}{2\langle\theta^{-1}\rangle_\pi} - 2\frac{\Gamma(\frac{l}{2}+\frac{1}{4})}{\Gamma(l)}v^{l-1/2} \qquad \text{for } v \ll 1, \tag{3.53}$$

as well as the lower bounds

$$\beta_l(v) > \beta^{(>)}(v) \qquad \text{for } l > 1, \tag{3.54}$$

$$\beta_l(v) \geq \beta^{(<)}(v) \qquad \forall l. \tag{3.55}$$

Here $\Gamma(z)$ is the Gamma function, and $M(a,b,z)$ is a confluent hypergeometric function [101].

As mentioned above, we need to show that $1+\zeta$ is positive. Thus the quantity of interest is really $1+\beta_l(v)$, as opposed to $\beta_l(v)$. In Fig. (3.1) we plot $1+\bar{\beta}_l$ for $0 \leq l \leq 4$, together with its asymptotic form $1+\beta^{(>)}(v)$ for large values of the argument v.

Having looked at the general behavior of the functions $1+\beta_l(v)$, let us now obtain the lower bounds $1+\bar{\beta}_l$ for $1+\zeta$, and show that they are positive for $l \neq 1$. For $l=4$, (and, as $\beta_l(v)$ grows with l, for all $l \geq 4$), $\beta_l(v)$ is positive for all nonzero v, and thus $\bar{\beta}_l = \beta_l(0) = 0$. For $1 \leq l \leq 3$, $\bar{\beta}_l$ is obtained by numerically minimizing Eq. (3.51). In table (3.1), we give the numerical values for those bounds.

The results in table (3.1) prove that all eigenvalues of the Hessian are positive for $l \neq 1$.

Let us focus now on the case $l=1$. Since for this case our lower bound is negative, we can not draw any conclusion from it. We have shown that there is a zero mode, but there could still be a negative eigenvalue. A numerical diagonalization of the radial equation (3.26) for this case yields, within numerical error, the following two lowest eigenvalues:

$$1+\zeta_{10} = 0.000 \pm 0.001 \qquad 1+\zeta_{11} = 0.984 \pm 0.001 \tag{3.56}$$

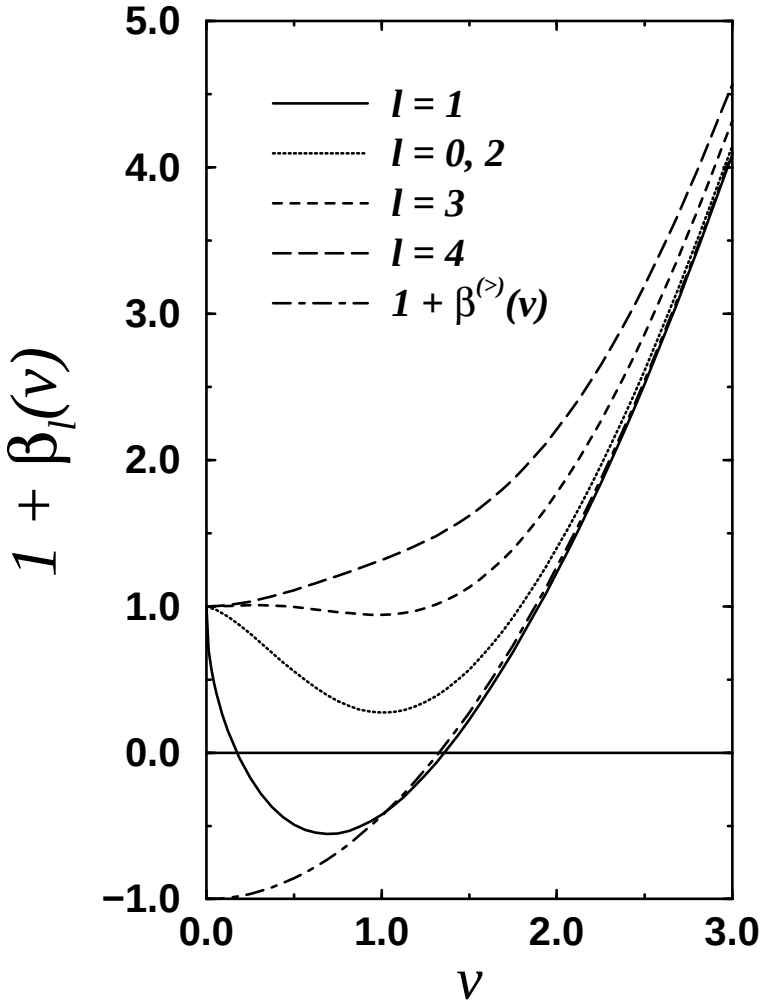

Figure 3.1: Plot of lower bound functions for the stability matrix eigenvalue problem. Lower bound functions $1 + \beta_l(v)$ (for $0 \leq l \leq 4$) and $1 + \beta^{(>)}(v)$ as functions of v.

Clearly, ζ_{10} corresponds to the expected zero mode, and we can conclude that there are no further zero modes and that all other eigenvalues are positive definite.

Let us summarize the results obtained up to now. The eigenvalues for the extended Hessian have the general form

$$\kappa_{lr}(\tilde{\mathbf{k}}) = (1 + \zeta_{lr})\epsilon + \frac{\tilde{\mathbf{k}}^2}{2}, \tag{3.57}$$

with

$$1 + \zeta_{10} = 0 \tag{3.58}$$

Table 3.1: Lower bounds for eigenvalues of the Hessian matrix.

l	$1+\bar{\beta}_l$
1	-0.55571
0, 2	0.27326
3	0.94274
≥ 4	1

and

$$1+\zeta_{lr} > 0 \qquad \text{for } lr \neq 10. \tag{3.59}$$

Therefore there is a zero mode corresponding to $lr = 10$ and $\tilde{\mathbf{k}} = \mathbf{0}$, which is continued by a branch of soft modes with eigenvalues

$$\kappa_{10}(\tilde{\mathbf{k}}) = \frac{\tilde{\mathbf{k}}^2}{2} \qquad (> 0 \text{ for } \tilde{\mathbf{k}} \neq \mathbf{0}). \tag{3.60}$$

All other eigenvalues are positive, with one continuous branch of modes labeled by $\tilde{\mathbf{k}}$ for each value of lr. The minimum eigenvalue for each branch is given by

$$\kappa_{lr}(\mathbf{0}) = (1+\zeta_{lr})\epsilon > 0, \tag{3.61}$$

which goes to zero as the transition is approached (i.e. when $\epsilon \to 0$).

3.3.3 The one-replica sector

We now need to return to the issue that we postponed earlier, namely that we have extended the Hessian matrix defined by Eq. (3.6) to be defined also in the one replica sector.

Since the original Hessian matrix exactly decouples fluctuations with different values of $\tilde{\mathbf{k}}$, it is consistent to consider separately MTI fluctuations (with $\tilde{\mathbf{k}} = \mathbf{0}$) and non-MTI fluctuations (with $\tilde{\mathbf{k}} \neq \mathbf{0}$).

For the case of MTI fluctuations, their components in the one replica sector are exactly zero, because the conditions $\hat{k} \in$ 1rs and $\check{\mathbf{k}} = \mathbf{0}$ are incompatible. This implies that for this case the extended Hessian that was diagonalized coincides with the original Hessian. Consequently our results are rigorously valid in this case.

For the case of non-MTI fluctuations, we will show that in the limit $n \to 0$, the hrs and 1rs are not coupled by the extended Hessian matrix. Furthermore, each one of its eigenvectors belong to one of the sectors and has a vanishing overlap with vectors in the other.

To understand this question, we need to look at the form that the 1rs and hrs take in the replica limit.

For a wave-vector

$$\hat{p} = (\mathbf{0}, \ldots, \mathbf{0}, \mathbf{p}, \mathbf{0}, \ldots, \mathbf{0}) \tag{3.62}$$

in the one replica sector, we have

$$\tilde{\mathbf{p}} = \mathbf{p} \qquad \hat{p}^2 = \mathbf{p}^2, \tag{3.63}$$

and, using Eq. (3.8) with $\hat{v} = \hat{w} = \hat{p}$,

$$|\breve{p}| = \sqrt{\hat{p}^2 - \frac{\tilde{\mathbf{p}}^2}{1+n}} = \sqrt{\mathbf{p}^2 - \frac{\mathbf{p}^2}{1+n}} = \sqrt{\frac{n}{1+n}}|\mathbf{p}|. \tag{3.64}$$

This means that the radial coordinate $|\breve{p}|$ goes to zero like $n^{1/2}$ in the replica limit $n \to 0$.

Besides, for a each fixed value of $\tilde{\mathbf{p}} = \mathbf{p}$, the $n+1$ wavevectors defined by

$$\begin{aligned} \hat{e}_\alpha(\mathbf{p}) &\equiv (\mathbf{e}^0, \mathbf{e}^1, \cdots, \mathbf{e}^n), \\ \mathbf{e}^\beta &\equiv \mathbf{0} \qquad \text{for } \beta \neq \alpha, \\ \mathbf{e}^\alpha &\equiv \mathbf{p}, \end{aligned} \tag{3.65}$$

with $\alpha = 0, \ldots, n$ are the only ones in the one replica sector that satisfy the condition that the sum of their $(n+1)$ component d-dimensional wavevectors is equal to $\mathbf{p}$.

These two results tell us that the 1rs corresponds, in the parametrization we are using, to a set of $n+1$ points that, in the replica limit, converge to the origin of $\breve{p}$ space. In the case $n=0$ the origin is the only point in the 1rs.

Consequently, to see whether or not a given eigenvector has any overlap with the 1rs, one needs to look at the properties of the corresponding radial eigenfunction near the origin.

Let us then consider the scaled radial equation (3.25) for the region very close to the origin, and let us keep $n > 0$ for the moment. Using the small argument behavior of the Bessel function (for $\nu \neq -1, -2, \ldots$)

$$I_\nu(z) \approx \frac{(z/2)^\nu}{\Gamma(\nu+1)}, \tag{3.66}$$

we obtain the asymptotic form of the kernel for $x \ll 1$ and $x' \lesssim 1$

$$\eta_l^{(n)}(x,x') \approx 2\,\frac{x^{l+(nd-1)/2}}{\Gamma(l+nd/2)}\,m_l(x'), \tag{3.67}$$

with

$$m_l(y) \equiv \int_0^\infty d\theta\,\pi(\theta)\,\theta^{-l}\,\mathrm{e}^{-y^2/\theta}\,y^{l+(nd-1)/2}. \tag{3.68}$$

By inserting this into Eq. (3.25), we obtain

$$(\zeta - \frac{x^2}{2})u(x) \approx \frac{-4x^{l+(nd-1)/2}}{\Gamma(l+nd/2)}\,U_l, \tag{3.69}$$

with

$$U_l \equiv \int_0^\infty dy\; m_l(y)\,u(y). \tag{3.70}$$

For n positive and small, Eq. (3.69) can only be satisfied for $\zeta \neq 0$ [102]. The term proportional to x^2 is thus negligible, and we obtain, for $x \ll 1$,

$$u(x) \approx \frac{-4\,U_l}{\Gamma(l+nd/2)}\,\frac{x^{l+(nd-1)/2}}{\zeta}. \tag{3.71}$$

The leading behavior of this radial eigenfunction for nd small and positive depends on the degree $l = |\sigma|$ of the surface harmonic. For $l = 0$ there is one eigenfunction that diverges at

the origin like $x^{(nd-1)/2}$. Its eigenvalue ζ_- is given by the expression

$$\zeta_- \approx -\frac{4\int_0^\infty dy \int_0^\infty d\theta\, \pi(\theta)\, \mathrm{e}^{-y^2/\theta}\, y^{nd-1}}{\Gamma(nd/2)}, \tag{3.72}$$

which, in the replica limit, reduces to

$$\lim_{n\to 0} \zeta_- = -2. \tag{3.73}$$

The presence of this eigenfunction as a solution of Eq. (3.25) depends crucially on the singularity of $\eta_0^{(n)}(x,x')$ at the origin for n small but positive. It is *not* a solution of Eq. (3.26), which is always regular at the origin. We will show below that this eigenfunction corresponds in the replica limit to an unphysical fluctuation in the one replica sector. In fact, from Eqs. (3.29) and (3.72), we see that its eigenvalue $\kappa_-(\tilde{\mathbf{k}})$ is negative for small $\tilde{\mathbf{k}}$:

$$\kappa_-(\tilde{\mathbf{k}}) = -\epsilon + \frac{\tilde{\mathbf{k}}}{2}. \tag{3.74}$$

Still for $l = 0$, all other radial eigenfunctions will be orthogonal to the one just found, and thus will cancel the integral U_l. Their behavior is controlled by the next power in the expansion of $\eta_0^{(n)}(x,x')$, and consequently they vanish for $x \to 0$ at least as fast as $x^{(nd+3)/2}$.

For $l > 0$, by Eq. (3.71) all the radial eigenfunctions vanish for $x \to 0$ as $x^{l+(nd-1)/2}$ or faster.

These results can be condensed as follows: all the radial eigenfunctions except one are regular at the origin. The singular eigenfunction corresponds to $l = 0$ and scales like $x^{(nd-1)/2}$ for $x \ll 1$. The regular eigenfunctions can have any value of l and vanish for $x \to 0$ as $x^{(|l-1|+1/2)}$ or faster.

In all the cases where the eigenfunction is regular at the origin, it is permissible to take the limit $n \to 0$ in Eq. (3.25). This is because these eigenfunctions vanish at the origin fast enough that they do not pick up any extra contribution from the singularity of $\eta_l^{(n)}(x,x')$ [which, by Eqs. (3.67) and (3.68), is at most of order $nd(xx')^{(nd-1)/2}$]. Thus the spectrum of

eigenvalues of Eq. (3.26) is the same as the limit of the spectrum of Eq. (3.25) when $n \to 0$, except that the spurious eigenvalue ζ_- is absent.

We now show that the one replica sector fluctuations decouple from the higher replica sector fluctuations in the replica limit.

Consider the following orthonormal basis set for the fluctuations in the one replica sector with fixed $\tilde{\mathbf{p}} = \mathbf{p}$:

$$\begin{aligned} w_j(\hat{k}) &\equiv \sum_{\alpha=0}^{n} w_{j,\alpha}\, \delta_{\hat{k},\hat{e}_\alpha(\mathbf{p})} \\ w_{j,\alpha} &\equiv \frac{V^{n/2}}{\sqrt{n+1}}\, \mathrm{e}^{i2\pi j\alpha/(n+1)}, \end{aligned} \tag{3.75}$$

where $j = 0, \ldots, n$.

Let us compute the scalar product of one of these basis functions in the one replica sector with one of the eigenfunctions of the extended Hessian, which have the general form given in Eq. (3.15):

$$\begin{aligned} \langle w_j | \psi_{r,\tilde{\mathbf{p}},\sigma} \rangle &= \frac{1}{V^n} \sum_{\hat{k} \neq \hat{0}} w_j^*(\hat{k}) \psi_{r,\tilde{\mathbf{p}},\sigma}(\hat{k}) \\ &= \frac{1}{V^n} \sum_{\alpha=0}^{n} w_{j,\alpha}^* \Big[(1+n)^{d/4} (2\pi)^{nd/2} S_\sigma(\phi_{\breve{k}}) \Big(\sqrt{\frac{n}{1+n}} |\mathbf{p}| \Big)^{\frac{1-nd}{2}} R_r\Big(\sqrt{\frac{n}{1+n}} |\mathbf{p}| \Big) \Big]. \end{aligned} \tag{3.76}$$

Here we have made use of the relation Eq.(3.64). There are two possible cases, depending on whether or not R_r is singular at the origin. If it is singular, we have $l = 0$ and, for small k,

$$R(k) = \epsilon^{-1/4} u(k/\sqrt{\epsilon}) \approx \mathcal{N} \epsilon^{-nd/4} k^{(nd-1)/2}, \tag{3.77}$$

where $\mathcal{N}$ is a normalization constant, determined by Eq. (3.16). Its value is given by

$$\mathcal{N} = \sqrt{nd}(1 + \mathcal{O}(nd)). \tag{3.78}$$

The angular part of $\psi_{r,\tilde{\mathbf{p}},\sigma=0}$ is isotropic, and is given by

$$S_0(\phi) = \sqrt{\frac{1}{\tau_{nd}}} = \sqrt{\frac{\Gamma(nd/2)}{2\pi^{nd/2}}} = (nd)^{-1/2}(1 + \mathcal{O}(nd)), \tag{3.79}$$

where $\tau_{nd} = 2\pi^{nd/2}/\Gamma(nd/2)$ is the surface of the unit sphere in nd-dimensions. By combining Eqs. (3.76), (3.77), (3.78), and (3.79), we obtain

$$\begin{aligned} \langle w_j|\psi_{r,\tilde{\mathbf{p}},\sigma}\rangle &= \sum_{\alpha=0}^{n} w^*_{j,\alpha}(1+\mathcal{O}(n)) = \langle w_j|w_0\rangle(1+\mathcal{O}(n)) \\ &= \delta_{j,0}(1+\mathcal{O}(n)) \end{aligned} \tag{3.80}$$

Now let us consider the case when R_r is non-singular at the origin. In this case the radial eigenfunction has the form, for small k,

$$R(k) = \epsilon^{-1/4} u(k/\sqrt{\epsilon}) \lesssim \mathcal{N}\epsilon^{-(|l-1|+1)/2} k^{(|l-1|+1/2)}, \tag{3.81}$$

where the normalization constant $\mathcal{N}$ does not vanish in the replica limit.

As, in this regular case, l need not be zero, we have to obtain an estimate for the normalization constant of the surface harmonic for all values of l. Consider a monomial $M_m(\phi)$ defined on the D-dimensional unit sphere

$$M_m(\phi) = \phi_1^{m_1}\cdots\phi_D^{m_D} = \frac{x_1^{m_1}\cdots x_D^{m_D}}{r^{m_1+\cdots+m_D}}. \tag{3.82}$$

Here $(x_1,\ldots,x_D)$ are the Cartesian coordinates of a point x, $r = (x_1^2+\cdots+x_D^2)^{1/2}$ is the radial coordinate for the same point, and $\phi = (\phi_1,\ldots,\phi_D) = x/r$ is the unit vector pointing in the direction of x. The integral of the monomial over the unit sphere is

$$\begin{aligned} \int d\phi\, M_m(\phi) &= \frac{\int d^D x\ x_1^{m_1}\cdots x_D^{m_D}\ \mathrm{e}^{-(x_1^2+\cdots+x_D^2)}}{\int_0^\infty dr\ r^{D-1}\ r^{m_1+\cdots+m_D}\ \mathrm{e}^{-r^2}} \\ &= \begin{cases} \dfrac{2\prod_{j=1}^D \Gamma(\frac{1+m_j}{2})}{\Gamma\left(\frac{D+\sum_{j=1}^D m_j}{2}\right)} & \text{if } m_j \text{ even } \forall j, \\ \\ 0 & \text{otherwise.} \end{cases} \end{aligned} \tag{3.83}$$

In the case of interest to us $D = nd$, and $\sum_{j=1}^D m_j = 2|\sigma|$. From this result we conclude that the normalization factor N_σ for a surface harmonic S_σ has the asymptotic form

$$N_\sigma \sim \sqrt{\Gamma(\frac{nd}{2}+|\sigma|)} \sim \begin{cases} n^{-1/2} & \text{for } |\sigma| = 0, \\ n^0 & \text{for } |\sigma| \neq 0. \end{cases} \tag{3.84}$$

Here, we have ignored factors that have finite limits when $n \to 0$. This result can be summarized as follows

$$\begin{aligned} S_\sigma(\phi) &\sim n^{\upsilon(\sigma)} \\ \upsilon(\sigma) &= \begin{cases} -1/2 & \text{for } |\sigma| = 0, \\ 0 & \text{for } |\sigma| \neq 0. \end{cases} \end{aligned} \tag{3.85}$$

By inserting Eqs. (3.81) and (3.85) into Eq.(3.76), we obtain the following scaling with n for the scalar product:

$$\begin{aligned} |\langle w_j | \psi_{r,\tilde{\mathbf{p}},\sigma} \rangle| &\lesssim (\sqrt{n}|\tilde{\mathbf{k}}|)^{1/2} (\sqrt{n}|\tilde{\mathbf{k}}|)^{1/2+|l-1|} n^{\upsilon(\sigma)}, \\ &\lesssim \begin{cases} n^{1/2} & \text{for } l = 0, \\ n^{(|l-1|+1)/2} & \text{for } l \neq 0. \end{cases} \end{aligned} \tag{3.86}$$

For completeness, we compute explicitly the matrix elements of the extended Hessian between members of the basis set $\{w_j\}_{j=0}^n$ for the one replica sector fluctuations,

$$\begin{aligned} \langle w_m | H | w_j \rangle &= \frac{1}{V^{2n}} \sum_{\hat{k},\hat{l}} w_m^*(\hat{k})\, H_{\hat{k},\hat{l}}\, w_j(\hat{l}) \\ &= \frac{1}{V^n (1+n)} \Big[\sum_{\alpha=0}^{n} \Big(\epsilon + \frac{\mathbf{p}^2}{2} \Big) w_{m,\alpha}^* w_{j,\alpha} - 2\epsilon \int_0^\infty d\theta\, \pi(\theta) \sum_{\alpha,\beta=0}^{n} \mathrm{e}^{-[\hat{e}_\alpha(\mathbf{p}) - \hat{e}_\beta(\mathbf{p})]^2/\epsilon\theta} w_{m,\alpha}^* w_{j,\beta} \Big] \\ &= \delta_{m,j} \Big(-\epsilon + \frac{\mathbf{p}^2}{2} \Big) + \mathcal{O}(n). \end{aligned} \tag{3.87}$$

Thus we see that, as expected, the eigenvalue obtained here is same as the one obtained in Eq. (3.74) for the singular eigenfunction of the extended Hessian.

In summary, in the replica limit all regular eigenfunctions of the extended Hessian are orthogonal to all of the 1rs vectors, and the singular eigenfunction of the extended Hessian coincides with the isotropic fluctuation in the 1rs. Consequently, in the replica limit, the higher replica sector is an invariant subspace for the extended Hessian, and therefore the regular eigenfunctions of the extended Hessian are the eigenfunctions of the original Hessian. More significantly, the eigenvalues of the original Hessian are the eigenvalues of the

extended Hessian for its regular eigenfunctions. Thus, all the conclusions obtained about the eigenvalues of the extended Hessian apply well equally to the original Hessian.

3.4 Randomly crosslinked macromolecules

We now consider the semi-microscopic theory of the amorphous solidification transition for randomly crosslinked linear macromolecules.

Let us notice here that the amorphous solid stationary point in this theory is the same as in the Landau theory discussed before, i.e., it is also described by Eqs. (2.115), (2.116), (2.108), and (2.131).

We now expand the free energy functional to quadratic order around a stationary point, and obtain its second derivatives with respect to the fields $\{\Omega_{\hat{q}}\}$. In this section we use the notations H and $\bar{H}$ to refer to the exact Hessian for the microscopic theory and the extended Hessian for the Landau theory respectively.

For $\hat{k}$ and $\hat{k}'$ both in the higher replica sector,

$$\begin{aligned}
\frac{\delta^2[nd\mathcal{F}_n]}{\delta\Omega_{\hat{k}}\delta\Omega_{-\hat{k}'}} &= H^{hh}_{\hat{k},\hat{k}'} \\
&= \frac{\mu^2}{V^n}\left(\delta_{\hat{k},\hat{k}'} - \frac{\mu^2}{V^n}\langle\rho_{-\hat{k}}\rho_{\hat{k}'}\rangle^{W,\bar{\Omega}}_{n+1,c}\right) \\
&= \frac{\mu^2}{3}\Big[\delta_{\hat{k},\hat{k}'}\Big(\epsilon+\frac{\hat{k}^2}{2}\Big) - \delta_{\tilde{\mathbf{k}},\tilde{\mathbf{k}}'}2\epsilon\int_0^\infty d\theta\,\pi(\theta)\mathrm{e}^{-(\hat{k}-\hat{k}')^2/\epsilon\theta}\Big] + \mathcal{O}(\epsilon^2) \\
&= \frac{1}{3}\,\bar{H}^{hh}_{\hat{k},\hat{k}'} + \mathcal{O}(\epsilon^2).
\end{aligned} \tag{3.88}$$

For $\hat{k}$ in the higher replica sector and $\hat{p}$ in the one replica sector,

$$\begin{aligned}
\frac{\delta^2[nd\mathcal{F}_n]}{\delta\Omega_{\hat{k}}\delta\Omega_{-\hat{p}}} &= H^{h1}_{\hat{k},\hat{p}} \\
&= -i\tilde{\lambda}_n^2\frac{N\mu^2}{V^{1+n}}\langle\rho_{-\hat{k}}\rho_{\hat{p}}\rangle^{W,\bar{\Omega}}_{n+1,c} \\
&= -i\frac{\tilde{\lambda}_n^2}{V}\frac{N\mu^2}{3}\delta_{\tilde{\mathbf{k}},\tilde{\mathbf{p}}}2\epsilon\int_0^\infty d\theta\,\pi(\theta)\mathrm{e}^{-(\hat{k}-\hat{p})^2/\epsilon\theta} + \mathcal{O}(\epsilon^2) \\
&= \frac{i\tilde{\lambda}_n^2 N}{3V}\,\bar{H}^{h1}_{\hat{k},\hat{p}} + \mathcal{O}(\epsilon^2).
\end{aligned} \tag{3.89}$$

Finally, for both $\hat{p}$ and $\hat{p}'$ in the one replica sector,

$$\begin{aligned}\frac{\delta^2[nd\mathcal{F}_n]}{\delta\Omega_{\hat{p}}\delta\Omega_{-\hat{p}'}} &= H^{11}_{\hat{p},\hat{p}'} \\ &= \frac{\tilde{\lambda}_n^2 N}{V}\Big(\delta_{\hat{p},\hat{p}'} + \frac{\tilde{\lambda}_n^2 N}{V}\langle\rho_{-\hat{p}}\rho_{\hat{p}'}\rangle^{W,\bar{\Omega}}_{n+1,c}\Big) \\ &= \delta_{\hat{p},\hat{p}'}\frac{\tilde{\lambda}_n^2 N}{V}\Big\{1 + \frac{\tilde{\lambda}_n^2 N}{V}[1 + \mathcal{O}(\epsilon) + \mathcal{O}(\hat{p}^2)]\Big\}. \end{aligned} \tag{3.90}$$

In these formulas we made use of the definition Eq. (2.83).

The notations H^{hh}, H^{h1}, and H^{11} respectively refer to the higher replica, cross-sector, and one replica parts of the Hessian matrix.

As MTI (i.e., $\tilde{\mathbf{k}} = \mathbf{0}$) fluctuations do not have any component in the 1rs, the relevant Hessian in that case is just $H^{hh} = (1/3)\bar{H}^{hh}$. Consequently the results obtained for the Landau theory tell us that there is a zero eigenvalue for the zero mode, and that the rest of the eigenvalues are positive.

Let us now consider general fluctuations. We will show that, in the replica limit, the eigenvectors of the Hessian H for the semi-microscopic theory are the same as the eigenvectors of the extended Hessian $\bar{H}$ for the Landau theory, and the one replica and higher replica sectors are again invariant subspaces for this Hessian.

Let us consider a regular eigenvector $|\psi_{r,\tilde{\mathbf{p}},\sigma}\rangle$ of $\bar{H}$ and one of the elements of the basis set $\{|w_j\rangle\}_{j=0}^n$ of the one replica sector fluctuations. By Eq. (3.90),

$$\begin{aligned} H^{11}|w_j\rangle &= \kappa_{1\mathrm{rs}}|w_j\rangle, \\ \kappa_{1\mathrm{rs}} &= \frac{\tilde{\lambda}_n^2 N}{V}\Big\{1 + \frac{\tilde{\lambda}_n^2 N}{V}[1 + \mathcal{O}(\epsilon) + \mathcal{O}(\tilde{\mathbf{p}}^2) + \mathcal{O}(n\tilde{\mathbf{p}}^2)]\Big\}, \end{aligned} \tag{3.91}$$

and therefore

$$|\langle w_j|H^{11}|\psi_{r,\tilde{\mathbf{p}},\sigma}\rangle| = |\kappa_{1\mathrm{rs}}\langle w_j|\psi_{r,\tilde{\mathbf{p}},\sigma}\rangle| \lesssim \mathcal{O}(\sqrt{n}). \tag{3.92}$$

Analogously, by Eq. (3.87),

$$\bar{H}^{11}|w_j\rangle = \Big(-\epsilon + \frac{\mathbf{p}^2}{2}\Big)|w_j\rangle + \mathcal{O}(n), \tag{3.93}$$

and

$$|\langle w_j|\bar{H}^{11}|\psi_{r,\tilde{\mathbf{p}},\sigma}\rangle| = \Big|\Big(-\epsilon + \frac{\mathbf{p}^2}{2}\Big)\langle w_j|\psi_{r,\tilde{\mathbf{p}},\sigma}\rangle\Big| \lesssim \mathcal{O}(\sqrt{n}). \tag{3.94}$$

By combining Eqs. (3.89), (3.92), and (3.94), we can now estimate the matrix element

$$\begin{aligned}
|\langle w_j|H|\psi_{r,\tilde{\mathbf{p}},\sigma}\rangle| &= |\langle w_j|H^{11} + H^{1h}|\psi_{r,\tilde{\mathbf{p}},\sigma}\rangle| \\
&= |\langle w_j|H^{1h}|\psi_{r,\tilde{\mathbf{p}},\sigma}\rangle + \mathcal{O}(\sqrt{n})| \\
&= |\langle w_j|\frac{i\tilde{\lambda}_n^2 N}{3V}\,\bar{H}^{1h}|\psi_{r,\tilde{\mathbf{p}},\sigma}\rangle + \mathcal{O}(\sqrt{n})| \\
&= \Big|\frac{i\tilde{\lambda}_n^2 N}{3V}\,\langle w_j|\bar{H}^{1h} + \bar{H}^{11}|\psi_{r,\tilde{\mathbf{p}},\sigma}\rangle + \mathcal{O}(\sqrt{n})\Big| \\
&= \Big|\frac{i\tilde{\lambda}_n^2 N}{3V}\,\langle w_j|\bar{H}\,|\psi_{r,\tilde{\mathbf{p}},\sigma}\rangle + \mathcal{O}(\sqrt{n})\Big| \\
&\lesssim \mathcal{O}(\sqrt{n}).
\end{aligned} \tag{3.95}$$

This means that in the replica limit $H|\psi_{r,\tilde{\mathbf{p}},\sigma}\rangle$ has no projection in the one replica sector, and also that $H|w_j\rangle$ has no projection in the higher replica sector. Therefore, also in this problem the one replica sector and the higher replica sector are decoupled invariant subspaces of the Hessian. In the one replica sector, the eigenvalue is $\kappa_{1\mathrm{rs}} > 0$. In the higher replica sector, since $H^{hh} = (1/3)\bar{H}^{hh}$, the eigenvectors are the same as for the Landau theory, and the eigenvalues are obtained from the ones in the Landau theory by multiplying by 1/3. All of these eigenvalues are positive, except for the zero eigenvalue corresponding to the zero mode. Thus, also for the semi-microscopic theory of randomly crosslinked macromolecules, the amorphous solid state is stable near the transition.

3.5 Concluding remarks

In this chapter we have shown that in a system with random constraints near the liquid–amorphous-solid transition, the amorphous solid state is a stable thermodynamic state. In order to do this, we have examined the spectra of the stability matrices, in the context of both the Landau theory for the transition and the semi-microscopic model of randomly crosslinked

macromolecular systems. In both cases the spectrum turned out to be non-negative, with only a single zero eigenvalue, and all the others positive.

Let us remark that even though we *do* find a zero eigenvalue for the stability matrix, we still declare that the stationary point is locally *stable*, as opposed to locally *marginally stable*. This is because in this system translational and rotational invariance are spontaneously broken, and therefore there is a manifold of equivalent states that have exactly the same free energy and are connected to each other by the continuous symmetries of the system. The zero eigenvalue (a.k.a. Goldstone mode) simply indicates that the free energy does not change if one applies an infinitesimal translation or rotation to the thermodynamic state.

In close analogy to the phonon spectra of ordinary solids, the fluctuation eigenvalues can be classified into two types: a soft branch of modes associated with "almost rigid" displacements of the whole system (analogous to the acoustic branch), with eigenvalues $\kappa_{10}(\tilde{\mathbf{k}}) = \tilde{\mathbf{k}}^2/2$, and a set of "massive" modes in which the structure of the system is altered more strongly (analogous to the set of optical branches), with eigenvalues $\kappa_{lr}(\tilde{\mathbf{k}}) = \epsilon(1+\zeta_{lr})+ \tilde{\mathbf{k}}^2/2$. In addition, there is in our case a "softening" of the system, because the eigenvalues of the "massive" modes go to zero at the transition.

It is an intriguing problem, which is left open for further study, to investigate whether there is any manifestation of a similar structure in the dynamics of the system and, in particular, to establish how the softening of the system manifests itself in the dynamics.

Chapter 4

Elastic properties of the amorphous solid state

4.1 Introduction

The amorphous solidification transition that we have been discussing has two main equilibrium signatures: (i) a nonzero fraction of the monomers become localized around random mean positions and with random localization lengths (structure); and (ii) the system, as a whole, acquires a nonzero static shear modulus (response). In the previous chapters, we have focused our discussion on the former signature; the purpose of the present chapter is to address the latter signature. Specifically, our aim is to develop a statistical-mechanical theory of the elastic properties of the amorphous solid state in the vicinity of the vulcanization transition. This theory incorporates both annealed (i.e. thermally equilibrating) and quenched random (i.e. crosslink specifying) variables. Its primary conclusions are: (a) that the amorphous solid [in the sense of signature (i)] state emerging at the vulcanization transition is indeed a solid [in the sense of signature (ii)]; (b) that the shear modulus vanishes continuously as the transition is approached, and does so with the third power of the excess

crosslink density (i.e. the amount by which the crosslink density exceeds its critical value); and (c) that the shearing of the container associated with elastic deformations does *not* lead to a shearing of the probability clouds associated with the thermal fluctuations of localized particles about their mean positions.

The elastic properties of vulcanized matter and related chemically-bonded systems, especially those near the amorphous solidification transition, have received considerable attention, to date. Notable approaches include the classical ones [16, 17, 18], in which it was argued that near the transition the elastic entropy in the solid phase (and consequently the static shear modulus E) grow as the third power of the excess crosslink density ϵ, i.e., $E \sim \epsilon^t$ with $t = 3$. Subsequently, it was proposed that the amorphous solidification transition of polymer systems be identified with a percolation process [5, 25, 26]. Thus, the exponent t was identified with the critical exponent μ for percolation of conductivity (with $\mu \approx 2.0$ in 3 spatial dimensions). Later, it was observed that the elasticity percolation exponent for a random network is substantially higher than μ when the forces are central [103].

More microscopically oriented approaches to the elastic properties of vulcanized matter have also been made, in which macromolecular degrees of freedom feature explicitly. Among these are the "phantom network" [104] and "affine network" [6] approaches, as well as the comprehensive discussion of rubber elasticity by Deam and Edwards [20], and others [23]. These approaches focus on the well-crosslinked regime rather than the lightly-crosslinked regime near the vulcanization transition [2].

Experimentally, the exponent t has been addressed for several systems (although mostly for gelation rather than vulcanization): the results vary from $t \approx 2$ [105] to $t \gtrsim 3$ [106]. This wide discrepancy is not understood.

Stimulating though they certainly are, it must be recognized that neither the classical [8, 9, 16, 17, 18] nor the percolation [5, 25, 26] approaches to the physics of vulcanized matter explicitly include both crucial ingredients: *thermal fluctuations* and *quenched disorder*. In

the previous chapters, an approach to the vulcanization transition was followed that takes into account both of these ingredients in the context of a semi-microscopic model for flexible, randomly crosslinked macromolecules. Up to this point, the results obtained refer to the *structure* of the amorphous solid state near the vulcanization transition. In this chapter, we use the same approach, but now to study the *response* of the amorphous solid state to shear deformations.

The outline of the rest of this chapter is as follows. In Sec. 4.2 the changes that have to be introduced in the theory in order to describe deformed systems are discussed. In Sec. 4.3 an order parameter hypothesis is proposed to describe the amorphous solid state in the deformed system. In Sec. 4.4 it is shown that the proposed order parameter does satisfy the stationary-point equations for the deformed system, and it is found that despite the externally imposed stress, the fluctuation regions for individual particles remain spherical. In Sec. 4.5, the free energy change due to the deformation is computed, and it is shown that the shear modulus scales as ϵ^3, in agreement with the results of the classical theory. In Sec. 4.6, some brief concluding remarks are presented.

The research discussed in the present chapter has been reported on in a short format in Ref. [44], and a full version is in preparation [45].

4.2 Changes in the model due to the deformation

In this section we discuss the ways in which the theoretical description of the system is affected by the deformation.

4.2.1 Description of the deformation

We characterize the deformation by the $(d \times d)$ matrix $\mathbf{S}$, which describes the change in position of any point $\mathbf{b}$ at the boundary of the system as follows: $\mathbf{b} \to \mathbf{S} \cdot \mathbf{b}$. For example,

for $d = 3$ and for a deformation in which the x, y and z Cartesian components of the position vector are, respectively, elongated by the factors λ_x, λ_y and λ_z, the matrix $\mathbf{S}$ has the form $\mathrm{diag}(\lambda_x, \lambda_y, \lambda_z)$. As we are concerned with the effects of pure shear strains, we shall consider only deformations that leave the volume V of the system unchanged, i.e.,

$$\det \mathbf{S} = 1. \tag{4.1}$$

For considering infinitesimal strains, it is convenient to define the (symmetric) strain tensor

$$\mathbf{J} \equiv \frac{1}{2}(\mathbf{S} + \mathbf{S}^{\mathrm{T}}) - \mathbf{I}. \tag{4.2}$$

Here $\mathbf{S}^{\mathrm{T}}$ is the transpose of $\mathbf{S}$, and $\mathbf{I}$ is the identity matrix. For small shear deformations, we have

$$1 = \det \mathbf{S} = 1 + \mathrm{tr}\,(\mathbf{S} - \mathbf{I}) + \mathcal{O}((\mathbf{S} - \mathbf{I})^2), \tag{4.3}$$

and consequently

$$\mathrm{tr}\,\mathbf{J} = 0, \tag{4.4}$$

to first order in the deformation.

4.2.2 Deformation and replicas

Before taking the thermodynamic limit, the system is finite in extent, and thus the Fourier representation of any function of position consists of a superposition of plane waves with wave-vectors belonging to a discrete set. This set of wave vectors is determined by the periodic boundary conditions. In particular, the order parameter is represented by a function $\Omega_{\hat{k}}$ on replicated Fourier space that is only defined at a discrete set of points. Now, under strain the boundaries in position space are displaced and, as a consequence, the discretization in replicated Fourier space changes. As the replica $\alpha = 0$ represents the degrees of freedom of the original system before crosslinking, and replicas $\alpha = 1, \ldots, n$ represent the actual system being studied, any external strain applied to the system after the permanent constraints

have been created will affect replicas $\alpha = 1, \ldots, n$, but not replica $\alpha = 0$ [20] Therefore, the change in the discretization of the wave vectors occurs only for $\alpha = 1, \ldots, n$, but not $\alpha = 0$. For replicas $\alpha = 1, \ldots, n$, the set of allowed d-dimensional wave vectors r^{u} corresponding to the unstrained system is replaced by a new set r^{s} corresponding to the strained system. Consequently, the set R^{u} of allowed replicated wave-vectors in the unstrained system [defined just after Eq. (2.48)] is replaced by a set R^{s} of allowed replicated wave-vectors in the strained system. The set R^{s} is composed of all replicated wave vectors $\hat{k} = \{\mathbf{k}^0, \mathbf{k}^1, \cdots, \mathbf{k}^n\}$ such that $\mathbf{k}^0 \in r^{\mathrm{u}}$ and $\mathbf{k}^\alpha \in r^{\mathrm{s}}$ for replicas $\alpha = 1, \ldots, n$.

4.2.3 Free energy functional for the deformed system

Conceptually, there are two sources for the change in free energy, Eq. (2.78), under deformation: the change in the expression for the free energy functional itself, and the consequent change in the value of the order parameter that solves the stationary-point equation. The free-energy functional for the strained system $\mathcal{F}_n^{\mathrm{s}}(\{\Omega_{\hat{k}}\})$ is obtained by repeating, step-by-step, the procedure followed in Secs. 2.4 and 2.5 to construct the free-energy functional for the unstrained system $\mathcal{F}_n(\{\Omega_{\hat{k}}\})$. The only change resides in the fact that integrals over the positions of the monomers now range over the region occupied by the strained sample instead of the region occupied by the unstrained sample, and consequently the periodic delta function of Eq. (2.46) now involves a summation over the new set R^{s} of wave vectors in replicated space:

$$\delta(\hat{c}) = \frac{1}{V^{1+n}} \sum_{\hat{p} \in R^{\mathrm{s}}} \exp\left(i\hat{p} \cdot \hat{c}\right). \tag{4.5}$$

Consequently, Eq. (2.48) is replaced by

$$\frac{\mu^2 V}{2N} \sum_{i,j=1}^{N} \int_0^1 ds \int_0^1 dt\, \delta\left(\hat{c}_i(s) - \hat{c}_j(t)\right) = \frac{\mu^2 N}{2V^n} \sum_{\hat{p} \in R^{\mathrm{s}}} |Q_{\hat{p}}|^2, \tag{4.6}$$

and the expression for $[\bar{Z}^n]$ in terms of monomer densities given in Eq. (2.53) is replaced by

$$[\bar{Z}^n] = \frac{\mathrm{e}^{-Nn\phi}\int \mathcal{D}\hat{c}\ \ \exp\Big\{-\frac{1}{2}\sum_{i=1}^{N}\int_0^1 ds\left|\frac{d\hat{c}_i(s)}{ds}\right|^2 - N\tilde{\lambda}_n^2\frac{N}{V}\tilde{\sum}^{\dagger}_{\hat{p}\in R^s}|Q_{\hat{p}}|^2 + N\frac{\mu^2}{V^n}\overline{\sum}^{\dagger}_{\hat{k}\in R^s}|Q_{\hat{k}}|^2\Big\}}{\int \mathcal{D}\mathbf{c}\ \ \exp\Big\{-\frac{1}{2}\sum_{i=1}^{N}\int_0^1 ds\left|\frac{d\mathbf{c}_i(s)}{ds}\right|^2 - N\tilde{\lambda}_0^2\frac{N}{V}\sum^{\dagger}_{\mathbf{p}}|Q_{\mathbf{p}}|^2\Big\}}. \tag{4.7}$$

Two features should be noted here. One is that the denominator in the last formula is unaffected by the deformation, because it is the normalization factor for the disorder distribution, which has not changed. Thus the normalization constant $\mathcal{N}$ in Eq. (2.63), which reads

$$\mathcal{N} = \frac{\exp(-Nn\phi)}{\int \mathcal{D}\mathbf{c}\ \ \exp\Big\{-\frac{1}{2}\sum_{i=1}^{N}\int_0^1 ds\left|\frac{d\mathbf{c}_i(s)}{ds}\right|^2 - N\tilde{\lambda}_0^2\frac{N}{V}\sum^{\dagger}_{\mathbf{p}}|Q_{\mathbf{p}}|^2\Big\}}, \tag{4.8}$$

is unchanged by the deformation, as anticipated in Sec. 2.5. The second feature is that no changes have appeared in any of the prefactors in front of the terms in Eq. (2.53) that *are* affected by the deformation.

From Eq. (4.7), one immediately obtains, with the Hubbard Stratonovich transformation of Sec. 2.5, the free energy functional

$$\begin{aligned} nd\mathcal{F}_n^{\mathrm{s}}(\{\Omega_{\hat{k}}\}) = {} & \tilde{\lambda}_n^2\frac{N}{V}\tilde{\sum}^{\dagger}_{\hat{p}\in R^s}|\Omega_{\hat{p}}|^2 + \frac{\mu^2}{V^n}\overline{\sum}^{\dagger}_{\hat{k}\in R^s}|\Omega_{\hat{p}}|^2 \\ & - \ln\left\langle \exp\left(i\tilde{\lambda}_n^2\frac{2N}{V}\tilde{\sum}^{\dagger}_{\hat{p}\in R^s}\mathrm{Re}\,\Omega_{\hat{p}}\rho^*_{\hat{p}} + \frac{2\mu^2}{V^n}\overline{\sum}^{\dagger}_{\hat{k}\in R^s}\mathrm{Re}\,\Omega_{\hat{k}}\rho^*_{\hat{k}}\right)\right\rangle^{W}_{n+1}. \end{aligned} \tag{4.9}$$

Having this expression for the free energy functional would allow us to compute the free energy for the deformed system in the stationary-point approximation by using Eq. (2.78). However, we are going to take one further step, and restrict ourselves for the moment to the regime near the amorphous solidification transition.

In the regime close to the transition, we can expand the free energy functional in powers of the order parameter and the wave vectors, and obtain the analog of Eq. (2.123) for the deformed system:

$$nd\mathcal{F}_n^{\mathrm{s}}(\{\Omega_{\hat{k}}\}) = \overline{\sum}_{\hat{k}\in R^s}\big(-\epsilon + \frac{1}{2}|\hat{k}|^2\big)|\Omega_{\hat{k}}|^2 - \overline{\sum}_{\hat{k}_1\hat{k}_2\hat{k}_3\in R^s}\Omega_{\hat{k}_1}\,\Omega_{\hat{k}_2}\,\Omega_{\hat{k}_3}\,\delta_{\hat{k}_1+\hat{k}_2+\hat{k}_3,\hat{0}}\,. \tag{4.10}$$

As a result, the stationary-point equation for the strained system becomes

$$0 = 2\Big(-\epsilon + \frac{1}{2}|\hat{k}|^2\Big)\Omega_{\hat{k}} - 3 \overline{\sum_{\hat{k}_1 \hat{k}_2 \in R^s}} \Omega_{\hat{k}_1}\, \Omega_{\hat{k}_2}\, \delta_{\hat{k}_1+\hat{k}_2,\hat{k}}\,. \tag{4.11}$$

4.3 Proposing a hypothesis for the order parameter

We shall obtain the order parameter by finding a solution for Eq. (4.11). We use physical arguments similar to the ones used in the unstrained case to motivate our guess for a possible solution. As our guess will turn out to solve Eq. (4.11) exactly, this justifies *a posteriori* our physical assumptions. As the shear modulus is determined by an expansion of the free energy to quadratic order in the deformation, for the moment we will only consider infinitesimal deformations.

For each localized monomer in the unstrained system we envisage that its old mean position $\mathbf{b}_i(s)$ is displaced to a new mean position $\mathbf{b}_i^{\mathrm{s}}(s) = \mathbf{S}\cdot\mathbf{b}_i(s) + \mathbf{t}_i(s)$. Up to this point the only assumption is the physically intuitive one that the same monomers will be localized in the undeformed and the deformed system. The vector $\mathbf{S}\cdot\mathbf{b}_i(s)$ is the affine displacement of the old position [6]. We now make the assumption that $\mathbf{t}_i(s)$ is a random additional displacement, uncorrelated with $\mathbf{b}_i(s)$.

For each localized monomer, we also need some conjecture about the size and shape of the region within which it thermally fluctuates. We assume that this localization region need not be spherical (as it was in the unstrained system), but that it might now be deformed due to the external strain. We will consider the position fluctuations for the monomers:

$$\delta\mathbf{c}^{\mathrm{u}} = \mathbf{c}_i(s) - \mathbf{b}_i(s) \tag{4.12}$$

for the unstrained system, and

$$\delta\mathbf{c}^{\mathrm{s}} = \mathbf{c}_i(s) - (\mathbf{S}\cdot\mathbf{b}_i(s) + \mathbf{t}_i(s)) \tag{4.13}$$

for the strained system, and also the individual monomer densities for the unstrained and strained system, $\rho^{\rm u}_{i,s,\chi}(\mathbf{r})$ and $\rho^{\rm s}_{i,s,\chi}(\mathbf{r})$, as defined by Eq. (2.20).

One possible assumption is that the fluctuation region deforms affinely, i.e., that

$$\delta\mathbf{c}^{\rm u} \to \delta\mathbf{c}^{\rm s} = \mathbf{S}\cdot\delta\mathbf{c}^{\rm u}. \tag{4.14}$$

This gives rise to the individual monomer density

$$\rho^{\rm s}_{i,s,\chi}(\mathbf{r}) = \rho^{\rm u}_{i,s,\chi}(\mathbf{S}^{-1}(\mathbf{r}-\mathbf{b}^{\rm s}_i(s))+\mathbf{b}_i(s)) \tag{4.15}$$

in real space, and

$$\langle {\rm e}^{i\mathbf{k}\cdot\mathbf{c}_i(s)}\rangle^{\rm s}_\chi = \exp\left(i\mathbf{k}\cdot\{\mathbf{S}\cdot\mathbf{b}_i(s)+\mathbf{t}_i(s)\}\right)\exp\left(-\xi_i^2(s)\,\mathbf{k}\cdot\left\{\mathbf{S}^{\rm T}\cdot\mathbf{S}\right\}\cdot\mathbf{k}/2\right) \tag{4.16}$$

for the Fourier-transformed version. In what follows, we will replace the matrix $\mathbf{S}^{\rm T}\cdot\mathbf{S}$ by its expansion to first order in the deformation:

$$\mathbf{S}^{\rm T}\cdot\mathbf{S} \approx \mathbf{I} + 2\mathbf{J} + \mathcal{O}(\mathbf{J}^2). \tag{4.17}$$

Thus, for an infinitesimal strain, the assumption of affine distortion of the fluctuation region gives the density

$$\langle {\rm e}^{i\mathbf{k}\cdot\mathbf{c}_i(s)}\rangle^{\rm s}_\chi = \exp\left(i\mathbf{k}\cdot\{\mathbf{S}\cdot\mathbf{b}_i(s)+\mathbf{t}_i(s)\}\right)\exp\left(-\xi_i^2(s)\,\mathbf{k}\cdot\{\mathbf{I}+2\mathbf{J}\}\cdot\mathbf{k}/2\right). \tag{4.18}$$

An alternative assumption is that the fluctuation region remains spherical as in the unstrained system, i.e., that

$$\delta\mathbf{c}^{\rm u} \to \delta\mathbf{c}^{\rm s} = \delta\mathbf{c}^{\rm u}. \tag{4.19}$$

This, in turn, gives rise to the individual monomer density

$$\rho^{\rm s}_{i,s,\chi}(\mathbf{r}) = \rho^{\rm u}_{i,s,\chi}(\mathbf{r}-\mathbf{b}^{\rm s}_i(s)+\mathbf{b}_i(s)) \tag{4.20}$$

in real space, and

$$\langle {\rm e}^{i\mathbf{k}\cdot\mathbf{c}_i(s)}\rangle^{\rm s}_\chi = \exp\left(i\mathbf{k}\cdot\{\mathbf{S}\cdot\mathbf{b}_i(s)+\mathbf{t}_i(s)\}\right)\exp\left(-\xi_i^2(s)\mathbf{k}^2/2\right) \tag{4.21}$$

in wave vector space.

Motivated by the above special cases, we propose the following parametrization for $\langle e^{i\mathbf{k}\cdot\mathbf{c}_i(s)}\rangle_\chi^{\mathbf{s}}$, that contains Eqs. (4.18) and (4.21) as particular limits:

$$\langle e^{i\mathbf{k}\cdot\mathbf{c}_i(s)}\rangle_\chi^{\mathbf{s}} = \exp\left(i\mathbf{k}\cdot\{\mathbf{S}\cdot\mathbf{b}_i(s)+\mathbf{t}_i(s)\}\right)\exp\left(-\xi_i^2(s)\,\mathbf{k}\cdot\{\mathbf{I}+\eta_i(s)\,\mathbf{J}\}\cdot\mathbf{k}/2\right). \tag{4.22}$$

The rationale for this generalization goes as follows. In the undeformed system, we know that the probability cloud is asymptotically isotropic. For an infinitesimal deformation, one could expect the localization region to be slightly distorted. To lowest order in the deformation, the matrix characterizing it is $\mathbf{J}$. (As we are attempting to specify a quadratic form, only the symmetric part of the matrix defining it is relevant.) The other ingredient that can influence the shape of the localization region is the disorder: we thus include a random factor $\eta_i(s)$ that weights the departure of the localization region from spherical symmetry. For example, if $\eta_i(s) = 2$, Eq. (4.22) reduces to Eq. (4.18), meaning that the probability cloud is affinely distorted. On the other hand, if $\eta_i(s) = 0$ Eq. (4.22) reduces to Eq. (4.21), i.e., the probability cloud remains spherical, as it is in the undeformed system. In the same spirit as in the undeformed case, we assume that the parameters η and ξ describing the extent (and shape) of the fluctuation region are uncorrelated with the original mean position $\mathbf{b}$.

By considering g real copies of the system, and adding the contributions from all the monomers, we can explicitly construct the order parameter of Eq. (2.24):

$$\begin{aligned}\Omega_{\mathbf{k}^1,\cdots,\mathbf{k}^g} &= (1-q)\,\delta_{\mathbf{k}^1,\mathbf{0}}\cdots\delta_{\mathbf{k}^g,\mathbf{0}} + q\int\frac{d\mathbf{b}}{V}\,e^{i(\mathbf{k}^1+\cdots+\mathbf{k}^g)\cdot\mathbf{S}\cdot\mathbf{b}} \\ &\quad\times\int d\mathbf{t}\int_0^\infty d\tau\int_{-\infty}^\infty d\eta\,\psi(\mathbf{t},\tau,\eta)\,e^{i(\mathbf{k}^1+\cdots+\mathbf{k}^g)\cdot\mathbf{t}}e^{-\xi^2(\mathbf{k}^1\cdot\{\mathbf{I}+\eta\,\mathbf{J}\}\cdot\mathbf{k}^1+\cdots+\mathbf{k}^g\cdot\{\mathbf{I}+\eta\,\mathbf{J}\}\cdot\mathbf{k}^g)/2}.\end{aligned} \tag{4.23}$$

Here, $\psi(\mathbf{t},\tau,\eta)$ is the statistical distribution for the parameters $\mathbf{t}$, τ and η. In order for the above equation to reduce to the order parameter of Eq. (2.36) in the limit of zero strain, we impose the condition:

$$\lim_{\mathbf{S}\to\mathbf{I}}\psi(\mathbf{t},\tau,\eta) = \delta(\mathbf{t})p(\tau)\delta(\eta). \tag{4.24}$$

The integral over $\mathbf{b}$ in Eq. (4.23) factorizes for the same reason as in the undeformed system, namely because $\mathbf{b}$ is uncorrelated with all the other parameters.

In order to solve the stationary-point equations, we need an expression for $\Omega_{\hat{k}}$, where $\hat{k}$ is a generic replicated wave vector in R^{s}. Obtaining this expression is slightly less straightforward than in the undeformed case. We have to take into account the fact that replica $\alpha = 0$ is different from all the others because it is not affected by the deformation. This suggests that for localized monomers we parametrize the Fourier-transformed individual particle density by using Eq. (2.31) for $\alpha = 0$ but Eq. (4.22) for $\alpha = 1, \ldots, n$, thus obtaining the following form for $\Omega_{\hat{k}}$:

$$\begin{aligned}
\Omega_{\hat{k}} &= (1-q) \prod_{\alpha=0}^{n} \delta_{\mathbf{k}^\alpha,\mathbf{0}} + q \int \frac{d\mathbf{b}}{V} \, \mathrm{e}^{i(\mathbf{k}^0\cdot\mathbf{b} + \sum_{\alpha=1}^{n} \mathbf{k}^\alpha \cdot \mathbf{S}\cdot\mathbf{b})} \\
&\quad \times \int d\mathbf{t} \int_0^\infty d\tau \int_{-\infty}^{\infty} d\eta \, \psi(\mathbf{t},\tau,\eta) \, \mathrm{e}^{i(\sum_{\alpha=1}^{n} \mathbf{k}^\alpha)\cdot\mathbf{t}} \mathrm{e}^{-((\mathbf{k}^0)^2 + \sum_{\alpha=1}^{n} \mathbf{k}^\alpha \{\mathbf{I}+\eta\,\mathbf{J}\}\mathbf{k}^\alpha)/2\tau}, \quad (4.25) \\
&= (1-q)\,\delta_{\hat{k},\hat{0}} + q\,\delta_{\mathbf{k}^0 + \mathbf{S}^{\mathrm{T}}\cdot\sum_{\alpha=1}^{n}\mathbf{k}^\alpha,\mathbf{0}} \; W^{\mathrm{s}}(\hat{k}). \quad (4.26)
\end{aligned}$$

In the second line we have recognized that the product of wave-vector delta functions corresponds to a delta function for replicated wave vectors, we have identified the integral over $\mathbf{b}$ as a representation of a Kronecker delta function in wave vector space, and we have labeled the integral over $\mathbf{t}$, τ and η as $W^{\mathrm{s}}(\hat{k})$, the continuous part of the order parameter in the strained system.

Although it is not trivial to propose a general form for the probability distribution $\psi(\mathbf{t},\tau,\eta)$, under fairly mild conditions it is possible to expand its Fourier transform with respect to the random displacement $\mathbf{t}$ to first order in the strain and to lowest nontrivial order in wavevectors:

$$\int d\mathbf{t} \, \mathrm{e}^{i\mathbf{p}\cdot\mathbf{t}} \, \psi(\mathbf{t},\tau,\eta) = p(\tau)\,\delta(\eta) + m(\tau,\eta)\,\mathbf{p}\cdot\mathbf{J}\cdot\mathbf{p} + \mathcal{O}(\mathbf{J}^2), \quad (4.27)$$

with $m(\tau,\eta)$ an unknown function. The value of the right hand side in the limit of zero strain is dictated by the assumption of Eq. (4.24). The correction to first order in the strain

is determined by assuming that it has to be invariant under a rotation of the coordinate system (which is equivalent to a simultaneous rotation of $\mathbf{p}$ and $\mathbf{J}$). This condition only allows for the following terms: (i) a linear function of $\mathbf{p}\cdot\mathbf{J}\cdot\mathbf{p}$ times any function of $\mathbf{p}^2$ and (ii) a product of an invariant linear function of $\mathbf{J}$ times any function of $\mathbf{p}^2$. The only quantity linear in $\mathbf{J}$ and invariant under rotations is $\mathrm{tr}\,\mathbf{J}$, which is zero for infinitesimal shear strains, as mentioned above. Thus we only have term (i), which, to lowest nontrivial order in wave vectors, reduces to the contribution appearing in Eq. (4.27). The integral over $\mathbf{t}$ that appears in Eq. (4.25) is the same one of Eq. (4.27), with $\mathbf{p}$ replaced by

$$\begin{aligned}\sum_{\alpha=1}^{n}\mathbf{k}^{\alpha} &= -(\mathbf{S}^{\mathrm{T}})^{-1}\cdot\mathbf{k}^{0}\\ &\approx -\mathbf{k}^{0}\end{aligned} \tag{4.28}$$

The approximation in the second line is consistent with keeping only terms linear in the deformation in Eq. (4.27).

We are now in a condition to simplify the form of Eq. (4.25) substantially, by taking the following steps: (i) by using Eqs. (4.27) and (4.28) to perform the integration over the random displacement $\mathbf{t}$, (ii) by expanding all terms consistently to linear order in $\mathbf{J}$, and (iii) by defining scaling variables in a way analogous to the one shown in Eq. (2.129). The result of these manipulations is the following hypothesis for the continuous part of the order parameter:

$$W^{\mathrm{s}}(\hat{k}) = q\int_0^\infty d\theta\, \mathrm{e}^{-\hat{k}^2/\epsilon\theta}\Big(\pi(\theta) - \frac{\zeta(\theta)}{\epsilon}\mathbf{k}^0\cdot\mathbf{J}\cdot\mathbf{k}^0 - \frac{\varpi(\theta)}{\epsilon}\sum_{\alpha=1}^{n}\mathbf{k}^{\alpha}\cdot\mathbf{J}\cdot\mathbf{k}^{\alpha}\Big). \tag{4.29}$$

Here, $\zeta(\theta)$ and $\varpi(\theta)$ are new scaling functions, which describe the change in the continuous part of the order parameter due to the deformation. They are unknown at this point, but they will be determined later by demanding that the hypothesis of Eq. (4.29) satisfy the stationary-point equations for the deformed system.

There is an alternative way of motivating the above hypothesis for the order parameter, by using symmetry arguments. Let us assume that for small strains $W^{\mathrm{s}}(\hat{k})$ is unchanged

by a rotation of the coordinate system (or, equivalently, by simultaneous rotations of $\mathbf{S}$ and $\hat{k}$). This is evidently true for $W^{\rm u}(\hat{k})$ (which is a function of $\hat{k}^2$). Therefore the difference between the two quantities $W^{\rm s}(\hat{k})$ and $W^{\rm u}(\hat{k})$ has the same property. If we further assume the presence of permutation symmetry among replicas $\alpha = 1, \ldots, n$, this difference can only contain, up to lowest nontrivial order in the deformation and in the wave vectors, the following terms: (i) a product of an invariant linear function of $\mathbf{J}$ with a linear combination of a constant, $(\mathbf{k}^0)^2$, and $\sum_{\alpha=1}^n (\mathbf{k}^\alpha)^2$; (ii) a linear function of $\mathbf{k}^0 \cdot \mathbf{J} \cdot \mathbf{k}^0$; (iii) a linear function of $\sum_{\alpha=1}^n \mathbf{k}^\alpha \cdot \mathbf{J} \cdot \mathbf{k}^\alpha$; and (iv) a linear function of $(\sum_{\alpha=1}^n \mathbf{k}^\alpha) \cdot \mathbf{J} \cdot (\sum_{\beta=1}^n \mathbf{k}^\beta)$. The only quantity linear in $\mathbf{J}$ and invariant under rotations is $\mathrm{tr}\,\mathbf{J}$, which is zero for infinitesimal shear strains, as mentioned above. In addition, using Eq. (4.28), any term of type (iv) is reduced to a term of type (ii). Thus only terms of type (ii) and (iii) are left, and we recover Eq. (4.29).

4.4 Solving the stationary-point equations

We now show that the hypothesis just proposed does satisfy the stationary point equations in the deformed system, provided that the gel fraction q and the scaling functions $\pi(\theta)$, $\zeta(\theta)$, and $\varpi(\theta)$ satisfy appropriate conditions.

In order to perform the summation over wave vectors in the stationary point equation, Eq. (4.11), one has to take into account the fact that the sum excludes vectors in the one and zero replica sectors. For any expression $f_{\hat{k}}$ that is zero in the one replica sector, the following identity is valid in the large volume limit:

$$\overline{\sum}_{\hat{k}} f_{\hat{k}} = V \int_{\hat{k}} f_{\hat{k}} - \lim_{\hat{k} \to \hat{0}} f_{\hat{k}}. \tag{4.30}$$

To simplify our notation, we make use of the shorthand:

$$\int_{\hat{k}} f_{\hat{k}} \equiv V^n \int \frac{d\hat{k}}{(2\pi)^{(1+n)d}} f_{\hat{k}}, \tag{4.31}$$

the factor V^n in front of the integral will be irrelevant in the replica limit $n \to 0$, and we will ignore it from now on. The stationary-point equation for the deformed system can be

rewritten as follows:

$$0 = 2\Big(3q - \epsilon + \frac{1}{2}|\hat{k}|^2\Big)\Omega_{\hat{k}} - 3V\int_{\hat{p}} \Omega_{\hat{p}}\,\Omega_{\hat{k}-\hat{p}}\ . \tag{4.32}$$

Two observations are in order here. One is technical, namely that the volume prefactor in the second term, although it might appear dangerous, is in fact compensated by a $1/V$ factor coming from the integrand. The second is more profound, and will be discussed in detail later: at this point in the argument, the only dependence that the stationary-point equation still has on the deformation is that the "external" wave vector $\hat{k}$ has to belong to the discrete set $R^{\rm s}$; the other source of dependence on the deformation, namely the fact that the sum over wave vectors in the second term was taken for wave vectors restricted to the discrete set $R^{\rm s}$, has now been eliminated.

By inserting the hypothesis for the order parameter, given by Eqs. (4.26) and (4.29), into the stationary point condition, Eq. (4.32), and expanding to first order in the strain, we obtain

$$\begin{aligned}
0 = \delta_{\tilde{\mathbf{k}}^{\rm s},\mathbf{0}}\ \Big\{ & 2\left(3q^2 - \epsilon q + q\hat{k}^2/2\right)\int_0^\infty d\theta\,\pi(\theta)\ \mathrm{e}^{-\hat{k}^2/\epsilon\theta} \\
& \quad -3q^2\int_{\hat{p}}\int_0^\infty d\theta_1\,\pi(\theta_1)\int_0^\infty d\theta_2\,\pi(\theta_2)\ \mathrm{e}^{-\hat{p}^2/\epsilon\theta_1}\,\mathrm{e}^{-(\hat{k}-\hat{p})^2/\epsilon\theta_2}\int d\mathbf{m}\,\mathrm{e}^{i\mathbf{m}\cdot\tilde{\mathbf{p}}^{\rm s}} \\
& -2\left(3q^2 - \epsilon q + q\hat{k}^2/2\right)\int_0^\infty d\theta\,\frac{\zeta(\theta)}{\epsilon}\mathbf{k}^0\cdot\mathbf{J}\cdot\mathbf{k}^0\,\mathrm{e}^{-\hat{k}^2/\epsilon\theta} \\
& \quad +6q^2\int_{\hat{p}}\int_0^\infty d\theta_1\,\frac{\zeta(\theta_1)}{\epsilon}\mathbf{p}^0\cdot\mathbf{J}\cdot\mathbf{p}^0\int_0^\infty d\theta_2\,\pi(\theta_2)\ \mathrm{e}^{-\hat{p}^2/\epsilon\theta_1}\,\mathrm{e}^{-(\hat{k}-\hat{p})^2/\epsilon\theta_2}\int d\mathbf{m}\,\mathrm{e}^{i\mathbf{m}\cdot\tilde{\mathbf{p}}^{\rm s}} \\
& -2\left(3q^2 - \epsilon q + q\hat{k}^2/2\right)\int_0^\infty d\theta\,\frac{\varpi(\theta)}{\epsilon}\sum_{\alpha=1}^{n}\mathbf{k}^\alpha\cdot\mathbf{J}\cdot\mathbf{k}^\alpha\,\mathrm{e}^{-\hat{k}^2/\epsilon\theta} \\
& \quad +6q^2\int_{\hat{p}}\int_0^\infty d\theta_1\,\frac{\varpi(\theta_1)}{\epsilon}\sum_{\alpha=1}^{n}\mathbf{p}^\alpha\cdot\mathbf{J}\cdot\mathbf{p}^\alpha\int_0^\infty d\theta_2\,\pi(\theta_2)\ \mathrm{e}^{-\hat{p}^2/\epsilon\theta_1}\,\mathrm{e}^{-(\hat{k}-\hat{p})^2/\epsilon\theta_2}\int d\mathbf{m}\,\mathrm{e}^{i\mathbf{m}\cdot\tilde{\mathbf{p}}^{\rm s}}\Big\}\,.
\end{aligned} \tag{4.33}$$

Here we have made use of the notation

$$\tilde{\mathbf{k}}^{\rm s} \equiv \mathbf{k}^0 + \mathbf{S}^{\rm T}\cdot\sum_{\alpha=1}^{n}\mathbf{k}^\alpha, \tag{4.34}$$

and the integral representation for the Kronecker delta

$$\delta_{\mathbf{k},\mathbf{0}} = \frac{1}{V}\int d\mathbf{m}\, \mathrm{e}^{i\mathbf{m}\cdot\mathbf{k}}. \tag{4.35}$$

After performing the integrations, first over $\hat{p}$, then over $\mathbf{m}$, Eq. (4.33) reduces to:

$$
\begin{aligned}
0 \;=\; & \left\{ 2\left(3q^2 - \epsilon q + q\hat{k}^2/2\right) \int_0^\infty d\theta\, \pi(\theta)\, \mathrm{e}^{-\hat{k}^2/\epsilon\theta} - 3q^2 \int_0^\infty d\theta_1 \int_0^\infty d\theta_2\, \pi(\theta_1)\pi(\theta_2)\, \mathrm{e}^{-\hat{k}^2/\epsilon(\theta_1+\theta_2)} \right\} \\
& -\frac{1}{\epsilon}\left\{ \mathbf{k}^0 \cdot \mathbf{J} \cdot \mathbf{k}^0 \right\} \left\{ 2\left(3q^2 - \epsilon q + q\hat{k}^2/2\right) \int_0^\infty d\theta\, \zeta(\theta)\, \mathrm{e}^{-\hat{k}^2/\epsilon\theta} \right. \\
& \qquad \left. - 6q^2 \int_0^\infty d\theta_1 \int_0^\infty d\theta_2 \left(\frac{\theta_1}{\theta_1+\theta_2}\right)^2 \zeta(\theta_1)\pi(\theta_2)\, \mathrm{e}^{-\hat{k}^2/\epsilon(\theta_1+\theta_2)} \right\} \\
& -\frac{1}{\epsilon}\left\{ \sum_{\alpha=1}^{n} \mathbf{k}^\alpha \cdot \mathbf{J} \cdot \mathbf{k}^\alpha \right\} \left\{ 2\left(3q^2 - \epsilon q + q\hat{k}^2/2\right) \int_0^\infty d\theta\, \varpi(\theta)\, \mathrm{e}^{-\hat{k}^2/\epsilon\theta} \right. \\
& \qquad \left. - 6q^2 \int_0^\infty d\theta_1 \int_0^\infty d\theta_2 \left(\frac{\theta_1}{\theta_1+\theta_2}\right)^2 \varpi(\theta_1)\pi(\theta_2)\, \mathrm{e}^{-\hat{k}^2/\epsilon(\theta_1+\theta_2)} \right\}. \qquad (4.36)
\end{aligned}
$$

By taking the limit $\hat{k}^2 \to 0$ we recover the condition for the gel fraction

$$
0 = -2q\epsilon + 3q^2, \qquad (4.37)
$$

which implies that $q = 2\epsilon/3$ for $\epsilon > 0$. It is not surprising that we obtain the same gel fraction for the amorphous solid state as in the unstrained system, as in our motivation for the order parameter hypothesis we assumed that the monomers that were localized in the strained system would also be those that were localized in the unstrained system.

Demanding that Eq. (4.36) be valid for all $\hat{k} \in R^3$ is equivalent to the above equation for the gel fraction plus the following integro-differential equations for the scaling functions $\pi(\theta)$, $\zeta(\theta)$, and $\varpi(\theta)$:

$$
\begin{aligned}
\frac{\theta^2}{2}\frac{d\pi}{d\theta} &= (1-\theta)\,\pi(\theta) - \int_0^\theta d\theta' \pi(\theta')\pi(\theta-\theta'), && (4.38)\\
\frac{\theta^2}{2}\frac{d\zeta}{d\theta} &= (1-\theta)\,\zeta(\theta) - \frac{2}{\theta^2}\int_0^\theta d\theta'\, \theta'^2\, \zeta(\theta')\,\pi(\theta-\theta'), && (4.39)\\
\frac{\theta^2}{2}\frac{d\varpi}{d\theta} &= (1-\theta)\,\varpi(\theta) - \frac{2}{\theta^2}\int_0^\theta d\theta'\, \theta'^2\, \varpi(\theta')\,\pi(\theta-\theta'). && (4.40)
\end{aligned}
$$

The boundary conditions for the scaling functions $\pi(\theta)$, $\zeta(\theta)$ and $\varpi(\theta)$ are obtained by studying the values of the order parameter in different regions of $\hat{k}$ space.

As noticed in Sec. 2.3.2 for the case of $p(\tau)$, the fact that the order parameter is unity

at the origin determines that the following normalization condition for $\pi(\theta)$ be satisfied:

$$\int_0^\theta d\theta\, \pi(\theta) = 1. \tag{4.41}$$

To derive boundary conditions for $\zeta(\theta)$ and $\varpi(\theta)$, we observe that, from Eq. (2.24),

$$\lim_{(\mathbf{k}^1)^2+\cdots+(\mathbf{k}^g)^2\to\infty} \Omega_{\mathbf{k}^1,\cdots,\mathbf{k}^g} = 0 \tag{4.42}$$

and, consequently, that

$$\lim_{\hat{k}^2\to\infty} \Omega_{\hat{k}} = 0. \tag{4.43}$$

In order to benefit from this information, we perform the change of variables

$$y \equiv \hat{k}^2/\epsilon\theta \tag{4.44}$$

in Eq. (4.29), thus obtaining

$$W^{\mathrm{s}}(\hat{k}) = q\int_0^\infty dy\, \mathrm{e}^{-y}\Big\{\frac{\epsilon}{\hat{k}^2}\,\tilde{\pi}\Big(\hat{k}^2/\epsilon y\Big) - \tilde{\zeta}\Big(\hat{k}^2/\epsilon y\Big)\,\mathbf{x}^0\cdot\mathbf{J}\cdot\mathbf{x}^0 - \tilde{\varpi}\Big(\hat{k}^2/\epsilon y\Big)\,\sum_{\alpha=1}^{n}\mathbf{x}^\alpha\cdot\mathbf{J}\cdot\mathbf{x}^\alpha\Big\}. \tag{4.45}$$

Here, we have defined the functions $\tilde{\pi}(\theta)$, $\tilde{\zeta}(\theta)$, and $\tilde{\varpi}(\theta)$ by

$$\tilde{\pi}(\theta) \equiv \theta^2\pi(\theta); \qquad \tilde{\zeta}(\theta) \equiv \theta^2\zeta(\theta); \qquad \tilde{\varpi}(\theta) \equiv \theta^2\varpi(\theta); \tag{4.46}$$

and the unit vector $\hat{x} = \{\mathbf{x}^0, \ldots, \mathbf{x}^n\}$ by

$$\mathbf{x}^\alpha \equiv \frac{\mathbf{k}^\alpha}{\sqrt{\hat{k}^2}}, \qquad\qquad (\alpha = 0, \ldots, n). \tag{4.47}$$

From the expression (4.45) for the order parameter hypothesis, it follows immediately that

$$\lim_{\hat{k}^2\to\infty} \Omega_{\hat{k}} = -\lim_{\theta\to\infty}\Big(\tilde{\zeta}(\theta)\,\mathbf{x}^0\cdot\mathbf{J}\cdot\mathbf{x}^0 + \tilde{\varpi}(\theta)\sum_{\alpha=1}^{n}\mathbf{x}^\alpha\cdot\mathbf{J}\cdot\mathbf{x}^\alpha\Big). \tag{4.48}$$

However, this limit must be zero regardless of the direction of $\hat{x}$, and consequently we obtain the following boundary conditions for $\zeta(\theta)$ and $\varpi(\theta)$:

$$0 = \lim_{\theta\to\infty}\theta^2\zeta(\theta), \tag{4.49}$$

$$0 = \lim_{\theta\to\infty}\theta^2\varpi(\theta). \tag{4.50}$$

To obtain boundary conditions at the origin, one only needs to examine the integro-differential equations themselves. Near the origin, the integral terms can be neglected, and all three equations reduce to the form:

$$\frac{\theta^2}{2}\frac{df}{d\theta} = (1-\theta)\, f(\theta), \tag{4.51}$$

where f stands for π, ζ, or ϖ. This is a first order linear differential equation that has the solution

$$f(\theta) = A\frac{\mathrm{e}^{-2/\theta}}{\theta^2}, \tag{4.52}$$

with A an arbitrary constant. Consequently, all three of the scaling functions vanish rapidly at the origin.

As the reader has probably already noticed, the integro-differential equation and the boundary condition that apply to both $\zeta(\theta)$ and $\varpi(\theta)$ are linear and homogeneous. This implies that one of two possibilities must hold for each one of these functions: either it is identically zero, or it is only determined up to an arbitrary multiplicative constant. The latter possibility does not seem to be easy to justify on physical grounds, as it would imply that the stationary point equations leave the order parameter undetermined. In fact, if this were the case, there would be a continuous family of order parameters such that the continuous parts $W^{\mathrm{s}}(\hat{k})$ for different members of the family differ in different degrees from the continuous part of the order parameter corresponding to the amorphous solid state of the unstrained system. One could, however, imagine that we are missing another physical constraint that fixes the scale of these two functions, and therefore the above argument is suggestive but not conclusive. In what follows we are going to show that both functions are zero, doing so by the analytic manipulation of the integro-differential equations and boundary conditions. [By contrast, in the case of $\pi(\theta)$, the integro-differential equation (4.38) is nonlinear, and the condition of Eq. (4.41) is linear but inhomogeneous.]

As the equations and boundary conditions are identical for $\zeta(\theta)$ and $\varpi(\theta)$, it is enough

to show that $\zeta(\theta) = 0$ for all θ. This is done in Appendix L.

The fact that both $\zeta(\theta)$ and $\varpi(\theta)$ are identically null implies the *a priori* most surprising result of this chapter: the continuous part of the order parameter *does not change* to first order in the strain, i.e., $W^{\rm s}(\hat{k}) = W^{\rm u}(\hat{k})$. This conclusion is consistent with the phantom network picture [2, 104]. It also suggests that $W^{\rm s}(\hat{k}) = W^{\rm u}(\hat{k})$ for finite (and not merely infinitesimal) deformations. Indeed, our order-parameter hypothesis turns out to satisfy the stationary-point equation for arbitrarily strained systems. To see this, let us go back to the stationary-point equation, Eq. (4.32). As was mentioned earlier, Eq. (4.32) applies both for the unstrained and for the strained systems, the only difference between the two cases being that in the unstrained case, the "external" replicated wave vector $\hat{k}$ belongs to the discrete set $R^{\rm u}$, while in the strained case, $\hat{k}$ belongs to the set $R^{\rm s}$. By inserting the form for the order parameter given by Eq. (4.26), but now with $W^{\rm s}(\hat{k}) = W^{\rm u}(\hat{k})$, i.e., given by Eq. (4.29) with $\zeta(\theta) = \varpi(\theta) = 0$, we find that the stationary-point equation is satisfied provided $\pi(\theta)$ satisfies Eq. (2.108).

One could be tempted at this point to assume that the order parameter is completely unchanged when the system is deformed. However, this is not quite correct. In addition to the stationary-point equation, the order parameter has to satisfy the boundary conditions in real space for the deformed system. This means that the hypothesis of Eq. (4.26) for $\Omega_{\hat{k}}$ is physically meaningful only for $\hat{k}$ belonging to the set of allowed replicated wave vectors $R^{\rm s}$. If the order parameter corresponding to the unstrained system were maintained, there would be a factor $\delta_{\tilde{\mathbf{k}},\mathbf{0}}$ in the term corresponding to the localized monomers that would be zero for generic values of the deformation matrix $\mathbf{S}$ unless *both* $\mathbf{k}^0 = \mathbf{0}$ and $\sum_{\alpha=1}^{n} \mathbf{k}^\alpha = \mathbf{0}$. As in the undeformed system this same factor is nonzero for $\sum_{\alpha=1}^{n} \mathbf{k}^\alpha = -\mathbf{k}^0 \neq \mathbf{0}$, this would give rise to an unphysical discontinuity in the order parameter as a function of the deformation. On the other hand, the modified delta factor $\delta_{\tilde{\mathbf{k}}^{\rm s},\mathbf{0}}$ that appears in Eq. (4.26) takes into account the shift in the reciprocal lattice due to the deformation, and displays no such discontinuity.

4.5 Change in free energy with the deformation; shear modulus

We now have all the ingredients necessary to calculate the change in the free energy Δf, to leading order in ϵ, due to the deformation of the system:

$$\Delta f = d \lim_{n \to 0} \left[\mathcal{F}_n^{\rm s}(\{\Omega_{\hat{k}}^{\rm s}\}) - \mathcal{F}_n(\{\Omega_{\hat{k}}^{\rm u}\}) \right]. \tag{4.53}$$

Here $\Omega_{\hat{k}}^{\rm s}$ and $\Omega_{\hat{k}}^{\rm u}$ are, respectively, the stationary-point values of the order parameter for the strained and unstrained systems. We need to compute $\mathcal{F}_n^{\rm s}(\{\Omega_{\hat{k}}^{\rm s}\})$ as a function of the deformation matrix $\mathbf{S}$.

From Eq. (4.10) we see that $\mathcal{F}_n^{\rm s}(\{\Omega_{\hat{k}}^{\rm s}\})$ contains both a quadratic and a cubic term in $\Omega_{\hat{k}}^{\rm s}$. We first study the quadratic term. We make use of Eq. (4.30) to write, in the large volume limit,

$$\overline{\sum}_{\hat{k} \in R^{\rm s}} \Big(-\epsilon + \frac{1}{2}|\hat{k}|^2 \Big) |\Omega_{\hat{k}}|^2 = \epsilon \lim_{\hat{k} \to \hat{0}} |\Omega_{\hat{k}}|^2 + V \int_{\hat{k}} \Big(-\epsilon + \frac{1}{2}|\hat{k}|^2 \Big) |\Omega_{\hat{k}}|^2. \tag{4.54}$$

The term associated to the limit $\hat{k} \to \hat{0}$ has the value ϵq^2, independent of $\mathbf{S}$, and is thus irrelevant for our purposes. We concentrate on computing the integral

$$I \equiv V \int_{\hat{k}} \Big(-\epsilon + \frac{1}{2}|\hat{k}|^2 \Big) |\Omega_{\hat{k}}|^2. \tag{4.55}$$

To make the algebra more digestible, we define the notations

$$\int_\theta \cdots \equiv \int_0^\infty d\theta \cdots \pi(\theta) \quad \text{and} \quad a \equiv \frac{2}{\epsilon}\Big(\frac{1}{\theta_1} + \frac{1}{\theta_2}\Big). \tag{4.56}$$

The first step is to insert the form of the order parameter for the solid phase, Eqs. (4.25) and (4.29), and use the fact that $\zeta(\theta) = \varpi(\theta) \equiv 0$. We then have

$$\begin{aligned} I &= V \int_{\hat{k}} \Big(-\epsilon + \frac{1}{2}|\hat{k}|^2 \Big) \left(q\, \delta_{\tilde{\mathbf{k}}^{\rm s}, \mathbf{0}} \int_\theta \mathrm{e}^{-\hat{k}^2/\epsilon\theta} \right)^2 \\ &= q^2 \int_{\theta_1} \int_{\theta_2} \int_{\hat{k}} \Big(-\epsilon + \frac{1}{2}|\hat{k}|^2 \Big) \mathrm{e}^{-a\hat{k}^2/2} \int d\mathbf{m}\, \mathrm{e}^{i\mathbf{m}\cdot(\mathbf{k}^0 + \mathbf{S}^{\rm T}\cdot\sum_{\alpha=1}^n \mathbf{k}^\alpha)} \\ &= q^2 V^n \int_{\theta_1} \int_{\theta_2} \Big(-\epsilon - \frac{d}{da} \Big) \int d\mathbf{m}\, \frac{\mathrm{e}^{-m^2/2a}}{(2\pi a)^{d/2}} \Big(\frac{\mathrm{e}^{-(\mathbf{S}m)^2/2a}}{(2\pi a)^{d/2}} \Big)^n \end{aligned} \tag{4.57}$$

$$
\begin{aligned}
&= q^2 V^n \int_{\theta_1}\int_{\theta_2}\Big(-\epsilon - \frac{d}{da}\Big)\Big\{(2\pi a)^{nd}[\det(\mathbf{I}+n\mathbf{S}^{\mathrm{T}}\mathbf{S})]\Big\}^{-1/2} \\
&= q^2(1+n\ln V)(-\epsilon+\mathcal{O}(n))\Big(1-\frac{n}{2}\mathrm{tr}\,(\mathbf{S}^{\mathrm{T}}\cdot\mathbf{S})\Big)+\mathcal{O}(n^2),
\end{aligned}
\tag{4.58}
$$

where we have only kept low powers of the number n of replicas in the result. The change in this term due to the deformation is

$$
\Delta I = \frac{n}{2}\epsilon q^2 \mathrm{tr}\,(\mathbf{S}^{\mathrm{T}}\mathbf{S}-\mathbf{I})+\mathcal{O}(n^2). \tag{4.59}
$$

Now, for the cubic term, by using Eq. (4.30) repeatedly we obtain

$$
-\overline{\sum}_{\hat{k}_1\hat{k}_2\hat{k}_3\in R^s}\Omega_{\hat{k}_1}\,\Omega_{\hat{k}_2}\,\Omega_{\hat{k}_3}\,\delta_{\hat{k}_1+\hat{k}_2+\hat{k}_3,\hat{0}} = -V^2\int_{\hat{k}_1}\int_{\hat{k}_2}\Omega_{\hat{k}_1}\,\Omega_{\hat{k}_2}\,\Omega_{-\hat{k}_1-\hat{k}_2}+3Vq\int_{\hat{k}}|\Omega_{\hat{k}}|^2-2q^3. \tag{4.60}
$$

then, inserting the form of the order parameter, the first term on the r.h.s yields

$$
\begin{aligned}
J &\equiv -q^3\int_{\theta_1}\int_{\theta_2}\int_{\theta_3}\int_{\hat{k}_1}\int_{\hat{k}_2} \mathrm{e}^{-\hat{k}_1^2/\epsilon\theta_1-\hat{k}_2^2/\epsilon\theta_2-(\hat{k}_1+\hat{k}_2)^2/\epsilon\theta_3} \\
&\times\int d\mathbf{m}_1\,\mathrm{e}^{i\mathbf{m}_1\cdot(\mathbf{k}_1^0+\mathbf{S}^{\mathrm{T}}\cdot\sum_{\alpha=1}^n\mathbf{k}_1^\alpha)}\int d\mathbf{m}_2\,\mathrm{e}^{i\mathbf{m}_2\cdot(\mathbf{k}_2^0+\mathbf{S}^{\mathrm{T}}\cdot\sum_{\alpha=1}^n\mathbf{k}_2^\alpha)} \\
&= -q^3V^{2n}\int_{\theta_1}\int_{\theta_2}\int_{\theta_3}\int d\mathbf{m}_1\int d\mathbf{m}_2\,\frac{\exp\left\{-\frac{1}{2}(\mathbf{m}_1\;\mathbf{m}_2)\cdot\mathbf{A}\cdot\begin{pmatrix}\mathbf{m}_1\\ \mathbf{m}_2\end{pmatrix}\right\}}{(4\pi^2\det\mathbf{A})^{d/2}} \\
&\times\left(\frac{\exp\left\{-\frac{1}{2}(\mathbf{S}\cdot\mathbf{m}_1\;\mathbf{S}\cdot\mathbf{m}_2)\mathbf{A}\begin{pmatrix}\mathbf{S}\cdot\mathbf{m}_1\\ \mathbf{S}\cdot\mathbf{m}_2\end{pmatrix}\right\}}{(4\pi^2\det\mathbf{A})^{d/2}}\right)^n,
\end{aligned}
\tag{4.61}
$$

where the 2×2 matrix $\mathbf{A}$ is the inverse of the matrix

$$
\frac{2}{\epsilon}\begin{pmatrix}\frac{1}{\theta_1}+\frac{1}{\theta_3} & \frac{1}{\theta_3}\\ \frac{1}{\theta_2} & \frac{1}{\theta_2}+\frac{1}{\theta_3}\end{pmatrix}. \tag{4.62}
$$

By performing the gaussian integration over m_1 and m_2, and expanding in powers of n, we obtain

$$
\begin{aligned}
J &= -q^3V^{2n}\int_{\theta_1}\int_{\theta_2}\int_{\theta_3}(4\pi^2\det\mathbf{A})^{-nd/2}\Big\{\det(\mathbf{I}+n\mathbf{S}^{\mathrm{T}}\mathbf{S})\Big\}^{-1} \\
&= -q^3(1+2n\ln V)(1-n\mathrm{tr}\,(\mathbf{S}^{\mathrm{T}}\cdot\mathbf{S}))(1+\mathcal{O}(n))+\mathcal{O}(n^2).
\end{aligned}
\tag{4.63}
$$

For this term, the change due to the deformation is

$$\Delta J = nq^3 \mathrm{tr}\,(\mathbf{S}^{\mathrm{T}} \cdot \mathbf{S} - \mathbf{I}) + \mathcal{O}(n^2). \tag{4.64}$$

Similarly, the second term on the r.h.s. of Eq. (4.60) evaluates to

$$\begin{aligned} K &= 3Vq \int_{\hat{k}} |\Omega_{\hat{k}}|^2 \\ &= 3q^3(1 + n \ln V)(1 - \frac{n}{2}\mathrm{tr}\,(\mathbf{S}^{\mathrm{T}} \cdot \mathbf{S}))(1 + \mathcal{O}(n)) + \mathcal{O}(n^2), \end{aligned} \tag{4.65}$$

and its change under deformation is

$$\Delta K = \frac{-3n}{2} q^3 \mathrm{tr}\,(\mathbf{S}^{\mathrm{T}} \cdot \mathbf{S} - \mathbf{I}) + \mathcal{O}(n^2). \tag{4.66}$$

By combining the contributions shown in Eqs. (4.59), (4.64) and (4.66), dividing by the number n of replicas, and taking into account the fact that $q = \frac{2}{3}\epsilon$, we obtain the free-energy change due to the deformation:

$$\begin{aligned} \Delta f &= d \lim_{n \to 0} \left\{ \mathcal{F}_n^{\mathrm{s}}(\{\Omega_{\hat{k}}^{\mathrm{s}}\}) - \mathcal{F}_n(\{\Omega_{\hat{k}}^{\mathrm{u}}\}) \right\} \\ &= \frac{2\epsilon^3}{27} \mathrm{tr}\,(\mathbf{S} \cdot \mathbf{S}^{\mathrm{T}} - \mathbf{I}). \end{aligned} \tag{4.67}$$

Thus we can extract the value of the static shear modulus for the amorphous solid state near the solidification transition (with physical units restored):

$$E = k_{\mathrm{B}} T N C \epsilon^3, \tag{4.68}$$

where k_{B} is Boltzmann's constant, T is the temperature, and C is a model-dependent positive constant. Hence, we see that the static shear modulus near the vulcanization transition is characterized by the exponent $t = 3$, in agreement with the classical result [5, 16, 17, 18]. A simple scaling argument, viz., that the modulus should scale as two powers of the order parameter (q^2) and two powers of the gradient (ξ_{typ}^{-2}), leads to the same value for the exponent t.

4.6 Concluding remarks

In this chapter we have presented a microscopic derivation of the static elastic response of a system of randomly crosslinked macromolecules near the amorphous solidification transition.

From the technical point of view, we modeled the deformation of the system by changing the boundary conditions in real space, and reformulating the theory presented in Chap. 2 under these new conditions. A point that required special care was how to include in our formulation the physical information that the system had been crosslinked *before* it was deformed. This results in an asymmetry in the replica formulation of the problem: in the case we are studying, replica $\alpha = 0$ describes the system *before* the deformation is applied, and replicas $\alpha = 1, \ldots, n$ describe the system in its actual state of deformation.

The physical picture that emerges from the results of this chapter has the following features: (i) the amorphous solid state, which was shown in Chap. 2 to be characterized structurally by the localization of a nonzero fraction of particles, is also characterized by having a nonzero static shear modulus; (ii) the static shear modulus scales as the third power of the excess crosslink density (beyond its value at the transition) [107]; and (iii) the form of localization exhibited by the particles is left unchanged by the strain.

A possible explanation for the spherical localization regions that the particles exhibit even under externally applied stress might be that in the regime near the transition most monomers in the infinite cluster are very loosely connected, and thus their behavior is dominated by the maximization of entropy, which is obtained by allowing them to fluctuate in all directions. It is not implausible that strain-induced changes in the pattern of localization would emerge from a more detailed analysis of the effects of the excluded-volume interaction, at least at higher crosslink densities. This is because at higher crosslinks densities, the macromolecular network is more tightly bound, and the topological barriers generated by interlocking of polymer loops are more significant.

Finally, let us point out that since the treatment presented here only depends on the form of the free-energy functional [88] near the transition, and not any specific semi-microscopic model, the approach to elasticity described here should be generally applicable not only to systems of randomly crosslinked flexible macromolecules, but also to other equilibrium amorphous solid forming systems.

Appendix A

Wiener correlator

In this appendix we derive the basic correlators associated with the Wiener measure:

$$\Big\langle \exp\Big(-i\sum_{\rho=1}^{r}\mathbf{k}_\rho\cdot\mathbf{c}(s_\rho)\Big)\Big\rangle_1^{\mathrm{W}} = \delta^{(d)}_{\mathbf{0},\sum_{\rho=1}^{r}\mathbf{k}_\rho}\exp\Big(-\frac{1}{2}\sum_{\rho,\rho'=1}^{r}\mathcal{S}_{\rho\rho'}\,\mathbf{k}_\rho\cdot\mathbf{k}_{\rho'}\Big), \tag{A.1}$$

and

$$\Big\langle \exp\Big(-i\sum_{\rho=1}^{r}\hat{k}_\rho\cdot\hat{c}(s_\rho)\Big)\Big\rangle_{1+n}^{\mathrm{W}} = \delta^{(nd+d)}_{\hat{0},\sum_{\rho=1}^{r}\hat{k}_\rho}\exp\Big(-\frac{1}{2}\sum_{\rho,\rho'=1}^{r}\mathcal{S}_{\rho\rho'}\,\hat{k}_\rho\cdot\hat{k}_{\rho'}\Big), \tag{A.2}$$

where $\mathcal{S}_{\rho\rho'}$ is a function of the pair of arclength coordinates s_ρ and $s_{\rho'}$ defined via

$$\mathcal{S}_{\rho\rho'} \equiv \min(s_\rho, s_{\rho'})\,. \tag{A.3}$$

In terms of the Wiener measure, the correlator is given, up to normalization, by

$$\Big\langle \exp\Big(-i\sum_{\rho=1}^{r}\mathbf{k}_\rho\cdot\mathbf{c}(s_\rho)\Big)\Big\rangle_1^{\mathrm{W}} \propto \int\mathcal{D}\mathbf{c}\,\exp\Big(-\frac{1}{2}\int_0^1 ds|\dot{\mathbf{c}}(s)|^2\Big)\exp\Big(-i\sum_{\rho=1}^{r}\mathbf{k}_\rho\cdot\mathbf{c}(s_\rho)\Big), \tag{A.4}$$

where the overdot denotes a derivative with respect to s. We express the configuration of the macromolecule in terms of the position of the end at $s=0$, together with the tangent vector $\dot{\mathbf{c}}(s)$ via: $\mathbf{c}(s) = \mathbf{c}(0) + \int_0^1 ds'\dot{\mathbf{c}}(s')\theta(s-s')$, where $\theta(s)$ is the Heaviside θ-function. Then the measure $\mathcal{D}\mathbf{c}$ is given by $\mathcal{D}\dot{\mathbf{c}}\,d\mathbf{c}(0)$, and the correlator becomes proportional to

$$\int d\mathbf{c}(0)\,\exp\Big(-i\mathbf{c}(s_0)\cdot\sum_{\rho=1}^{r}\mathbf{k}_\rho\Big)\int\mathcal{D}\dot{\mathbf{c}}\,\exp\Big(-\frac{1}{2}\int_0^1 ds|\dot{\mathbf{c}}(s)|^2\Big)\exp\Big(-i\int_0^1 ds\,\dot{\mathbf{c}}(s)\cdot\sum_{\rho=1}^{r}\mathbf{k}_\rho\theta(s_\rho-s)\Big). \tag{A.5}$$

By performing the integral over $\mathbf{c}(0)$ we obtain the Kronecker δ-function factor: $\delta^{(d)}_{\mathbf{0},\sum_{\rho=1}^{r}\mathbf{k}_\rho}$. By performing the integrals over the tangent vectors $\dot{\mathbf{c}}(s)$ we obtain the gaussian factor:

$$\exp\Big(-\frac{1}{2}\sum_{\rho,\rho'=1}^{r}\mathbf{k}_\rho\cdot\mathbf{k}_{\rho'}\int_0^1 ds\theta(s_\rho-s)\theta(s_{\rho'}-s)\Big). \tag{A.6}$$

By performing the arclength integral, and by setting to zero the wave vectors $\{\mathbf{k}_\rho\}_{\rho=1}^{r}$ in order to establish the correct normalization factor, we obtain the Wiener measure correlator Eq. (A.1). It should be noted that because $\min(s_\rho,s_{\rho'}) = \frac{1}{2}(s_\rho+s_{\rho'})-\frac{1}{2}|s_\rho-s_{\rho'}|$, and because of the Kronecker δ-function factor, the exponent of the Wiener measure correlator can also be expressed as $\sum_{\rho,\rho'=1}^{r}\mathbf{k}_\rho\cdot\mathbf{k}_{\rho'}|s_\rho-s_{\rho'}|/4$.

In the case of the *replicated* Wiener measure, since there is no coupling between the replicas, the analogous correlator is just the product over replicas of the corresponding one-replica correlators, which is exactly Eq. (A.2).

Appendix B

Debye function and related functions

In this appendix we derive the basic Debye function $g_0(|\mathbf{k}|^2)$. The Debye function $g_0(|\mathbf{k}|^2)$ is defined as the integral over arclength variables of the Wiener correlator Eq. (A.1) for the case $r = 2$ and $-\mathbf{k}_1 = \mathbf{k}_2 = \mathbf{k}$:

$$\begin{aligned} g_0(|\mathbf{k}|^2) &\equiv \int_0^1 ds_1 ds_2 \left\langle \mathrm{e}^{i\mathbf{k}\cdot\left(\mathbf{c}(s_1)-\mathbf{c}(s_2)\right)} \right\rangle_1^{\mathrm{W}} = \int_0^1 ds_1 ds_2 \, \mathrm{e}^{-k^2|s_1-s_2|/2} \\ &= \frac{\mathrm{e}^{-k^2/2} - \left(1 - \frac{1}{2}k^2\right)}{\frac{1}{2}\left(\frac{1}{2}k^2\right)^2} \sim \begin{cases} 1 - k^2/6, & \text{if } k^2 \ll 1; \\ 4/k^2 & \text{if } k^2 \gg 1. \end{cases} \end{aligned} \tag{B.1}$$

Appendix C

Free energy functional evaluated for the order parameter hypothesis

C.1 Quadratic contribution

We now compute the contribution in the $n \to 0$ limit to the free energy functional, Eq. (2.64), that is quadratic in $\Omega_{\hat{k}}$, for the specific form of $\Omega_{\hat{k}}$ given in Eq. (2.36). No approximations will be made. To this end we focus on the quantity

$$\lim_{n\to 0} \frac{1}{n} \frac{2}{V^n} \overline{\sum_{\hat{k}}}^{\dagger} |\Omega_{\hat{k}}|^2. \tag{C.1}$$

Inserting $\Omega_{\hat{k}}$ from Eq. (2.36), we obtain

$$\begin{aligned}
\frac{2}{V^n} \overline{\sum_{\hat{k}}}^{\dagger} |\Omega_{\hat{k}}|^2 &= \frac{1}{V^n} \overline{\sum_{\hat{k}}} |\Omega_{\hat{k}}|^2 \\
&= \frac{1}{V^n} \overline{\sum_{\hat{k}}} q^2 \int_0^\infty d\tau_1\, p(\tau_1) \int_0^\infty d\tau_2\, p(\tau_2)\, \delta^{(d)}_{\tilde{\mathbf{k}},\mathbf{0}} \exp\Big(- \hat{k}^2 (\tau_1^{-1} + \tau_2^{-1})/2 \Big) \\
&= q^2 \int_0^\infty d\tau \int_0^\infty d\tau_1\, p(\tau_1) \int_0^\infty d\tau_2\, p(\tau_2)\, \delta\Big(\tau - (\tau_1^{-1} + \tau_2^{-1})^{-1}\Big) \\
&\qquad \times \frac{1}{V^n} \overline{\sum_{\hat{k}}} \delta^{(d)}_{\tilde{\mathbf{k}},\mathbf{0}} \exp\Big(-\hat{k}^2/2\tau\Big)\,.
\end{aligned} \tag{C.2}$$

We now add and subtract the terms in the 0- and 1-replica sectors in order to relax the constraint on the summation over $\hat{k}$ indicated by the overbar on the summation symbol. In fact, owing to the factor of $\delta^{(d)}_{\tilde{\mathbf{k}},\mathbf{0}}$, the summand vanishes for $\hat{k}$ in the 1-replica sector, so that we obtain

$$\frac{2}{V^n}\overline{\sum_{\hat{k}}}^{\dagger}|\Omega_{\hat{k}}|^2 = -\frac{q^2}{V^n} + q^2\int_0^\infty d\tau \int_0^\infty d\tau_1\, p(\tau_1)\int_0^\infty d\tau_2\, p(\tau_2)\,\delta\left(\tau - (\tau_1^{-1}+\tau_2^{-1})^{-1}\right) \times\frac{1}{V^n}\sum_{\hat{k}}\delta^{(d)}_{\tilde{\mathbf{k}},\mathbf{0}}\exp\left(-\hat{k}^2/2\tau\right). \quad \text{(C.3)}$$

We now focus on the remaining, unconstrained summation on the right hand side of Eq. (C.3), which we compute via the following steps. First, we introduce an integral representation of $\delta^{(d)}_{\tilde{\mathbf{k}},\mathbf{0}}$, viz.,

$$\delta^{(d)}_{\tilde{\mathbf{k}},\mathbf{0}} = \frac{1}{V}\int_V d\mathbf{c}\exp\left(i\mathbf{c}\cdot\textstyle\sum_{\alpha=0}^n \mathbf{k}^\alpha\right), \quad \text{(C.4)}$$

where the integral is taken over the volume V. Then we convert the summation over $\hat{k}$ into an integral by using

$$\frac{1}{V^{n+1}}\sum_{\hat{k}}\cdots \to \int đ\hat{k}\cdots, \quad \text{(C.5)}$$

where $đ\hat{k} \equiv \prod_{\alpha=0}^n đ\mathbf{k}^\alpha$ and $đ\mathbf{k} \equiv (2\pi)^{-d}d\mathbf{k}$, and the integral is taken over the entire $\hat{k}$ space. Thus we obtain

$$\begin{aligned}\frac{1}{V^n}\sum_{\hat{k}}\delta^{(d)}_{\tilde{\mathbf{k}},\mathbf{0}}\exp\left(-\hat{k}^2/2\tau\right) &= \int đ\hat{k}\exp\left(-\hat{k}^2/2\tau\right)\int_V d\mathbf{c}\exp\left(i\mathbf{c}\cdot\textstyle\sum_{\alpha=0}^n\mathbf{k}^\alpha\right)\\ &= \int_V d\mathbf{c}\left\{\int đ\mathbf{k}\exp\left(-\mathbf{k}\cdot\mathbf{k}/2\tau\right)\exp\left(i\mathbf{k}\cdot\mathbf{c}\right)\right\}^{n+1}\\ &= (\tau/2\pi)^{(n+1)d/2}\int_V d\mathbf{c}\exp\left(-(n+1)\tau\mathbf{c}\cdot\mathbf{c}/2\right)\\ &= (\tau/2\pi)^{nd/2}(1+n)^{-d/2}, \quad \text{(C.6)}\end{aligned}$$

where we have used the gaussian integral and, in the last step, have assumed that $\tau^{-1/2} \ll V^{1/d}$ for inverse square localization lengths that are given significant weight by the distribution $p(\tau)$, Eq. (2.36). Thus we find

$$\frac{2}{V^n}\overline{\sum_{\hat{k}}}^{\dagger}|\Omega_{\hat{k}}|^2 = -\frac{q^2}{V^n} + q^2\int_0^\infty d\tau \int_0^\infty d\tau_1\, p(\tau_1)\int_0^\infty d\tau_2\, p(\tau_2)\,\delta\Big(\tau - (\tau_1^{-1}+\tau_2^{-1})^{-1}\Big) \times(\tau/2\pi)^{nd/2}(1+n)^{-d/2}. \tag{C.7}$$

As we shall need this quadratic term only in the vicinity of $n = 0$, we expand for small n, and by taking the $n \to 0$ limit we obtain

$$\lim_{n\to 0}\frac{1}{n}\frac{2}{V^n}\overline{\sum_{\hat{k}}}^{\dagger}|\Omega_{\hat{k}}|^2 = \frac{d}{2}q^2\int_0^\infty d\tau_1\, p(\tau_1)\int_0^\infty d\tau_2\, p(\tau_2)\ln\left(\frac{V^{2/d}}{2\pi \mathrm{e}}\left(\tau_1^{-1}+\tau_2^{-1}\right)^{-1}\right). \tag{C.8}$$

C.2 Logarithmic contribution

We now compute the contribution in the $n \to 0$ limit to the free energy functional, Eq. (2.64), that can be identified and the partition function of a single macromolecule coupled to $\Omega_{\hat{k}}$ for the specific form of $\Omega_{\hat{k}}$ given in Eq. (2.36). The calculation will be undertaken as a perturbation expansion in the typical inverse square localization length, to first order in this quantity. Thus, we focus on the quantity

$$\Big\langle \exp\Big(2\mu^2 V^{-n}\overline{\sum_{\hat{k}}}^{\dagger}\mathrm{Re}\,\Omega_{\hat{k}}^*\int_0^1 ds\,\mathrm{e}^{i\hat{k}\cdot\hat{c}(s)}\Big)\Big\rangle_{n+1}^{\mathrm{W}}. \tag{C.9}$$

First, we observe that only for $\hat{k}\cdot\hat{n} > 0$ are the variables $\Omega_{\hat{k}}$ independent, and that $\Omega_{\hat{k}} \equiv \Omega_{-\hat{k}}^*$ for $\hat{k}\cdot\hat{n} < 0$, as follows from the discussion after Eq. (2.63). This allows us to eliminate the Re operation and to extend the range of the summation in Eq. (C.9), which becomes

$$\Big\langle \exp\Big(\mu^2 V^{-n}\overline{\sum_{\hat{k}}}\Omega_{\hat{k}}\int_0^1 ds\,\mathrm{e}^{-i\hat{k}\cdot\hat{c}(s)}\Big)\Big\rangle_{n+1}^{\mathrm{W}}. \tag{C.10}$$

Next, we insert $\Omega_{\hat{k}}$ from Eq. (2.36), which gives

$$\Big\langle \exp\Big(\mu^2 q V^{-n}\overline{\sum_{\hat{k}}}\delta_{\tilde{\mathbf{k}},\mathbf{0}}^{(d)}\int_0^\infty d\tau\, p(\tau)\mathrm{e}^{-\hat{k}^2/2\tau}\int_0^1 ds\,\mathrm{e}^{-i\hat{k}\cdot\hat{c}(s)}\Big)\Big\rangle_{n+1}^{\mathrm{W}}. \tag{C.11}$$

We now add and subtract the terms in the 0- and 1-replica sectors to the summation over $\hat{k}$ in order to relax the constraint indicated by the overbar on the summation symbol. In fact,

owing to the factor of $\delta^{(d)}_{\tilde{\mathbf{k}},\mathbf{0}}$, the summand vanishes for $\hat{k}$ in the 1-replica sector, so that we obtain

$$\exp\Big(-\mu^2 qV^{-n}\Big)\Big\langle \exp\Big(\mu^2 qV^{-n}\sum\nolimits_{\hat{k}}\delta^{(d)}_{\tilde{\mathbf{k}},\mathbf{0}}\int_0^\infty d\tau\, p(\tau)\,\mathrm{e}^{-\hat{k}^2/2\tau}\int_0^1 ds\,\mathrm{e}^{-i\hat{k}\cdot\hat{c}(s)}\Big)\Big\rangle^{\mathrm{W}}_{n+1}. \tag{C.12}$$

The next step is to make the power series expansion of the exponential in the expectation value, and make r-fold use of the integral representation of the Kronecker δ-function,

$$\delta^{(d)}_{\mathbf{k},\mathbf{0}} = \frac{1}{V}\int_V d\mathbf{c}\exp\Big(i\mathbf{c}\cdot\mathbf{k}\Big), \tag{C.13}$$

in which the $\mathbf{c}$-integral is taken over the volume V, to obtain

$$\begin{aligned}
&\exp\Big(\mu^2 qV^{-n}\Big)\Big\langle \exp\Big(2\mu^2 V^{-n}\overline{\sum_{\hat{k}}}^{\dagger}\mathrm{Re}\,\Omega^*_{\hat{k}}\int_0^1 ds\,\mathrm{e}^{i\hat{k}\cdot\hat{c}(s)}\Big)\Big\rangle^{\mathrm{W}}_{n+1}\\
&\quad = 1+\frac{1}{V}\sum_{r=1}^{\infty}\frac{\mu^{2r}q^r}{V^{nr}\,r!}\sum_{\hat{k}_1,\ldots,\hat{k}_r}\int_V\frac{d\mathbf{c}_1}{V}\cdots\frac{d\mathbf{c}_r}{V}\exp\Big(i\sum_{\rho=1}^{r}\mathbf{c}_\rho\cdot\sum_{\alpha=0}^{n}\mathbf{k}^\alpha_\rho\Big)\\
&\qquad\times\int_0^\infty d\tau_1 p(\tau_1)\cdots d\tau_r p(\tau_r)\exp\Big(-\frac{1}{2}\sum_{\rho=1}^{r}\frac{1}{\tau_\rho}\sum_{\alpha=0}^{n}|\mathbf{k}^\alpha_\rho|^2\Big)\\
&\qquad\qquad\times\int_0^1 ds_1\cdots ds_r\Big\langle\exp\Big(-i\sum_{\rho=1}^{r}\sum_{\alpha=0}^{n}\mathbf{k}^\alpha_\rho\cdot\mathbf{c}^\alpha(s_\rho)\Big)\Big\rangle^{\mathrm{W}}_{n+1}.
\end{aligned}\tag{C.14}$$

The remaining expectation value in Eq. (C.14), $\langle\exp(-i\sum_{\rho=1}^{r}\sum_{\alpha=0}^{n}\mathbf{k}^\alpha_\rho\cdot\mathbf{c}^\alpha(s_\rho))\rangle^{\mathrm{W}}_{n+1}$, factorizes on the replica index, giving $\prod_{\alpha=0}^{n}\langle\exp(-i\sum_{\rho=1}^{r}\mathbf{k}^\alpha_\rho\cdot\mathbf{c}(s_\rho))\rangle^{\mathrm{W}}_{1}$. Each factor in this product is of the form of the expectation value computed in App. A, in terms of which we express the remaining expectation value in Eq. (C.14). The result contains an $(n+1)$-fold product of Kronecker δ-functions, which we replace with the integral representation

$$\prod_{\alpha=0}^{n}\delta^{(d)}_{\mathbf{0},\sum_{\rho=1}^{r}\mathbf{k}^\alpha_\rho} = \frac{1}{V^{n+1}}\int_V d\mathbf{m}^0\ldots d\mathbf{m}^n\exp\Big(-i\sum_{\alpha=0}^{n}\mathbf{m}^\alpha\cdot\sum_{\rho=1}^{r}\mathbf{k}^\alpha_\rho\Big), \tag{C.15}$$

in which each of the $(n+1)$ $\mathbf{m}$-integrals is taken over the volume V. Next, we convert the summations over $\{\hat{k}_1,\cdots,\hat{k}_r\}$ to integrations by using Eq. (C.5) r times, after which the summation on the right hand side of Eq. (C.14) becomes

$$\frac{1}{V^n}\sum_{r=1}^{\infty}\frac{\mu^{2r}q^r}{r!}\int_0^1 ds_1\cdots ds_r\int_0^\infty d\tau_1 p(\tau_1)\cdots d\tau_r p(\tau_r)\frac{1}{V}\int_V\frac{d\mathbf{c}_1}{V}\cdots\frac{d\mathbf{c}_r}{V}\int_V d\mathbf{m}^0\cdots d\mathbf{m}^n$$

$$\times \int đ\hat{k}_1 \cdots đ\hat{k}_r \exp\Big(i \sum_{\alpha=0}^{n} \sum_{\rho=1}^{r} \mathbf{k}_\rho^\alpha \cdot (\mathbf{c}_\rho - \mathbf{m}^\alpha)\Big) \exp\Big(-\frac{1}{2} \sum_{\rho,\rho'=1}^{r} \mathcal{R}^{(r)}_{\rho\rho'} \sum_{\alpha=0}^{n} \mathbf{k}_\rho^\alpha \cdot \mathbf{k}_{\rho'}^\alpha\Big)$$
$$= \frac{1}{V^n} \sum_{r=1}^{\infty} \frac{\mu^{2r} q^r}{r!} \int_0^1 ds_1 \cdots ds_r \int_0^\infty d\tau_1 p(\tau_1) \cdots d\tau_r p(\tau_r) \frac{1}{V} \int_V \frac{d\mathbf{c}_1}{V} \cdots \frac{d\mathbf{c}_r}{V}$$
$$\times \Big(\int_V d\mathbf{m} \int đ\mathbf{k}_1 \cdots đ\mathbf{k}_r \exp\Big(i \sum_{\rho=1}^{r} \mathbf{k}_\rho \cdot (\mathbf{c}_\rho - \mathbf{m})\Big) \exp\Big(-\frac{1}{2} \sum_{\rho,\rho'=1}^{r} \mathcal{R}^{(r)}_{\rho\rho'} \mathbf{k}_\rho \cdot \mathbf{k}_{\rho'}\Big)\Big)^{n+1}. \tag{C.16}$$

Here, $\mathcal{R}^{(r)}_{\rho\rho'}$ is an $(r \times r)$-matrix–valued function of the r arclength coordinates $\{s_\nu\}_{\nu=1}^r$ and the r inverse square localization lengths $\{\tau_\nu\}_{\nu=1}^r$, defined in Eq. (E.1). We now focus on the quantity in this expression that is raised to the $(n+1)^{\text{th}}$ power.

By performing the gaussian integrations, first over $\{\mathbf{k}_1, \ldots, \mathbf{k}_r\}$ and then over $\mathbf{m}$, we obtain

$$\int_V d\mathbf{m} \int đ\mathbf{k}_1 \cdots đ\mathbf{k}_r \exp\Big(i \sum_{\rho=1}^{r} \mathbf{k}_\rho \cdot (\mathbf{c}_\rho - \mathbf{m})\Big) \exp\Big(-\frac{1}{2} \sum_{\rho,\rho'=1}^{r} \mathcal{R}^{(r)}_{\rho\rho'} \mathbf{k}_\rho \cdot \mathbf{k}_{\rho'}\Big)$$
$$= (2\pi)^{-(r-1)d/2} \Big(\mathcal{W}^{(r)} \det{}^{(r)} \mathcal{R}^{(r)}\Big)^{-d/2} \exp\Big(-\frac{1}{2} \sum_{\rho,\rho'=1}^{r} \mathcal{C}^{(r)}_{\rho\rho'} \mathbf{c}_\rho \cdot \mathbf{c}_{\rho'}\Big), \tag{C.17}$$

where we have introduced the $(r \times r)$-matrix–valued function $\mathcal{C}^{(r)}$ of the r arclength coordinates $\{s_\nu\}_{\nu=1}^r$ and the r inverse square localization lengths $\{\tau_\nu\}_{\nu=1}^r$, which is built from $\mathcal{R}^{(r)}$, Eq. (E.1), in a manner described in App. E. The gaussian integrals in Eq. (C.17) are convergent, owing to the positive-definiteness of the eigenvalue spectrum of $\mathcal{R}^{(r)}$ and of $\mathcal{W}^{(r)}$ for finite τ. By inserting the result (C.17) into expression (C.16) we obtain

$$\frac{1}{V^n} \sum_{r=1}^{\infty} \frac{\mu^{2r} q^r}{r!} \int_0^1 ds_1 \cdots ds_r \int_0^\infty d\tau_1 p(\tau_1) \cdots d\tau_r p(\tau_r) \frac{1}{V} \int_V \frac{d\mathbf{c}_1}{V} \cdots \frac{d\mathbf{c}_r}{V}$$
$$(2\pi)^{-(r-1)(n+1)d/2} \Big(\mathcal{W}^{(r)} \det{}^{(r)} \mathcal{R}^{(r)}\Big)^{-(n+1)d/2} \exp\Big(-\frac{n+1}{2} \sum_{\rho,\rho'=1}^{r} \mathcal{C}^{(r)}_{\rho\rho'} \mathbf{c}_\rho \cdot \mathbf{c}_{\rho'}\Big). \tag{C.18}$$

The quantity $\mathcal{W}^{(r)}$ is built from $\mathcal{R}^{(r)}$, Eq. (E.1), in a manner described in App. E.

Next we perform the integration over $\{\mathbf{c}_1, \ldots, \mathbf{c}_r\}$. This integration is not quite gaussian, instead being quasi-gaussian, owing to the presence of a single *zero-mode*, the eigenvalue

spectrum of $\mathcal{C}^{(r)}$ containing a single zero eigenvalue, the remaining $r-1$ eigenvalues being positive-definite. The presence of this zero-mode can readily be ascertained by observing that from the definition of $\mathcal{C}^{(r)}$, Eq. (E.4), we identically have $\sum_{\rho'=1}^{r} \mathcal{C}^{(r)}_{\rho\rho'} = 0$, i.e., the normalized r-vector $(1,1,\ldots,1)/\sqrt{r}$ is an eigenvector of $\mathcal{C}^{(r)}_{\rho\rho'}$ with zero eigenvalue. The necessary quasi-gaussian integral is computed in App. D. By using it, Eq. (C.18) becomes

$$\frac{1}{V^n}\sum_{r=1}^{\infty}\frac{\mu^{2r}q^r}{r!}\int_0^1 ds_1\cdots ds_r\int_0^\infty d\tau_1 p(\tau_1)\cdots d\tau_r p(\tau_r)(2\pi)^{-(r-1)nd/2}$$
$$\times\left(\mathcal{W}^{(r)}\det{}^{(r)}\mathcal{R}^{(r)}\right)^{-nd/2}(n+1)^{-(r-1)d/2}\left(r^{-1}\mathcal{W}^{(r)}\det{}^{(r)}\mathcal{R}^{(r)}\,\tilde{\det}{}^{(r)}\mathcal{C}^{(r)}\right)^{-d/2}$$
, (C.19)

where $\tilde{\det}{}^{(r)}\mathcal{C}^{(r)}$ indicates the *quasi-determinant* of $\mathcal{C}^{(r)}$, i.e., the product of all the nonzero eigenvalues of $\mathcal{C}^{(r)}$; see [108]. We now make use of the result, established in App. F, that the factor $r^{-1}\mathcal{W}^{(r)}\det{}^{(r)}\mathcal{R}^{(r)}\,\tilde{\det}{}^{(r)}\mathcal{C}^{(r)}$ is identically unity. Thus, Eq. (C.19) is simplified, becoming

$$\frac{1}{V^n}\sum_{r=1}^{\infty}\frac{\mu^{2r}q^r}{r!}\int_0^1 ds_1\cdots ds_r\int_0^\infty d\tau_1 p(\tau_1)\cdots d\tau_r p(\tau_r)$$
$$\times(2\pi)^{-(r-1)nd/2}\left(\mathcal{W}^{(r)}\det{}^{(r)}\mathcal{R}^{(r)}\right)^{-nd/2}(n+1)^{-(r-1)d/2}. \quad \text{(C.20)}$$

We take this expression and insert it into Eq. (C.14) to obtain an expression for

$$\left\langle \exp\left(2\mu^2 V^{-n}\overline{\sum_{\hat{k}}}^{\dagger}\mathrm{Re}\,\Omega^*_{\hat{k}}\int_0^1 ds\,\mathrm{e}^{i\hat{k}\cdot\hat{c}(s)}\right)\right\rangle^{\mathrm{W}}_{n+1} \quad \text{(C.21)}$$

that is valid for $n > -1$. By expanding this result for small n, we finally obtain the desired quantity:

$$\lim_{n\to 0}\frac{2}{nd}\ln\left\langle \exp\left(2\mu^2 V^{-n}\overline{\sum_{\hat{k}}}^{\dagger}\mathrm{Re}\,\Omega^*_{\hat{k}}\int_0^1 ds\,\mathrm{e}^{i\hat{k}\cdot\hat{c}(s)}\right)\right\rangle^{\mathrm{W}}_{n+1}$$
$$=\left(\mathrm{e}^{-\mu^2 q}-(1-\mu^2 q)\right)\ln\left(V^{2/d}/2\pi\mathrm{e}\right)-\mathrm{e}^{-\mu^2 q}\sum_{r=1}^{\infty}\frac{\mu^{2r}q^r}{r!}$$
$$\times\int_0^1 ds_1\cdots ds_r\int_0^\infty d\tau_1 p(\tau_1)\cdots d\tau_r p(\tau_r)\ln\left(\mathcal{W}^{(r)}\det{}^{(r)}\mathcal{R}^{(r)}\right). \quad \text{(C.22)}$$

Appendix D

Quasi-gaussian integration

Consider the following integral,

$$\frac{1}{V}\int_V d\mathbf{c}_1\cdots d\mathbf{c}_r \exp\Big(-\frac{1}{2}\sum_{\rho,\rho'=1}^{r}\mathcal{C}^{(r)}_{\rho\rho'}\,\mathbf{c}_\rho\cdot\mathbf{c}_{\rho'}\Big)\exp\Big(-i\sum_{\rho=1}^{r}\mathbf{c}_\rho\cdot\mathbf{J}_\rho\Big), \tag{D.1}$$

taken over r copies of the volume V, in which $\mathcal{C}^{(r)}$ has as its sole non-positive definite eigenvalue the zero eigenvalue corresponding to the r-eigenvector $(1,1,\ldots,1)/\sqrt{r}$. We shall need both the general case, in which the sources $\{\mathbf{J}_\rho\}_{\rho=1}^r$ are arbitrary, and also the special case, in which the sources $\{\mathbf{J}_\rho\}_{\rho=1}^r$ all vanish. By working in a basis in which $\mathcal{C}^{(r)}$ is diagonal and assuming that V is sufficiently large (or, equivalently that no nonzero eigenvalue of $\mathcal{C}^{(r)}$ is arbitrarily small) one finds that this *quasi-gaussian* integral is given by

$$r^{d/2}\,(2\pi)^{(r-1)d/2}\Big(\tilde{\det}^{(r)}\,\mathcal{C}^{(r)}\Big)^{-d/2}\exp\Big(-\frac{1}{2}\sum_{\rho,\rho'=1}^{r}\tilde{\mathcal{C}}^{(r)}_{\rho\rho'}\,\mathbf{J}_\rho\cdot\mathbf{J}_{\rho'}\Big)\,\delta^{(d)}_{\mathbf{0},\sum_{\rho=1}^r\mathbf{J}_\rho}\,, \tag{D.2}$$

where $\tilde{\mathcal{C}}^{(r)}$ is the *quasi-inverse* of $\mathcal{C}^{(r)}$, i.e., the eigenvector expansion of the inverse of $\mathcal{C}^{(r)}$ from which the term corresponding to the zero eigenvalue has been omitted; see [108]. Similarly, as mentioned in Sec. C.2, $\tilde{\det}^{(r)}\,\mathcal{C}^{(r)}$ indicates the *quasi-determinant* of $\mathcal{C}^{(r)}$; see [108]. The factor of $r^{d/2}$ is subtle, but is familiar from the context of so-called collective coordinates. It arises from the fact that owing to the presence of the zero eigenvalue there are d integration directions for which convergence is not controlled by a gaussian integrand. Not only do the

corresponding integrations yield a volume factor; they also each yield a factor of $r^{1/2}$ by virtue of the limits on them determined by the form of the corresponding eigenvector. For the special case in which the sources $\{\mathbf{J}_\rho\}_{\rho=1}^r$ all vanish we have:

$$\frac{1}{V}\int_V d\mathbf{c}_1 \cdots d\mathbf{c}_r \exp\Big(-\frac{1}{2}\sum_{\rho,\rho'=1}^{r} \mathcal{C}^{(r)}_{\rho\rho'}\,\mathbf{c}_\rho\cdot\mathbf{c}_{\rho'}\Big) = r^{d/2}\,(2\pi)^{(r-1)d/2}\Big(\tilde{\det}^{(r)}\,\mathcal{C}^{(r)}\Big)^{-d/2}. \qquad \text{(D.3)}$$

Appendix E

Perturbation expansion at long localization lengths: free energy

Consider the quantity $\mathcal{R}^{(r)}$, an $(r \times r)$-matrix–valued function of the r arclength coordinates $\{s_\nu\}_{\nu=1}^r$ and the r inverse square localization lengths $\{\tau_\nu\}_{\nu=1}^r$, given by

$$\mathcal{R}^{(r)}_{\rho\rho'} \equiv \tau_\rho^{-1}\,\delta_{\rho\rho'} + \mathcal{S}_{\rho\rho'}, \tag{E.1}$$

where $\mathcal{S}$ is given by Eq. (A.3). We have found it useful to construct from $\mathcal{R}^{(r)}$ several auxiliary quantities:

$$\mathcal{U}^{(r)}_\rho \equiv \sum_{\rho'=1}^{r} \left(\mathcal{R}^{(r)}\right)^{-1}\Big|_{\rho\rho'}, \tag{E.2}$$

$$\mathcal{W}^{(r)} \equiv \sum_{\rho=1}^{r} \mathcal{U}^{(r)}_\rho, \tag{E.3}$$

$$\mathcal{C}^{(r)}_{\rho\rho'} \equiv \left(\mathcal{R}^{(r)}\right)^{-1}\Big|_{\rho\rho'} - \mathcal{U}^{(r)}_\rho\,\mathcal{U}^{(r)}_{\rho'}\big/\mathcal{W}^{(r)}. \tag{E.4}$$

We shall need to develop perturbative expansions in $\{\tau_\nu\}_{\nu=1}^r$ of $\ln\left(\mathcal{W}^{(r)}\det{}^{(r)}\,\mathcal{R}^{(r)}\right)$ to linear order and of $\mathcal{C}^{(r)}$ to quadratic order. To this end, we introduce the $(r \times r)$ identity matrix $\mathcal{I}^{(r)} \equiv \delta_{\rho\rho'}$, and make the definition

$$\mathcal{R}^{(r)}_0\Big|_{\rho\rho'} \equiv \tau_\rho^{-1}\,\delta_{\rho\rho'}, \tag{E.5}$$

so that $(\mathcal{R}_0^{(r)})^{-1}|_{\rho\rho'} \equiv \tau_\rho\,\delta_{\rho\rho'}$. First, we consider $\ln\det{}^{(r)}\,\mathcal{R}^{(r)}$:

$$\begin{aligned}
\ln\det{}^{(r)}\,\mathcal{R}^{(r)} &= \ln\det{}^{(r)}\left(\mathcal{R}_0^{(r)}+\mathcal{S}\right)\\
&= \ln\det{}^{(r)}\,\mathcal{R}_0^{(r)}\cdot\left(\mathcal{I}^{(r)}+\left(\mathcal{R}_0^{(r)}\right)^{-1}\cdot\mathcal{S}\right)\\
&= \ln\det{}^{(r)}\,\mathcal{R}_0^{(r)}+\ln\det{}^{(r)}\left(\mathcal{I}^{(r)}+\left(\mathcal{R}_0^{(r)}\right)^{-1}\cdot\mathcal{S}\right)\\
&= \ln\det{}^{(r)}\,\mathcal{R}_0^{(r)}+\mathrm{tr}^{(r)}\,\ln\left(\mathcal{I}^{(r)}+\left(\mathcal{R}_0^{(r)}\right)^{-1}\cdot\mathcal{S}\right)\\
&= \ln\left(\textstyle\prod_{\rho=1}^{r}\tau_\rho^{-1}\right)+\mathrm{tr}^{(r)}\left(\left(\mathcal{R}_0^{(r)}\right)^{-1}\cdot\mathcal{S}+\cdots\right)\\
&= -\textstyle\sum_{\rho=1}^{r}\ln\tau_\rho+\sum_{\rho=1}^{r}\tau_\rho\,\mathcal{S}_{\rho\rho}+\mathcal{O}(\tau^2),
\end{aligned}\tag{E.6}$$

where $\mathrm{tr}^{(r)}$ denotes the trace of an $r\times r$ matrix. Second, we consider $(\mathcal{R}^{(r)})^{-1}$. From Eq. (E.1) we have $\mathcal{R}^{(r)}=\mathcal{R}_0^{(r)}+\mathcal{S}$, from which follows the Dyson-type equation

$$\left(\mathcal{R}^{(r)}\right)^{-1}=\left(\mathcal{R}_0^{(r)}\right)^{-1}-\left(\mathcal{R}_0^{(r)}\right)^{-1}\cdot\mathcal{S}\cdot\left(\mathcal{R}^{(r)}\right)^{-1}.\tag{E.7}$$

Iterating the Dyson-type equation once and then truncating gives

$$\left(\mathcal{R}^{(r)}\right)^{-1}\Big|_{\rho\rho'}=\tau_\rho\delta_{\rho\rho'}-\tau_\rho\mathcal{S}_{\rho\rho'}\tau_{\rho'}+\mathcal{O}(\tau^3).\tag{E.8}$$

By using this result in Eqs. (E.2) and (E.3) we obtain

$$\mathcal{U}_\rho^{(r)} = \tau_\rho-\tau_\rho\sum_{\rho'=1}^{r}\mathcal{S}_{\rho\rho'}\tau_{\rho'},\tag{E.9}$$

$$\mathcal{W}^{(r)} = \sum_{\rho=1}^{r}\tau_\rho-\sum_{\rho,\rho'=1}^{r}\tau_\rho\mathcal{S}_{\rho\rho'}\tau_{\rho'}+\mathcal{O}(\tau^3).\tag{E.10}$$

Third, we use Eqs. (E.6) and (E.10) to obtain

$$\ln\left(\mathcal{W}^{(r)}\det{}^{(r)}\,\mathcal{R}^{(r)}\right)=\ln\left(\frac{\sum_{\rho=1}^{r}\tau_\rho}{\prod_{\rho=1}^{r}\tau_\rho}\right)+\left(\sum_{\rho=1}^{r}\tau_\rho\mathcal{S}_{\rho\rho}-\frac{\sum_{\rho,\rho'=1}^{r}\tau_\rho\,\mathcal{S}_{\rho\rho'}\,\tau_{\rho'}}{\sum_{\sigma=1}^{r}\tau_\sigma}\right)+\mathcal{O}(\tau^2).\tag{E.11}$$

Finally, by using Eqs. (E.8), (E.9) and (E.10) in Eq. (E.4) we obtain

$$\begin{aligned}
\mathcal{C}_{\rho\rho'}^{(r)} &= \left(\tau_\rho\delta_{\rho\rho'}-\frac{\tau_\rho\tau_{\rho'}}{\sum_{\sigma=1}^{r}\tau_\sigma}\right)\\
&\quad+\left(-\tau_\rho\,\mathcal{S}_{\rho\rho'}\,\tau_{\rho'}+\tau_\rho\tau_{\rho'}\frac{\sum_{\nu=1}^{r}\tau_\nu(\mathcal{S}_{\nu\rho'}+\mathcal{S}_{\rho\nu})}{\sum_{\sigma=1}^{r}\tau_\sigma}-\tau_\rho\tau_{\rho'}\frac{\sum_{\nu,\nu'=1}^{r}\tau_\nu\tau_{\nu'}\,\mathcal{S}_{\nu\nu'}}{(\sum_{\sigma=1}^{r}\tau_\sigma)^2}\right)+\mathcal{O}(\tau^3).
\end{aligned}\tag{E.12}$$

In reducing the free energy (2.91) to the form (2.95) we have used, *inter alia*, the perturbation expansion (E.11). In this way, the free energy reduces to an assembly of terms each being a functional of $p(\tau)$. Each term has a coefficient determined by integration over the arclength variables $\{s_1, \ldots, s_r\}$ of integrands arising from factors of $\mathcal{S}_{\rho\rho'}$, defined in Eq. (A.3), which depend on the arclength variables. The necessary integrals are readily expressed in terms of the following ones:

$$\int_0^1 ds_1\, \mathcal{S}_{11} = \int_0^1 ds_1\, \min(s_1, s_1) = \int_0^1 ds_1\, s_1 = 1/2, \tag{E.13}$$

$$\int_0^1 ds_1 \int_0^1 ds_2\, \mathcal{S}_{12} = \int_0^1 ds_1 \int_0^1 ds_2\, \min(s_1, s_2) = 2\int_0^1 ds_1 \int_0^{s_1} ds_2\, s_2 = 1/3. \tag{E.14}$$

Appendix F

A useful identity

We make repeated use of the identity

$$r^{-1}\,\mathcal{W}^{(r)}\,\det{}^{(r)}\,\mathcal{R}^{(r)}\;\tilde{\det}^{(r)}\,\mathcal{C}^{(r)}=1, \tag{F.1}$$

where $\mathcal{R}^{(r)}$, $\mathcal{W}^{(r)}$ and $\mathcal{C}^{(r)}$ are, respectively, defined in Eqs. (E.1), (E.3) and (E.4) of App. E. To derive this identity, we evaluate the following quantity [which arises, e.g., in Eq. (C.16)] in two ways:

$$V^{-1}\int\limits_{V} d\mathbf{m}\int đ\mathbf{k}_1\cdots đ\mathbf{k}_r\,\exp\Big(i\sum_{\rho=1}^{r}\mathbf{k}_\rho\cdot(\mathbf{c}_\rho-\mathbf{m})\Big)\;\exp\Big(-\frac{1}{2}\sum_{\rho,\rho'=1}^{r}\mathcal{R}^{(r)}_{\rho\rho'}\mathbf{k}_\rho\cdot\mathbf{k}_{\rho'}\Big). \tag{F.2}$$

First, by integrating over $\{\mathbf{c}_\rho\}_{\rho=1}^{r}$, then over $\{\mathbf{k}_\rho\}_{\rho=1}^{r}$, and then over $\mathbf{m}$ we obtain the result: unity. Second, by integrating over $\{\mathbf{k}_\rho\}_{\rho=1}^{r}$,then over $\mathbf{m}$, and then, by using the quasi-gaussian integral Eq. (D.3), over $\{\mathbf{c}_\rho\}_{\rho=1}^{r}$, we obtain the result:

$$\Big(r^{-1}\mathcal{W}^{(r)}\,\det{}^{(r)}\,\mathcal{R}^{(r)}\,\tilde{\det}^{(r)}\,\mathcal{C}^{(r)}\Big)^{-d/2}; \tag{F.3}$$

hence the identity Eq. (F.1).

Appendix G

Laplace representation of free energy

In this appendix we describe in detail how to exchange the dependence of the three contributions to $\bar{f}^{\rm var}$, Eq. (2.95), from $p(\tau)$ to its Laplace transform $\hat{p}(\hat{\tau})$. We begin by noting two integrals:

$$\ln \tau = \int_0^\infty \frac{d\hat{\tau}}{\hat{\tau}} \left(e^{-\hat{\tau}} - e^{-\hat{\tau}\tau} \right), \tag{G.1}$$

$$\frac{1}{\tau} = \int_0^\infty d\hat{\tau} e^{-\hat{\tau}\tau}. \tag{G.2}$$

The latter integral is elementary; the former is an example of a Frullanian integral; see Ref. [109]. We use Eq. (G.1) to express the first contribution to $\bar{f}^{\rm var}$ as

$$\begin{aligned} \left\{ \ln \left(\frac{\tau_1 + \tau_2}{\tau_1 \tau_2} \right) \right\}_\tau &= \left\{ \ln(\tau_1 + \tau_2) - \ln(\tau_1) - \ln(\tau_2) \right\}_\tau \\ &= \int_0^\infty d\tau_1 p(\tau_1) \int_0^\infty d\tau_2 p(\tau_2) \int_0^\infty \frac{d\hat{\tau}}{\hat{\tau}} \left(-e^{-\hat{\tau}} - e^{-\hat{\tau}(\tau_1+\tau_2)} + e^{-\hat{\tau}\tau_1} + e^{-\hat{\tau}\tau_2} \right) \\ &= \int_0^\infty \frac{d\hat{\tau}}{\hat{\tau}} \left(-\hat{p}(\hat{\tau})^2 + 2\hat{p}(\hat{\tau}) - e^{-\hat{\tau}} \right), \end{aligned} \tag{G.3}$$

where the curly braces $\{\cdots\}_\tau$ were defined immediately following Eq. (2.95). By following the identical strategy, we use Eq. (G.1) to express the second contribution to $\bar{f}^{\rm var}$ as

$$\begin{aligned} \left\{ \ln \left(\frac{\tau_1 + \tau_2 + \tau_3}{\tau_1 \tau_2 \tau_3} \right) \right\}_\tau &= \left\{ \ln(\tau_1 + \tau_2 + \tau_3) - \ln(\tau_1) - \ln(\tau_2) - \ln(\tau_3) \right\}_\tau \\ &= \int_0^\infty \frac{d\hat{\tau}}{\hat{\tau}} \left(-\hat{p}(\hat{\tau})^3 + 3\hat{p}(\hat{\tau}) - 2e^{-\hat{\tau}} \right). \end{aligned} \tag{G.4}$$

To express the third contribution to $\bar{f}^{\rm var}$ in terms of $\hat{p}(\hat{\tau})$ we make use of Eq. (G.2). This yields

$$\begin{aligned}\left\{\frac{\tau_1\tau_2}{\tau_1+\tau_2}\right\}_\tau &= \int_0^\infty d\tau_1 p(\tau_1)\int_0^\infty d\tau_2 p(\tau_2)\frac{\tau_1\tau_2}{\tau_1+\tau_2} \\ &= \int_0^\infty d\tau_1 p(\tau_1)\tau_1\int_0^\infty d\tau_2 p(\tau_2)\tau_2\int_0^\infty d\hat{\tau}\,\mathrm{e}^{-\hat{\tau}(\tau_1+\tau_2)} = \int_0^\infty d\hat{\tau}(d\hat{p}/d\hat{\tau})^2. \quad \text{(G.5)}\end{aligned}$$

We now take the functional derivative with respect to $\hat{p}(\hat{\tau})$ of these three contributions to $\bar{f}^{\rm var}$. Being local, the first two are straightforward to compute, respectively yielding

$$\frac{\delta}{\delta\hat{p}(\hat{\tau})}\left\{\ln\left(\frac{\tau_1+\tau_2}{\tau_1\tau_2}\right)\right\}_\tau = \frac{2}{\hat{\tau}}\Big(1-\hat{p}(\hat{\tau})\Big), \quad \text{(G.6)}$$

$$\frac{\delta}{\delta\hat{p}(\hat{\tau})}\left\{\ln\left(\frac{\tau_1+\tau_2+\tau_3}{\tau_1\tau_2\tau_3}\right)\right\}_\tau = \frac{3}{\hat{\tau}}\Big(1-\hat{p}(\hat{\tau})^2\Big). \quad \text{(G.7)}$$

To evaluate the functional derivative with respect to $\hat{p}(\hat{\tau})$ of the third contribution to $\bar{f}^{\rm var}$ requires an integration by parts. The integrated piece vanishes because $\hat{p}(\hat{\tau})$ is to be varied at neither $\hat{\tau}=0$ nor $\hat{\tau}=\infty$, due to the boundary conditions. Thus we obtain for the third contribution to $\bar{f}^{\rm var}$:

$$\frac{\delta}{\delta\hat{p}(\hat{\tau})}\left\{\frac{\tau_1\tau_2}{\tau_1+\tau_2}\right\}_\tau = -2\frac{d^2\hat{p}}{d\hat{\tau}^2}. \quad \text{(G.8)}$$

Appendix H

Order-parameter weighted averages

In this appendix we focus on the computation of the following quantity, defined for arbitrary $\hat{l}$ and $\hat{l}'$:

$$\Big\langle \int_0^1 dt\, \mathrm{e}^{-i\hat{l}\cdot\hat{c}(t)} \int_0^1 dt'\, \mathrm{e}^{-i\hat{l}'\cdot\hat{c}(t')} \times \exp\Big(\mu^2 q V^{-n} \sum_{\hat{k}} \int_0^1 ds\, \mathrm{e}^{-i\hat{k}\cdot\hat{c}(s)}\, \delta^{(d)}_{\tilde{\mathbf{k}},\mathbf{0}} \int_0^\infty d\tau\, p(\tau) \exp\big(-\hat{k}^2/2\tau\big)\Big)\Big\rangle^{\mathrm{W}}_{n+1} . \tag{H.1}$$

In addition, we make two applications of it. We proceed by expanding the exponential, which yields

$$\Big\langle \int_0^1 dt\, \mathrm{e}^{-i\hat{l}\cdot\hat{c}(t)} \int_0^1 dt'\, \mathrm{e}^{-i\hat{l}'\cdot\hat{c}(t')}\Big\rangle^{\mathrm{W}}_{n+1} + \sum_{r=1}^{\infty} \frac{\mu^{2r} q^r}{V^{nr} r!} \int_0^1 ds_1 \cdots ds_{r+2} \int_0^\infty d\tau_1 p(\tau_1) \cdots d\tau_r p(\tau_r) \times \sum_{\hat{k}_1,\ldots,\hat{k}_r} \prod_{\rho=1}^{r} \delta^{(d)}_{\tilde{\mathbf{k}}_\rho,\mathbf{0}} \exp\Big(-\frac{1}{2}\sum_{\rho=1}^{r} \frac{1}{\tau_\rho}\hat{k}_\rho^2\Big) \Big\langle \mathrm{e}^{-i\hat{l}\cdot\hat{c}(s_{r+1})} \mathrm{e}^{-i\hat{l}'\cdot\hat{c}(s_{r+2})} \mathrm{e}^{-i\sum_{\rho=1}^{r}\hat{k}_\rho\cdot\hat{c}(s_\rho)}\Big\rangle^{\mathrm{W}}_{n+1} . \tag{H.2}$$

Next, we observe the factorization of the Wiener measure correlators on the replica index, use the explicit result for this correlator given in App. A, use integral representations for the Kronecker δ-functions [Eqs. (C.15) and (C.13)], and convert summations to integrals by using Eq. (C.5), thus obtaining

$$
\begin{aligned}
&\delta^{(nd+d)}_{\hat{l}+\hat{l}',\hat{0}} \int_0^1 dt \int_0^1 dt'\, \mathrm{e}^{-|t-t'|\hat{l}^2} \\
&+\frac{1}{V^n}\sum_{r=1}^{\infty}\frac{\mu^{2r}q^r}{r!}\int_0^1 ds_1\cdots ds_{r+2}\int_0^{\infty} d\tau_1 p(\tau_1)\cdots d\tau_r p(\tau_r)\frac{1}{V}\int_V d\mathbf{c}_1\ldots d\mathbf{c}_r\int_V d\mathbf{m}^0\cdots d\mathbf{m}^n \\
&\times\int đ\hat{k}_1\cdots đ\hat{k}_r \exp\Big(i\sum_{\rho=1}^{r}\mathbf{c}_\rho\cdot\sum_{\alpha=0}^{n}\mathbf{k}_\rho^\alpha\Big)\exp\Big(-i\sum_{\alpha=0}^{n}\mathbf{m}^\alpha\cdot(\mathrm{l}^\alpha+\mathrm{l}'^\alpha+\sum_{\rho=1}^{r}\mathbf{k}_\rho^\alpha)\Big)\exp\Big(-\sum_{\rho=1}^{r}\hat{k}_\rho^2/2\tau_\rho\Big) \\
&\times\exp\Big(-\frac{1}{2}\sum_{\alpha=0}^{n}\sum_{\rho,\rho'=1}^{r}\mathbf{k}_\rho^\alpha\cdot\mathbf{k}_{\rho'}^\alpha\,\mathcal{S}_{\rho\rho'}\Big)\exp\Big(-\sum_{\alpha=0}^{n}\sum_{\rho=1}^{r}\mathrm{l}^\alpha\cdot\mathbf{k}_\rho^\alpha\,\mathcal{S}_{r+1,\rho}\Big)\exp\Big(-\sum_{\alpha=0}^{n}\sum_{\rho=1}^{r}\mathrm{l}'^\alpha\cdot\mathbf{k}_\rho^\alpha\,\mathcal{S}_{r+2,\rho}\Big) \\
&\times\exp\Big(-\frac{1}{2}\hat{l}^2\,\mathcal{S}_{r+1,r+1}\Big)\exp\Big(-\frac{1}{2}\hat{l}'^2\,\mathcal{S}_{r+2,r+2}\Big)\exp\Big(-\hat{l}\cdot\hat{l}'\,\mathcal{S}_{r+1,r+2}\Big). \qquad \text{(H.3)}
\end{aligned}
$$

We now recognize that the integrals over $\{\mathbf{m}^\alpha\}_{\alpha=0}^n$ and $\{\mathbf{k}_1^\alpha,\ldots,\mathbf{k}_r^\alpha\}_{\alpha=0}^n$ factorize on the replica index, giving

$$
\begin{aligned}
&\delta^{(nd+d)}_{\hat{l}+\hat{l}',\hat{0}} \int_0^1 dt \int_0^1 dt'\, \mathrm{e}^{-|t-t'|\hat{l}^2}+\frac{1}{V^n}\sum_{r=1}^{\infty}\frac{\mu^{2r}q^r}{r!}\int_0^1 ds_1\cdots ds_{r+2}\int_0^{\infty} d\tau_1 p(\tau_1)\cdots d\tau_r p(\tau_r) \\
&\times\exp\Big(-\frac{1}{2}\hat{l}^2\,\mathcal{S}_{r+1,r+1}-\frac{1}{2}\hat{l}'^2\,\mathcal{S}_{r+2,r+2}-\hat{l}\cdot\hat{l}'\,\mathcal{S}_{r+1,r+2}\Big)\frac{1}{V}\int_V d\mathbf{c}_1\cdots d\mathbf{c}_r \\
&\times\prod_{\alpha=0}^{n}\Big(\int_V d\mathbf{m}\int đ\mathbf{k}_1\cdots đ\mathbf{k}_r\exp\Big(i\sum_{\rho=1}^{r}\mathbf{c}_\rho\cdot\mathbf{k}_\rho\Big)\exp\Big(-i\mathbf{m}\cdot(\mathrm{l}^\alpha+\mathrm{l}'^\alpha+\sum_{\rho=1}^{r}\mathbf{k}_\rho)\Big) \\
&\times\exp\Big(-\sum_{\rho=1}^{r}\mathbf{k}_\rho^2/2\tau_\rho\Big)\exp\Big(-\frac{1}{2}\sum_{\rho,\rho'=1}^{r}\mathbf{k}_\rho\cdot\mathbf{k}_{\rho'}\,\mathcal{S}_{\rho\rho'}\Big) \\
&\times\exp\Big(-\sum_{\rho=1}^{r}\mathrm{l}^\alpha\cdot\mathbf{k}_\rho\,\mathcal{S}_{r+1,\rho}\Big)\exp\Big(-\sum_{\rho=1}^{r}\mathrm{l}'^\alpha\cdot\mathbf{k}_\rho\,\mathcal{S}_{r+2,\rho}\Big)\Big). \qquad \text{(H.4)}
\end{aligned}
$$

At this stage we focus on the factorized integrals over $\{\mathbf{k}_\rho^\alpha\}_\rho^r$ and $\mathbf{m}^\alpha$ occurring under the product. As they are gaussian integrals they can straightforwardly be performed (we prefer to integrate over $\{\mathbf{k}_\rho^\alpha\}_{\rho=1}^r$ first and $\mathbf{m}^\alpha$ second), yielding

$$
\begin{aligned}
&(2\pi)^{-(r-1)d/2}(\mathcal{W}^{(r)}\,\det\mathcal{R}^{(r)})^{-d/2}\exp\Big(-|\mathrm{l}^\alpha+\mathrm{l}'^\alpha|^2/2\mathcal{W}^{(r)}\Big) \\
&\quad\times\exp\Big(-\frac{1}{2}\sum_{\rho,\rho'=1}^{r}\mathcal{C}^{(r)}_{\rho\rho'}(\mathbf{c}_\rho+i\mathrm{l}^\alpha\,\mathcal{S}_{r+1,\rho}+i\mathrm{l}'^\alpha\,\mathcal{S}_{r+2,\rho})\cdot(\mathbf{c}_{\rho'}+i\mathrm{l}^\alpha\,\mathcal{S}_{r+1,\rho'}+i\mathrm{l}'^\alpha\,\mathcal{S}_{r+2,\rho'})\Big) \\
&\quad\times\exp\Big(-\frac{i}{\mathcal{W}^{(r)}}(\mathrm{l}^\alpha+\mathrm{l}'^\alpha)\cdot\sum_{\rho=1}^{r}\mathcal{U}^{(r)}_\rho\,(\mathbf{c}_\rho+i\mathrm{l}^\alpha\,\mathcal{S}_{r+1,\rho}+i\mathrm{l}'^\alpha\,\mathcal{S}_{r+2,\rho})\Big), \qquad \text{(H.5)}
\end{aligned}
$$

where $\mathcal{U}^{(r)}$, $\mathcal{W}^{(r)}$ and $\mathcal{C}^{(r)}$ are respectively defined in Eqs. (E.2), (E.3) and (E.4). Next, we insert the result of integrating over $\{\mathbf{k}_\rho^\alpha\}_{\rho=1}^r$ and $\mathbf{m}^\alpha$ into Eq. (H.4) and focus on the

remaining integrals over $\{\mathbf{c}_\rho\}_{\rho=1}^r$. Just as we encountered in App. C, this integration is not quite gaussian, instead being quasi-gaussian, owing to the presence a single zero in the eigenvalue spectrum of $\mathcal{C}^{(r)}$. The necessary quasi-gaussian integral is computed in App. D. By using it, Eq. (H.4) becomes

$$\begin{aligned}
&\delta^{(nd+d)}_{\hat{l}+\hat{l}',\hat{0}} \int_0^1 dt \int_0^1 dt'\, \mathrm{e}^{-|t-t'|\hat{l}^2} \\
&\quad + \delta^{(d)}_{\tilde{\mathbf{l}}+\tilde{\mathbf{l}}',\mathbf{0}} \frac{1}{V^n} \sum_{r=1}^{\infty} \frac{\mu^{2r} q^r}{r!} \int_0^1 ds_1 \cdots ds_{r+2} \int_0^\infty d\tau_1 p(\tau_1) \cdots d\tau_r p(\tau_r) \\
&\quad \times (2\pi)^{-(r-1)nd/2} (\mathcal{W}^{(r)} \det{}^{(r)} \mathcal{R}^{(r)})^{-nd/2} (n+1)^{-(r-1)d/2} \\
&\quad \times (r^{-1} \mathcal{W}^{(r)} \det{}^{(r)} \mathcal{R}^{(r)} \tilde{\det}{}^{(r)} \mathcal{C}^{(r)})^{-d/2} \\
&\quad \times \exp\Big((\mathcal{W}^{(r)})^{-1} \sum_{\rho=1}^r \mathcal{U}_\rho^{(r)} \big(\hat{l}^2 \mathcal{S}_{r+1,\rho} + \hat{l}'^2 \mathcal{S}_{r+2,\rho} + \hat{l} \cdot \hat{l}' (\mathcal{S}_{r+1,\rho} + \mathcal{S}_{r+2,\rho}) \big) \Big) \\
&\quad \times \exp\Big(-(\hat{l}^2 \mathcal{S}_{r+1,r+1} + \hat{l}'^2 \mathcal{S}_{r+2,r+2} + 2\hat{l} \cdot \hat{l}' \mathcal{S}_{r+1,r+2})/2 \Big) \\
&\quad \times \exp\Big(\frac{1}{2} \hat{l}^2 \sum_{\rho,\rho'=1}^r \mathcal{C}^{(r)}_{\rho\rho'} \mathcal{S}_{r+1,\rho} \mathcal{S}_{r+1,\rho'} + \frac{1}{2} \hat{l}'^2 \sum_{\rho,\rho'=1}^r \mathcal{C}^{(r)}_{\rho\rho'} \mathcal{S}_{r+2,\rho} \mathcal{S}_{r+2,\rho'} + \hat{l} \cdot \hat{l}' \sum_{\rho,\rho'=1}^r \mathcal{C}^{(r)}_{\rho\rho'} \mathcal{S}_{r+1,\rho} \mathcal{S}_{r+2,\rho'} \Big) \\
&\quad \times \exp\Big(-(\hat{l}^2 + \hat{l}'^2 + 2\hat{l} \cdot \hat{l}')/2\mathcal{W}^{(r)} \Big) \\
&\quad \times \exp\Big(-(n+1)^{-1} \sum_{\rho,\rho'=1}^r \mathcal{C}^{(r)}_{\rho\rho'} (\tilde{\mathbf{l}} \mathcal{S}_{r+1,\rho} + \tilde{\mathbf{l}}' \mathcal{S}_{r+2,\rho}) \cdot (\tilde{\mathbf{l}} \mathcal{S}_{r+1,\rho'} + \tilde{\mathbf{l}}' \mathcal{S}_{r+2,\rho'})/2 \Big). \qquad \text{(H.6)}
\end{aligned}$$

We have simplified this result by making use of the identity given in Eq. (F.1) of App. F. We have further simplified it by observing that as $\tilde{\mathcal{C}}^{(r)}$ is the quasi-inverse [108] of $\mathcal{C}^{(r)}$ (see App. E and footnote [108]), the relevant zero-mode being $(1,1,\ldots,1)/\sqrt{r}$, we have

$$\tilde{\mathcal{C}}^{(r)} \cdot \mathcal{C}^{(r)}\big|_{\rho\rho'} = \delta_{\rho\rho'} - r^{-1}, \qquad \text{(H.7)}$$

$$\mathcal{C}^{(r)} \cdot \tilde{\mathcal{C}}^{(r)} \cdot \mathcal{C}^{(r)} = \mathcal{C}^{(r)}. \qquad \text{(H.8)}$$

In addition, we have used the fact that there is a single zero-mode to ascertain that

$$\tilde{\det}{}^{(r)} ((n+1)\mathcal{C}^{(r)}) = (n+1)^{r-1} \tilde{\det}{}^{(r)} \mathcal{C}^{(r)}. \qquad \text{(H.9)}$$

As our first application of Eq. (H.6), we set $\hat{l} = \hat{l}' = \hat{0}$, thus obtaining a normalization factor that we shall use subsequently:

$$1 + \frac{1}{V^n} \sum_{r=1}^{\infty} \frac{\mu^{2r} q^r}{r!} \int_0^1 ds_1 \cdots ds_{r+2} \int_0^\infty d\tau_1 p(\tau_1) \cdots d\tau_r p(\tau_r)$$

$$\times(2\pi)^{-(r-1)nd/2}(\mathcal{W}^{(r)}\det{}^{(r)}\mathcal{R}^{(r)})^{-nd/2}(n+1)^{-(r-1)d/2}. \qquad \text{(H.10)}$$

As our second application of Eq. (H.6) we compute the right hand side of Eq. (2.110) by forming the quotient of Eq. (H.6) with $\hat{l}' = \hat{0}$ and Eq. (H.10). By making use of the identity Eq. (F.1) and taking the limit $n \to 0$ we obtain Eqs. (2.111) and (2.112).

Appendix I

Perturbation expansion at long localization lengths: order parameter

In this appendix we compute the perturbative expansions of $\Upsilon^{(1)}$ and $\Upsilon^{(2)}$ needed to compute the right hand side of Eq. (2.114). By using the definitions (A.3), (E.2), (E.3) and (E.4), we find

$$\Upsilon^{(1)} = \left(\tau_1^{-1} + |s_1 - s_2|\right)^{-1} = \tau_1 - |s_1 - s_2|\tau_1^2 + \mathcal{O}(\tau^3), \tag{I.1}$$

$$\Upsilon^{(2)} = \tau_1 + \tau_2 + \mathcal{O}(\tau^2). \tag{I.2}$$

By inserting these results into Eq. (2.114), and using Eq. (2.113), we obtain

$$\begin{aligned} qp(\tau) &= (1-q)\mu^2 q \int_0^1 ds_1 ds_2 \int_0^\infty d\tau_1 p(\tau_1)\, \delta(\tau - \tau_1 + \tau_1^2|s_1 - s_2|) \\ &\quad + \frac{1}{2}\mu^4 q^2 \int_0^1 ds_1 ds_2 ds_3 \int_0^\infty d\tau_1 p(\tau_1)\, d\tau_2 p(\tau_2)\, \delta(\tau - \tau_1 - \tau_2) + \mathcal{O}(\epsilon^2). \end{aligned} \tag{I.3}$$

Next, we expand the Dirac δ-function, $\delta(\tau - \tau_1 + \tau_1^2|s_1 - s_2|) \approx \delta(\tau - \tau_1) + \tau_1^2|s_1 - s_2|\delta'(\tau - \tau_1)$, and perform the τ and s integrals. (Equivalently, we take the Laplace transform of Eq. (I.3), expand the resulting exponential function, perform the τ and s integrals, and back-transform the resulting nonlinear ordinary differential equation.) Finally, we transform to the scaling form $\pi(\theta)$ defined in Eq. (2.102), and observe that it satisfies Eq. (2.108).

Appendix J

Computation of the non-diagonal matrix elements for the Hessian matrix

In this appendix we collect some useful information concerning surface harmonics, and later use it to compute the matrix elements of the non-diagonal part H^O of the Hessian in the basis $\{\varphi_{p,\tilde{\mathbf{p}},\sigma}\}$.

The Gegenbauer (also called hyperspherical) polynomials play a role in D dimensions and with regard to the surface harmonics S_σ analogous to that played by the Legendre polynomials in 3 dimensions and with regard to the spherical harmonics Y_{lm}. The Gegenbauer polynomial $C_l^\nu(x)$ of degree r is defined by the generating function (see, e.g., [97], Sec. 11.1.2)

$$(1 - 2xt + t^2)^{-\nu} = \sum_{l=0}^{\infty} C_l^\nu(x)\, t^l. \tag{J.1}$$

There is a generalization to dimension $D = p + 2$ of the addition theorem for spherical harmonics, which relates the Gegenbauer polynomial to a sum of surface harmonics (see,

e.g., [97], Sec. 11.4):

$$\begin{aligned} C_l^{p/2}(\phi'\cdot\phi) &= \frac{C_l^{p/2}(1)\tau_D}{h(l,p)}\sum_{|\sigma|=l} S_\sigma^*(\phi')S_\sigma(\phi), \\ &= \frac{4\pi^{1+p/2}}{(2l+p)\Gamma(p/2)}\sum_{|\sigma|=l} S_\sigma^*(\phi')S_\sigma(\phi). \end{aligned} \tag{J.2}$$

Here ϕ' and ϕ are any unit D-dimensional vectors, $h(l,p)$ is the number of linearly independent surface harmonics of degree l in dimension $p+2$, and $\tau_D = 2\pi^{D/2}/\Gamma(D/2)$ is the area of the D-dimensional unit sphere. As $C_l^{1/2}(x)$ is equal to the Legendre polynomial $P_l(x)$, the above formula reduces, in the case $D=3$, to the usual addition theorem.

We will also make use of the identity (see, e.g., [97], Vol. II, Sec. 7.15)

$$z^\nu \mathrm{e}^{xz} = 2^\nu \Gamma(\nu)\sum_{n=0}^{\infty}(n+\nu)\, C_n^\nu(x)\, I_{n+\nu}(z) \tag{J.3}$$

In the case of dimension $D=nd$, by combining Eqs. (J.2) and (J.3), the following identity is obtained

$$\exp(x\phi'\cdot\phi) = 2\pi^{nd/2}(x/2)^{1-nd/2}\sum_{l=0}^{\infty} I_{l-1+nd/2}(x)\sum_{\sigma,|\sigma|=l} S_\sigma^*(\phi')\, S_\sigma(\phi). \tag{J.4}$$

Here x is any real number, ϕ' and ϕ are unit nd-dimensional vectors, $I_\nu(x)$ is the modified Bessel function of order ν, and $|\sigma|$ is the degree of S_σ as a homogeneous trigonometric polynomial.

Let us now compute the matrix elements of the non-diagonal part H^O of the Hessian in the basis $\{\varphi_{p,\tilde{\mathbf{p}},\sigma}\}$. By using Eqs. (3.13) and (3.9) we obtain

$$\begin{aligned} \langle\varphi_{p'\tilde{\mathbf{p}}'\sigma'}|H^O|\varphi_{p\tilde{\mathbf{p}}\sigma}\rangle &= V^2\int \frac{d\tilde{\mathbf{k}}\, d\tilde{\mathbf{l}}\, d\breve{k}\, d\breve{l}}{(1+n)^d(2\pi)^{(1+n)2d}}(1+n)^{d/2}(2\pi)^{nd}p'^{\frac{1-nd}{2}}\delta_{\tilde{\mathbf{p}}'\tilde{\mathbf{k}}}\,\delta(|\breve{k}|-p')\, S_{\sigma'}^*(\phi_{\breve{k}}) \\ &\quad\times p^{\frac{1-nd}{2}}\delta_{\tilde{\mathbf{p}}\tilde{\mathbf{l}}}\delta(|\breve{l}|-p)S_\sigma(\phi_{\breve{l}})\delta_{\tilde{\mathbf{k}}\tilde{\mathbf{l}}}\ \ (-2\epsilon)\int_0^\infty d\theta\,\pi(\theta)\mathrm{e}^{-(\breve{k}-\breve{l})^2/\epsilon\theta}, \qquad \text{(J.5)} \\ &= \frac{-2\epsilon\ (2\pi)^{-nd}}{(1+n)^{d/2}}\sum_{\tilde{\mathbf{k}},\tilde{\mathbf{l}}}\delta_{\tilde{\mathbf{p}}'\tilde{\mathbf{k}}}\delta_{\tilde{\mathbf{p}}\tilde{\mathbf{l}}}\delta_{\tilde{\mathbf{k}}\tilde{\mathbf{l}}}\ \ \int_0^\infty\delta(|\breve{k}|-p')\,|\breve{k}|^{nd-1}d|\breve{k}| \\ &\quad\times\int_0^\infty\delta(|\breve{l}|-p)\,|\breve{l}|^{nd-1}d|\breve{l}|\ \ (pp')^{\frac{1-nd}{2}}\int_0^\infty d\theta\,\pi(\theta)\,\mathrm{e}^{-(p^2+p'^2)/\epsilon\theta} \\ &\quad\times\int d\phi_{\breve{k}}\int d\phi_{\breve{l}}\, S_{\sigma'}^*(\phi_{\breve{k}})\,\exp(2pp'\phi_{\breve{k}}\cdot\phi_{\breve{l}}/\epsilon\theta)\, S_\sigma(\phi_{\breve{l}})\ . \qquad \text{(J.6)} \end{aligned}$$

In the second step we have separated the $\breve{k}$ and $\breve{l}$ integrals into radial and angular parts. The angular integrals can be performed (with the help of the identity Eq. (J.4), and using the orthogonality of the surface harmonics) to obtain

$$\langle \varphi_{p'\tilde{\mathbf{p}}'\sigma'} | H^O | \varphi_{p\tilde{\mathbf{p}}\sigma} \rangle = \delta_{\tilde{\mathbf{p}}',\tilde{\mathbf{p}}} \delta_{\sigma',\sigma} \frac{(-2\epsilon)\epsilon^{(nd-1)/2}}{2^{nd}\pi^{nd/2}(1+n)^{d/2}} \times 2\sqrt{pp'/\epsilon} \int_0^\infty \frac{d\theta\, \pi(\theta)}{\theta^{1-nd/2}} \, \mathrm{e}^{-(p'^2+p^2)/\epsilon\theta} \, I_{|\sigma|-1+nd/2}\left(\frac{2p'p}{\epsilon\theta}\right), \tag{J.7}$$

which is equivalent to Eqs. (3.18), (3.19) and (3.20).

Appendix K

Computation of lower bounds for the eigenvalues of the Hessian matrix

In this appendix we study in detail the bound function $\beta_l(v)$. We decompose $\beta_l(v)$ as follows:

$$\begin{aligned} \beta_l(v) &= \frac{v^2}{2\langle\theta^{-1}\rangle_\pi} - 2j_l(v) \\ j_l(v) &\equiv 2\int_0^\infty du\,\sqrt{uv}\,\mathrm{e}^{-(u^2+v^2)} I_{l-1}(2uv) \end{aligned} \tag{K.1}$$

We now analytically compute the integral defining $j_l(v)$

$$\begin{aligned} j_l(v) &= \sqrt{v}\mathrm{e}^{-v^2}\int_0^\infty dy\, y^{-1/4}\mathrm{e}^{-y} I_{l-1}(2v\sqrt{y}) \\ &= \frac{\Gamma(l/2+1/4)}{\Gamma(l)} v^{l-1/2} e^{-v^2} M\Big(\frac{l}{2}+\frac{1}{4}, l, v^2\Big). \\ &= \frac{\Gamma(l/2+1/4)}{\Gamma(l)} v^{l-1/2} M\Big(\frac{l}{2}-\frac{1}{4}, l, -v^2\Big). \end{aligned} \tag{K.2}$$

By inserting this expression into Eq. (K.1), we obtain Eq. (3.51).

We can obtain more information by using the following integral formula for the confluent hypergeometric function [101], valid for $\mathrm{Re}\, a > 0$ and $\mathrm{Re}\, b > 0$:

$$\frac{\Gamma(b-a)\Gamma(a)}{\Gamma(b)} M(a,b,z) = \int_0^1 \mathrm{e}^{zt} t^{a-1}(1-t)^{b-a-1} dt. \tag{K.3}$$

In our case, we have

$$j_l(v) = \frac{(v^2)^{\frac{l}{2}-\frac{1}{4}}}{\Gamma(\frac{l}{2}-\frac{1}{4})} \int_0^1 \mathrm{e}^{-tv^2} t^{(\frac{l}{2}-\frac{1}{4})-1}(1-t)^{(\frac{l}{2}+\frac{1}{4})-1} dt. \tag{K.4}$$

By considering the fact that the exponential in the integrand is always smaller than or equal to 1, this formula can immediately be bounded above, as follows:

$$\begin{aligned} j_l(v) &\leq \frac{(v^2)^{\frac{l}{2}-\frac{1}{4}}}{\Gamma(\frac{l}{2}-\frac{1}{4})} \int_0^1 t^{(l/2-1/4)-1}(1-t)^{(l/2+1/4)-1} dt, \\ &= \frac{(v^2)^{\frac{l}{2}-\frac{1}{4}}}{\Gamma(\frac{l}{2}-\frac{1}{4})} B(\frac{l}{2}-\frac{1}{4}, \frac{l}{2}+\frac{1}{4}) = \frac{\Gamma(\frac{l}{2}+\frac{1}{4})}{\Gamma(l)} v^{l-1/2}. \end{aligned} \tag{K.5}$$

By combining this with Eq. (K.1) we obtain the bound stated in Eq. (3.55). In addition, in the limit of $v \ll 1$, it is legitimate to replace the exponential by 1 inside the integral, and thus the same expression gives the asymptotic form in that limit, as quoted in Eq. (3.53).

An additional bound can be obtained for the case $l > 1$ by taking into account that the factor $(1-t)^{(l/2+1/4)-1}$ in the integrand is smaller than or equal to one

$$j_l(v) \leq \frac{(v^2)^{\frac{l}{2}-\frac{1}{4}}}{\Gamma(\frac{l}{2}-\frac{1}{4})} \int_0^\infty \mathrm{e}^{-tv^2} t^{(l/2-1/4)-1} dt = 1. \tag{K.6}$$

This gives the lower bound of Eq. (3.54). The same expression provides the asymptotic form for all values of l when $v \gg 1$, Eq. (3.52), as in that limit the integral is dominated by the region near the origin, and the factor $(1-t)^{(l/2+1/4)-1}$ is close to unity in that region.

Appendix L

Correction to the order parameter under stress

In this appendix we show that the only solution to Eq. (4.39) that satisfies the boundary condition Eq. (4.49) is the null function $\zeta(\theta) \equiv 0$ for all θ. Our approach is to assume that a nonzero solution exists, and then to arrive at a contradiction.

It is convenient to work with $\tilde{\zeta}(\theta)$ instead of $\zeta(\theta)$. In terms of $\tilde{\zeta}(\theta)$, the integro-differential equation reads:

$$\frac{\theta^2}{2}\frac{d\tilde{\zeta}}{d\theta} = \tilde{\zeta}(\theta) - 2\int_0^\theta d\theta'\, \tilde{\zeta}(\theta')\, \pi(\theta - \theta'). \tag{L.1}$$

The boundary condition is simply

$$\lim_{\theta\to\infty} \tilde{\zeta}(\theta) = 0. \tag{L.2}$$

It turns out that it is possible to derive a simple differential equation for the Laplace transform $\hat{\varrho}(s)$ of the function

$$\varrho(\theta) \equiv \frac{d\tilde{\zeta}}{d\theta}. \tag{L.3}$$

Starting from Eq. (L.1), and using properties of the Laplace transform, one obtains (after some algebra) the equation

$$\frac{d^2\hat{\varrho}(s)}{ds^2} = \frac{2}{s}\hat{\varrho}(s)(1 - \hat{\pi}(s)), \tag{L.4}$$

and the boundary condition

$$\hat{\varrho}(0) = \int_0^\infty d\theta \, \frac{d\tilde{\zeta}}{d\theta} = \lim_{\theta\to\infty} \tilde{\zeta}(\theta) - \tilde{\zeta}(0) = 0. \tag{L.5}$$

The function $\hat{\pi}(s)$ appearing in Eq. (L.4) is the Laplace transform [defined in Eq. (2.104)] of the scaled probability distribution $\pi(\theta)$ for the unstrained system. By using its expansion for small s,

$$\hat{\pi}(s) = 1 - s\langle\theta\rangle_\pi + \mathcal{O}(s^2), \tag{L.6}$$

one can immediately show that Eq. (L.4) has a regular singular point at the origin, and thence use the Frobenius method [110] to obtain the asymptotic forms near the origin of two linearly independent solutions:

$$\hat{\varrho}_1(s) = s - s^2 + \mathcal{O}(s^3), \tag{L.7}$$

$$\hat{\varrho}_2(s) = \frac{1}{2} - s\ln s + \mathcal{O}(s). \tag{L.8}$$

Any solution of Eq. (L.4) can be written as a linear combination of these two. Due to the boundary condition (L.5), the coefficient of $\hat{\varrho}_2(s)$ must be zero. Therefore $\hat{\varrho}(s)$ is some real multiple of $\hat{\varrho}_1(s)$.

We haven't been able to integrate Eq. (L.4) analytically. However, it is easy to integrate it numerically, using the behavior given by Eq. (L.7) as the initial condition. The numerical solution thus obtained diverges at infinity; but as $\hat{\varrho}(s)$ is the Laplace transform of a function, it has to go to zero at infinity. Therefore, by assuming that a nonzero solution can be found satisfying both Eq. (4.39) and Eq. (4.49), we have arrived at a contradiction.

References

[1] For an overview of the physics and chemistry of elastomers, see, e.g., L. R. G. Treloar, *The Physics of Rubber Elasticity* (Clarendon Press, Oxford, 1975), and also Refs. [2] and [3].

[2] J. E. Mark and B. Erman, *Rubberlike Elasticity, a Molecular Primer* (John Wiley, New York, 1988).

[3] J. M. G. Cowie, *Polymers: Chemistry and Physics of Modern Materials* (Blackie, Glasgow, 1991).

[4] For an introduction to Polymer Physics from the point of view of modern Statistical Mechanics, see Ref. [5]. For a more chemically oriented presentation, see, e.g., Refs. [6] and [3].

[5] P.-G. de Gennes, *Scaling Concepts in Polymer Physics* (Cornell University Press, Ithaca, 1979).

[6] P. J. Flory, *Principles of Polymer Chemistry* (Cornell University Press, Ithaca, 1971).

[7] As it is commonly done in Statistical Mechanics, we keep the dimensionality as a variable here. A question that merits future study but falls outside of the scope of the mean field theory presented in this work is what are the critical dimensions for the vulcanization transition.

[8] P. J. Flory, J. Amer. Chem. Soc. **63**, 3083 (1941); **63**, 3091 (1941); **63**, 3096 (1941).

[9] W. H. Stockmayer, J. Chem. Phys. **11**, 45 (1943); **12**, 125 (1944).

[10] A derivation of this result can be found, e.g., in [5], Sec. V.2.5.

[11] See, e.g., [12] and [13].

[12] G. R. Dobson and M. Gordon, J. Chem. Phys. **41**, 2389 (1964).

[13] B. H. Zimm and W. H. Stockmayer, J. Chem. Phys. **17**, 1301 (1949).

[14] See, e.g., Refs. [6], [15] and [2].

[15] M. Plischke and B. Joós, Physics in Canada **53**, 184 (1997).

[16] J. Scanlan, J. Polymer Sci. **43**, 501 (1960).

[17] L. C. Case, J. Polymer Sci. **45**, 397 (1960).

[18] M. Gordon and S. B. Ross-Murphy, Pure App. Chem **43**, 1 (1975).

[19] S. F. Edwards, Proc. Phys. Soc. (London) **85**, 613 (1965).

[20] R. T. Deam and S. F. Edwards, Phil. Trans. R. Soc. **280A**, 317 (1976).

[21] R. C. Ball and S. F. Edwards, Macromol. **13** (1980) 748.

[22] M. Doi and S. F. Edwards, *The Theory of Polymer Dynamics* (Oxford University Press, New York, 1986).

[23] See, e.g., S. V. Panyukov, Zh. Eksp. Teor. Fiz. **103** (1993) 1644 [Sov. Phys. JETP **76** (1993) 808]; Pis'ma Zh. Eksp. Teor. Fiz. **55** (1992) 584 [JETP Lett. **55** (1992) 608].

[24] S. Panyukov and Y. Rabin, Phys. Rep. **269**, 1 (1996).

[25] P.-G. de Gennes, J. Phys. (Paris) **37**, L1 (1976); **36**, 1049 (1975).

[26] D. Stauffer, J. Chem. Soc., Faraday Trans. II **72**, 1354 (1976).

[27] For reviews of the percolative aspects of the gelation transition, see D. Stauffer, A. Coniglio, and M. Adam, Adv. in Polym. Sci. **44** (1982) 103, and Ref. [5].

[28] For a general discussion of percolation, see, e.g., D. Stauffer and A. Aharony *Introduction to Percolation Theory*, (Taylor and Francis, London, 1994).

[29] P.-G. de Gennes, J. Phys. (Paris) **38**, L355 (1977).

[30] P. M. Goldbart and N. Goldenfeld, Phys. Rev. Lett. **58**, 2676 (1987); Macromol. **22** (1989) 948; Phys. Rev. A **39** (1989) 1402; **39** (1989) 1412; P. M. Goldbart and N. Goldenfeld, in *Synergetics* **43**: *Cooperative Dynamics in Complex Physical Systems*, H. Takayama (ed.), (Springer, Berlin, 1989) p. 208.

[31] S. F. Edwards and P. W. Anderson, J. Phys. F **5**, 965 (1975).

[32] See, e.g., M. Mézard, G. Parisi and M. A. Virasoro, *Spin Glass Theory and Beyond*, (World Scientific, Singapore, 1987); and K. Binder and A. P. Young, Rev. Mod. Phys. **58**, 801 (1986).

[33] A. Zippelius, P. M. Goldbart and N. Goldenfeld, Europhys. Lett. **23**, 451 (1993).

[34] P. M. Goldbart and A. Zippelius, Phys. Rev. Lett. **71**, 2256 (1993).

[35] C. Roos, A. Zippelius and P. M. Goldbart, J. Phys. A **30**, 1967 (1997).

[36] M. Huthmann, M. Rehkopf, A. Zippelius, and P. M. Goldbart, Phys. Rev. E **54**, 3943 (1996).

[37] P. M. Goldbart and A. Zippelius, Europhys. Lett. **27** (1994) 599.

[38] K. A. Shakhnovich and P. M. Goldbart, manuscript in preparation.

[39] K. Broderix, P. M. Goldbart and A. Zippelius, Phys. Rev. Lett. **79**, 3688 (1997).

[40] An example of approximate treatment of permanent entanglements is the "sliplink model" presented in: R. C. Ball, M. Doi, S. F. Edwards and M. Warner, Polymer **22**, 1010 (1981).

[41] H. E. Castillo, P. M. Goldbart and A. Zippelius, Europhys. Lett. **28**, 519 (1994).

[42] P. M. Goldbart, H. E. Castillo and A. Zippelius, Adv. Phys. **45**, 393 (1996).

[43] H. E. Castillo, P. M. Goldbart and A. Zippelius, manuscript in preparation.

[44] H. E. Castillo and P. M. Goldbart, Phys. Rev. E **58**, R24 (1998).

[45] H. E. Castillo and P. M. Goldbart, manuscript in preparation.

[46] See, e.g., Y. Oono, Adv. Chem. Phys. **61**, 301 (1985).

[47] As, in the context of noninteracting macromolecules, the statistical weight of a semi-microscopic configuration $\{\mathbf{c}_i(s)\}_{i=1}^N$ is simply proportional to the number of microscopic configurations consistent with it, $-k_{\rm B}W_1$ is an entropy, and therefore does not carry a factor of $1/T$.

[48] It is straightforward to see that in terms of dimensionful variables the Edwards measure takes the form

$$\exp\left(-\frac{d}{2}\sum_{i=1}^{N}\int_0^L\frac{d\sigma}{\ell}\left|\frac{d}{d\sigma}\mathbf{R}_i(\sigma)\right|^2-\frac{u_0}{2}\sum_{i,i'=1}^{N}\int_0^L\frac{d\sigma}{\ell}\int_0^L\frac{d\sigma'}{\ell}\,\delta^{(d)}(\mathbf{R}_i(\sigma)-\mathbf{R}_{i'}(\sigma'))\right),$$

where the excluded-volume parameter u_0 is given by $u_0 = (\ell L/d)^{d/2}\,(\ell/L)^2\,\lambda^2$, the units of which are those of volume.

[49] At the microscopic level, a pair of monomers participating in a crosslink are not located at precisely the same position, being instead separated by the length of the bond that connects them. At the semi-microscopic level, however, positions are not resolved beyond a scale of order ℓ. Thus, it is adequate to model the constraints via the Dirac δ-function. A more detailed description, involving the modeling of the constraint via a function that varies on the scale of the bond-length, would yield a theory that differs only at scales on the order of ℓ: the results of the present semi-microscopic approach would thus be unchanged.

[50] J. W. Gibbs *Elementary Principles in Statistical Mechanics* (Scribners, New York, 1902), pp. 206-7.

[51] Two remarks are in order here. As a point of practice, only crosslink locations that differ by more than ℓ can be distinguished in our semi-microscopic approach. Besides, as a point of principle, the set of possible crosslink locations is discrete, owing to the underlying quantum-mechanical nature of the chemical bonds. Thus, the cluster index a is discrete. If it were continuous, one would reasonably expect that for all cluster species (other than the uncrosslinked species) the likelihood of having more that one specimen would be zero.

[52] The thermodynamic limit ($N \to \infty$, $V \to \infty$, N/V fixed, μ^2 fixed) will eventually be taken, in a manner that is discussed in detail in Sec. 2.6.1.

[53] This can be achieved, e.g., by some suitable photo-chemical process. Such schemes have the virtue that they are accurately determined by the equilibrium properties of the system prior to crosslinking. To describe crosslinking processes that are not simultaneous and instantaneous would require information pertaining to the kinetics of the system as the number of crosslinks grows.

[54] A rough estimate gives $[M]/N \sim \mu^2/2$; see Ref. [35].

[55] D. Sherrington and S. Kirkpatrick, Phys. Rev. Lett. **35** (1975) 1792; Phys. Rev. B **17** (1978) 4384.

[56] P. M. Goldbart and A. Zippelius, J. Phys. A **27** 6375 (1994).

[57] For an analysis of related issues in the specific context of supervised learning by neural networks, see S. Seung, H. Sompolinsky and N. Tishby, Phys. Rev. A **45** (1992) 6065, especially Sec. V.D.

[58] See, e.g., I. M. Lifshitz, A. Yu. Grosberg and A. R. Khokhlov, Rev. Mod. Phys. **50**, 683 (1978).

[59] E. Schrödinger, *What is Life*? (Cambridge University Press, 1944), especially Chap. 5.

[60] A. Einstein, Ann. der Physik, **22** (1907) 180. In fact, Ref. [34] presents a more direct connection with the Einstein model, because there all monomers are considered to be identically localized; see also [30].

[61] See, *inter alia*, E. I. Shakhnovich and A. M. Gutin, J. Phys. A **22**, 1647 (1989); M. Mézard and G. Parisi, J. Phys. (Paris) *I* **1**, 809 (1991); Y. Y. Goldschmidt and T. Blum, Phys. Rev. E **48**, 161 (1993); M. Mézard and G. Parisi, J. Phys. (Paris) *I* **2**, 2231 (1992); Ref. [34]; A. Engel, Nucl. Phys. **B410** [FS] 617 (1994).

[62] This hypothesis amounts to adopting the form $\Omega_{\hat{k}} = (1-q)\,\delta_{\hat{k},\hat{0}} + q\,\delta_{\tilde{\mathbf{k}},\mathbf{0}}\,\varpi(\hat{k}^2)$, subject to the mild technical restriction that $\varpi(z)$ be analytic for $\mathrm{Re}\, z \geq 0$ and vanish sufficiently fast at infinity so as to guarantee that $\varpi(z)$ can be expressed as the Laplace transform of another function; see, e.g., [63].

[63] G. Doetsch, *Introduction to the Theory and Application of the Laplace Transformation* (New York: Springer-Verlag, 1974).

[64] See, e.g., F. Mezei, in *Neutron scattering and collective dynamics*, in: *Liquides, crystallisation et transition vitreuse*, edité par J. P. Hansen, D. Levesque et J. Zinn-Justin (Les Houches Session LI, 3-28 Juillet 1989).

[65] We thank S. K. Sinha for a useful discussion of this and related matters.

[66] R. Oeser, B. Ewen, D. Richter and B. Farago, Phys. Rev. Lett. **60** (1988) 1041.

[67] J. Kärger and G. Fleischer, Trends in Analytical Chem. **13** (1994) 145.

[68] V. D. Skirda *et al.*, Makromol. Chem., Rapid Commun. **9** (1988) 603.

[69] P. N. Pusey and W. Van Megen, Physica **A 157** (1989) 705.

[70] J. G. H. Joosten, E. T. F. Geladé, and P. N. Pusey, Phys. Rev. A **42** (1990) 2161.

[71] It may seem strange that $\{\mathbf{k}^0, \mathbf{k}^1, \ldots, \mathbf{k}^g\}$ can be kept fixed in Eq. (2.59) as $n \to 0$. However, in practice the computation of this limit generally involves quantities of the form $w(n, \sum_{a=0}^{g} \mathbf{k}^a, \sum_{a=0}^{g} |\mathbf{k}^a|^2) = w(n, \tilde{\mathrm{l}}, \hat{l}^2)$, and one can simply take the limit for the first variable, while keeping the other two constant.

[72] As is conventional in statistical mechanics, we use the same notation, Ω, for the equilibrium value of the order parameter and for the fluctuating variable (of which it is the expectation value and which features in the Landau free energy). Which meaning is implied can be readily ascertained from the context.

[73] We believe that this is the appropriate order in which to take the thermodynamic and replica limits, although this order is opposite to that commonly used in the context of spin glass theory; see, e.g., §3C of the second citation in Ref. [32].

[74] We have not explored the curious feature of the non–positive-definiteness of $\hat{k}^2$, which arises for modes, say, in the $(n-2)$-replica sector. In principle, this feature could modify the notion that the least stable modes are the long wavelength modes.

[75] In Ref. [34] the instability of the liquid state was found to occur at a higher density of crosslinks, corresponding to $\mu^2 \approx 1.59$. This was due to the variational hypothesis adopted there, which did not allow for a fraction of delocalized monomers to be present in the amorphous solid state.

[76] P. Erdős and A. Rényi, Magyar Tud. Akad. Mat. Kut. Int. Közl. **5**, 17 (1960), especially Theorem 9b; reprinted in Ref. [77], Chap. 14, article [324]. For an informal discussion, see P. Erdős and A. Rényi, Bull. Inst. Internat. Statist. **38**, 343 (1961); reprinted in Ref. [77], Chap. 14, article [v].

[77] *Paul Erdős: The Art of Counting*, edited by J. Spencer (MIT Press, 1973).

[78] If we had chosen to include the delocalized monomers along with the localized monomers in the distribution $p(\tau)$ then $p(\tau)$ would have a term of the form $(1-q)\delta(\tau)$. Such a singularity at $\tau = 0$ would lead to $\hat{p}(\infty) = (1-q)$, which would in general be nonzero. As this would be a technical inconvenience, we have chosen to exclude the delocalized

monomers from $p(\tau)$, separating them from the localized monomers, as was done explicitly in Sec. 2.3.

[79] It is noteworthy that a divergent length scale emerges already at the level of mean-field theory. The analysis of fluctuations around the stationary-point solution would presumably reveal a second length scale, the conventional correlation length, which characterizes the decay of order-parameter correlations. It is not clear at present whether these two length scales are related.

[80] See, e.g., T. W. Körner, *Fourier Analysis* (Cambridge University Press, 1988), §75.

[81] Equation (2.107) was integrated numerically using the Bulirsch-Stoer method [83]. Choosing the solution that satisfies the boundary conditions is a delicate matter because the differential equation is unstable in the following sense. Assuming that $\hat{\pi}(0) = 1$, there is a unique value of $d\hat{\pi}/d\hat{\theta}|_{\hat{\theta}=0}$ that gives rise to $\hat{\pi}(\infty) = 0$: if $d\hat{\pi}/d\hat{\theta}|_{\hat{\theta}=0}$ is larger then $\hat{\pi}(\hat{\theta})$ will oscillate indefinitely about unity; if $d\hat{\pi}/d\hat{\theta}|_{\hat{\theta}=0}$ is smaller then $\hat{\pi}(\hat{\theta})$ will become negative and diverge to $-\infty$. We determined $d\hat{\pi}/d\hat{\theta}|_{\hat{\theta}=0}$ by using a variant of the shooting method for which we defined a monotonic function $t(x)$ via (i) $t(x) = 1/\theta^*$ if integrating Eq. (2.107) with $\hat{\pi}(0) = 1$ and $d\hat{\pi}/d\hat{\theta}|_{\hat{\theta}=0} = x$ gives a solution for which $\hat{\pi}(\hat{\theta}^*) = 1$ and $0 < \hat{\pi}(\hat{\theta}) < 1$ for $0 < \hat{\theta} < \hat{\theta}^*$; and (ii) $t(x) = -1/\theta^*$ if integrating Eq. (2.107) with $\hat{\pi}(0) = 1$ and $d\hat{\pi}/d\hat{\theta}|_{\hat{\theta}=0} = x$ gives a solution for which $\hat{\pi}(\hat{\theta}^*) = 0$ and $0 < \hat{\pi}(\hat{\theta}) < 1$ for $0 < \hat{\theta} < \hat{\theta}^*$. We identified the desired value of $d\hat{\pi}/d\hat{\theta}|_{\hat{\theta}=0}$ as the root of $t(x) = 0$.

[82] Equation (2.108) was also integrated numerically using the Bulirsch-Stoer method [83]. To satisfy the normalization condition we first analytically obtained the asymptotic solution of Eq. (2.107) for $\hat{\theta} \gg 1$. We identified the numerical prefactor by comparison with the numerical solution, and then inverse-Laplace-transformed this asymptotic form to obtain $\pi(\theta) \sim 4.554\theta^{-2}\exp(-2/\theta)$ (for $\theta \ll 1$). We used this form to start the integration of Eq. (2.108) at a small but nonzero value of θ, thus avoiding the singularity at $\theta = 0$. After integrating to obtain the full function $\pi(\theta)$ we computed $\int_0^\infty d\theta\, \pi(\theta)$ numerically, and verified (to within numerical accuracy) that the value was unity. As a second check, we computed $\hat{\pi}(\hat{\theta})$ as the (numerical) Laplace transform of our (numerically obtained) solution of Eq. (2.108), and established that it coincided (to within numerical accuracy) with the numerical solution of Eq. (2.107).

[83] W. H. Press, S. A. Teukolsky, W. T. Vetterling and B. P. Flannery, *Numerical Recipes in FORTRAN*, Second Edition (Cambridge University Press, 1992), Chap. 16, subroutines `bsstep.for`, `rzextr.for` and `mmid.for`.

[84] A different field-theoretic treatment, intended for the well-crosslinked regime (in which the many-macromolecule system is modeled by a single, linear, self-crosslinked macromolecule) can be found in Ref. [23]. For a review of this work, see Ref. [24].

[85] See Ref. [5], Sec. V.2

[86] S. J. Barsky and M. Plischke, Phys. Rev. E **53**, 871 (1996).

[87] S. J. Barsky, Ph.D. thesis, Simon Fraser University, Canada (unpublished, 1996); S. J. Barsky and M. Plischke (unpublished, 1997).

[88] W. Peng, H. E. Castillo, P. M. Goldbart, and A. Zippelius, Phys. Rev. B **57**, 839 (1998); cond-mat/9709250.

[89] A constant is ignored here that has to do with the symmetry under permutations of the macromolecules. See Sec. 2.2.6 for a full discussion.

[90] For an ϵ dependence to appear in the scaling function $\pi(\theta)$, terms of order ϵ^4 need to be included in the free-energy functional, or equivalently terms of order ϵ^3 need to be included in the stationary-point equation.

[91] Y. Kantor, M. Kardar, D. R. Nelson, Phys. Rev. Lett. **57**, 791 (1986); Phys. Rev. A **35**, 3056 (1987).

[92] For a review, see *Jerusalem Winter School for Theoretical Physics: Statistical Mechanics of Membranes and Surfaces*, edited by D. Nelson, T. Piran, S. Weinberg (World Scientific, Singapore, 1989).

[93] J. R. L. de Almeida and D. J. Thouless, J. Phys. **A11**, 983 (1977).

[94] G. Parisi, Phys. Lett. **73A**, 203 (1979).

[95] C. De Dominicis and I. Kondor, Phys. Rev. B **27**, 606 (1983).

[96] See, e.g., [97], Volume II, Chapter XI, Section 11.3.

[97] Bateman Manuscript Project, *Higher Transcendental Functions*, (McGraw-Hill, New York, 1953-55)

[98] We choose the axis of quantization to be parallel to $\check{a}$. In any dimension there exists one surface harmonic that is proportional to the coordinate along the axis of quantization. We use the notation $\sigma = (1, 0)$ to denote this specific surface harmonic, by analogy with the case of 3 dimensions, in which it corresponds to $Y_{10} \sim z$.

[99] I. S. Gradshteyn and I. M. Ryzhik, *Table of Integrals, Series and Products*, (Academic Press, New York, 1965).

[100] The greatest lower bound of a nonempty set $\mathcal{S}$ of real numbers is a real number c such that for any lower bound b of the set $\mathcal{S}$ it is true that $c \geq b$. Such a number always exists for any set that has at least a lower bound. See, e.g., H. L. Royden, *Real Analysis*, (Macmillan, New York, 1968), Chapter 2.

[101] M. Abramowitz and I. A. Stegun, *Handbook of mathematical functions with formulas, graphs, and mathematical tables*, (Dover, New York, 1965), Chapter 13.

[102] One could attempt to solve Eq. (3.69) assuming $\zeta = 0$, but this leads to the condition

$$4\langle\theta^{-1+nd/2}\rangle_\pi = l - 1 + nd/2,$$

which can at most be satisfied for isolated values of n. In particular, by using Eq.(3.48) we see that for $n = 0$ the left hand side is not an integer, and the equation is not satisfied.

[103] S. Feng and P. N. Sen, Phys. Rev. Lett. **52**, 216 (1984).

[104] H. M. James and E. Guth, J. Chem. Phys. **15**, 669 (1947).

[105] M. Adam et al., Pure Appl. Chem. **53**, 1489 (1981); C. Allain and L. Salomé, Polymer Commun. **28**, 109 (1987); Macromol. **20**, 2957 (1987); M. A. V. Axelos and M. Kolb, Phys. Rev. Lett. **64**, 1457 (1990).

[106] M. Adam et al., Pure Appl. Chem. **53**, 1489 (1981); M. Adam, M. Delsanti, and D. Durand, Macromol. **18**, 2285 (1985); B. Gauthier-Manuel et al., J. Phys. (Paris) **47**, 869 (1987); T. Woignier et al., J. Phys. (Paris) **49**, 289 (1988).

[107] It is unclear why the ad hoc strategy for computing the shear modulus used, e.g., by Huthmann et al. [36] gives too large a value of t.

[108] Let $\mathcal{M}$ be a real and symmetric but otherwise arbitrary $r \times r$ matrix, having elements $\mathcal{M}_{\rho,\rho'}$. Let $\{\mathbf{m}^j\}_{j=1}^r$ be a complete set of orthonormal eigenvectors, having components $\{m_\rho^j\}_{j,\rho=1}^r$, and let $\{\mu^j\}_{j=1}^r$ be the set of corresponding eigenvalues. The quasi-determinant $\tilde{\det}^{(r)}\,\mathcal{M}$ and quasi-inverse $\tilde{\mathcal{M}}$ associated with $\mathcal{M}$ are extensions of the standard determinant and inverse of $\mathcal{M}$ that are relevant if $\mathcal{M}$ is singular (i.e., has one or more vanishing eigenvalues, which we refer to as zero-modes). They can be expressed in the following way:

$$\begin{aligned} \tilde{\det}^{(r)}\,\mathcal{M} &\equiv \prod_{\substack{j=1 \\ (\mu^j \neq 0)}}^{r} \mu^j, \\ \tilde{\mathcal{M}}_{\rho,\rho'} &\equiv \sum_{\substack{j=1 \\ (\mu^j \neq 0)}}^{r} \frac{m_\rho^j\, m_{\rho'}^j}{\mu^j}, \end{aligned}$$

terms corresponding to vanishing eigenvalues being omitted from the product and summation. Thus, in contrast with their conventional counterparts, the quasi-determinant fails to vanish and the quasi-inverse continues to exist for singular matrices.

[109] See, e.g., Daniel Zwillinger, *Handbook of Integration* (Jones and Bartlett, London, 1992), §35.

[110] See, e.g., C. M. Bender and S. A. Orszag, *Advanced Mathematical Methods for Scientists and Engineers* (Mc Graw-Hill, New York, 1978).

Vita

Horacio Emilio Castillo was born in Buenos Aires, Argentina, on October 2, 1961. He received his Licenciado en Ciencias Físicas degree from the University of Buenos Aires in 1986, and his M.S. from the University of Illinois in 1993.